Studies of ultra-relativistic macroscopic phenomena including real time correlations

By

TOSHALI MITRA

PHYS10201804004

The Institute of Mathematical Sciences, Chennai

A thesis submitted to the

Board of Studies in Physical Sciences

In partial fulfillment of requirements

for the Degree of

DOCTOR OF PHILOSOPHY

of

HOMI BHABHA NATIONAL INSTITUTE

21/07/2023

Homi Bhabha National Institute

Recommendations of the Viva Voce Committee

As members of the Viva Voice Committee, we certify that we have read the dissertation prepared by TOSHALI MITRA entitled "Studies of ultra-relativistic macroscopic phenomena including real time correlations" and recommend that it may be accepted as fulfilling the thesis requirement for the award of Degree of Doctor of Philosophy.

Date: 21/07/2023

Chairman - Sibasish Ghosh

Date: 21/07/2023

Guide/Convenor - V. Ravindran

Date: 21/07/2023

Co-guide - Ayan Mukhopadhyay

Date: 21/07/2023

Examiner - Diptarka Das

Date: 21/07/2023

Member 1 - Venkata Suryanarayana Nemani

Date: 21/07/2023

Member 2 - Sujay K Ashok

Date: 21/07/2023

Member 3 - D. Indumathi

Date: 21/07/2023

Member 4 - Suresh Govindarajan

Final approval and acceptance of this thesis is contingent upon the candidate's submission of the final copies of the thesis to HBNI.

We hereby certify that we have read this thesis prepared under our direction and recommend that it may be accepted as fulfilling the thesis requirement.

Date: 21/07/2023

Place: Chennai

Guide

STATEMENT BY AUTHOR

This dissertation has been submitted in partial fulfillment of requirements for an advanced degree at Homi Bhabha National Institute (HBNI) and is deposited in the Library to be made available to borrowers under rules of the HBNI.

Brief quotations from this dissertation are allowable without special permission, provided that accurate acknowledgement of source is made. Requests for permission for extended quotation from or reproduction of this manuscript in whole or in part may be granted by the Competent Authority of HBNI when in his or her judgement the proposed use of the material is in the interests of scholarship. In all other instances, however, permission must be obtained from the author.

Toshali Mitra

TOSHALI MITRA

21/07/2023

DECLARATION

I hereby declare that the investigation presented in the thesis has been carried out by me. The work is original and has not been submitted earlier as a whole or in part for a degree/diploma at this or any other Institution / University.

Toshali Mitra

TOSHALI MITRA

21/07/2023

LIST OF PUBLICATIONS ARISING FROM THE THESIS

Publications:

- **Published**

  1. **T. Mitra**, A. Mukhopadhyay and A. Soloviev, "Hydrodynamic attractor and novel fixed points in superfluid Bjorken flow," Phys. Rev. D 103 (2021) no.7, 076014 doi:10.1103/PhysRevD.103.076014 [arXiv:2012.15644 [hep-ph]].

- **Submitted**

  1. PRR submission - A. Banerjee, **T. Mitra** and A. Mukhopadhyay, "Correlation functions of the Bjorken flow in the holographic Schwinger-Keldysh approach," [arXiv:2207.00013 [hep-th]].

- **In Preparation**

  1. **Toshali Mitra**, Sukrut Mondkar, Ayan Mukhopadhyay, Anton Rebhan, Alexander Soloviev, On thermalization in Semi-holography, Manuscript under preparation (2023).

Toshali Mitra
Toshali Mitra
21/07/2023

List of other publications, Not included in the thesis

1. A. Banerjee and **T. Mitra** and A. Mukhopadhyay and A. Soloviev, "How Gubser flow ends in a holographic conformal theory", [arXiv:2307.10384[hep-th]]

2. **T. Mitra**, S. Mondkar, A. Mukhopadhyay, A. Rebhan and A. Soloviev, "Hydrodynamization in hybrid Bjorken flow attractors," [arXiv:2211.05480 [hep-ph]].

3. **T. Mitra**, S. Mondkar, A. Mukhopadhyay, A. Rebhan and A. Soloviev, "Hydrodynamic attractor of a hybrid viscous fluid in Bjorken flow," Phys. Rev. Res. 2 (2020) no.4, 043320 doi:10.1103/PhysRevResearch.2.043320 [arXiv:2006.09383 [hep-ph]].

List of presentations and participation at conferences

1. **Title**: Real time correlation function of Bjorken flow in holographic approach,
   Conference: Chennai String Meet, 2023 IMSc, Chennai, in person.

2. **Title**: Real time correlation function of Bjorken flow in holographic approach,
   Conference: 2022 Chennai Southampton Workshop, STAG Research Centre, Southampton University, Center for Strings, Gravitation and Cosmology, IIT Madras, Chennai, 2022, Hybrid.

3. **Title**: Scalar correlation functions and Transients in an attractor background
   Conference: Chennai String Meet, 2021, Online edition.

4. **Title**: Bottom up thermalization and hydrodynamization on hybrid attractor surface
   Conference: Strong-Electro Weak Matter 2021, Online edition.

5. **Title**: Hybrid hydrodynamic attractors, Bottom up thermalization and more
   Conference: Extreme non-equilibirum QCD, ICTS Bangalore, 2020, Online edition.

6. **Title**: Attractive hydrodynamic coupling and QGP
   Conference: National String Meetings 2019, IISER Bhopal, in person.

Research visits and seminars

1. Research visit: Prof. Edmond Iancu, Institut de Physique Théorique, Saclay; Paris.

2. Attended:Strong-Electro Weak Matter, 2022, Institut de Physique Théorique, Saclay; Sorbonne Université, Campus Jussieu, Paris.

3. Attended: Chennai Symposium Gravitation and Cosmology, IIT Madras, Chennai, 2020.

4. Attended: The Myriad colourful ways of understanding extreme QCD matter, ICTS, Bangalore, 2019.

To my family

ACKNOWLEDGEMENTS

The five years journey in IMSc would not have been possible without the help of numerous individuals. I am extremely thankful to my supervisor Dr V Ravindran for his assistance, support and advice during the PhD. I am indebted to my co-supervisor Dr Ayan Mukhopadhyay for his invaluable guidance, patience and continuous support during my PhD study. His optimistic and enthusiastic attitude towards research has inspired me throughout the research. I would also like to thank the members of the Doctoral Committee for their suggestions and encouragement.

I would like to extend my gratitude towards Dr Alexander Soloviev for his valuable guidance during collaboration and also while writing the thesis. I am grateful to Dr Avik Banerjee for his assistance and direction throughout the collaborative projects and thesis writing. I am thankful to my colleague Sukrut Mondkar for helping and challenging me intellectually while working together on various projects. I'd like to thank Professor Anton Rebhan for his insightful comments and discussions during the collaboration. Professor Edmond Iancu's support and invitation to IPHT Saclay, Paris, are also greatly appreciated. In addition, I'd like to thank the entire administrative staff and various IMSc departments for their consistent support.

I am grateful to my close friends Pavan and Gopal for their support during difficult times, as well as for being fun-loving and food-loving besides physics-loving. I would like to thank my friends Hareram and Tanay for their encouragement and help during the journey. I'd like to thank the two Tanmays, Saha and Sengupta, for their help throughout the process. Also, I want to thank my friend Lakshitha for giving me constant moral support.

I am extremely grateful to my parents for being understanding and supportive throughout my life. I would like to thank my sister Ankita Mitra for being always there for me. I want to thank my in-laws for being supportive while writing the thesis. I want to thank my life partner

Akhil Antony for his constant support, patience and encouragement from the very beginning of PhD life. Thank you for inspiring me and making me a better person.

Abstract

The existence of hydrodynamic attractors in various microscopic theories and phenomenological models has paved the way for understanding hydrodynamization in out-of-equilibrium systems. The thesis studies a far-away-from equilibrium system undergoing Bjorken flow, a boost-invariant expansion in the longitudinal direction. It explores the effect of continuous symmetry breaking and the corresponding phase transition on hydrodynamization in the Bjorken expanding system. Followed by this, it computes the real-time hydrodynamic correlation functions of the expanding system using the holographic method. In addition, the thesis also investigates the thermalisation of a hybrid system coupled in a semi-holographic framework.

We begin with a review of the necessary theoretical background required to follow the work included in the thesis. Then we discuss the construction of an effective description of a dissipative superfluid by extending the quantum effective approach of Son and Nicolis and incorporating dissipation in Müller-Isreal-Stewart (MIS) formalism. We include the Goldstone boson and the condensate together with the hydrodynamic modes as the effective degrees of freedom. We show that the evolution of the superfluid undergoing boost invariant expansion is governed by the conventional hydrodynamic attractor with unbroken $U(1)$ symmetry and an even number of novel non-dissipative fixed points with broken symmetry. If the initial temperature is super-critical, then the condensate becomes exponentially small very rapidly and the system is trapped by the hydrodynamic attractor for a long intermediate time before it reheats rapidly and switches to one of the symmetry-breaking fixed points eventually. Finally, we show that the fixed points are unstable against inhomogeneous perturbations that should lead to spinodal decomposition. We conclude that these features should be generic beyond the MIS formalism.

Next, we develop a method to compute the Schwinger-Keldysh correlation functions of an expanding system in a holographic approach in the limit in which the state hydrodynamizes.

We implement the horizon cap prescription of Crossley-Glorioso-Liu to an asymptotically dynamical AdS_{d+1} geometry which is dual to Bjorken flow in the boundary. We provide a new and elegant proof of consistency of the horizon cap prescription with the KMS (Kubo-Martin-Schwinger) periodicity and the ingoing boundary condition for the retarded propagator at any arbitrary frequency and momentum. The trick of Weyl rescaling the Bjorken flow at the boundary lifts to appropriate bulk diffeomorphism, which implies that the dual black hole's event horizon attains constant surface gravity and area at a late time. Subsequently, at late time the temperature and entropy density for the dual state maps to a constant which otherwise has a perfect fluid-like expansion. One of our key results is that in the limit of perfect fluid expansion, the Schwinger-Keldysh correlation functions are simply thermal at an appropriate temperature when expressed in terms of reparametrized spacetime arguments. A generalized bi-local thermal structure holds to all orders. We also argue a transseries form of the hydrodynamic correlation functions that can decode the details of the initial state.

Finally, we investigate the thermalization of a hybrid system involving a weakly self-interacting perturbative and a strongly self-interacting non-perturbative (holographic) sector, democratically coupled in semi-holographic framework. We first provide a generic proof of thermalisation, in which the entropy of the full system is maximised only when the physical temperatures of the respective sectors coincide at any fixed total energy. We show that if we consider a generic state in which observable like the full energy-momentum tensor is like in a pseudo-equilibrium state, the total entropy of this non-equilibrium state is that of global equilibrium. Then we study dynamical situations such as an effective two-fluid model described by BRSSS formalism. We show that there exist macroscopic fluctuations about any pseudo-equilibrium state which keep the total energy fixed and take the system to a non-equilibrium state whose total entropy is close to that of global equilibrium entropy up to a good degree of precision. Based on these results we formulate how to study the thermalization of the full isolated hybrid system in the full quantum theory in the large N limit.

Contents

Synopsis

The robust success of heavy ion colliders, namely Relativistic Heavy Ion Colliders (RHIC) at Brookhaven National Laboratory and Large Hadron Colliders (LHC) at CERN, in recreating the hot and dense QCD matter has unveiled new opportunities in understanding the dynamics of strongly interacting gauge theories. The QCD matter formed in the head-on collision of two nuclei evolves into a deconfined state of quarks and gluons known as Quark Gluon Plasma(QGP) in the intermediate stage. Various experimental observations such as rapid thermalization (at about 1fm/c), low ratio of shear viscosity to entropy density, and collective flow provide evidence of strong interaction and fluid-like behaviour of the QGP. The most relevant effective theory that describes the observables of collective flow is relativistic hydrodynamics with a low value of the ratio of shear viscosity to entropy density.

One of the surprising aspects of the phenomenology of QGP is that a hydrodynamic description is valid even when it is far away from equilibrium and has large pressure anisotropies. Various phenomenological causal models of hydrodynamics, such as Baier-Romatschke-Son-Starinets-Stephanov (BRSSS) theory [1] which is a refinement of Müller-Israel-Stewart (MIS) theory [1, 2], have been developed and applied in rather extreme conditions. The term hydrodynamization has been coined to describe such phenomena in which the evolution of a system when monitored by coarse-grained variables such as the energy-momentum tensor and conserved currents, can be described by hydrodynamics even far away from equilibrium. A recent theoretical understanding of hydrodynamization [3, 4] arises from the discovery of hydrodynamic attractors [5] which have been shown to exist in various microscopic descriptions such as kinetic theory and the holographic description of $\mathcal{N} = 4$ Super Yang-Mills theory at large $\mathcal{N}$ and strong coupling.

Chiral symmetry, and the associated chiral phase transition from the unbroken to broken phase which accompanies the deconfinement-confinement transition, play a prominent role in the dynamics of the expanding nuclear matter formed in heavy ion collision. The phase di-

agram of QCD shows smooth crossover at smaller baryon chemical potential and a first order transition at larger values separated by a critical point. Lattice simulations suggest that the critical point shows $O(4)$ scaling. The effect of finite but small quark masses on chiral susceptibility has been studied by lattice methods [6, 7].

In the chiral limit (vanishing quark masses), the Goldstone modes should be included together with the hydrodynamic variables parameterizing the conserved currents governed by the Ward identities. In case of small quark masses, we obtain pseudo-Goldstone bosons instead of the Goldstone bosons. The construction of an effective description of the composite dissipative system of pseudo-Goldstone bosons interacting with usual hydrodynamic degrees of freedom is a direction of intense research.

Superfluid fluctuations should have significant effects on macroscopic flow of matter formed in heavy ion collisions if the system gets close to the critical point in the course of its evolution in time, as shown in [8]. At length scales below a dynamically determined decoherence length scale, which can be larger than the microscopic scales in a superfluid, the fluctuations are of quantum origin. Stochastic hydrodynamics [9] is a formalism for incorporating macro(meso)scopic classical statistical fluctuations at length scales larger than the mean free path, and studying how they alter the long-time evolution of the system. However, for superfluids, a quantum generalization of stochastic hydrodynamics is necessary for incorporating the effects of macro(meso)scopic fluctuations between the decoherence length scale and the mean free path.

Experimental evidence suggests an interplay between strong and weak degrees of freedom in the QCD matter formed in heavy ion collision from the very initial stage till the time the particle reaches the detector. Semi-holographic approach [10–12], incorporates both these degrees of freedom consistently in a single framework. In this framework, the low energy sector coupled with the holographic sector is expected to thermalise with the latter. In this case, fluctuation plays a crucial role in leading the system towards global equilibrium from a pseudo-equilibrium state. Particularly in the large N limit, fluctuation dominates the understanding of

quantum thermalisation of the system.

The work included in the thesis is divided into three parts. The first part deals with constructing the effective description of a dissipative relativistic superfluid and understanding the nature of the Bjorken flow [13] of such a system.

The second part deals with the development of a holographic method for computing real-time hydrodynamic (out-of-equilibrium) correlation functions of a strongly coupled relativistic system undergoing Bjorken flow. This is not only the first step for the study of a quantum superfluid incorporating macroscopic fluctuations, but also for a more fundamental understanding of non-equilibrium dynamics with diverse applications to the phenomenology of heavy-ion collisions.

In the third work included in the thesis, we study the thermalisation of a democratically coupled system in the semi-holographic framework.

MIS formalism of superfluidity

In the first work, we have developed a causal MIS formalism for superfluid in which we add both the order parameter and dissipation to the Son-Nicolis effective action framework [14, 15]. We have restricted ourselves here to the case of a $U(1)$ symmetry breaking but our work can be easily generalized to non-Abelian cases. Our formalism reproduces the superfluid diffusion mode found in other effective approaches [16] while pointing towards spinodal instabilities below a certain temperature.

We use our MIS-superfluid formalism to study symmetry breaking in out-of-equilibrium situations in the context of Bjorken flow. For initial temperature above the critical temperature, T_c, the condensate decays exponentially fast while the phase evolves over a similar timescale to satisfy the Josephson condition. Then the full system gets trapped very close to a conventional *hydrodynamic attractor* over a very long period of time during which the system approaches a perfect fluid expansion with unbroken symmetries. However, the long time

physics is somewhat surprising.

It turns out that the superfluid system has an even number of symmetry breaking non-dissipative fixed points in which the full system undergoes expansion at a *constant* temperature (determined by the equation of state and the potential) and with a *constant* value of the condensate. These fixed points are possible because the condensate lowers the energy with respect to the vacuum, allowing the expanding system to maintain a self-consistent constant temperature.

When the initial temperature T, is above the critical temperature T_c and otherwise the initial conditions are generic, the superfluid system switches rapidly to one of these symmetry-breaking fixed points after spending time in very close proximity to the conventional *hydrodynamic attractor* with unbroken symmetries. The basin of attraction of these fixed points has complicated interlacing and possibly fractal boundaries. If $T < T_c$ initially, then the superfluid system generically evolves to one of the fixed points without getting trapped near the hydrodynamic attractor (unless the initial condition is close to the boundary between the basins of attraction of the fixed points). We observe that the symmetry-breaking fixed points are independent of the relaxation mechanism, and are determined only by the equation of state and the potential of the condensate. Furthermore, the hydrodynamic attractor is a feature in any phenomenological framework incorporating relaxation. Therefore, the dynamic features of superfluid flow, especially concerning the role of the hydrodynamic attractor and the fixed point should be universal. We also analyze the linearized perturbations around thermal equilibrium and show that the fixed points are unstable against inhomogeneous perturbations that should lead to spinodal decomposition.

Schwinger Keldysh correlation function of Bjorken flow

To study the real-time correlation function of a strongly coupled non-equilibrium system in the hydrodynamic limit, we have implemented a holographic approach. We generalize the horizon cap prescription due to Crossley, Glorioso and Liu (CGL) [17] to a dynamical asymptotically

AdS_{d+1} (anti-de Sitter) bulk geometry dual to the Bjorken flow in the field theory, and obtain the out-of-equilibrium correlation functions in the hydrodynamic limit in the late time expansion. The horizon cap prescription originally proposed for the static black brane dual to the thermal state realizes the Schwinger-Keldysh contour by a *horizon cap*, in which the ingoing Eddington-Finkelstein radial coordinate goes around the horizon in the complex plane in a little circle of radius ϵ before going back to the real axis and reaching the second boundary. Thus the two arms of the Schwinger-Keldysh contour at the two boundaries are connected continuously in the bulk through the bulk radial contour. The horizon cap implements the appropriate analytic continuation of bulk fields from one arm of the bulk geometry to the other with the sources specified independently at the two boundaries.

We first provide a novel, elegant and simple proof that the CGL horizon cap prescription reproduces the Kubo-Martin-Schwinger (KMS) periodicity at thermal equilibrium which relates the various real-time correlation functions, and that it also reproduces the Son-Starinets ingoing boundary prescription for the retarded correlation function (implying that it is given by causal response) at arbitrary frequency and momenta. This proof relies on deriving a simple matrix factorization of thermal correlation functions and also showing that the on-shell action is localised at the two boundaries receiving contributions only from the cross terms between the in-going and out-going modes.[1] Both of these features are also crucial for the extension of the CGL method to the out-of-equilibrium hydrodynamic Bjorken flow and also for crucial consistency checks of the prescription.

The primary tool for extending the CGL prescription into the hydrodynamic regime is the utilization of a Weyl rescaling of the Bjorken flow. At late time this rescaling maps the perfect fluid expansion to a flow with constant temperature and entropy density. However, there is no time-translation symmetry (time-like Killing vector). The Weyl rescaling leads to expansion in the longitudinal direction and contraction in the transverse direction with proper time evolution in a way such that the total spatial volume density is a constant. This Weyl

[1]The in-going and out-going modes are defined at the horizon but each of them extend all the way to the boundary. The Dirichlet boundary conditions at the two boundaries give a unique solution of the sclar field in the full geometry.

transformation can be lifted to a bulk diffeomorphism. At late proper time, the dual black hole's event horizon (and also the apparent horizon which coincides with it at late time) reaches a fixed location. The area and surface gravity of the event horizon remain constant at late time, but the event horizon shrinks in the directions transverse to the flow while expanding in the longitudinal direction. The latter necessitates the viscous and higher order hydrodynamic corrections (in this Weyl rescaled version) so that the horizon is smooth. The computation of viscous and higher order corrections is just a special case of the fluid/gravity correspondence [18] and has been worked out up to very high orders for the Bjorken flow.

The out-of-equilibrium correlation functions of a scalar operator can be obtained from the on-shell action of a scalar field in the doubled version of the bulk Bjorken flow geometry. At the leading order, the Klein-Gordon equation for the bulk massive scalar field dual to the operator can be mapped to that in the static black brane with appropriate co-moving momenta, thus generalizing the result of Janik and Peschanski for the homogeneous case [19], after adequate spacetime reparametrizations manifested via the Weyl rescaling mentioned above. It follows that the Schwinger-Keldysh (real time) correlation functions at late time can be mapped to thermal correlation functions with appropriate reparametrizations of the proper time, the rapidity and the transverse coordinates, up to an overall Weyl rescaling.

We show that the scalar field can be solved order by order in the late time expansion such that the regularity of the horizon cap is preserved provided the latter is located at the perturbative event horizon. Furthermore, with an additional log correction to the time-reparametrization, we obtain systematic corrections to the real time correlation functions to the perfect fluid limit in the late time expansion. We show that the all order result for the hydrodynamic Schwinger-Keldysh correlation functions exhibits a hidden thermal structure (mimicking the matrix factorization property) which satisfies crucial field theory consistency conditions that are relevant even out of equilibrium. The pinning of the horizon cap to the event horizon mimics the causal nature of Schwinger-Keldysh correlation functions which govern the evolution of the real time correlation functions in the dual field theory. We also comment on the trans-series

resummation of hydrodynamic correlation functions and how Stokes data can capture initial conditions.

Thermalization in semiholography

In this part of the thesis, we investigate thermalization of a hybrid system involving a weakly self-interacting perturbative sector and a strongly self-interacting non-perturbative (holographic) sector. The two sectors are coupled using effective metric coupling technique inspired by semi-holographic framework. The effective metrics of each subsector is determined by the energy-momentum tensor of the complementary one in a way which leads to a conserved energy-momentum tensor of the full system in the physical background metric. This setup manifests a continuum of pseudo-equilibrium states in the large N limit where the two sectors can equilibrate at two arbitrary and distinct physical temperatures. Earlier, it was shown in [20], that the setup nevertheless admits a consistent thermodynamic description in which demanding the equality of the two physical temperatures of the respective subsectors is consistent with the thermodynamic identities of the full system, and furthermore the total entropy of the system is also the sum of the entropies of the two sectors with respective effective spatial volume corrections. The latter is consistent with statistical mechanics since the two sectors are isolated except for the effective metric background being determined in a self-consistent way.

We first give a generic proof that the entropy of the full system is maximised only when the two physical temperatures of the two sectors coincide at any fixed total energy. This result completely establishes that the semi-holographic framework leads to a consistent and unique global equilibrium state in the large N limit.

We furthermore study dynamical situations, such as an effective two fluid model and a kinetic system coupled to a holographic black hole via the effective metric coupling [20], and show that there exists non-equilibrium macroscopic fluctuations about any pseudo-equilibrium state which keep the total energy fixed and increases the total entropy. However, any non-

equilibrium macroscopic fluctuation about the global equilibrium state only reduces the entropy. Based on these results we formulate how to study the thermalization of the full isolated hybrid system in the full quantum theory in the large N limit. In particular, we show that the entanglement of the two systems provide a natural origin of the fluctuations which will lead to the large N dynamics of thermalization.

****

We conclude the thesis with a summary of the results, and discussing the planned future research which extends the work described here and which should lead to a better understanding of macroscopic dynamics of relativistic quantum systems, particularly quantum gauge theories.

List of Figures

Chapter 1

Introduction

With the advent of heavy-ion colliders, namely Relativistic Heavy-ion Colliders (RHIC) at Brookhaven National Laboratory and Large Hadron Collider (LHC) at CERN, the relativistic heavy-ion collision has unveiled new opportunities in understanding the fundamental nature of strongly interacting gauge theories. The hot and dense nuclear matter formed in the head-on collision of Lorentz contracted disc of large nuclei such as Au or Pb, in the intermediate stage evolves into a deconfined state of quarks and gluons known as Quark Gluon Plasma(QGP). Such an exotic state of matter forms the key to understand and explore the deconfined and confined states of quarks and gluons via the phase diagram of QCD (quantum chromodynamics) [32]. Moreover, this deconfined phase of quarks and gluons pervaded the Universe for a few seconds after the Big Bang [33].

Experimental observations for heavy ion collision at the colliders exhibit collective phenomena like elliptic flow [34, 35], giving evidence of strong interaction among the partons liberated by collisions. This strongly interacting partonic matter rapidly approaches thermal equilibrium which is consistent with the relatively short thermalization time of order $\tau \sim 1$fm/c [36]. The expansion and cooling of the QGP suggest the dependence of temperature on space and time, implying a scenario close to local thermal equilibrium. Moreover, the estimated value of certain observables such as the ratio of shear viscosity (η) to entropy density (s) of the QGP

formed at CERN and RHIC lie in the ballpark of the ratio $\eta/s = 1/(4\pi)$ [37], computed by Policastro, Son and Starinets [38] and was later conjectured to be the universal lower bound by Kovtun, Son, and Starinets [39]. The most relevant effective theory that captures these fluid-like features of QGP is the relativistic theory of hydrodynamics [9, 40, 41]. Surprisingly, one of the remarkable aspects of the phenomenology of QGP is that a hydrodynamic description is valid even when it is far away from equilibrium and has large pressure anisotropies. The effective theory of hydrodynamics studies the long-range behaviour of fluid near local thermal equilibrium, governed by the conservation equation of the energy-momentum tensor and global currents. The applicability of hydrodynamics to a dynamical evolution away from local equilibrium led to further development in the theory. Various causal models like Muller-Israel-Stewart (MIS) theory [2, 42], where the dissipation is treated as a dynamical variable, Baier-Romatschke-Son-Starinets-Stephanov (BRSSS) theory [1] which systematically studies the second order gradient expansions, have been developed and applied in rather extreme conditions. In addition, there are extensive studies to acknowledge the diverging behaviour of the hydrodynamic gradient expansion [25, 26] and its consistency with the theory of resurgence at large order [43].

The applicability of hydrodynamics to a system far away from equilibrium has been explained by the discovery of hydrodynamic attractors [25]. Attractor is a feature of a dissipative system that can be defined as a state of the system towards which the non-equilibrium dynamics of the system evolves irrespective of any initial conditions. The attractors can be represented as a point or set of points, curve, surface or complicated fractal structure. The emergence of attractor phenomena in a causal hydrodynamic model as well as in microscopic theories such as kinetic theory [44, 45] and the holographic description of $\mathcal{N} = 4$ Super Yang-Mills (SYM) theory at large N and strong coupling [24], can be attributed to the observation that the non-hydrodynamic modes present in the dynamics decay to same late time behaviour, governed by hydrodynamic degrees of freedom for arbitrary initial conditions. Moreover, the attractors can be also defined as the resummation of hydrodynamic gradient expansion up to all orders. This phenomenon in which the evolution of a system is controlled by macroscopic variables such as energy-momentum tensor and conserved currents, and described by hydrodynamics, even at far

away from equilibrium has been termed as *hydrodynamization* [23].

The fluid description of the QGP includes only the hydrodynamic variables such as fluid velocity, temperature and charge densities via the constitutive relations of the energy-momentum tensor and global currents (refer to chapter 2). However, the presence of chiral symmetry breaking, the salient feature of the nuclear matter is not captured in this usual hydrodynamic description. Chiral symmetry and the associated chiral phase transition from the unbroken to the broken phase, which involves the deconfinement-confinement transition, play a significant role in the dynamics of the expanding nuclear matter produced by heavy ion collisions [46]. The evolution of the nuclear matter through the chiral unbroken and broken phase can be understood by studying the QCD phase diagram 1.1. A phase diagram is the graphical representation of the physical states of a system under different conditions of thermodynamical variables. The QCD phase diagram tells the tale of distinct phases of QCD matter that occur and co-exist at different ranges of temperature T and chemical potential μ. The phase diagram of QCD is an active research subject which has shown much progress with lattice simulation [32] and experimental searches at experiments in RHIC and CERN.

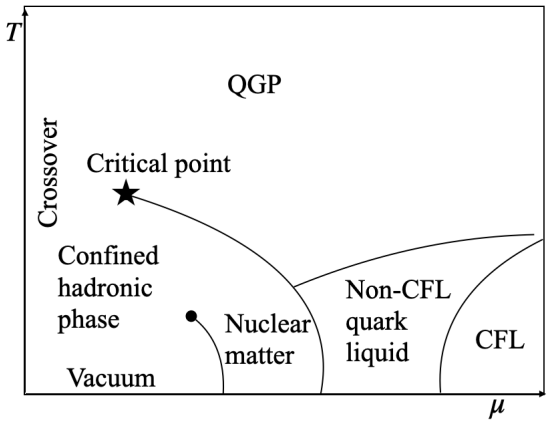

Figure 1.1: Schematic view of QCD phase diagram [21].

Here we sketch a schematic understanding of the QCD phase diagram: We start with zero temperature T and chemical potential μ, where vacuum exists and then vary the temperature along with μ. At a low value of T and baryon chemical potential μ, there exists the colour-neutral bound state of quarks and gluons which is the chiral symmetry broken phase.

At higher temperatures, we have the deconfined state of quarks and gluons which respects the approximate chiral symmetry that becomes exact with zero quark mass. These two phases at some intermediate temperature show a smooth crossover at smaller baryon chemical potential which is a good approximation of QCD transition in the early Universe and a first-order transition at a relatively higher value of chemical potential separated by a second-order critical point marked by a star. Now with temperature close to zero, if we increase the chemical potential we find that at a low value of μ there exists a phase boundary between nuclear matter and vacuum. Then with a further increase in μ, there exists a more compressed phase of nuclear matter, which brings us closer to the neutron star. Besides these phases of QCD matter, for higher value of the chemical potential at low temperature, one predicts a color-flavor-locked (CFL) phase of color-superconducting quark matter [47, 48] and some other unknown phase marked as non-CFL quark liquid.

The existence of this crossover region in the phase diagram indicates the presence of a small but finite quark mass, implying that the chiral symmetry has been explicitly broken. This complicates the distinction between the confined and deconfined QCD phases by any global symmetry. Lattice simulations suggest that the critical point shows $O(4)$ scaling [46, 49]. Using the $O(4)$ scaling function, the lattice computation of the chiral condensate as a function of quark mass has been able to explain the properties of chiral crossover [6, 7]. Also, there has been an effort to understand the scaling of dynamic correlators in the crossover region by performing the real-time simulation of the $O(4)$ critical region [50]. However as mentioned, the effect of neither explicit nor spontaneous chiral symmetry breaking has been incorporated in the hydrodynamic description of nuclear matter formed in heavy ion collisions.

In the chiral limit, hydrodynamic description obeys the underlying symmetry of QCD, $U(1)\times SU_L(2)\times SU_R(2)$, while below the transition temperature, the symmetry is spontaneously broken to $U(1)\times SU_V(2)$, resulting into the development of chiral condensate. In this limit below the transition temperature, the occurrence of Goldstone modes necessitates their inclusion in the hydrodynamic description which leads to an effective theory similar to the non-abelian

superfluid [15, 51]. Further, the presence of small but finite quark mass implies the generation of pseudo-Goldstone modes due to the explicit breaking of the symmetry. Recently, the effect of this pseudo-Goldstone mode has been incorporated into the hydrodynamics using stochastic formalism, where it has been shown that the hydrodynamic transport coefficients get a correction from the quark masses [52]. Therefore, this shows the need to include the dynamics of the broken symmetry together with the hydrodynamic variables characterizing the conserved currents governed by the Ward identities. Hence, the formulation of an effective description of the composite dissipative system of pseudo-Goldstone bosons interacting with ordinary hydrodynamic degrees of freedom is a direction of intense research. This can further lead to the understanding of the interplay between the symmetry-breaking dynamics and that of the hydrodynamic attractors.

The study of hydrodynamic description in the regime of continuous symmetry breaking describes the theory of superfluidity. Superfluidity, first discovered in helium−4 isotopes by Pyotr Kapitsa [53] and independently by John F. Allen and Don Misener [54] in 1937, is a characteristic of fluid with zero viscosity which means the fluid can flow without loss of kinetic energy. The theory of superfluidity was developed long ago by Landau [55] in the non-relativistic case which was later extended to the relativistic domain [56, 57]. In heavy ion collisions, owing to the limited size of the system, superfluid fluctuation plays an essential role in the dynamical evolution of the system, especially near the $O(4)$ critical point of QCD. In [8], using stochastic hydrodynamic formalism, it has been investigated how these fluctuations modify the transport coefficients of QCD. They have also provided a phenomenological understanding of the effect of the chiral fluctuations on the momentum spectrum of soft pions near pseudo-critical points. Stochastic hydrodynamics is a formalism for incorporating macro(meso)scopic classical statistical fluctuations at length scales larger than the mean free path, and studying how they alter the long-time evolution of the system [9]. At length scales below a dynamically determined decoherence length scale, which can be larger than the microscopic scales in a superfluid, the fluctuations are of quantum origin. Therefore for superfluids, a quantum generalization of stochastic hydrodynamics is necessary for incorporating the effect of this fluctuation at a length

scale shorter that the scattering time and the mean free path by using techniques such as the holographic approach.

The AdS/CFT correspondence, an example of the holographic principle, is a proposed relationship between the quantum gauge theories and the quantum theory of gravity in one higher dimension with appropriate boundary conditions. In the limit of strong coupling and large N, the quantum gravity theory reduces to the classical theory of gravity. The duality forms an important toolkit to study the strongly interacting dynamics of quarks and gluons by solving the dynamics of the classical Einstein equation of the gravity dual. In quantum gauge theories, real-time correlation functions are important for various observables such as S-matrix which leads to the computation of scattering amplitudes. At finite temperature and density of the gauge theory, the real-time correlation functions are essential to apprehend the response of the thermal ensemble to fluctuations that drives the system out of equilibrium. Further, these correlation functions also provides an understanding of decoherence and thermalization in the weak coupling limit.

The first prescription to study the real-time correlation function using the holographic method is due to Son and Starinets [51], where they have computed the retarded correlation function of thermal states. Schwinger Keldysh formalism [58] gives a systematic way to study real-time correlation functions in non-equilibrium and thermal systems via path ordering. The implementation of this formalism to holographic dual was first achieved by Son and Herzog [59], where they mapped the Schwinger Keldysh contour to a thermal black brane. In addition to this, different ways were developed using holographic techniques to compute the real-time correlation functions such as Skenderis and van Rees prescription [31, 60, 61] which is best defined for initial states that can be built using Euclidean path integrals. However, the computation of Schwinger-Keyldsh correlation functions for non-equilibrium processes which hydrodynamizes at a late time such as the dynamics of QGP, does not require any understanding of initial states. For such cases, the computation of hydrodynamic Schwinger-Keldysh correlation functions demands a simpler approach.

Further, in heavy ion collisions, the evolution of the QCD matter is not only governed by the strongly interacting degrees of freedom (non-perturbative) but also by weakly interacting degrees of freedom (perturbative). Both these degrees of freedom play a crucial role from the very initial stage of color glass condensate to the freeze-out stage until the particle reaches the detector. The presence of both these interactions can be attributed to one of the features of QCD called asymptotic freedom. Asymptotic freedom indicates asymptotically weaker interaction of the quarks and gluon with an increase in energy or decreases in the length scale. The dynamics of QCD in this limit have been well explained by the perturbative theory. While at low energy, the strong interaction of quarks and gluons resulting in composite hadrons requires non-perturbative descriptions such as Gauge/gravity duality and lattice simulation. Therefore, there seems a need for a single framework that can incorporate both these degrees of freedom consistently. Such a unified and consistent framework is provided by the semi-holographic approach.

The semi-holographic framework was initially developed in the context of holographic non-fermi liquid models by Polchinski and Faulkner [10]. Later this model has been generalised by Mukhopadhyay and Policastro to study the effective description for a large set of non-Fermi liquids [11]. In this formulation a strongly coupled conformal theory with a gravity dual is coupled to a dynamical boundary field, hence the term semi-holography. In the context of heavy ion collisions, this model couples classical Yang-Mill fields defining the weakly coupled gluon modes to strongly coupled soft modes, defined by strongly coupled holographic theory [12]. The model has been constructed in a way to have phenomenological implications. This is achieved by the democratic coupling mechanism [62] in which one can describe the physical system consistently at any given scale including both perturbative and non-perturbative effects without the knowledge of microscopic details of both the sectors. This democratic coupling has been utilized to study hybrid fluid model [20], where it was shown that the setup admits a consistent thermodynamic description provided the physical temperatures of the two subsectors are equal and consistent with the full system thermodynamic identities. In addition, the total entropy of the system is a sum of the entropies of the individual sectors with effective spatial

volume corrections which is consistent with statistical mechanics. The hybrid fluid model has been extended by adding viscosity using MIS formalism [63]. This viscous fluid model shows the emergence of hybrid hydrodynamic attractors and also captures the feature which is reminiscent of the Bottom-up scenario of thermalisation in the heavy-ion collision. Further, the coupling of MIS with holography in a democratic manner [64] suggests a possibility of the MIS sector to thermalise with the holographic sector. This motivates the study of thermalisation in semi-holographic framework where fluctuation plays a crucial role in driving the system towards global equilibrium. Particularly in the limit of large N, the quantum thermalisation of the system is dominated by macroscopic fluctuations.

The thesis has been organised as follows: Chapter 2 describes the relevant theoretical concepts required to follow later chapters in the thesis. This chapter reviews the theory of relativistic hydrodynamics followed by a discussion on the AdS/CFT correspondence and the Schwinger-Keldysh formalism. In chapter 3 we discuss the formulation of an effective description of a dissipative relativistic superfluid by including both order parameter and dissipation to the Son-Nicolis effective action framework [14, 15] using MIS formalism. Here we have restricted ourselves to $U(1)$ symmetry breaking. Then in chapter 4, we develop a holographic method for computing real-time hydrodynamic correlation functions of a strongly coupled relativistic system which hydrodynamizes at a late time using the horizon cap prescription of Crossley, Glorioso and Liu (CGL) [17]. The computation of this hydrodynamic real-time correlation function prepares the foundation to study quantum superfluid by incorporating macroscopic fluctuations. In addition, it can also provide a fundamental understanding of non-equilibrium processes with applications to the phenomenology of heavy-ion collisions. In chapter 5, we study the thermalisation in a hybrid system coupled in a democratic manner via the effective metric of the weakly self-interacting perturbative sector and a strongly self-interacting non-perturbative sector in the semi-holographic framework. Chapter 6 summarises the thesis and discusses the future research plan to extend the work done to have a better understanding of the dynamics of relativistic quantum systems in macroscopic length scale. In the end, the longer calculations are included in the Appendices.

Chapter 2

Theoretical background

2.1 Relativistic Hydrodynamics

Hydrodynamics is an effective description of many-body physics that explains the long wavelength limit of the underlying microscopic theory. It investigates small fluctuations in local thermal equilibrium where the macroscopic length scale is much larger than the microscopic scale. In recent years, hydrodynamic modelling of various non-equilibrium processes has gained much momentum owing to its success in characterising the out-of-equilibrium observables. One such example is the hydrodynamic description of the QGP phase formed in heavy ion collision [65–68].

The validity of hydrodynamic applicability can be examined based on the Knudsen number Kn, defined as a ratio of the microscopic to the macroscopic scale of the underlying theory. Typically for $Kn \ll 1$, the system approaches the local thermal equilibrium and can hold an effective description of hydrodynamics while a large value of the Kn renders the application of hydrodynamics questionable. However, there are evidences where a system away from local equilibrium holds a fluid dynamical description. For instance, in [22], it has been observed that the Knudsen number defined as the ratio of relaxation time to the expansion rate (or gradient of energy density) attains a large value of 0.5 for $\eta/S = 0.08$. This value marks the edge of validity

of the hydrodynamic description of the QGP formed in ultra-relativistic heavy ion collision, as seen in Fig. 2.1. In such cases, the success of hydrodynamic applicability has been attributed to the discovery of the hydrodynamic attractor [25, 69, 70].

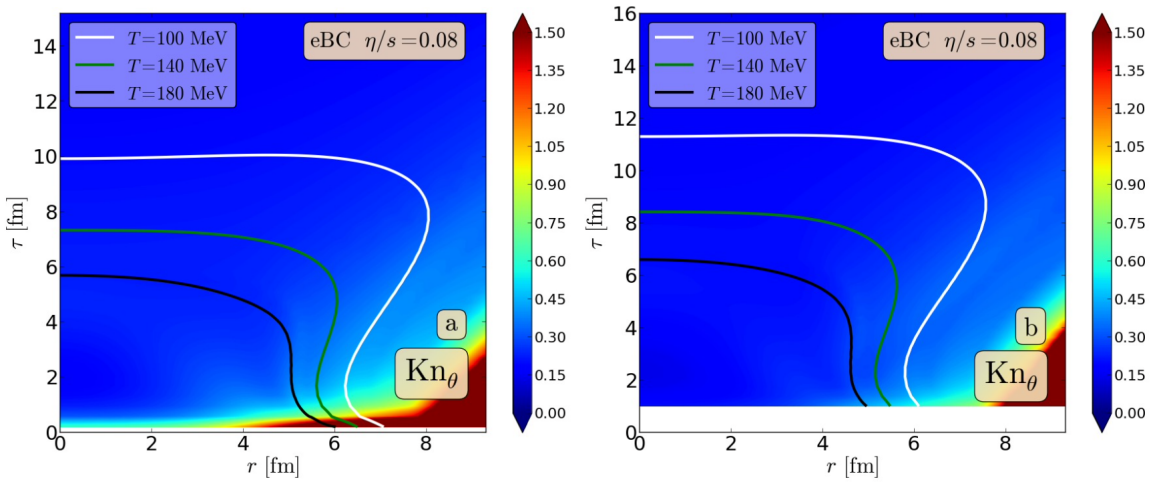

Figure 2.1: Spacetime evolution of Knudsen number Kn_θ in a Pb+Pb collision of the 20 − 30 centrality class at the LHC, for eBC (energy density is proportional to the density of binary collision) initial state. In the left panel, the initial time $\tau_0 = 0.2$ fm, while in the right panel, $\tau_0 = 1.0$ fm, the shear viscosity to entropy density ratio is $\eta/s = 0.08$. Figure taken from [22].

A system in a hydrodynamic regime is characterized by the conservation equation of the energy-momentum tensor $T^{\mu\nu}$ and other global currents J^μ_a,

$$\nabla_\mu T^{\mu\nu} = 0, \tag{2.1}$$

$$\nabla_\mu J^\mu_a = 0. \tag{2.2}$$

The stress tensor $T^{\mu\nu}$ and conserved currents follow a constitutive relation and can be expressed as gradient expansion of local hydrodynamic degrees of freedom (eg. velocity, temperature etc), respecting the symmetry of the system.

In this section, we study the conformal symmetry of hydrodynamics along with its action formalism and gradient expansion. We also discuss Bjorken flow, the one-dimensional boost-invariant flow of fluid and hydrodynamic attractors.

2.1.1 Conformal symmetry of hydrodynamics

A theory is said to follow conformal symmetry if the action $\mathcal{S}[\phi, g_{\mu\nu}]$ is invariant under Weyl transformation,

$$g_{\mu\nu} \to e^{-2\phi(x)} g_{\mu\nu} \tag{2.3}$$

where $\phi(x)$ is an arbitrary function of space-time coordinate. Subsequently, the stress tensor, defined as $T^{\mu\nu} \equiv -\frac{1}{2\sqrt{-g}}\frac{\delta \mathcal{S}}{\delta g_{\mu\nu}}$, is traceless at the classical level while at the quantum level, the stress tensor has a non-vanishing trace,

$$g_{\mu\nu} T^{\mu\nu}_{cl} = -\frac{1}{2}\frac{\delta \mathcal{S}}{\delta \phi(x)} = 0, \tag{2.4}$$

$$g_{\mu\nu}\langle T^{\mu\nu}\rangle = W_d[g_{\mu\nu}] \tag{2.5}$$

where W_d is the Weyl anomaly [71, 72] in d dimensions which is identically zero for odd d. For any even $d = 2k$, W_{2k} contains $2k$ derivatives of the metric. For instance, for $d = 4$, the Weyl anomaly W_4 has four derivatives,

$$W_4[g_{\mu\nu}] = -\frac{a}{16\pi^2}(R_{\mu\nu\lambda\rho}R^{\mu\nu\lambda\rho} - 4R_{\mu\nu}R^{\mu\nu} + R^2) + \frac{c}{16\pi^2}(R_{\mu\nu\lambda\rho}R^{\mu\nu\lambda\rho} - 2R_{\mu\nu}R^{\mu\nu} + \frac{1}{3}R^2), \tag{2.6}$$

$R^{\mu\nu\lambda\rho}$ and $R_{\mu\nu}$ are the Riemann tensor and Ricci tensor, a and c are constants (in $\mathcal{N} = 4$ Super Yang-Mills (SYM) theory $a = c = \frac{1}{4}(N_c^2 - 1)$ [73]).

In a hydrodynamic theory, the existence of Weyl anomaly depends on the order of hydrodynamic gradient expansion. For second-order hydrodynamics, the anomaly in $d = 4$ dimension vanishes because of the fourth-order derivatives in $W_4[g_{\mu\nu}]$. This implies, for a larger even $d-$ dimension, one needs to keep even higher orders in hydrodynamics for a non-vanishing Weyl anomaly. Thus, one can ignore the anomaly and assume that lower-order hydrodynamic theory is invariant under Weyl transformation. In this case, following the Weyl transformation

(2.3), the traceless energy-momentum tensor transforms homogeneously as,

$$T^{\mu\nu} \to e^{(d+2)\phi(x)} T^{\mu\nu}. \tag{2.7}$$

Likewise, one can also show that the global current under the Weyl rescaling of the metric follows a homogeneous transformation,

$$J^{\mu} \to e^{d\phi(x)} J^{\mu}, \tag{2.8}$$

d is the space-time dimension of the theory. In general, any tensor $\mathcal{Q}^{\mu_1\cdots\mu_m}_{\nu_1\cdots\nu_n}$ is said to be conformally invariant if it transforms homogeneously under Weyl transformation (2.3), $\mathcal{Q}^{\mu_1\cdots\mu_m}_{\nu_1\cdots\nu_n} \to e^{w\phi(x)}\mathcal{Q}^{\mu_1\cdots\mu_m}_{\nu_1\cdots\nu_n}$. Here, w is a real number and is known as conformal weight which is $(d+2)$ for energy-momentum tensor and d for global currents.

2.1.2 Hydrodynamics from action formalism

Hydrodynamic descriptions can be thought of as a large wavelength (infrared) effective description of quantum field theory. There are various approaches [74–76] to understand the constitutive relation of hydrodynamics from effective action formalism. In [75], the author has formulated the effective action of an uncharged fluid from Lagrangian fluid element[1] variables in a systematic derivative expansion and derived the non-dissipative energy-momentum tensor up to second-order. In the case of a charged fluid, one can refer [78] to study the derivation of the perfect fluid energy-momentum tensor from the effective action formalism.

We start with an effective action $S[g_{\mu\nu}]$,

$$S[g_{\mu\nu}] = \int d^d x \sqrt{-g} p(T) \tag{2.9}$$

[1]Lagrangian description of fluid flow means, individual fluid cells are labelled and their position and velocity are defined as a function of time [77].

where $p(T)$ is the pressure of the perfect fluid and T is the temperature and g is the determinant of the d dimensional spacetime metric $g_{\mu\nu}$. The temperature T has been defined through a new variable β^μ as,

$$T \equiv (-\beta^\mu g_{\mu\nu}\beta^\nu)^{-1/2} \tag{2.10}$$

where $\beta^\mu = u^\mu/T$ and u^μ is the fluid velocity normalised to $u^\mu u_\mu = -1$. By varying the action with respect to the metric $g_{\mu\nu}$ and using the thermodynamic identities $s = \frac{\partial p}{\partial T}$ and $\epsilon + p = sT$, we recover the energy-momentum tensor of the perfect fluid.

$$\begin{aligned}
\delta S &= \int d^d x\Big(\delta\sqrt{-g}p(T) + \sqrt{-g}\frac{\partial p}{\partial T}\delta T\Big) \\
&= \int d^d x\sqrt{-g}\Big(g^{\mu\nu}p(T) + sT^3\beta^\mu\beta^\nu\Big)\delta g_{\mu\nu} \\
&= \int d^d x\sqrt{-g}\Big(g^{\mu\nu}p(T) + sTu^\mu u^\nu\Big)\delta g_{\mu\nu}
\end{aligned} \tag{2.11}$$

where we recognize the energy-momentum tensor to be,

$$T^{\mu\nu} = (\epsilon + p)u^\mu u^\nu + g^{\mu\nu}p. \tag{2.12}$$

Here ϵ is the energy density and s is the entropy density of the fluid. Further, under diffeomorphisms of x^μ,

$$x^\mu \to x^\mu + \xi^\mu, \tag{2.13}$$

we get

$$\delta g_{\mu\nu} = \nabla_\mu\xi_\nu + \nabla_\nu\xi_\mu \tag{2.14}$$

which directly leads to the conservation of the energy-momentum tensor after partial integra-

tion,

$$\nabla_\mu T^{\mu\nu} = 0. \tag{2.15}$$

Hence, from the effective action (2.9), we have recovered the energy-momentum tensor for the perfect fluid and further, the diffeomorphism invariance gives the conservation of energy-momentum tensor. This action formalism will be used in chapter 3 for the MIS formalism of superfluid.

2.1.3 Hydrodynamics as gradient expansion

Hydrodynamic constitutive relations can be expressed in terms of the gradient of hydrodynamic variables like fluid velocity, temperature and chemical potential. In this section, we analyse hydrodynamics as gradient expansion up to the second order.

Perfect fluid

At local equilibrium or zeroth order of gradient expansion, a system living on a d dimensional metric $g_{\mu\nu}$ is defined by an isotropic stress tensor and conserved current of the form,

$$T^{\mu\nu}_{(0)} = \epsilon\, u^\mu u^\nu + p(\epsilon)\Delta^{\mu\nu}, \tag{2.16}$$

$$J^\mu_{a(0)} = q_a u^\mu \tag{2.17}$$

where ϵ is the energy density, and q_a is the net charge density of the fluid. u^μ is the normalised relativistic velocity ($u^\mu u_\mu = -1$) which in the local rest frame takes the form $u^\mu = (1, \underbrace{0, 0, ..., 0}_{(d-1)})$. The fluid pressure $p(\epsilon)$ is given by the thermodynamic equation of state. In the case of a conformal system, the tracelessness of the energy-momentum tensor gives the equation of state to be $p(\epsilon) = \epsilon/(d-1)$ where ϵ can be defined in terms of temperature T as, $\epsilon = const\ T^d$. $\Delta^{\mu\nu}$

is the spatial projection operator given by

$$\Delta^{\mu\nu} = u^\mu u^\nu + g^{\mu\nu} \tag{2.18}$$

which satisfies the condition,

$$\Delta^{\mu\nu} u_\nu = 0, \qquad \Delta^{\mu\rho}\Delta_{\rho\nu} = \Delta^\mu_\nu. \tag{2.19}$$

In absence of any sources, the conservation equation (2.1) gives the relativistic Euler equation,

$$\nabla_\mu T^{\mu\nu}_{(0)} = 0, \tag{2.20}$$

and the conservation equation for current is

$$\nabla_\mu J^\mu_{a(0)} = 0. \tag{2.21}$$

The projection of (2.20) in the direction parallel and perpendicular to fluid velocity gives the fundamental equation for energy and momentum,

$$u_\nu \nabla_\mu T^{\mu\nu}_{(0)} \equiv D\epsilon + (\epsilon + p)\nabla_\mu u^\mu = 0, \tag{2.22}$$

$$\Delta^\alpha_\nu \nabla_\mu T^{\mu\nu}_{(0)} \equiv (\epsilon + p) D u^\alpha + \nabla^\alpha p = 0 \tag{2.23}$$

where $D \equiv u^\mu \nabla_\mu$ and $\nabla^\alpha \equiv \Delta^{\mu\alpha}\nabla_\mu$. In addition, using the thermodynamic identities one can find that the entropy current defined as $s^\mu = s\, u^\mu$ is conserved i.e., $\nabla_\mu s^\mu = 0$. This shows that there is no entropy production for a perfect fluid.

Dissipative fluid

Dissipative fluids can be studied by adding perturbations to the equilibrium state. The perturbative corrections can be expressed as a gradient of hydrodynamic variables. At the first order

of gradient expansion which gives the well-known *Navier-Stokes equation*, $\nabla_\mu T^{\mu\nu} = 0$, the energy-momentum tensor and the conserved current read as,

$$T^{\mu\nu} = T^{\mu\nu}_{(0)} + \Pi^{\mu\nu}_{(1)}, \tag{2.24}$$

$$J^\mu_a = J^\mu_{a(0)} + \mathcal{J}^\mu_a \tag{2.25}$$

where $\mathcal{J}^\mu_a$ and $\Pi^{\mu\nu}_{(1)}$ are first order in gradient of hydrodynamic variables. The correction terms chosen are arbitrary and can be fixed by the choice of reference frame. In the case of the Landau frame, the energy density ϵ and the fluid velocity u^μ are treated as timelike eigenvalue and eigenvector of the stress tensor in the local rest frame,

$$T^\mu_\nu u^\nu = -\epsilon u^\mu. \tag{2.26}$$

This implies that there is no flow of energy density in the local rest frame and the correction $\Pi^{\mu\nu}_{(1)}$ follows the transverse condition, $\Pi^{\mu\nu}_{(1)} u_\nu = 0$. The other commonly chosen frame is the Eckart frame where there is no flow of charge density in the local rest frame. In the thesis, we will follow the convention of the Landau frame.

To obtain the expression for $\Pi^{\mu\nu}_{(1)}$ and $\mathcal{J}^\mu_a$ in terms of hydrodynamic variables, we use the conservation equation of energy-momentum tensor projected along the fluid velocity,

$$u_\nu \nabla_\mu T^{\mu\nu} \equiv D\epsilon + (\epsilon + p)\nabla_\mu u^\mu + u_\nu \nabla_\mu \Pi^{\mu\nu}_{(1)} = 0, \tag{2.27}$$

and the thermodynamic identities along with the second law of thermodynamics,

$$\epsilon + p = sT + \mu_a q_a, \qquad dp = sdT + q_a d\mu_a, \qquad \text{and} \qquad \nabla_\mu s^\mu \geq 0, \tag{2.28}$$

T is the local temperature and μ_a is the chemical potential. These identities together with (2.27)

gives

$$\nabla_\mu s^\mu \equiv -\frac{\Pi^{\mu\nu}_{(1)}}{T}\nabla_\mu u_\nu - \mathcal{J}^\mu_a \nabla_\mu \frac{\mu_a}{T} \geq 0 \tag{2.29}$$

where the positivity condition demands that

$$\Pi^{\mu\nu}_{(1)} = -\eta\sigma^{\mu\nu} - \zeta\Delta^{\mu\nu}\nabla_\lambda u^\lambda \quad \text{and} \quad \mathcal{J}^\mu_a = -\kappa_{ab}\,\partial^\mu\Big(\frac{\mu^b}{T}\Big). \tag{2.30}$$

Here $\sigma^{\mu\nu}$ is the first-order derivative in fluid velocity,

$$\sigma^{\mu\nu} = (\nabla_\alpha u_\beta + \nabla_\beta u_\alpha)\Delta^{\alpha\beta}\Delta^{\mu\nu} - \frac{2}{d-1}\nabla_\lambda u^\lambda \Delta^{\mu\nu}, \tag{2.31}$$

and $\eta(\epsilon)$ and $\zeta(\epsilon)$ are the first-order transport coefficients, known as shear viscosity and bulk viscosity. These are associated with shear stress $\pi^{\mu\nu} = -\eta\sigma^{\mu\nu}$ and bulk stress $\Pi = -\zeta\nabla_\lambda u^\lambda$. κ_{ab} is the transport coefficient connected to the charge diffusion constant. These transport coefficients are given as input based on the microscopic details of the theory. Further, for a conformal system, the bulk viscosity $\zeta = 0$ which implies that $\Pi^{\mu\nu}_{(1)}$ is traceless (Note: By definition the shear stress is traceless i.e. $\pi^\mu_\mu = 0$).

Acausality

The relativistic Navier-Stokes equation leads to acausality for being parabolic in nature [23,79]. This acausality can be understood easily by considering the diffusion equation obtained by adding linear perturbations to the initial equilibrium state of the system. The dispersion relation of the corresponding diffusion equation turns out to be,

$$\omega = i\frac{\eta_0}{\epsilon_0 + p_0}k^2 \tag{2.32}$$

which can be used to determine the velocity of propagation with wavenumber k,

$$v_T(k) = \frac{d\omega}{dk} = 2i\frac{\eta_0}{\epsilon_0 + p_0}k, \tag{2.33}$$

η_0, ϵ_0, and p_0 are some initial equilibrium conditions associated with shear viscosity, the energy density, and the pressure of the system. Equation (2.33) shows that for larger values of k, the velocity of propagation $v_T(k)$ can exceed the speed of light. Thus violating causality at short wavelength. Hydrodynamics being a long wavelength theory, $k \to 0$ limit does not seem to cause any threat to causality. However, hydrodynamics is an initial value problem which requires well-posed initial conditions. It has been observed in various examples [79, 80] that this acausality leads to instabilities in solving the Navier Stokes equation numerically for any generic initial conditions.

The problem of acausality leads to a series of approaches to modify the hydrodynamic equations to a causal one. In this section we discuss two simple solutions to it, the MIS theory [25] and the BRSSS theory [1].

Conformal MIS theory

In MIS theory [2, 42], the problem of causality has been resolved by promoting the shear stress tensor, $\pi^{\mu\nu}$, to an independent dynamical variable that follows the relaxation type equation of the form,

$$(\tau_\pi D + 1)\pi^{\mu\nu} = -\eta\sigma^{\mu\nu}, \qquad D = u^\mu\nabla_\mu \tag{2.34}$$

where τ_π is a phenomenological parameter known as relaxation time. The equation (2.34) along with the energy-momentum conservation equation forms the set of dynamical equations in MIS formalism. The relaxation type equation (2.34) introduces damped non-hydrodynamic modes in the theory which modifies the dispersion relation. The modified dispersion relation leads to

a finite velocity of propagation provided the relaxation time satisfies the condition,

$$\tau_\pi \geq \frac{2}{T}\frac{\eta}{s} \tag{2.35}$$

where s is the entropy density. Therefore the theory is causal as long as the relaxation time obeys the above condition (2.35).

BRSSS theory

BRSSS theory [1] allows systematic addition of all possible terms of second-order gradient expansion to the first-order hydrodynamics. The stress tensor reads as,

$$T^{\mu\nu} = T^{\mu\nu}_{(0)} + \underbrace{\Pi^{\mu\nu}_{(1)} + \Pi^{\mu\nu}_{(2)}}_{\Pi^{\mu\nu}}. \tag{2.36}$$

Following the Landau frame of reference and conformal invariance of the system, the second-order correction $\Pi^{\mu\nu}_{(2)}$ should also be transverse and traceless as earlier. With these constraints, this order has eight contributions to the stress tensor which further reduces to five combinations that transform homogeneously under Weyl transformations.

$$\mathcal{O}_1^{\mu\nu} = R^{\langle\mu\nu\rangle} - (d-2)\Big(\nabla^{\langle\mu}\nabla^{\nu\rangle}\ln T - \nabla^{\langle\mu}\ln T\nabla^{\nu\rangle}\ln T\Big), \tag{2.37}$$

$$\mathcal{O}_2^{\mu\nu} = R^{\langle\mu\nu\rangle} - (d-2)u_\alpha R^{\alpha\langle\mu\nu\rangle\beta}u_\beta, \tag{2.38}$$

$$\mathcal{O}_3^{\mu\nu} = \sigma^{\langle\mu}{}_\lambda\sigma^{\nu\rangle\lambda}, \quad \mathcal{O}_4^{\mu\nu} = \sigma^{\langle\mu}{}_\lambda\Omega^{\nu\rangle\lambda}, \quad \mathcal{O}_5^{\mu\nu} = \Omega^{\langle\mu}{}_\lambda\Omega^{\nu\rangle\lambda} \tag{2.39}$$

where $\Omega^{\mu\nu}$ is the vorticity defined as, $\Omega^{\mu\nu} = \frac{1}{2}\Delta^{\mu\alpha}\Delta^{\nu\beta}(\nabla_\alpha u_\beta - \nabla_\beta u_\alpha)$. Further for convenience and easy comparison with MIS theory, one redefines the combination of $\mathcal{O}_1^{\mu\nu}$ to ${}^{\langle}D\sigma^{\mu\nu\rangle}$[2] $+ \frac{1}{d-1}(\nabla.u)$

[2] $^{\langle}A^{\mu\nu\rangle} \equiv \frac{1}{2}\Delta^{\mu\alpha}\Delta^{\nu\beta}(A_{\alpha\beta} + A_{\beta\alpha}) - \frac{1}{d-1}\Delta^{\mu\nu}\Delta^{\alpha\beta}A_{\alpha\beta}$.

[1, 81], such that the final expression up to second-order in gradient expansion becomes,

$$\begin{aligned}\Pi^{\mu\nu} &= -\eta\sigma^{\mu\nu} + \eta\tau_{\Pi}\Big[{}^{\langle}D\sigma^{\mu\nu\rangle} + \frac{1}{d-1}\sigma^{\mu\nu}(\nabla.u)\Big] + \kappa\,[R^{\langle\mu\nu\rangle} - (d-2)u_{\alpha}R^{\alpha\langle\mu\nu\rangle\beta}u_{\beta}] \\ &+ \lambda_1\sigma^{\langle\mu}{}_{\lambda}\sigma^{\nu\rangle\lambda} + \lambda_2\sigma^{\langle\mu}{}_{\lambda}\Omega^{\nu\rangle\lambda} + \lambda_3\Omega^{\langle\mu}{}_{\lambda}\Omega^{\nu\rangle\lambda} \end{aligned} \tag{2.40}$$

where τ_{Π}, κ, $\lambda_{1,2,3}$ are the transport coefficients which are determined by the underlying microscopic theory. The first constant τ_{Π} has a time dimension and can be thought of as a relaxation time. κ is zero when we are in a flat space. The constants $\lambda_{1,2,3}$ are non-linear in velocity and can be ignored if we wish for small perturbations. Also if we consider irrotational flow, terms associated with $\lambda_{2,3}$ can be neglected. However, in a non-linear viscous fluid, the flow is characterized by all the six transport coefficients which can be explicitly determined for a fluid with holographic dual [18, 82, 83] and also for fluid whose underlying microscopic theory is kinetic theory [84]. In particular, for $\mathcal{N} = 4$ Super Yang-Mills (SYM) in $d = 4$ dimension the values of the six transport coefficients [83] are given by,

$$\begin{aligned}\frac{\eta}{s} &= \frac{1}{4\pi}, \qquad \tau_{\Pi} \equiv \tau_{\pi} = \frac{2-\ln 2}{2\pi}, \qquad \kappa = \frac{\eta}{\pi T} \\ \lambda_1 &= \frac{\eta}{2\pi T}, \qquad \lambda_2 = \frac{\eta \ln 2}{\pi T}, \qquad \lambda_3 = 0 \end{aligned} \tag{2.41}$$

which can be written in generic closed form for a $d-$ dimensional fluid dual to AdS_{d+1} [82, 85],

$$\begin{aligned}\eta &= \frac{1}{16\pi G_N^{(d+1)}}\Big(\frac{4\pi}{d}T\Big)^{d-1} = \frac{s}{4\pi}, \qquad \tau_{\Pi} = \frac{d}{4\pi T}\Big[1 + \frac{1}{d}\mathrm{Harmonic}\Big(\frac{2}{d} - 1\Big)\Big], \\ \kappa &= \frac{d}{2\pi(d-2)}\frac{\eta}{T}, \qquad \lambda_1 = \frac{d}{8\pi}\frac{\eta}{T}, \\ \lambda_2 &= \frac{1}{2\pi}\mathrm{Harmonic}\Big(\frac{2}{d} - 1\Big)\frac{\eta}{T}, \qquad \lambda_3 = 0. \end{aligned} \tag{2.42}$$

Further, with the identification $\Pi^{\mu\nu} = \pi^{\mu\nu} = \eta\sigma^{\mu\nu}$ and $D\eta = \eta\nabla.u$, the BRSSS expansion up to second order (2.40) can be written as,

$$\begin{aligned}\Pi^{\mu\nu} &= -\eta\sigma^{\mu\nu} - \tau_\Pi\Big[{}^{\langle}D\Pi^{\mu\nu\rangle} + \frac{d}{d-1}\Pi^{\mu\nu}(\nabla.u)\Big] + \kappa\left[R^{\langle\mu\nu\rangle} - (d-2)u_\alpha R^{\alpha\langle\mu\nu\rangle\beta}u_\beta\right] \\ &+ \frac{\lambda_1}{\eta^2}\Pi^{\langle\mu}{}_\lambda\Pi^{\nu\rangle\lambda} + \frac{\lambda_2}{\eta}\Pi^{\langle\mu}{}_\lambda\Omega^{\nu\rangle\lambda} + \lambda_3\Omega^{\langle\mu}{}_\lambda\Omega^{\nu\rangle\lambda} \qquad (2.43)\end{aligned}$$

which on truncating at first order reduces to the MIS equation (2.34),

$$(\tau_\Pi D + 1)\Pi^{\mu\nu} = -\eta\sigma^{\mu\nu}. \qquad (2.44)$$

Entropy and Entropy current

As discussed above, the demand of causality modifies the relativistic hydrodynamic equations by including a dynamical dissipative term and by extending the first-order hydrodynamic to second-order gradient expansion. In these cases, one can question whether the modified theory has a positive entropy current.

To study the positive divergence of entropy current we use (2.27) and the thermodynamic identity to define the entropy current as,

$$T\nabla_\mu(su^\mu) = -\Pi^{\mu\nu}\nabla_\mu u_\nu \qquad (2.45)$$

where s corresponds to equilibrium entropy density and $\Pi^{\mu\nu}$ holds a second-order derivative structure for BRSSS theory and is equivalent to $\pi^{\mu\nu}$ for MIS theory. Here one can write $\nabla_\mu u_\nu$ in terms of $\sigma^{\mu\nu}/2$ using its definition in (2.27). This gives the entropy current as,

$$T\nabla_\mu(su^\mu) = -\Pi^{\mu\nu}\sigma_{\mu\nu}/2. \qquad (2.46)$$

Then by using the BRSSS expansion (2.40), the dissipative entropy current (2.46) takes the

form,

$$\nabla_\mu(su^\mu) = \frac{1}{2\eta T}\Pi^{\mu\nu}\Pi_{\mu\nu} + \frac{\tau_\pi}{\eta T}\frac{\Pi_{\mu\nu}}{2}\Big[\langle D\Pi^{\mu\nu\rangle} + \frac{d}{d-1}\Pi^{\mu\nu}\nabla.u\Big] + \cdots . \tag{2.47}$$

Further, with the identification $\eta/\tau_\Pi = const.T^{-d}$, the equation (2.47) can be rearranged to give,

$$\begin{aligned}\nabla_\mu(s_{neq}u^\mu) &= \frac{1}{2\eta T}\Pi^{\mu\nu}\Pi_{\mu\nu} - \Big[\frac{\tau_\pi}{\eta T}\frac{d}{d-1}\Pi_{\mu\nu}\Pi^{\mu\nu}\nabla_\alpha u^\alpha\Big] \\ &+ \Big[\frac{\tau_\pi}{2\eta T}\frac{d}{d-1}\Pi_{\mu\nu}\Pi^{\mu\nu}\nabla.u\Big] + \cdots\end{aligned} \tag{2.48}$$

where we have used the lowest order equation (2.22) in terms of temperature T as $D\ln T = -\frac{1}{d-1}\nabla.u$. The non-equilibrium entropy s_{neq} is defined as

$$s_{neq} = s - \Big(\frac{\tau_\Pi}{4\eta T}\Pi_{\mu\nu}\Pi^{\mu\nu}\Big). \tag{2.49}$$

We find that the entropy current (2.48) for BRSSS theory is non-decreasing with the assumption that the contribution from terms like $\kappa\Pi_{\mu\nu}\mathcal{O}_2^{\mu\nu}/\eta T$ which are not total derivative are small. However, in the case of MIS, the third term is absent from the equation (2.44) which means that the MIS theory does not have a well-defined non-decreasing entropy current. Therefore, to get a positive definite entropy current in MIS one can modify the equation by adding the extra term $\frac{d}{d-1}\Pi^{\mu\nu}\nabla.u$, such that the equation becomes,

$$\tau_\Pi\Big[\frac{\Pi^{\mu\nu}}{\tau_\Pi} + D\Pi^{\mu\nu}\Big] + \tau_\Pi\frac{d}{d-1}\Pi^{\mu\nu}\nabla_\alpha u^\alpha = -\eta\sigma^{\mu\nu}. \tag{2.50}$$

This gives the well-defined positive definite entropy current (2.48) for MIS theory where the non-equilibrium entropy is defined as (2.49). Further, following [86], we can also reproduce positive divergence of entropy current (2.49) in MIS theory as well as in BRSSS expansion by using Weylcovariant derivative $\mathcal{D}_\alpha$. With the Weyl covariant derivative, the MIS equation

becomes,

$$\Pi^{\mu\nu} + \tau_\Pi u^\alpha \mathcal{D}_\alpha \Pi^{\mu\nu} = -\eta\sigma^{\mu\nu} - \frac{\lambda_2}{\eta}(\Omega^\mu_\alpha \Pi^{\alpha\nu} + \Omega^\nu_\alpha \Pi^{\alpha\mu}) \tag{2.51}$$

where the action of $\mathcal{D}_\alpha$ on a tensor and its definition is mentioned in appendix A.

2.1.4 Bjorken flow and Weyl rescaling

Bjorken flow [13] is a simple model describing the expanding plasma produced by heavy ion collisions. This model is based on the assumptions of boost invariance and translational and rotational symmetries in the transverse directions of the expanding system. The evolution occurs inside a forward light cone as shown in Fig. 2.2. It is convenient to describe the Bjorken flow in

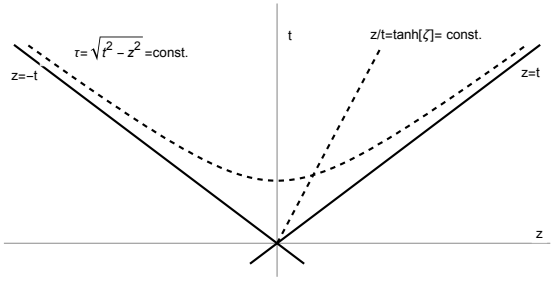

Figure 2.2: The schematic diagram of the Bjorken flow illustrates the evolution of an expanding system on the forward light cone. Here z is the longitudinal direction along which the system expands. The transverse directions have been suppressed. Initial data is specified on a constant τ hyperboloid.

the Milne proper time τ and the rapidity ζ which are related to the Minkowski (lab frame) time t and the longitudinal coordinate z (along which the system is expanding) as

$$t = \tau \cosh\zeta \qquad \text{and} \qquad z = \tau \sinh\zeta.$$

The transverse coordinates $x_\perp$ are the same in both Milne and Minkowski coordinate systems. In the Milne coordinates, the Minkowski metric takes the form

$$\mathrm{d}s^2 = -\mathrm{d}\tau^2 + \tau^2 \mathrm{d}\zeta^2 + \mathrm{d}s^2_\perp \tag{2.52}$$

where $ds_\perp$ is the line element in the transverse plane.

The symmetries of the Bjorken flow imply that the expectation value of any operator depends only on the proper time τ. Thus an ansatz for the expectation value of the energy-momentum tensor in a d-dimensional theory, which is also consistent with the transverse translational and rotational symmetries of the Bjorken flow, can take the form

$$\langle T_{\mu\nu}\rangle = \text{diag}(\epsilon(\tau),\, \tau^2 p_L(\tau),\, \underbrace{p_T(\tau),\, \cdots,\, p_T(\tau)}_{(d-2)\text{ times}}), \tag{2.53}$$

in the Milne coordinates for $d > 2$. Clearly, ϵ, p_L and p_T denote the energy density, and longitudinal and transverse pressures respectively.
The local conservation of energy and momentum $\nabla_\mu T^{\mu\nu} = 0$, implies that

$$p_L(\tau) = -\epsilon(\tau) - \tau\partial_\tau\epsilon(\tau), \tag{2.54}$$

and the conformal Ward identity $T^\mu_{\ \mu} = 0$ imposes

$$p_T(\tau) = \frac{2}{d-2}\left(\epsilon(\tau) + \frac{1}{2}\tau\partial_\tau\epsilon(\tau)\right). \tag{2.55}$$

Consequently, the evolution of the energy-momentum tensor is determined by $\epsilon(\tau)$ in a conformal field theory.

At large proper time τ, the Bjorken flow admits a hydrodynamic description [87]. To explicitly map the energy-momentum tensor (2.53) to that of a fluid, we need to set the flow velocity as

$$u^\mu = (1, \vec{0}),$$

i.e. $d\tau$ is co-moving with the flow in the Milne coordinates. In a conformal system, the large proper time expansion of $\epsilon(\tau)$ is given by a single parameter, namely

$$\mu := \epsilon_0 \tau_0^{\frac{d}{d-1}} \tag{2.56}$$

which is determined by the initial conditions — ϵ_0 is a constant energy density, and τ_0 can be chosen to be the value of τ where we intialize. The large proper time expansion of $\epsilon(\tau)$ takes the form

$$T^{\tau}_{\ \tau} = -\epsilon(\tau) = -\mu\tau^{-\frac{d}{d-1}}\left(1 + \sum_{n=1}^{\infty}\lambda_n\,\mu^{-\frac{n}{d}}\tau^{-n\frac{d-2}{d-1}}\right) \tag{2.57}$$

where λ_n are (state-independent) constants that are determined by the transport coefficients of the microscopic theory. As for instance, λ_1 is related to the shear viscosity η as

$$\lambda_1 = -\frac{\eta(\epsilon)}{\epsilon^{\frac{d-1}{d}}} \tag{2.58}$$

which should indeed be a constant in a conformal theory. The leading term of the expansion $\propto \tau^{-d/(d-1)}$ gives an exact solution of the Euler equations, and thus represents the expansion of a conformal perfect fluid.

Weyl rescaled Bjorken flow

In what follows in chapter 5, Weyl transformation of the Bjorken flow plays a crucial role in computing the real-time correlation function of Bjorken flow in hydrodynamic limit. In a conformal theory, the hydrodynamic equations are Weyl covariant [83]. We are ignoring the Weyl anomaly for the moment, but we will explicitly mention it later. Under a Weyl transformation which transforms the metric and the energy-momentum tensor as

$$\mathrm{d}s^2 \to \widetilde{\mathrm{d}s}^2 = \Omega(x)^2\mathrm{d}s^2, \quad T_{\mu\nu} \to \widetilde{T}_{\mu\nu} = \Omega(x)^{-d+2}T_{\mu\nu}, \tag{2.59}$$

the new solutions of the hydrodynamic equations are given by

$$u^\mu \to \tilde{u}^\mu = \Omega(x)^{-1}u^\mu, \quad \epsilon \to \tilde{\epsilon} = \Omega(x)^{-d}\epsilon, \tag{2.60}$$

in any conformal theory. Consider the combined operation of the time reparametrization

$$\sigma = \tau^{\frac{d-2}{d-1}} \tau_0^{\frac{1}{d-1}}, \tag{2.61}$$

and the Weyl scaling with

$$\Omega(\sigma) = \left(\frac{\tau_0}{\sigma}\right)^{\frac{1}{d-2}}, \tag{2.62}$$

under which the Milne metric (2.52) transforms to (with $\hat{\zeta} = \zeta\tau_0$)

$$\widetilde{\mathrm{d}s}^2 = -\frac{(d-1)^2}{(d-2)^2}\mathrm{d}\sigma^2 + \frac{\sigma^2}{\tau_0^2}\mathrm{d}\hat{\zeta}^2 + \left(\frac{\sigma}{\tau_0}\right)^{-\frac{2}{d-2}} \mathrm{d}s_\perp^2, \tag{2.63}$$

and the energy-momentum tensor given by (2.53), (2.54) and (2.55) transforms to

$$\begin{aligned}
\widetilde{T}_{\sigma\sigma} &= \Omega^{-d+2}\tau'(\sigma)^2\epsilon(\tau(\sigma)) \\
&= \frac{(d-1)^2}{(d-2)^2}\left(\frac{\sigma}{\tau_0}\right)^{\frac{d}{d-2}} \epsilon(\tau(\sigma)) \\
&= \frac{(d-1)^2}{(d-2)^2}\widetilde{\epsilon}(\sigma), \quad \left(\text{Note } \widetilde{\epsilon}(\sigma) := \left(\frac{\sigma}{\tau_0}\right)^{\frac{d}{d-2}} \epsilon(\tau(\sigma))\right) \\
\widetilde{T}_{\hat{\zeta}\hat{\zeta}} &= \Omega^{-d+2}\left(\frac{\tau(\sigma)}{\tau_0}\right)^2 p_L(\tau(\sigma)) \\
&= -\left(\frac{\sigma}{\tau_0}\right)^{\frac{3d-4}{d-2}} \Big(\epsilon(\tau(\sigma)) + \tau(\sigma)\epsilon'(\tau(\sigma))\Big) \\
&= \left(\frac{\sigma}{\tau_0}\right)^2 \frac{1}{d-1}\Big(\widetilde{\epsilon}(\sigma) - (d-2)\sigma\widetilde{\epsilon}'(\sigma)\Big), \\
\widetilde{T}_{ii} &= \Omega^{-d+2}P_T(\tau(\sigma)) \\
&= \frac{2}{d-2}\frac{\sigma}{\tau_0}\Big(\epsilon(\tau(\sigma)) + \frac{1}{2}\tau(\sigma)\epsilon'(\tau(\sigma))\Big) \\
&= \left(\frac{\sigma}{\tau_0}\right)^{-\frac{2}{d-2}} \frac{1}{d-1}\Big(\widetilde{\epsilon}(\sigma) + \sigma\widetilde{\epsilon}'(\sigma)\Big),
\end{aligned} \tag{2.64}$$

with $\widetilde{T}_{ii}$ denoting the diagonal transverse components and $'$ denoting the derivative w.r.t. the argument of the corresponding function. It follows that in the hydrodynamic limit, the Bjorken

expansion (2.57) takes the resultant form

$$\widetilde{T}^{\sigma}_{\sigma} \equiv -\widetilde{\epsilon}(\sigma) = -\left(\frac{\sigma}{\tau_0}\right)^{\frac{d}{d-2}} \epsilon(\tau(\sigma)) = -\epsilon_0 \left(1 + \sum_{n=1}^{\infty} \lambda_n \, \epsilon_0^{-\frac{n}{d}} \sigma^{-n}\right). \tag{2.65}$$

The Weyl scaled metric (2.63) has the property that

$$\sqrt{-\widetilde{g}} = \frac{d-1}{d-2}\,, \tag{2.66}$$

is a constant, and the spatial volume factor is unity, same as in the Minkowski coordinates. However, the longitudinal volume expands, while the transverse volume contracts with the evolution. Also note that for the Weyl scaled Bjorken flow (2.65), we have

$$\lim_{\sigma\to\infty} \widetilde{\epsilon}(\sigma) = \epsilon_0. \tag{2.67}$$

Therefore, instead of a perfect fluid expansion, the flow attains a constant temperature, energy and entropy densities at late time although no time-like Killing vector exists in the background metric. The latter feature leads to viscous and higher-order corrections. The large (reparametrised) proper time expansion is determined by ϵ_0, the final thermal value of the energy density, while τ_0 appears in the Weyl scaling factor Ω as explicit in Eq.(2.62).

The Weyl scaling depends explicitly on τ_0. However, note that for $\tau_0 \to \xi\tau_0$, we obtain from (2.61) that $\sigma \to \xi^{1/(d-1)}\sigma$. Thus the Weyl factor given by (2.62) scales as $\Omega \to \xi^{1/(d-1)}\Omega$, implying that $\widetilde{\mathrm{d}s}^2 \to \xi^{2/(d-1)}\widetilde{\mathrm{d}s}^2$ and $\epsilon_0 \to \xi^{-1/(d-1)}\epsilon_0$. Therefore, the dimensionless variables $\epsilon_0^{-1/d}\sigma^{-1}$ (which provides the proper time expansion parameter) and $\sigma^n \widetilde{T}^{\sigma}_{\sigma}$ are invariant under $\tau_0 \to \xi\tau_0$, and are thus independent of τ_0.

2.1.5 Hydrodynamic attractors

The emergence of hydrodynamic attractors resolves the puzzle of the applicability of relativistic hydrodynamics to a far away from equilibrium system with large pressure anisotropies. The

terminology attractor arises from the observation that the non-equilibrium system for any arbitrary initial conditions evolves to the same late-time behaviour, hence an attractor. This attractor incorporates all orders of hydrodynamic gradient expansion and at a sufficient late time, it coincides with the relativistic Navier-Stokes equation. Hence the term hydrodynamic attractor which at late time is characterised by hydrodynamic degrees of freedom, explains the applicability of the hydrodynamic theory in a far away from equilibrium system. The feature of the attractor being ignorant of the initial condition makes it a strong phenomenological candidate to identify universal behaviour in heavy ion collisions by distinguishing between observables that are and are not dependent on initial conditions.

In the context of heavy ion collisions, hydrodynamic attractors came into existence while investigating the boost-invariant expansion of plasma by Heller and Spalinski [25]. In addition, various microscopic theories based on the first principle show the decay of non-equilibrium solution to the hydrodynamic attractor for arbitrary initial conditions i.e., the transition to hydrodynamic behaviour [23]. The onset of hydrodynamic behaviour in a far away from equilibrium system can be studied by considering the example of Bjorken flow in which the whole physics is encoded in the energy density ϵ or the effective temperature T. Here, the evolution of the energy density approaches a hydrodynamic attractor [25, 26] where the energy density at late time has a perfect fluid-like behaviour. The attractor is a generic property of a many-body relativistic system irrespective of whether its degrees of freedom interact weakly or strongly (see [5] for a recent review).

The symmetry of the Bjorken flow, as mentioned above in section 2.1.4, ensures that the hydrodynamic degrees of freedom are functions of proper time τ. Therefore, the energy density ϵ, and the longitudinal and transverse pressure, p_L and p_T, as defined above are functions of τ. The departure of the pressures from the equilibrium pressure given by the equation of states, $p = \epsilon/(d-1)$, measures the anisotropy in the system i.e, how far the system is from the

local equilibrium. Based on this, one defines the normalised pressure anisotropy variable $\mathcal{A}$ as

$$\mathcal{A} = \frac{p_T - p_L}{p}, \tag{2.68}$$

whose evolution with proper time is studied with respect to the dimensionless variable $w = \tau T(\tau)$. This dimensionless variable can be thought of as a proper time in units of inverse temperature. This pressure anisotropy also admits a hydrodynamic expansion in w,

$$\mathcal{A}(w) = \sum_{n=1} a_n w^{-n}, \tag{2.69}$$

similar to the energy density above. Generally, one studies the evolution of $\mathcal{A}$ as a function of w to the attractor curve, marking the onset of hydrodynamic description, as shown in Fig. 2.3. This shows that irrespective of large pressure anisotropy, the system is governed by relativistic hydrodynamics.

Moreover, the hydrodynamic attractor can be defined as the evolution obtained by resummation of the hydrodynamic gradient expansion up to all orders [25]. The hydrodynamic gradient expansions such as (2.57) and (2.68) for arbitrary higher orders result in factorial growth of the coefficients with zero radius of convergence, as shown in the Fig. 2.4. The standard technique to remove factorial divergence is the Borel transform of the original series [88],

$$\mathcal{B}\mathcal{A}(\xi) = \sum_{n=0} \frac{a_n}{n!} \xi_n. \tag{2.70}$$

This transformed series has a finite radius of convergence due to the removal of the leading $n!$ growth. The subsequent inverse Borel transform, also known as Borel resummation is defined by the Laplace transform,

$$\mathcal{L}\mathcal{A}(\xi) = \int_C e^{-w\xi} \tilde{\mathcal{B}}\mathcal{A} \tag{2.71}$$

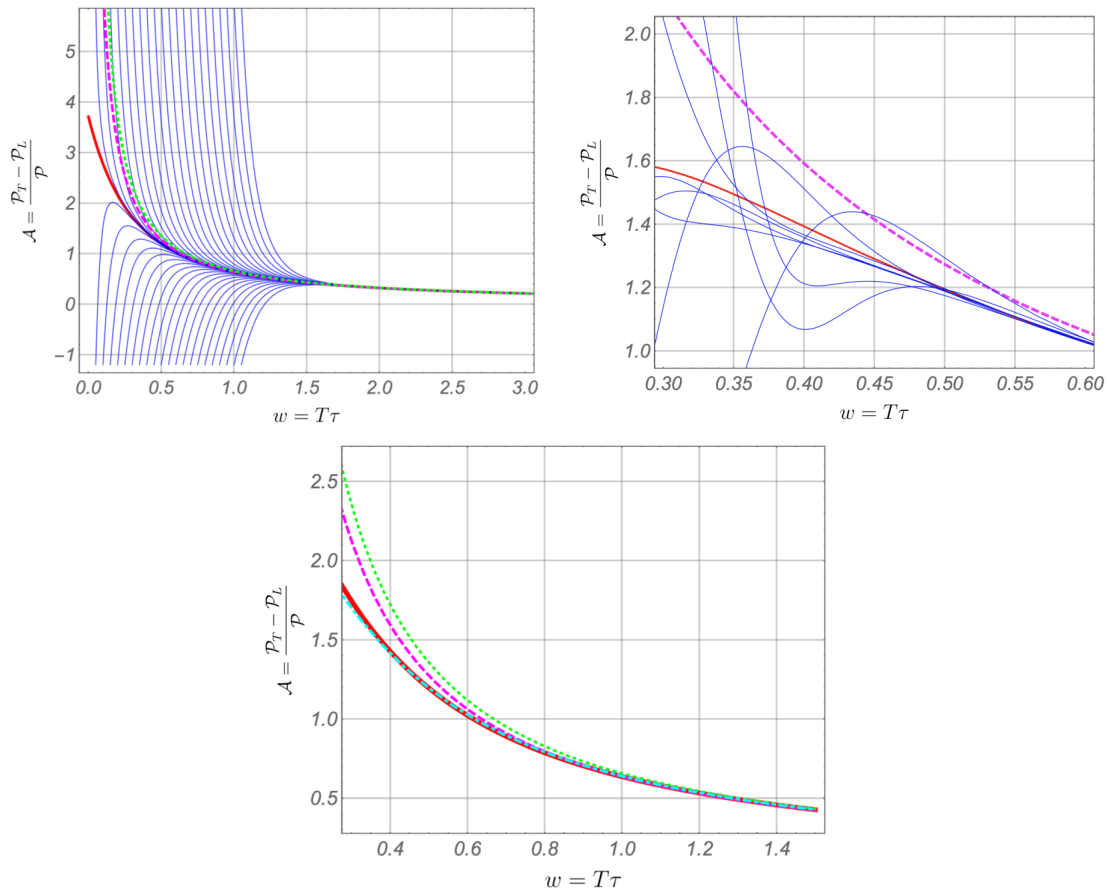

Figure 2.3: The left plot is the MIS attractor. It shows the evolution of the arbitrary initial conditions given by blue curves to the numerically determined attractor curve, the red one. The relaxation time τ_π is considered 3 times the relaxation time of $\mathcal{N} = 4$ SYM. The magenta and green dotted curves correspond to the hydrodynamics truncated at first and second-order derivatives. The right plot is the attractor of $\mathcal{N} = 4$ SYM plasma. The blue curves are the solutions for arbitrary initial conditions obtained by numerical simulation in AdS/CFT and the red colour is the Borel resummed attractor. The dotted magenta is first-order hydrodynamics. The bottom figure shows resummed attractor in dotted Cyan for MIS, the red one is the numerical attractor and the dotted magenta and green are the first-order and second-order hydrodynamics. Figure taken from [23–25].

where C is the integration contour in complex plane that connects from $\xi = 0$ to $\xi = \infty$. $\tilde{\mathcal{B}}\mathcal{A}$ is the analytic continuation of the Borel series achieved by Páde approximation [89]. This analytic continuation introduces singularities (simple pole) in the Borel plane which is related to the finite radius of convergence of the Borel series. The accumulation of these simple poles in the complex plane gives an image of branch cut in the plane and the distance of the closet pole from the origin is given by the inverse slope of the coefficients. For holographic theory, the nearest pole to the origin is associated with the lowest quasinormal modes [26] while in

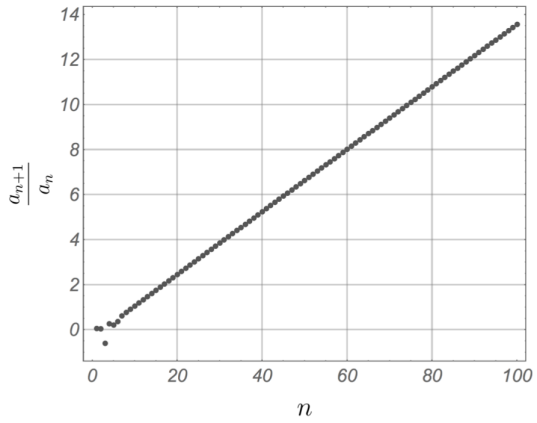

Figure 2.4: The figure shows linear growth in the ratio of the coefficients a_{n+1} and a_n for BRSSS hydrodynamics. This growth implies factorial divergence of the coefficients. Figure taken from [23].

quantum field theory, they can be associated with instantons [90].

The presence of singularities in the Borel plane introduces complex ambiguities in the Borel resummation, making the integration, contour dependent. This ambiguity as per the theory of resurgence indicates the contribution of an infinite set of exponentially suppressed non-perturbative corrections (non-hydrodynamic modes) to the hydrodynamic series. Hence, the hydrodynamic series takes the form of transseries [25],

$$\mathcal{A}(w) = \sum_m \Omega(w)^m \sum_n a_{n,m} w^{-n}. \tag{2.72}$$

The non-perturbative corrections are encoded in $\Omega(w)$ where $\Omega(w) = Cw^{-\gamma}e^{-\xi_0 w}$, γ is a constant which can be determined by analysing the residue along the branch cut. ξ_0 is the pole closest to the origin in branch cut and as mentioned is associated with the quasinormal modes or the instantons depending on the theory. The constant C is a complex parameter that must be chosen such that the ambiguity in the integration contour is cancelled by the subsequent terms in the transseries, yielding a real final result. This cancellation determines the parameter up to an arbitrary real constant which is parameterised by different initial conditions at early time. In the space of initial conditions one particular configuration finally gives the attractor solution. Therefore, the transseries form of hydrodynamic expansion captures the information about the

initial condition via the complex parameter C also known as Stokes parameter, unlike the divergent hydrodynamic expansion where the knowledge of the initial state of evolution vanishes. For further details in transseries form of hydrodynamics, one can refer to [91–94].

In $\mathcal{N} = 4$ SYM [26] or HJSW hydrodynamics [43], the poles are accumulated away from the positive real axis as shown in Fig. 2.5, hence one can perform the integration (2.71) by considering the contour along the positive real axis. The Borel resummability indicates the presence of Borel resummed all order hydrodynamics. This resummation results in a resummed attractor as shown in Fig. 2.3. However, for hydrodynamic models like MIS or BRSSS [25], the poles are accumulated on the positive real axis, as in Fig. 2.5, causing difficulty in integration along this axis. Here the integration is carried out by choosing the integration contour at an angle to the real axis by avoiding the poles. In this instance, the ambiguity in the contour can be eliminated by fixing the parameter, as stated previously where the real part of C is assumed to be associated with the integration constant for the MIS or BRSSS differential equation [25], and hence determined by the initial conditions. This then gives the Borel resummed attractor in MIS or BRSSS, shown in Fig. 2.3.

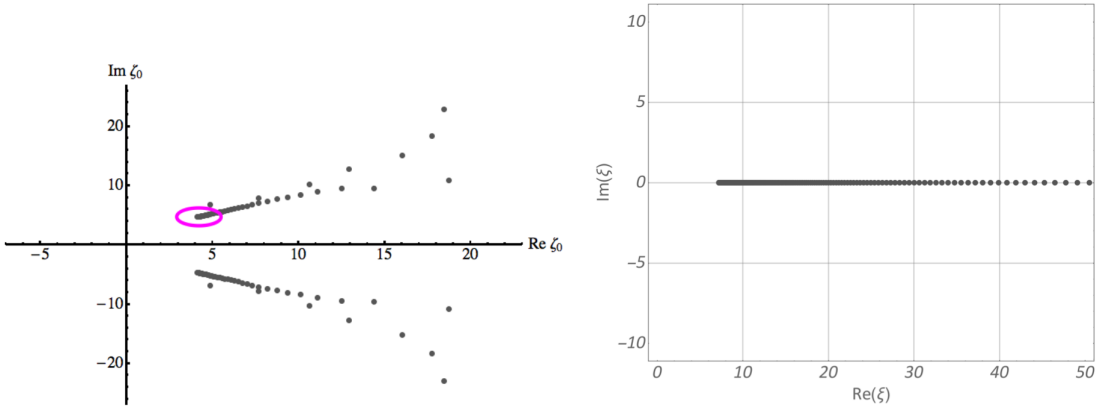

Figure 2.5: The figure shows the accumulation of poles of symmetric Pade approximant of the Borel transform of hydrodynamic gradient expansion. The high concentration of the poles gives an image of a branch cut and the pole closest to the origin governs the radius of convergence of the Borel transformed series. The left plot shows the poles obtained by doing Borel transform of energy density for $\mathcal{N} = 4$ SYM (páde approximation is done up to order of 240.). The right plot shows the poles obtained by doing the Borel transform of anisotropy measure $\mathcal{A}$ for BRSSS hydrodynamics. Figure taken from [23, 26].

Hydrodynamization

A non-equilibrium system is said to hydrodynamize if the evolution of the system is governed by hydrodynamic degrees of freedom. This transition to the hydrodynamics of a non-equilibrium system is known as hydrodynamization [95]. Hydrodynamization refers to the state of a dynamical system in which the average values of the energy-momentum tensor and conserved currents follow the constitutive relations of hydrodynamics up to a good approximation. It can also be defined in terms of the hydrodynamic attractor in phase space, which is the result of Borel resummed divergent series of the late-time effective hydrodynamic expansion (for a recent review see [5]). The Fig. 2.6 compares the time evolution of pressure anisotropy in a system governed by Bjorken flow according to numerical holography, EKT (Effective Kinetic Theory) and RTA (Relaxation Time Approximation) kinetic theory. In all these cases, the evolution of the initial conditions converges to first-order viscous hydrodynamics roughly around $\tilde{w} \approx 1$ with large pressure anisotropy $\mathcal{A} = 0.6 - 0.8$. $\tilde{w} = w/(4\pi\eta/s)$, is the rescaled variable which gives a universal feature to $\mathcal{A}$ at late time for microscopic theories such as strongly coupled hCFTs and the kinetic theory models [23]. The time when the systems are described by hydrodynamic degrees of freedom is known as hydrodynamization time. Precisely, the hydrodynamization time can be defined as the time when both the longitudinal and transverse pressure admits a first-order hydrodynamic description up to certain accuracy [3]. The work [96], explores hydrodynamization in a hybrid viscous fluid model coupled in a semi-holographic framework and shows how hydrodynamizaiton works in an asymptotically free gauge theory with both weakly and strongly interacting degrees of freedom.

2.2 Holography and AdS/CFT correspondence

The holographic principle first formulated by t'Hooft [97] and further refined by Susskind [98], states that in a theory of quantum gravity, the information stored in any region of the spacetime scales as the surface area enclosing the region rather than the volume of the region itself. This

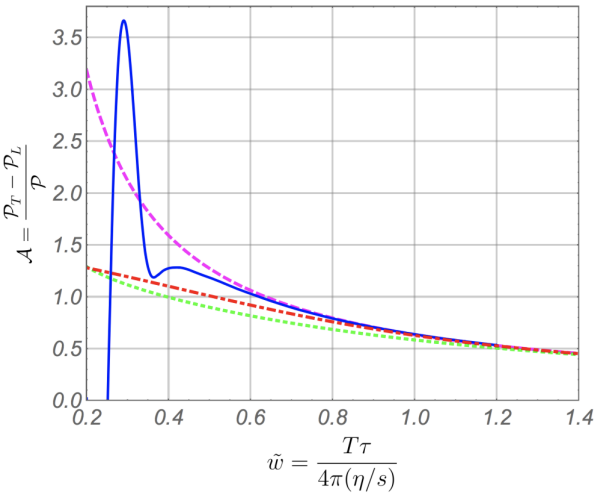

Figure 2.6: Comparison of hydrodynamization of EKT (dashed-dotted red), RTA kinetic theory and $\mathcal{N} = 4$ SYM (blue curve), with different values of η/s. The dashed brown curve is for $\eta/s = 1/4\pi$ and the dotted green is for $\eta/s = 0.624$. The dashed magenta is the first-order hydrodynamics. Figure taken from [23].

argument was inspired by black hole thermodynamics in which the maximum entropy of a black hole, known as the Bekenstein-Hawking entropy is proportional to the surface area of the black hole,

$$S_{BH} = \frac{A}{4G} \tag{2.73}$$

where G is the Newton constant. One concrete example of holography is the AdS/CFT correspondence, or gauge/gravity duality. The AdS/CFT correspondence is a proposed duality between conformal field theory and the theory of gravity in one higher dimension with an appropriate boundary condition. Precisely, it describes the same physics from two different perspectives by relating the strongly coupled gauge theories to the weakly coupled classical gravity descriptions.

The correspondence originally proposed by Maldacena [99] can be formally stated in the context of AdS_5/CFT_4 as [100],

$\mathcal{N} = 4$ Super Yang-Mills (SYM) theory with gauge group $SU(N)$ and coupling constant g_{YM} is dynamically equivalent to type IIB string theory with coupling constant g_s and string length $l_s = \sqrt{\alpha'}$ on $AdS_5 \times S^5$ with radius of curvature L. The correspondence maps the free parameters, g_s and the dimensionless ratio L/l_s on the string side to the free parameters on the field theory side, g_{YM} and N, by

$$g_{YM}^2 = 2\pi g_s \quad \text{and} \quad 2g_{YM}^2 N = L^4/l_s^4$$

where $g_{YM}^2 N = \lambda$ is the t'Hooft coupling and α' is the Regge slope [101]. This statement is referred to as the strongest form of the AdS_5/CFT_4 correspondence. In the t'Hooft limit, $N \to \infty$ with λ fixed and arbitrary, one realises the strong form of the correspondence where the AdS side reduces to classical string theory with $g_s \to 0$. In this limit, the string theory is realised by tree-level diagrams and all quantum corrections are neglected. Therefore, one can map $1/N$ expansion on the field theory to a string genus expansion for fixed λ. Since we are interested in strong/weak duality, we consider the weak form of AdS/CFT conjecture in the sense that the strongly coupled $\mathcal{N} = 4$ SYM on field theory side with $\lambda \to \infty$ is mapped to point-particle limit, $l_s/L \to 0$, of type IIB string theory (IIB supergravity) on $AdS_5 \times S^5$ space.

The correspondence establishes one-to-one relation between the gauge invariant operators in $\mathcal{N} = 4$ SYM and classical gravity field in $AdS_5 \times S^5$. This mapping is termed as AdS/CFT dictionary and is a result of the coincidence of the symmetries on both sides where the isometries SO(4,2) × SO(6) of $AdS_5 \times S^5$ has a one-to-one mapping with the supergroup SO(4,2) × SO(6) of $\mathcal{N} = 4$ SYM theory. Explicitly this argument leads to equality between the generating functional of connected correlation functions of gauge invariant operators in the field theory to the on-shell action of the classical gravity theory with an appropriate near-boundary expansion of the gravity field Φ where the leading term acts as a source $\phi_{(0)}$ to the corresponding field operators $\mathcal{O}$.

$$W[\phi_{(0)}] = \mathcal{S}_{Sugra}^{on-shell}[\Phi]. \tag{2.74}$$

The connected correlation function of the gauge invariant operator O_i can be obtained by functional differentiation of the generating functional or the on-shell action with respect to the sources $\phi_{(0)}$,

$$\langle O(x_1)\cdots O(x_n)\rangle = (-1)^{n+1}\frac{\delta^n \mathcal{S}^{on-shell}_{Sugra}}{\delta\phi_{(0)}(x_1)\cdots\delta\phi_{(0)}(x_n)}. \tag{2.75}$$

2.2.1 Scalar field in the bulk

The proposed relation between the gravity field and the operator of the dual field theory can be understood better by studying an example of a scalar field in bulk. Consider a scalar field Φ in AdS_{d+1} space whose action reads as,

$$\mathcal{S} = -\frac{1}{2}\int \mathrm{drd^dx}\,\sqrt{-g}(\mathrm{g^{mn}}\partial_\mathrm{m}\Phi\partial_\mathrm{n}\Phi + \mathrm{m^2}\Phi^2). \tag{2.76}$$

The AdS_{d+1} space is defined by the Poincaré metric given by,

$$\mathrm{ds^2} = \mathrm{g_{mn}dx^m dx^n} = \frac{\mathrm{L^2}}{\mathrm{r^2}}(\mathrm{dr^2} + \eta_{\mu\nu}\mathrm{dx^\mu dx^\nu}). \tag{2.77}$$

In this metric, the Klein-Gordon (KG) equation for the scalar field computed from the action takes the form,

$$(\Box_g - m^2)\Phi = 0 \tag{2.78}$$

where

$$\Box_g \equiv \frac{1}{\sqrt{-g}}\partial_m\Big(\sqrt{-g}g^{mn}\partial_n\Big) = \frac{1}{L^2}\Big(r^2\partial_r^2 - (d-1)r\partial_r + z^2\eta^{\mu\nu}\partial_\mu\partial_\nu\Big).$$

The most convenient approach to get the solution of the KG-equation is to perform Fourier transform of the field Φ in the x^μ coordinate and consider the field to be in the form of plane

wave ansatz, $\Phi(r, x) = e^{i\vec{k}.\vec{x}}\phi_k(r)$. Then the equation for the mode $\phi_k(r)$ becomes,

$$r^2\partial_r^2\phi_k(r) - (d-1)r\partial_r\phi_k(r) - (m^2L^2 + k^2r^2)\phi_k(r) = 0. \tag{2.79}$$

This equation has two independent solutions which near the boundary, $r \to 0$, has the following feature,

$$\phi_k(r) \approx A(k)r^{\Delta_+} + B(k)r^{\Delta_-} \tag{2.80}$$

where $\Delta_\pm$ is the root of the equation (2.79) near the boundary[3], defined as,

$$\Delta_\pm = \frac{d}{2} \pm \sqrt{\frac{d^2}{4} + m^2L^2}. \tag{2.81}$$

By definition, $\Delta_+ \geq \Delta_-$ and Δ_- can be expressed as $\Delta_- = d - \Delta_+$. These roots $\Delta_\pm$ are referred to as normalisable and non-normalisable. Δ_+ gives the normalisable solution which means the action evaluated on this solution is finite. This leads to normalisable mode. Δ_- corresponds to the non-normalisable mode. Near the boundary, the bulk field in the spacetime coordinates can be expanded in these modes as,

$$\Phi(r, x) = (\phi_{(0)}(x)r^{\Delta_-} + O(r) + \cdots) + (\phi_{(+)}(x)r^{\Delta_+} + O(r) + \cdots) \tag{2.82}$$

where the non-normalisable mode defines the boundary source $\phi_{(0)}(x)$ via

$$\phi_{(0)}(x) \equiv \lim_{r\to 0}\Phi(r, x)r^{-\Delta_-} = \lim_{r\to 0}\Phi(r, x)r^{\Delta_+-d}, \tag{2.83}$$

and the normalisable mode $\phi_{(+)}(x)$ is identified with the vacuum expectation value for a dual scalar field operator of dimension Δ_+.

Generally, for a consistent theory, we expect that m^2 should be positive or zero. Note that for $m = 0$, we have $\Delta_+ = d$ which means the dual operator is marginal, and for $m > 0$,

[3]Near the boundary for $\phi_r(k) = Exp(\Delta\, r)$ the equation becomes, $\Delta(\Delta - d) - m^2L^2 = 0$.

$\Delta_+ > d$, which means the dual operator is irrelevant. However, m^2 can be negative satisfying the Breitenlohner-Freedman bound [102, 103], $m^2L^2 \geq -d^2/4$. This condition states that the bulk scalar field Φ with mass, $0 > m^2L^2 \geq -d^2/4$, are dual to the relevant/marginal scalar field theory operators of conformal dimension Δ_+ with the condition $d \geq \Delta_+ \geq d/2$. For further details one can refer to [100].

2.2.2 Holographic renormalization

Correlation functions obtained in quantum field theory are affected by UV divergences which can be removed by the well-known methods of renormalisation. The duality relates this UV divergence on the field theory side to the IR divergence on the gravitational side and vice versa. On the gravity side, the long distance (IR) is equivalent to near the boundary. Holographic renormalisation [60, 104–106] ensures renormalised correlation function by dealing with these IR divergences via near-boundary analysis.

Here we review the holographic renormalisation of the stress-tensor of gravity based on the discussion in [105]. We consider a $(d+1)$ dimensional bulk manifold $\mathcal{M}$ which is foliated by a series of d dimensional timelike hypersurface defined by constant bulk radial coordinate, r. Near the boundary at $r \to \infty$, the bulk manifold leads to AdS spacetime. The dual conformal field theory lives on this d dimensional spacetime boundary. For any hypersurface defined by r = constant is spanned by the coordinates (x^μ, r) and can be referred to as the boundary $\partial\mathcal{M}_r$ to the region of spacetime $\mathcal{M}_r$ which is interior to $\partial\mathcal{M}_r$. This boundary is defined by the induced metric $\gamma_{\mu\nu}$ which is a function of x^μ and r and is evaluated at the boundary value of r. The bulk spacetime $\mathcal{M}$ can be expressed in terms of this induced metric $\gamma_{\mu\nu}$ in ADM-like decomposition [107],

$$ds^2 = N^2dr^2 + \gamma_{\mu\nu}(dx^\mu + N^\mu dr)(dx^\nu + N^\nu dr) \tag{2.84}$$

where N^μ is normal to r = constant hypersurface.

Now to compute the quasi-local stress tensor for the interior region we need to vary the gravitational action with respect to $\gamma_{\mu\nu}$. The renormalised gravitational action with cosmological constant $\Lambda = d(d-1)/2l^2$ (l is the AdS radius) read as,

$$\mathcal{S} = -\frac{1}{16\pi G}\int_{\mathcal{M}} d^{d+1}x\,\sqrt{g}\Big(R-\Lambda\Big) - \frac{1}{8\pi G}\int_{\partial\mathcal{M}} d^{d}x\,\sqrt{-\gamma}\Theta + \frac{1}{8\pi G}\mathcal{S}_{ct}(\gamma_{\mu\nu}). \tag{2.85}$$

The second term in the action is the Gibbons-Hawking term which is included here because the manifold $\mathcal{M}_r$ has a boundary $\partial\mathcal{M}_r$. This term ensures well-defined variational principles. Θ is the trace of extrinsic curvature of the boundary defined by the induced metric $\gamma_{\mu\nu}$. The counter term $\mathcal{S}_{ct}$ ensures a finite stress tensor. It should be chosen properly to remove the divergences arising due to the boundary limit of $\partial\mathcal{M}_r$ which is the AdS boundary $\partial\mathcal{M}$ of spacetime $\mathcal{M}$. The variation of the action in general includes a bulk term and a boundary term. Since we consider on-shell action, only the boundary term contributes to the action,

$$\delta\mathcal{S} = \int_{\partial\mathcal{M}_r} \mathrm{d^d x}\;\pi^{\mu\nu}\delta\gamma_{\mu\nu} + \frac{1}{8\pi \mathrm{G}}\int_{\partial\mathcal{M}_\mathrm{r}} \mathrm{d^d x}\frac{\delta \mathrm{S_{ct}}}{\delta\gamma_{\mu\nu}}\delta\gamma_{\mu\nu}. \tag{2.86}$$

Here $\pi^{\mu\nu}$ is the conjugate momentum of $\gamma_{\mu\nu}$ obtained at the boundary,

$$\pi^{\mu\nu} = \frac{1}{16\pi G}\sqrt{\gamma}(\Theta^{\mu\nu} - \Theta\gamma^{\mu\nu}), \tag{2.87}$$

where $\Theta^{\mu\nu}$ is the extrinsic curvature defined as,

$$\Theta^{\mu\nu} = -\frac{1}{2}(\nabla^{\mu}\hat{n}^{\nu} + \nabla^{\nu}\hat{n}^{\mu}). \tag{2.88}$$

$\hat{n}^{\nu}$ is the outward pointing normal vector to the boundary $\partial\mathcal{M}_r$. Therefore, the quasi-local stress tensor for the interior region, obtained by the variation of the renormalised gravitational action with respect to the induced metric $\gamma_{\mu\nu}$ read as,

$$T^{\mu\nu} = \frac{1}{8\pi G}\Big[\Theta^{\mu\nu} - \Theta\gamma^{\mu\nu} + \frac{2}{\sqrt{-\gamma}}\frac{\delta\mathcal{S}_{ct}}{\delta\gamma_{\mu\nu}}\Big]. \tag{2.89}$$

Since we are interested in the stress tensor of the boundary field theory, we evaluate $T^{\mu\nu}$ in the limit $\partial\mathcal{M}_r \to \partial\mathcal{M}$ which generically leads to divergence. To cancel the divergence in this procedure of renormalisation one considers $\mathcal{S}_{ct}$ to be local functional of the boundary metric [108]. This sets $\mathcal{S}_{ct}$ uniquely. For instance, the stress tensor for the boundary quantum field theory for AdS_5 becomes,

$$T^{\mu\nu} = \frac{1}{8\pi G}\Big[\Theta^{\mu\nu} - \Theta\gamma^{\mu\nu} - \frac{3}{l}\gamma^{\mu\nu} - \frac{l}{2}G^{\mu\nu}\Big] \tag{2.90}$$

where $G_{\mu\nu} = R_{\mu\nu} - \frac{1}{2}R\gamma_{\mu\nu}$ is the Einstein tensor of $\gamma_{\mu\nu}$.

Further, holographic renormalisation is also important to compute conformal anomalies on AdS space from the gravitational action [100]. These anomalies also known as trace anomalies, render the trace of the energy-momentum tensor non-zero for odd $(d+1)-$ dimensional AdS space. This is a consequence of the correspondence, as odd $(d+1)-$ dimensional bulk theory is dual to even $d-$ dimensional conformal theory where the trace is non-vanishing. For example, for $d = 2$ dimensional conformal theory at the boundary the trace anomaly is $T^{\mu}_{\mu} = -\frac{c}{24\pi}\mathcal{R}$ and the subsequent anomaly on AdS_3 space is $T^{\mu}_{\mu} = -\frac{l}{16\pi G}\mathcal{R}$, where $\mathcal{R}$ is the curvature of the induced metric $\gamma_{\mu\nu}$. These two anomalies agree when $c = 3l/2G$. While, for $d = 3$, the trace of the energy-momentum tensor on both sides is zero.

2.2.3 Fluid/gravity correspondence

The AdS/CFT correspondence can be extended to study effective descriptions of strongly coupled theory at long wavelength. In this limit, any interacting quantum field theory should equilibrate locally with high energy density, admitting a fluid dynamic description. In addition, with appropriate boundary conditions, the Einstein equation in this regime reduces to non-linear equation of fluid dynamics of d dimensional effective theories. This duality between the field theory at the boundary and gravity, at long wavelength, is termed as fluid/gravity correspondence [1, 18, 38, 83].

Consider a theory of pure gravitational dynamics in asymptotically AdS_{d+1} space. Einstein's equation with negative cosmological constant Λ is given by [4],

$$R_{MN} - \frac{1}{2}Rg_{MN} + \Lambda g_{MN} = 0, \qquad \Lambda = \frac{-d(d-1)}{2l^2} \tag{2.91}$$

where l is the AdS radius and is set to one for convenience, R_{MN} is the Ricci tensor and R is the Ricci scalar. In addition to the usual AdS_{d+1} solution, the equation admits a family of solutions given by the boosted black branes along the spatial direction x^i. For regularity in the future horizon, those family of solutions can be given by the ingoing Eddington-Finkelstein (EF) coordinates,

$$ds^2 = -2u_\mu dx^\mu dr - r^2\Big(f(br)\, u_\mu u_\nu - \Delta_{\mu\nu}\Big)\, dx^\mu dx^\nu \tag{2.92}$$

with $\Delta_{\mu\nu} = \eta_{\mu\nu} + u_\mu u_\nu$ and

$$f(br) = 1 - \frac{1}{(br)^d}, \qquad u^v = \frac{1}{\sqrt{1-\beta^2}} \qquad \text{and} \qquad u^i = \frac{\beta^i}{\sqrt{1-\beta^2}}. \tag{2.93}$$

Here u^μ is the relativistic fluid velocity and $b = 1/r_h$ which is related to the Hawking temperature by $T = d/(4\pi b)$. The d dimensional vector x^μ now has (v, x^i) as coordinates, where v is the ingoing Eddington-Finkelstein time coordinate [5]. The metric (2.92) describes the uniform black brane at constant temperature T moving with a velocity β_i with $\beta^2 = \beta^i\beta_i$.

The metric solution at the boundary leads to d dimensional perfect fluid with a conserved energy-momentum tensor. Now to describe dissipative fluid, one needs to add perturbation to this equilibrium solution. This can be achieved by promoting the constant parameter b and β^i as a slowly varying function of v and x^i which modifies the metric (2.92) to

$$ds^2 = -2u_\mu(x^\alpha)dx^\mu dr - r^2\Big(f(b(x^\alpha)r)\, u_\mu(x^\alpha)u_\nu(x^\alpha) - \Delta_{\mu\nu}(x^\alpha)\Big)\, dx^\mu dx^\nu. \tag{2.94}$$

[4] The uppercase letters $(M, N, \cdots)$ corresponds to the bulk direction and the Greek letters $(\mu, \nu, \cdots)$ represents boundary direction and the lowercase letters $(i, j, \cdots)$ represents spatial direction.

[5] The time coordinate v is defined as $v = t + r^*$, where r^* is the tortoise coordinate and t the usual time coordinate [100].

This modified metric denoted by $g_{\mu\nu}(u^i, b)$ with arbitrary functions is not a solution to Einstein's equation. The new solution can be obtained by solving the Einstein equation order by order in derivative expansion. This can be achieved by adding derivative corrections to the fluid velocity u^i, b and the metric $g_{\mu\nu}(u^i, b)$,

$$u^i = \sum_{m=0}^{n} u^{i,(m)}\epsilon^m, \qquad b = \sum_{m=0}^{n} b^{(m)}\epsilon^m, \qquad g_{\mu\nu} = \sum_{m=0}^{n} g^{(m)}_{\mu\nu}(u^i, b)\epsilon^m. \tag{2.95}$$

Here ϵ counts the order in the expansion. We insert the above ansatz in the Einstein equation and solve order by order in ϵ. Suppose the equation is solved up to the order ϵ^{n-1}, then at the order ϵ^n we get $(d+1)(d+2)/2$ inhomogeneous differential equations for the component of $g^{(n)}_{\mu\nu}$. The differential operator of these equations is given in terms of $g^{(0)}_{\mu\nu}(u^{i,(0)}, b^{(0)})$ and the source includes the derivative of $u^{i,(0)}$ and $b^{(0)}$. These equations can be distinguished as follow:

- $d(d+1)/2$ dynamical equations which fixes the unknown coefficient $g^{(n)}_{\mu\nu}$.
- $d+1$ constraint equations which include the conservation and the tracelessness of the boundary energy-momentum tensor up to order $n-1$ in the ϵ expansion,

$$\nabla_\mu T^{\mu\nu}_{(n-1)} = 0, \qquad T^{\mu}_{\mu(n-1)} = 0. \tag{2.96}$$

  This determines the coefficients $u^{i,(n-1)}$ and $b^{(n-1)}$.

For example, following this perturbative procedure, one can compute the first and second-order contribution to the metric and energy-momentum tensor and determine the transport coefficients as in [18, 100].

2.2.4 Holographic dual of Bjorken flow

The gravitational dual of the Bjorken flow [19, 26, 109–111] has been extensively studied in the literature with the late time evolution to perfect fluid. This provides a primary example of the

fluid/gravity correspondence where large order resummation of the hydrodynamic series [26] has been explicitly carried out revealing the hydrodynamization [25] of a far-from-equilibrium state. When a state hydrodynamizes, the energy-momentum tensor can be described as an optimally truncated (divergent and asymptotic) hydrodynamic series even when it is far from equilibrium [25, 26].

We consider an asymptotically AdS_{d+1} metric dual to a $d-$ dimensional conformal field theory governed by Bjorken flow at the boundary. The metric in ingoing Eddington-Finkelstein like coordinate takes the form

$$ds^2 = -\frac{2}{r^2}\mathrm{d}r\mathrm{d}\tau - \frac{A(r,\tau)}{r^2}\mathrm{d}\tau^2 + \left(1+\frac{\tau}{r}\right)^2 e^{L(r,\tau)}\mathrm{d}\zeta^2 + \frac{e^{K(r,\tau)}}{r^2}\mathrm{d}s_\perp^2, \tag{2.97}$$

with the following Dirichlet boundary condition

$$A(r,\tau)\to 1, \qquad K(r,\tau)\to 0 \qquad \text{and} \qquad L(r,\tau)\to 0 \qquad \text{as} \quad r\to 0. \tag{2.98}$$

r is the radial coordinate. These boundary conditions ensure that the boundary metric is the Milne metric (2.52). The corresponding vacuum solution, which is pure AdS_{d+1} spacetime with desired boundary metric is,

$$\mathrm{d}s^2 = -\frac{2}{r^2}\mathrm{d}r\mathrm{d}\tau - \frac{1}{r^2}\mathrm{d}\tau^2 + \left(1+\frac{\tau}{r}\right)^2 \mathrm{d}\zeta^2 + \frac{1}{r^2}\mathrm{d}s_\perp^2\,, \tag{2.99}$$

and is dual to the vacuum state of the Milne metric (2.52).

Now to study the late-time evolution of the geometry dual to Bjorken flow, the Einstein equations (2.91) can be readily solved in the late-time expansion, as functions of the scaling variable

$$s = r\left(\frac{\tau_0}{\tau}\right)^{\frac{1}{d-1}}, \tag{2.100}$$

and with the expansion parameter being

$$\left(\tilde{\mu}^{1/d}\tau^{\frac{d-2}{d-1}}\right)^{-1} \tag{2.101}$$

where $\tilde{\mu} := \varepsilon_0 \tau_0^{\frac{d}{d-1}}$ is a constant which will be related to the single parameter μ of the Bjorken flow defined in (2.56) (or equivalently to ϵ_0, below). Explicitly,

$$\begin{aligned} A(r,\tau) &= 1 - \varepsilon_0 s^d + \sum_{i=1}^{\infty} \left(\tilde{\mu}^{1/d}\tau^{\frac{d-2}{d-1}}\right)^{-i} a_{(i)}(\varepsilon_0^{\frac{1}{d}} s), \\ L(r,\tau) &= \sum_{i=1}^{\infty} \left(\tilde{\mu}^{1/d}\tau^{\frac{d-2}{d-1}}\right)^{-i} l_{(i)}(\varepsilon_0^{\frac{1}{d}} s), \\ K(r,\tau) &= \sum_{i=1}^{\infty} \left(\tilde{\mu}^{1/d}\tau^{\frac{d-2}{d-1}}\right)^{-i} k_{(i)}(\varepsilon_0^{\frac{1}{d}} s). \end{aligned} \tag{2.102}$$

The functions $a_{(i)}$, $l_{(i)}$ and $k_{(i)}$ satisfy ordinary differential equations with source terms at each order. These functions can be determined using the method discussed below.

Determining $a_{(i)}$, $l_{(i)}$ and $k_{(i)}$

We require that these functions do not blow up at the perturbative horizon which is at $s_h = \varepsilon_0^{-1/d}$, i.e. at

$$r_h = \varepsilon_0^{-\frac{1}{d}} \left(\frac{\tau}{\tau_0}\right)^{\frac{1}{d-1}}. \tag{2.103}$$

Together with the Dirichlet boundary conditions (2.98), these finiteness conditions ensure that we obtain solutions which are free of naked singularities in the perturbative expansion and which are unique up to terms which are determined by a single coefficient [26]. This coefficient captures the residual gauge freedom of the ingoing Eddington-Finkelstein coordinates which is the reparametrization of the radial coordinate r (without spoiling the manifest translational and rotational symmetries along the transverse directions). Usually, this residual gauge freedom is fixed by setting the radial location of the apparent or event horizon at (2.103) to all orders in the late proper time expansion [112]. Here we consider the example of $d = 4$ to illustrate the

computation of $a_{(i)}$, $l_{(i)}$ and $k_{(i)}$.

The late-time expansion of the six Einstein's equations ($E_{rr}, E_{rt}, E_{tt}, E_{\zeta\zeta}, E_{s_\perp s_\perp}$) based on the ansatz (2.97) along with (2.102), at each subleading order, can be repackaged to the following three equations

$$\begin{aligned} 2k''_{(i)}(x) + l''_{(i)}(x) &= S_{1,i}\,, \\ \left(x^4+3\right)\left(k'_{(i)}(x) - l'_{(i)}(x)\right) + x\left(x^4-1\right)\left(k''_{(i)}(x) - l''_{(i)}(x)\right) &= S_{2,i}\,, \\ \frac{3}{2}x^2 a''_{(i)}(x) - 6x a'_{(i)}(x) + 6a_{(i)}(x) - 2x^5\left(2k'_{(i)}(x) + l'_{(i)}(x)\right) &= S_{3,i} \end{aligned} \tag{2.104}$$

where $S_{1,i}$, $S_{2,i}$ and $S_{3,i}$ are the sources at the i-th order which depend on $a_{(j)}, l_{(j)}, k_{(j)}$ and their derivatives, for $j < i$. Now at each subleading order, the most general solutions to these equations are given by,

$$\begin{aligned} 2k_{(i)}(x) + l_{(i)}(x) &= \rho_i + \alpha_i x + PI_{1,i}\,, \\ k_{(i)}(x) - l_{(i)}(x) &= \xi_i - \frac{\kappa_i}{4}\log(1-x^4) + PI_{2,i}\,, \\ a_{(i)}(x) &= \beta_i x^4 + \alpha_i \frac{x(3+x^4)}{3} + PI_{3,i} \end{aligned} \tag{2.105}$$

where the Greek letters with subscript i correspond to the integration constants at i-th order and $PI_{1,i}, PI_{2,i}$ and $PI_{3,i}$ are the particular solutions determined by the sources $S_{1,i}$, $S_{2,i}$ and $S_{3,i}$ respectively. The expressions for the PIs for $i = 1$ are simple,

$$\begin{aligned} a_{(1)}(x) &= \alpha_1 \frac{x(1+x^4)}{3} + \frac{2x^4(1+x)}{3}, \\ k_{(1)}(x) &= \alpha_1 \frac{x}{3} + \frac{1}{2}g(x), \\ l_{(1)}(x) &= \alpha_1 \frac{x}{3} - g(x) \end{aligned} \tag{2.106}$$

where

$$g(x) = \frac{4}{3}x - \frac{1}{3}\ln(x^2+1) - \frac{2}{3}\ln(x+1) - \frac{2}{3}\arctan x. \tag{2.107}$$

For $i = 2$, the solution is given in the appendix B. The expressions for the particular solution get increasingly complicated at higher orders. However, the simple structure of the homogeneous solution remains the same in every order. The integration constants associated with the homogeneous solutions can be fixed in every order in the following way:

- The fixation of α_i can be done by setting the radial location of the event/apparent horizon at each order as in appendix C. The other way to set this integration constant has been detailed in chapter 4 ((4.83) – (4.85)) which ultimately leads to a fixed location of the event horizon. The same pattern repeats for the rest of $\alpha_{i>2}$.

- The integration constant β_i is fixed by mapping the coefficients of x^4 terms in (2.105) to $a_4(\tau)$, $l_4(\tau)$ and $k_4(\tau)$ of (2.112) and then solving the constraint equations (2.113).

- The constants ρ_i and ξ_i are fixed by demanding that the metric asymptotes to (2.63) at the boundary.

- Finally, the integration constants κ_i are fixed such that the dual geometry is regular at the horizon to all orders.

For $i = 1, 2$, this gives

$$\begin{aligned}
\beta_1 &= \frac{2}{3}, \quad \kappa_1 = 2, \quad \xi_1 = 0, \quad \rho_1 = 0, \\
\beta_2 &= -\frac{1}{54}\left(11 + 6\log(2)\right), \quad \kappa_2 = -\frac{1}{3}(2\log(2) - 3), \quad \rho_2 = -\frac{1}{3}, \\
\xi_2 &= \frac{1}{288} i\Big(- 24\pi\alpha_1 + 48iC - (48 - 96i)\mathrm{Li}_2\left(\frac{1}{2} + \frac{i}{2}\right) + (48 + 96i)\mathrm{Li}_2\left(\frac{1}{2} - \frac{i}{2}\right) + (7 + 6i)\pi^2 \\
&- 96i - 48\pi + 72i\log^2(2) - (24 - 60i)\pi\log(2) + 48\pi\log(2) + 24i\pi\log(1 - i)\Big)
\end{aligned} \tag{2.108}$$

where C is the Catalan's constant, $C = 0.915966$.

One can verify that these solutions reproduce the same late-time expansion of the stress

tensor

$$
\begin{aligned}
T_{\tau\tau} &\approx \tau^{-4/3} - \frac{2}{3}\tau^{-2} + \frac{1+2\log(2)}{18}\tau^{-8/3} + \cdots , && (2.109)\\
T_{\zeta\zeta} &\approx \frac{1}{3}\tau^{2/3} - \frac{2}{3} + \frac{5(1+2\log(2))}{54}\tau^{-2/3} + \cdots , && (2.110)\\
T_{x_\perp x_\perp} &\approx \frac{1}{3}\tau^{-4/3} - \frac{(1+2\log(2))}{54}\tau^{-8/3} + \cdots . && (2.111)
\end{aligned}
$$

It is crucial to emphasize that the residual gauge freedom involving the reparametrization of the radial coordinate is a proper diffeomorphism, i.e. it leaves *both* the boundary metric (which is the flat Milne background (2.52)) and also the $\langle T_{\mu\nu}\rangle$ of the dual Bjorken flow extracted from holographic renormalization *invariant*. It's useful to see this explicitly. For illustration, let's consider the AdS_5 case. We start with the asymptotic expansion of the metric functions, which after solving the Einstein equation (2.91) order by order in r takes the form:

$$
\begin{aligned}
A(r,\tau) &= 1 + r a_1(\tau) + r^2\left(\frac{a_1(\tau)^2}{4} - a_1'(\tau)\right) + r^4 a_4(\tau) + \cdots ,\\
K(r,\tau) &= r a_1(\tau) - r^2\frac{a_1(\tau)^2}{4} + r^3\frac{a_1(\tau)^3}{12} + r^4 k_4(\tau) + \cdots ,\\
L(r,\tau) &= r a_1(\tau) - r^2\left(\frac{a_1(\tau)^2}{4} + \frac{a_1(\tau)}{\tau}\right)\\
&\quad + r^3\left(\frac{a_1(\tau)^3}{12} + \frac{a_1(\tau)^2}{2\tau} + \frac{a_1(\tau)}{\tau^2}\right) + r^4 l_4(\tau) + \cdots . \qquad (2.112)
\end{aligned}
$$

Above, the function $a_1(\tau)$ is related to the residual gauge freedom, and can be chosen arbitrarily. Furthermore, the constraints of Einstein's equations (2.91) impose

$$
\begin{aligned}
a_4'(\tau) &= -\frac{a_1(\tau)^4}{12\tau} - \frac{4}{3\tau}a_4(\tau) - \frac{8}{3\tau}k_4(\tau),\\
l_4(\tau) + 2k_4(\tau) &= -\frac{a_1(\tau)}{\tau^3} - \frac{3}{4}\frac{a_1(\tau)^2}{\tau^2} - \frac{1}{4}\frac{a_1(\tau)^3}{\tau} - \frac{3}{32}a_1(\tau)^4. \qquad (2.113)
\end{aligned}
$$

Using these constraints, one can find via holographic renormalization that

$$\langle T_{\mu\nu}\rangle = \frac{3}{16\pi G_N}\times \begin{pmatrix} -a_4(\tau) & 0 & 0 & 0 \\ 0 & \tau^2\left(a_4(\tau)+\tau a_4'(\tau)\right) & 0 & 0 \\ 0 & 0 & -a_4(\tau)-\frac{1}{2}\tau a_4'(\tau) & 0 \\ 0 & 0 & 0 & -a_4(\tau)-\frac{1}{2}\tau a_4'(\tau) \end{pmatrix}. \tag{2.114}$$

Firstly, the above result is exact to *all* orders in the late proper time expansion. Secondly, we readily find that $\langle T_{\mu\nu}(\tau)\rangle$ is determined by $a_4(\tau)$ alone and is independent of the arbitrary function $a_1(\tau)$ capturing the residual gauge freedom in the asymptotic expansion *after* utilizing the constraints (2.113) in the renormalized Brown-York stress tensor (2.90). Thus $\langle T_{\mu\nu}(\tau)\rangle$ is invariant under the residual gauge transformation. Furthermore, comparing (2.114) with (2.53), (2.54) and (2.55) (for $d = 4$) we find that $\langle T_{\mu\nu}(\tau)\rangle$ takes the general form of the energy-momentum tensor of Bjorken flow with the identification

$$\epsilon(\tau) = -\frac{3}{16\pi G_N}a_4(\tau). \tag{2.115}$$

One can repeat the same exercise in arbitrary dimensions ($d > 2$) and show that $\langle T_{\mu\nu}(\tau)\rangle$ obtained from holographic renormalization takes the general form given by (2.53), (2.54) and (2.55) with the identification

$$\epsilon(\tau) = -\frac{d-1}{16\pi G_N}a_d(\tau) \tag{2.116}$$

where $a_d(\tau)$ is the coefficient of r^d in the asymptotic expansions of $A(r,\tau)$.

Further, extracting $a_d(\tau)$ from (2.102) we obtain that at the leading order in the late proper time expansion

$$\epsilon(\tau) \approx \frac{d-1}{16\pi G_N}\varepsilon_0\left(\frac{\tau_0}{\tau}\right)^{\frac{d}{d-1}} = \frac{d-1}{16\pi G_N}r_h(\tau)^{-d} = \frac{d-1}{16\pi G_N}\left(\frac{4\pi T(\tau)}{d}\right)^d \tag{2.117}$$

where we have used (2.103), and also $\beta = T^{-1} = \frac{4\pi r_h}{d}$ to define an instantaneous Hawking temperature $T(\tau)$ given by

$$T(\tau) = \frac{d}{4\pi}\varepsilon_0^{\frac{1}{d}}\left(\frac{\tau_0}{\tau}\right)^{\frac{1}{d-1}}. \tag{2.118}$$

Once again comparing with the general (hydrodynamic) late proper time expansion (2.57), we find that

$$\epsilon_0 = \frac{d-1}{16\pi G_N}\varepsilon_0. \tag{2.119}$$

For the case of AdS_5, the identification $\frac{1}{G_N} = \frac{2N^2}{\pi}$ implies that at late proper time

$$T(\tau) \approx \frac{1}{\pi}\varepsilon_0^{1/4}\left(\frac{\tau_0}{\tau}\right)^{\frac{1}{3}}, \qquad \epsilon(\tau) \approx \frac{3}{8}\pi^2 N^2 T(\tau)^4 = \frac{3}{8\pi^2}N^2\varepsilon_0\left(\frac{\tau_0}{\tau}\right)^{\frac{4}{3}}. \tag{2.120}$$

For any d, $\epsilon(\tau)$ is given by a perfect fluid expansion given by (2.117) at late time with

$$p_L(\tau) \approx p_T(\tau) \approx \frac{1}{d-1}\epsilon(\tau) \approx \frac{1}{16\pi G_N} r_h(\tau)^{-d}. \tag{2.121}$$

Thus, at late proper time, the energy density $\epsilon(\tau)$ and the pressures $p_L(\tau)$ and $p_T(\tau)$ are thus given by the thermal equation of state obtained from a static black brane geometry, but with a time-dependent temperature (2.118) which satisfy the Euler equations.

2.3 Schwinger Keldysh formalism

In zero temperature quantum field theory, the computation of observables such as S-matrix whose elements are known as scattering amplitudes, is achieved via Lehmann-Symanzik-Zimmermann (LSZ) reduction technique (eg. reader can refer to [113]) to the vacuum expectation value of time-ordered products of field operators. The operators acting on the vacuum state create an asymptotic state that corresponds to particles at infinite past or future. However, for field theory at finite temperatures, the computation of the expectation value of field operators becomes difficult. This is due to random interactions in the medium which do not preserve

the vacuum states. In these cases, Schwinger-Keldysh (SK) formalism (also known as real-time formalism) [58, 114–117] allows the computation of the expectation value of operators with arbitrary states.

The idea of the SK formalism is to construct a real-time contour consisting of two branches labelled as + and − running parallel to the real axis as shown in Fig. 2.7. The + branch runs forward in time and the − branch runs backwards in time which corresponds to time ordering $\mathcal{T}$ and anti-time ordering $\bar{\mathcal{T}}$. This real-time contour formalism introduces the notion of path ordering, P, where the path ordering automatically takes into account both time ordering and anti-time ordering in the following manner,

$$PO(x)O(y) = \begin{cases} \mathcal{T}O(x)O(y) & \text{if} \quad x^0, y^0 \in C_+, \\ \bar{\mathcal{T}}O(x)O(y) & \text{if} \quad x^0, y^0 \in C_-, \\ O(x)O(y) & \text{if} \quad x^0 \in C_-, y^0 \in C_+, \\ O(y)O(x) & \text{if} \quad x^0 \in C_+, y^0 \in C_- \end{cases} \tag{2.122}$$

where we have inserted operators at different positions x and y in the contour to show how path ordering encodes the time and anti-time ordering of the operators. Note in this formalism, the fields on the two branches of the contour are assumed to be distinct.

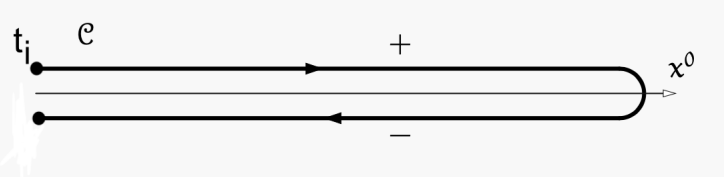

Figure 2.7: Real-time contour in the Schwinger-Keldysh formalism. C is the contour and x_0 is the time. Figure taken from [27].

In this section, we will discuss the computation of the correlation functions using SK formalism and the implementation of SK-contour in bulk geometry. We also briefly mention 2PI effective action.

2.3.1 Correlation functions using the Schwinger Keldysh formalism

Consider a non-equilibrium system whose initial state is defined by the density matrix ρ. The corresponding generating functional of the system is given by,

$$Z[J_+, J_-] = exp(iW[J_+, J_-]) = Tr(\rho P \exp(i \int d^d x (J_+ O_+ - J_- O_-)) \tag{2.123}$$

where P is the path ordering and $J_\pm$ is the source associated with the operator $O_\pm$ at the two branches of the contour, shown in Fig. 2.7. The negative sign in the exponent is due to time reversal in the second contour. The differentiation of this generating functional with respect to the source at each branch gives the real-time correlation function $G(x, y)$ where the correlation function has four components and can be written in matrix form as,

$$G(x, y) = \begin{pmatrix} G_{++}(x, y) & -G_{+-}(x, y) \\ -G_{-+}(x, y) & G_{--}(x, y) \end{pmatrix} \tag{2.124}$$

where,

- $G_{++}(x, y) = -i\langle \mathcal{T}(O_+(x), O_+(y))\rangle$.
- $G_{--}(x, y) = -i\langle \bar{\mathcal{T}}(O_-(x), O_-(y))\rangle$.
- $G_{+-}(x, y) = i\langle O_-(y) O_+(x)\rangle$.
- $G_{-+}(x, y) = i\langle O_-(x) O_+(y)\rangle$.

Here $G_{++}(x, y)$ is the time-ordered correlation function, also known as Feynman propagator, $G_{--}(x, y)$ is the anti-time ordered correlation function and the other two $G_{+-}(x, y)$ and $G_{-+}(x, y)$ are referred as greater and lesser correlation function. These four correlation functions are not independent of each other and they satisfy the following algebraic relation,

$$G_{++}(x, y) + G_{--}(x, y) = G_{+-}(x, y) + G_{-+}(x, y). \tag{2.125}$$

Further the retarded and the advanced propagator $G_R(x,y)$ and $G_A(x,y)$ which are defined as,

$$G_R(x,y) = -i\theta(x^0 - y^0)\langle[O(x), O(y)]\rangle, \tag{2.126}$$

$$G_A(x,y) = -i\theta(y^0 - x^0)\langle[O(y), O(x)]\rangle \tag{2.127}$$

can be expressed in terms of these real-time correlation functions as,

$$G_R(x,y) = G_{++}(x,y) - G_{+-}(x,y), \tag{2.128}$$

$$G_A(x,y) = G_{++}(x,y) - G_{-+}(x,y). \tag{2.129}$$

Above $\theta(x^0)$ is the step function. In the thermal equilibrium case, these correlation functions are further related by the fluctuation-dissipation relation, also known as the Kubo-Martin-Schwinger (KMS) relation which arises from the trace as discussed below. For a system in thermal equilibrium, generally, the SK closed time contour can be taken to be $C = [t_i, t_f] \cup [t_f, t_f - i\sigma] \cup [t_f - i\sigma, t_i - i\sigma] \cup [t_i - i\sigma, t_i - i\beta]$ with $0 \leq \sigma \leq \beta$, as shown in Fig. 2.8.

In this case, the density matrix describing the system is the thermal density matrix ρ_β. For the system in the canonical ensemble, the density matrix ρ_β is defined as,

$$\rho_\beta = \frac{e^{-\beta H}}{\mathrm{Tr}\, e^{-\beta H}}. \tag{2.130}$$

Above β is the inverse of the temperature T and H is the Hamiltonian that governs the dynamics of the system. The expectation value of an operator $O(t)$ [6] (in the Heisenberg picture) in this ensemble is given by

$$\begin{aligned}\langle O(t)\rangle = Tr(\rho_\beta O(t)) = \frac{\sum_n e^{-\beta E_n}\langle n|O(t)|n\rangle}{\sum_n e^{-\beta E_n}} = \frac{\sum_n e^{-\beta E_n}\langle n|e^{iHt}Oe^{-iHt}|n\rangle}{\sum_n e^{-\beta E_n}} \\ = \frac{\sum_n e^{-\beta E_n}\langle n|O|n\rangle}{\sum_n e^{-\beta E_n}},\end{aligned} \tag{2.131}$$

[6] In the limit, $T \to 0$, one can recover the vacuum expectation value, $\lim_{T\to 0} Tr(\rho_\beta O) = \langle O|O|O\rangle$.

where $|n\rangle$ denotes the eigenstates of the Hamiltonian H and E_n the corresponding eigenvalues. We have used $e^{-iHt}|n\rangle = e^{-iE_nt}|n\rangle$ and its conjugate relation above. We note that the expectation value of any operator in the thermal ensemble is time-independent. To compute the thermal correlation functions [59] one can differentiate the generating functional (2.123) with respect to the sources where the density matrix is the thermal density matrix. Then following the discussion in [59], the relation among the correlation functions in momentum space can be written as,

$$\begin{aligned} G_{++}(k) &= Re\, G_R(k) + i \coth\frac{\beta\omega}{2} Im\, G_R(k), \\ G_{+-}(k) &= \frac{2ie^{-(\beta-\sigma)\omega}}{1-e^{-\beta\omega}} Im\, G_R(k), \\ G_{-+}(k) &= \frac{2ie^{-\sigma\omega}}{1-e^{-\beta\omega}} Im\, G_R(k), \\ G_{--}(k) &= -Re\, G_R(k) + i \coth\frac{\beta\omega}{2} Im\, G_R(k) \end{aligned} \tag{2.132}$$

where for $\sigma = \beta/2$ we can obtain a symmetric matrix, $G_{-+}(k) = G_{+-}(k)$. In thermal equilibrium, all correlation functions can be thus obtained simply from the imaginary part of the retarded propagator in momentum space, as the real part of the retarded propagator can be further obtained from the imaginary part via the Kramers-Kronig relation that follows from the causal nature of the retarded correlator which implies that it is analytic in the upper half complex frequency plane.

Note that (2.125), (2.126) and (2.127) hold only for $\sigma = 0$ or $\sigma = \beta$.

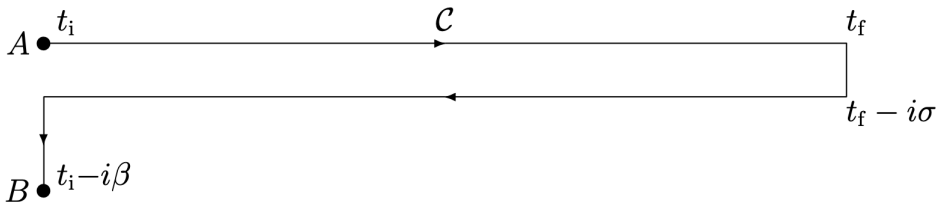

Figure 2.8: Thermal time contour in the Schwinger-Keldysh formalism. Figure is taken from [28].

Kubo-Martin-Schwinger condition

The thermal density operator ρ_β can be viewed as an evolution operator for the imaginary time shift, on which the field operator evolves as,

$$e^{-\beta H} O(x^0 - i\beta, \vec{x}) e^{\beta H} = O(x^0, \vec{x})$$

With this identity and cyclic property of trace one finds that the expectation value of the path-ordered operators obeys the KMS symmetry. For instance, the two-point correlation function obeys the relation,

$$\begin{aligned} \langle O_1(0,\vec{x}) O_2(t,\vec{x})\rangle &= Tr(e^{-\beta H} O_1(0,\vec{x}) O_2(t,\vec{x})) \\ &= Tr(e^{-\beta H} O_1(0,\vec{x}) e^{-\beta H} e^{\beta H} O_2(t,\vec{x})) \\ &= \langle O_2(t - i\beta,\vec{x}) O_1(0,\vec{x})\rangle \end{aligned} \tag{2.133}$$

which implies that the path-ordered correlation of $O_1(0,\vec{x})$ and $O_2(t,\vec{x})$ is periodic. This equality is called the Kubo-Martin-Schwinger (KMS) symmetry and it thus implies periodicity of bosonic correlation functions on the SK contour. For fermions, we have anti-periodicity and similar fluctuation-dissipation relations. More generally, for arbitrary σ, we obtain the relations (2.132) simply by considering the KMS relation in momentum space.

2.3.2 2PI effective action

The classical action $S[\Phi]$ entering the generating functional $Z[J]$ reflects interaction among the fields at the tree level, neglecting the higher-order corrections. However, the higher-order corrections are important to encapsulate various non-equilibrium phenomena such as early thermalisation in heavy ion collision [118]. These higher-order corrections are incorporated in the generating functional via loop corrections. This is achieved by the introduction of *n-particle irreducible (nPI) quantum effective action* which forms a functional integral technique that pro-

duces all orders of interactions solely from the tree-level contributions. The nPI effective action coincides with the classical action at the lowest level of perturbation theory.

The nPI effective action is a powerful non-perturbative approximation scheme that can be used to understand thermalisation as well as far from equilibrium dynamics from the first principle. Based on the discussion in [29], one can formulate the 2PI effective action from the classical action $S[\Phi]$ by doing Legendre transformation of the connected generating functional $W[J,R]$ given as,

$$\begin{aligned} Z[J,R] &= \exp(iW[J,R]) \\ &= \int \mathcal{D}\,\Phi \exp\Big(i\Big[S[\Phi] + \int_x J_a(x)\Phi_a(x) + \int_{xy} \frac{1}{2} R_{ab}\Phi_a(x)\Phi_b(y)\Big]\Big) \end{aligned} \tag{2.134}$$

where Φ_a is the $N-$ component real scalar field, J_a and R_{ab} are the two sources. The corresponding 2PI effective action of this generating functional is defined as,

$$\Gamma[\phi,G] = W[J,R] - \int_x \frac{\delta W[J,R]}{\delta J_a(x)} J_a(x) - \int_{xy} \frac{\delta W[J,R]}{\delta R_{ab}(x,y)} R_{ab}(x,y) \tag{2.135}$$

$$= W[J,R] - \int_x \phi_a(x) J_a(x) - \int_{xy} \phi_a(x)\phi_b(y) R_{ab}(x,y) - \frac{1}{2} Tr(GR) \tag{2.136}$$

where $\phi_a = \frac{\delta W[J,R]}{\delta J_a(x)}$ is the macroscopic field obtained by decomposing the field $\Phi_a(x)$ as $\Phi_a(x) \rightarrow \phi_a(x) + \eta_a(x)$, $\eta_a(x)$ being quantum correction and $\frac{\delta W[J,R]}{\delta R_{ab}(x,y)} = \frac{1}{2}(\phi_a(x)\phi_b(y) + G_{ab}(x,y))$. $G_{ab}(x,y)$ is the connected two-point Green's function. Further, using the definition of $W[J,R]$ one can write the 2PI effective action as,

$$\Gamma[\phi,G] = S[\phi] + \frac{i}{2} Tr \ln G^{-1} + \frac{i}{2} Tr \ln G_0^{-1}(\phi) G + \Gamma_2[\phi,G] + const. \tag{2.137}$$

Here $G^{-1}_{0,ab} = -i\delta^2 S[\phi]/(\delta\phi_a(x)\delta\phi_b(x))$ is the inverse classical propagator and $\Gamma_2[\phi,G]$ relates to the self energy $\Sigma_{ab}(x,y;\phi,G)$ via its functional G derivative i.e., $\Sigma_{ab}(x,y;\phi,G) \equiv 2i\frac{\delta\Gamma_2[\phi,G]}{\delta G_{ab}(x,y)}$. The diagrammatic representation of two-loop and three-loop 2PI effective action along with its self-energy $\Sigma_{ab}(x,y;\phi,G)$ is shown in the Fig. 2.9. The self-energy can be obtained by opening

one propagator line from the graph contributing to $\Gamma_2[\phi, G]$.

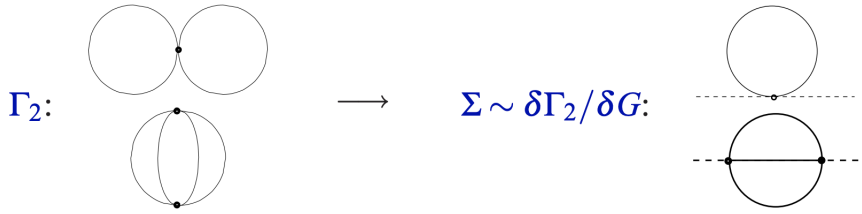

Figure 2.9: The diagram shows a two-loop and a three-loop graph for $\Gamma_2[\phi, G]$ and the corresponding self-energy. The diagram has been taken from [29].

In the case of non-equilibrium dynamics, one needs to specify the initial state given by the density matrix ρ as mentioned above. This density matrix at a given time t_0 can be in mixed state ($Tr\rho^2(t_0 = 0) < 1$) or pure state ($Tr\rho^2(t_0 = 0) = 1$). The corresponding generating functional for the non-equilibrium dynamics at the initial state given by $\rho(t_0 = 0)$ is defined as,

$$Z[J, R, \rho] = Tr\Big\{\rho(0)\mathcal{T}_C e^{i(\int_x J(x)\Phi(x) + \frac{1}{2}\int_{xy} R_{ab}(x,y)\Phi(x)\Phi(y))}\Big\} \tag{2.138}$$

where $\mathcal{T}_C$ is the time ordering along the real time path C, shown in Fig. 2.7. This generating functional can be further factorized into parts one of which includes the initial conditions and the other includes quantum dynamics. The factorization can be achieved by expressing (2.138) in terms of the eigenstate $|\phi^{(i)}\rangle$ of the Heisenberg field operator $\Phi^{(i)}(t = t_0, \mathbf{x})$ at initial time $t_0 = 0$ as,

$$\begin{aligned} Z[J, R, \rho] = \int\ & d\phi^{(1)}(\mathbf{x}) d\phi^{(2)}(\mathbf{x}) \langle\phi^{(1)}|\rho(0)|\phi^{(1)}\rangle \\ & \langle\phi^{(2)}|\mathcal{T}_C e^{i(\int_x J(x)\Phi(x) + \frac{1}{2}\int_{xy} R_{ab}(x,y)\Phi(x)\Phi(y))}|\phi^{(1)}\rangle \end{aligned} \tag{2.139}$$

where $\phi^{(i)}(\mathbf{x})$ are the eigenvalues. Using the time contour 2.7, one can express

$$Z[J, R, \rho] = \underbrace{\int d\phi^{(1)}(\mathbf{x})\, d\phi^{(2)}(\mathbf{x})\, \langle\phi^{(1)}|\rho(0)|\phi^{(1)}\rangle}_{\text{initial condition}} \underbrace{\int_{\phi^{(1)}(\mathbf{x}) = \phi^{(1)}(0^+, \mathbf{x})}^{\phi^{(2)}(\mathbf{x}) = \phi^{(2)}(0^-, \mathbf{x})} \mathcal{D}\phi e^{i(S[\phi] + \int_x J(x)\phi(x) + \frac{1}{2}\int_{xy} R_{ab}(x,y)\phi(x)\phi(y))}}_{\text{quantum dynamics}}. \tag{2.140}$$

After absorbing the contribution from the initial states in the sources J and R, one can obtain the 2PI effective action $\Gamma[\phi, G]$ for a closed time path using this generating functional (2.140).

The 2PI effective action formalism in thermal equilibrium recovers the standard form of fluctuation-dissipation relation from the evolution equation of the propagator G [29]. While in non-equilibrium, we get an exact coupled evolution equation which is equivalent to any kind of identity of two-point Greens function such as Schwinger-Dyson/Kadanoff-Baym equations. In [119], Cox and Berges showed that the Kadanoff-Baym equations can be treated numerically and also found that the studied scalar field reaches thermal equilibrium even in 1 + 1 dimensions, even though there is no binary collision on the level of Boltzmann equations. It was also shown in [120] that for a chiral quark meson model in 2PI formalism, the pre-thermalisation of various essential observables occurs on time scales shorter than thermal equilibration time. Moreover, the 2PI formalism provides an efficient framework to understand in and out of equilibrium quantum fields using suitable resummation techniques [29]. This resummation allows to compute self-consistent n-point functions to the desired accuracy. Fig. 2.10 shows large-N resummation in the $O(N)$ scalar field.

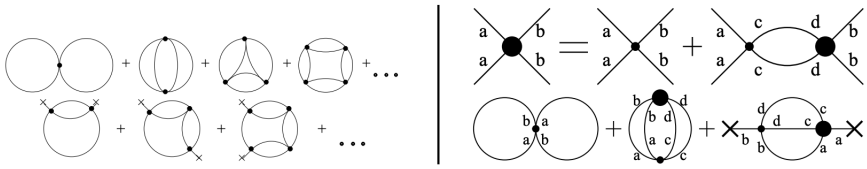

Figure 2.10: The left figure shows 2PI effective action to NLO in $1/N$ consists of an infinite series of diagrams which can be resummed by introducing self-consistent coupling, marked by big dots in the right figure. The diagram has been taken from [30].

2.3.3 Bulk dual of Schwinger Keldysh contour

The gauge/gravity duality discussed above suggests the computation of boundary correlation function from the gravity side by identifying the on-shell action of the bulk field with the generating functional of the field theory. Owing to this duality, it seems natural to implement the Schwinger Keldysh contour in the bulk and compute the real-time correlation function from the on-shell action. For the equilibrium state, the construction of contour in the bulk and computation of the respective correlation function is a complete story. However, the challenge lies in defining the real-time correlation function of the SK- contour in out-of-equilibrium situations.

The first step towards the implementation of the Schwinger-Keldysh contour in the bulk is due to Son and Herzog [59]. They mapped the Schwinger Keldysh contour at thermal equilibrium (Fig. 2.8) with the eternal black hole geometry (Fig. 2.11). The two boundaries of the geometry are identified with the forward and backward arms of the Schwinger-Keldysh contour with the backward arm displaced by $-i\beta/2$ (note $\beta = T^{-1}$) along the imaginary axis. For a $d+1-$ dimensional asymptotic AdS space, the metric defining the eternal black hole geometry reads as,

$$ds^2 = -f(r)dt^2 + \frac{dr^2}{f(r)} + r^2 d\vec{x}^2 \tag{2.141}$$

where $f(r)$ has zero at the event horizon r_h i.e., at $r = r_h$ and the inverse of temperature β is given by $\beta = \frac{4\pi}{f'(r_0)}$. The singularity at the horizon due to $f(r)$ motivates change of coordinate to Kruskal coordinate U and V defined as,

$$U = -e^{-\frac{2\pi}{\beta}u}, \qquad V = e^{\frac{2\pi}{\beta}v}, \qquad \text{for R-region,} \tag{2.142}$$

$$U = e^{-\frac{2\pi}{\beta}u}, \qquad V = -e^{\frac{2\pi}{\beta}v}, \qquad \text{for L-region.} \tag{2.143}$$

Here $v = t + r_*$ and $u = t - r_*$ are like the ongoing and outgoing coordinates. r_* is the tortoise

coordinate which near the horizon has the behaviour,

$$r_* = \frac{\beta}{4\pi} \log(r - r_h) + \cdots . \tag{2.144}$$

This coordinate removes the singularity and one can go beyond the horizon. For shift in time, $t \to t + \alpha$, we find that

$$U \to e^{-\frac{2\pi}{\beta}\alpha} U \qquad \text{and} \qquad V \to e^{\frac{2\pi}{\beta}\alpha} V \tag{2.145}$$

whose effect in the R-region and L-region is opposite. This shows that t increases in the R-region while decreases in the L-region. Note that the expression of U and V in the L-region can be simply obtained from the R-region by taking $t \to t - i\beta/2$. With t being opposite on both the sides, one can identify the full extended black hole geometry with the Schwinger Keldysh contour 2.8, provided $\sigma = \beta/2$. Then the correlation function can be computed by following the standard AdS/CFT procedure of obtaining the on-shell action which gets contribution from the boundary solution only.

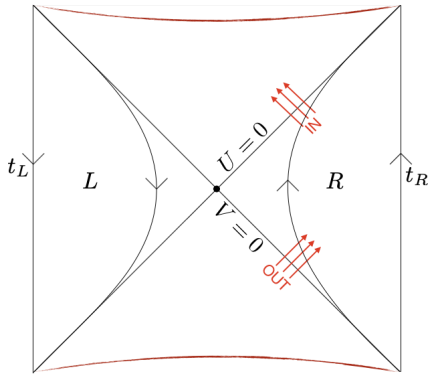

Figure 2.11: The figure shows the Penrose diagram for the eternal Schwarzschild AdS black hole. The red lines on the top and the bottom represents singularities. The solid line that meets at 45° is the horizon that meets at the bifurcation surface at the centre. L and R are the asymptotic regions outside the black hole. Figure taken from [28].

Further, to compute the bulk field solution of the whole geometry one can follow the trick of obtaining the solution in one region and then analytically continue it to the other. For example, for a bulk scalar field, the solution of the Klein-Gordon equation can be written as a

linear combination of two independent solutions χ_1 and χ_2, which near the boundary satisfies the condition

$$\lim_{r\to\infty}\chi_1(r,x)=\phi_1(x) \qquad \text{and} \qquad \lim_{r\to\infty}\chi_2(r,x)=\phi_2(x) \tag{2.146}$$

where $\phi_1(x)$ and $\phi_2(x)$ are the boundary sources. Near the horizon, the solutions in the R-region behave as,

$$\chi_1 = e^{-i\omega u} = e^{-i\omega v}(r-r_h)^{\frac{i\beta\omega}{2\pi}} \qquad \text{and} \qquad \chi_2 = e^{-i\omega v} \tag{2.147}$$

where modes depending on u are outgoing and on v are ongoing. Here we have used $u = v-\frac{\beta}{2\pi}\log(r-r_h)$. Following the prescription in [121], one can analytically continue this solution to L-region for arbitrary σ. The analytic continuation of $v\to v-i\sigma$ and $(r-r_h)\to e^{-2\pi i}(r-r_h)$ implies that the solution in the L-region differs from the R-region by a factor of $e^{\beta\omega}e^{-\sigma\omega}$ for χ_1 and $e^{-\sigma\omega}$ for χ_2,

$$\chi_1 = \left((r-r_h)^{\frac{i\beta\omega}{2\pi}}e^{-i\omega v}\right)e^{\beta\omega}e^{-\sigma\omega} \qquad \text{and} \qquad \chi_2 = e^{-i\omega v}e^{-\sigma\omega}. \tag{2.148}$$

Then with the solution of the entire geometry, one can compute the generating functional at the boundary by integrating over the bulk field with the source as a boundary condition.

The most concrete prescription of boundary SK-contour for real-time gauge-gravity duality for general initial states is due to Skenderis and van Rees [31, 61, 122]. The overall idea of the prescription is as follows, the gravity side SK-contour is constructed by associating the real-time branch of the dual SK-contour with the Lorentzian spacetime and the imaginary-time branch with the Euclidean spacetime. The different branches are then joined together using appropriate matching conditions, roughly, the bulk field and its derivative have to be continuous along the glueing surface. The arbitrary initial state defined by the density operator ρ is prepared in the Euclidean path integral and the generating functional for the entire contour is written as a combination of the Euclidean and Lorentzian path integral. Using this full path integral one

can follow the standard technique to compute the generating functional (2.123). Further by differentiating this generating functional with the two sources defined at the boundary one can obtain real-time correlation functions. However, in this construction, it is not easy to compute the generic initial states using Euclidean path integrals.

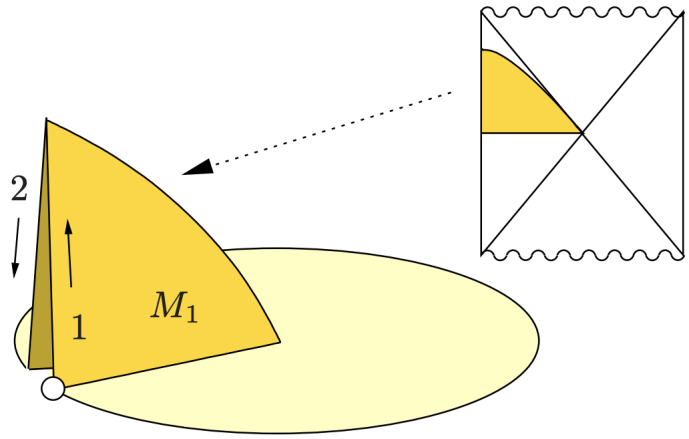

Figure 2.12: The two Lorentzian segments M_1 and M_2 which are the two copies of a part of an eternal black hole correspond to the two branches of the dual SK- contour. The vertical segment in Fig. 2.8 is filled in with Euclidean black hole solution which topologically fills the imaginary time circle with a disk. The Lorentzian segments are added to the Euclidean black hole solution by making a cut in the disk, up to the centre of the disk. Thus, completing the construction of the SK contour in the bulk. Figure taken from [31].

Recently, Crossley-Glorioso-Liu (CGL) gives the simple horizon cap prescription to realize Schwinger Keldysh contour in the bulk at thermal equilibrium [17]. The horizon cap prescription connects two copies of a complexified black brane geometry defined in Eddington Finkelstein (EF) gauge at the horizon r_h via anti-clockwise rotation of 2π. Here $\sigma = 0$, as there is no analytic continuation of the ingoing coordinate in EF gauge. Further, to have the same orientation in the fully complexified spacetime, the direction of the v coordinate is reversed. This construction will be discussed in detail in chapter 5 and will be extended to out-of-equilibrium bulk geometry to compute hydrodynamic real-time correlation functions.

Chapter 3

MIS formalism of superfluidity

Superfluidity, as defined in [123] is a frictionless flow of conserved charges. The superfluid phase was first discovered in the helium isotopes [53,54] where the liquid helium at low pressure and absolute zero temperature showed frictionless (zero viscosity) flow through a thin capillary tube. Here the conserved charge is considered to be the mass or the atoms of the helium. The phase transition of helium from normal fluid to superfluid phase, especially Helium-4, can be attributed to the formation of condensate below the transition temperature, where the helium atoms can occupy a single quantum state. This phase transition associated with conserved charges of the system can be characterized by the symmetry of the system. In the superfluid phase, the symmetry of the system accompanied by the conserved charges is spontaneously broken.

The theory of superfluidity studies hydrodynamics describing normal fluids with continuous symmetry breaking by including dynamics of Goldstone modes[1] with the hydrodynamic degree of freedom. Superfluidity can exist for a large variety of systems with different characteristic temperature scales below which the transition to superfluid phase occurs. For instance, ultra-cold atomic gases, dense quarks and nuclear matter below certain critical temperature show superfluidity.

[1] As per Goldstone's theorem [124–127], Goldstone modes are gapless excitations in the long-wavelength limit which exist due to spontaneous breaking of continuous symmetry.

In general, superfluid phase transitions in out-of-equilibrium systems is of interest for the physics of heavy-ion collisions [128, 129], cold atoms [130] and the early Universe [131]. Given the success of hydrodynamic theories for understanding out-of-equilibrium matter with both weak and strong self-interactions, there is sufficient motivation to construct frameworks that can describe superfluids by incorporating Goldstone mode(s) and the order parameter(s) (condensate(s)) associated with spontaneous breaking of global internal symmetries in hydrodynamic theories. Recently the demonstration of the ubiquitous presence of *hydrodynamic attractors* in a wide variety of phenomenological frameworks (eg. kinetic theory, holography, etc) has given us insights into how a system *hydrodynamizes* far away from equilibrium such that first order hydrodynamics can describe the evolution of the energy-momentum tensor and conserved currents even in presence large pressure gradients [23, 25, 132, 133]. It is therefore pertinent to ask if one can construct similar frameworks that incorporate Goldstone boson(s) and order parameter(s) along with hydrodynamic modes for superfluid states far from equilibrium.

A general framework for superfluids at finite density has its roots in the pioneering work of Son [15] (and generalized to finite temperature by Nicolis [14]), which utilized the quantum effective action for describing the low energy dynamics of the Goldstone bosons and superfluid vortices. An attractive feature of Son's approach is that the only microscopic input needed is simply the equation of state of the system at finite chemical potential and temperature (see [134] for a survey of related approaches and a broader discussion). Remarkably, the thermodynamic description emerges naturally from the energy-momentum tensor and conserved currents obtained from the quantum effective action and is not imposed by hand. The original context in which Son developed this approach was to describe baryonic matter at finite baryon density with spontaneous breaking of $U(1)$ baryon symmetry relevant for physics of neutron stars. Recently, generalizations of the quantum effective action have been studied incorporating both the pions and the hydrodynamic modes at finite chemical potential and temperature [52]. Further extensions to the case of phases with spontaneous spacetime symmetry breaking such as supersolids, etc [135–138] have been investigated as well but this is beyond the scope of this work.

In this work, we include the order parameter and add dissipation by merging the Son-Nicolis framework with the Müller-Israel-Stewart (MIS) formalism [2, 42] enabling a causal description. We use this to study symmetry breaking in out-of-equilibrium situations in the context of Bjorken flow. The study of evolution of many-body systems under Bjorken flow is particularly of interest not only for heavy-ion physics [133], but also for cold atomic systems in anisotropic laser traps [139, 140]. We restrict ourselves here to the case of a $U(1)$ symmetry breaking but our work can be easily generalized to non-Abelian cases.

At early time, the size of the expanding system undergoing Bjorken flow is sufficiently small so that fluctuations are significant. Therefore we should study the evolution of the system with generic initial conditions for the energy-momentum tensor, conserved currents and the condensate. Remarkably, we find that as long as we start above the critical temperature, T_c, the condensate decays exponentially while the phase evolves over a similar timescale to satisfy the Josephson condition. Then the full system gets trapped very close to a conventional *hydrodynamic attractor* over a very long period of time during which the system approaches a perfect fluid expansion with unbroken symmetries.

However, the long time physics is somewhat surprising. It turns out that the superfluid system has an even number of symmetry breaking non-dissipative fixed points in which the full system undergoes expansion at a *constant* temperature (determined by the equation of state and the potential) and with a *constant* value of the condensate. These fixed points are possible because the condensate lowers the energy with respect to the vacuum, allowing the expanding system to maintain a self-consistent constant temperature (with a non-trivial velocity profile). We find that with inital $T > T_c$ and otherwise generic initial conditions, the superfluid system switches rapidly to one of these symmetry breaking fixed points after spending a time in very close proximity to the conventional *hydrodynamic attractor*. The basin of attraction of these fixed points has complicated interlacing and possibly fractal boundaries. If $T < T_c$ initially, then the superfluid system generically evolves to one of the fixed points without getting trapped near the hydrodynamic attractor (unless the initial condition is close to the boundary between

the basins of attraction of the fixed points).

Summary of results

Our work demonstrates that the evolution of superfluid matter out of equilibrium is governed by the conventional hydrodynamic attractor with unbroken symmetry (which is rather like a saddle curve in the extended phase space) and non-trivial symmetry breaking fixed points which are determined by the potential of the condensate and the equation of state. The hydrodynamic attractor governs physics at intermediate time scales if the initial temperatures are above T_c, while the fixed points govern the physics at much longer time scales with a (typically) rapid crossover.

We observe that the symmetry breaking fixed points are independent of the relaxation mechanism, and are determined only by the equation of state and the potential of the condensate. Furthermore, the hydrodynamic attractor is a feature in any phenomenological framework incorporating relaxation as mentioned above. Therefore, the dynamical features of superfluid flow, especially with respect to the role of the hydrodynamic attractor and the fixed point should be universal.

However, if there is competition between various types of symmetry breaking as in neutron stars and some strongly correlated systems, we will need to incorporate a more general framework discussed in [141–143] that can couple multiple (super)fluids. This is beyond the scope of our present work. We also postpone a discussion regarding the relevance of our results for the quark-gluon plasma until the concluding section.

We also analyze the linearized perturbations around thermal equilibrium and show that the fixed points are unstable against inhomogeneous perturbations that should lead to spinodal decomposition. This can be studied using our MIS framework, which we postpone to future work.

The organization of the chapter is as follows. In section 3.1, we discuss the construc-

tion of the MIS theory of superfluids. In section 3.2, we derive the equations for Bjorken flow and then present our results in section 3.3. We further analyze the system by considering linearized perturbations in section 3.4.

3.1 The MIS formulation of superfluid effective theory

3.1.1 Effective action

The MIS formalism [2, 42] enables a causal description of a relativistic hydrodynamic system. In order to generalize this approach to a relativistic superfluid, we utilize aspects of the effective theory of superfluids due to Son and Nicolis [14, 15] at finite temperature. Furthermore, we include the order parameter as a dynamical variable to incorporate the possibility of out-of-equilibrium phase transition.

For simplicity, consider a complex field $\Sigma \equiv \rho e^{i\psi}$ charged under $U(1)$ global symmetry which is broken spontaneously below a critical temperature T_c due to the potential $V(\rho, \dots)$ where $\dots$ denote other variables of the effective theory. Crucially, the velocity u^μ and temperature T of the local thermal frame appear together as a new fundamental variable β^μ. Note that in this approach (local) thermodynamics emerge from the effective action and is not imposed separately. We first succinctly show how this works.

Due to Lorentz invariance, the effective action in a background metric $g_{\mu\nu}$ and gauge field A_μ (introduced to allow us to compute the energy-momentum tensor and conserved current efficiently) can depend on β^μ only via the *temperarture* T and *chemical potential* μ defined by the relations $T := (-\beta^\mu g_{\mu\nu}\beta^\nu)^{-1/2}$ and $\mu/T := A_\mu\beta^\mu$, respectively, at leading order in derivatives. Similarly, due to $U(1)$ gauge and Lorentz invariance, the dependence on Σ can be via the scalars $X := (D_\mu\Sigma)^\dagger(D^\mu\Sigma)$ and $Y := ((\beta\cdot D)\Sigma)^\dagger((\beta\cdot D)\Sigma)$, where

$$D_\mu\Sigma = (\nabla_\mu + iA_\mu)\Sigma = (\partial_\mu\rho + i\rho D_\mu\psi)e^{i\psi} \tag{3.1}$$

with $D_\mu\psi := \nabla_\mu\psi + A_\mu$ and ∇_μ is the covariant derivative constructed from the background metric. It will turn out (from absence of entropy production) that $(u \cdot D)\psi = 0$, i.e. $(u \cdot \nabla)\psi = \mu$ (a.k.a. the Josephson condition) must be satisfied in equilibrium while $\rho = \rho_*$, a constant, so that Y must vanish. On the other hand, we will find that X can assume an arbitrary non-trivial profile in equilibrium due to non-vanishing of derivatives of ψ in directions orthogonal to the four-velocity $u^\mu \equiv T\beta^\mu$. Since Y must vanish at equilibrium, we will drop it and retain X, T and μ as fundamental variables. Additionally we incorporate the gauge-invariant variable ρ to implement spontaneous symmetry breaking. Since derivatives of ρ (and ψ) appear in X, we must think of X and ρ as independent variables.[2]

We therefore consider an effective action of the form:

$$S = \int d^4x\sqrt{-g}\,[F(X,T,\mu) - V(\rho,T,\mu)] \tag{3.2}$$

where F is the kinetic piece of the action and V is the symmetry breaking potential. Simple instances of F and V are

$$F = -\frac{1}{2}X + p(T,\mu), \quad V(\rho,T,\mu) = \frac{\sigma(T-T_c)}{2}\rho^2 + \frac{\lambda}{4}\rho^4 \tag{3.3}$$

in which $\sigma, \lambda > 0$ and are both independent of T and μ. In Son's approach where only the dynamics of the Goldstone mode are considered [15], the condensate is set to its equilibrium value. The dependence of the generalized pressure F on the chemical potential μ then also determines its X dependence. In our case, the condensate is an independent variable and we truncate our theory to two-derivatives. To relate to Son's approach, we can simply expand the generalized pressure F in derivatives of the condensate and normalize the latter to get a standard two-derivative kinetic term. This leads to our simple ansatz (3.3). In what follows for the rest of this section, we consider a general $F(X,T,\mu)$.

[2]Note that as in a classical scalar field theory, ρ and its conjugate field momentum should also be thought of as independent variables since we need to set their initial conditions independently to specify an evolution. This implies that X and ρ should be thought of as independent variables.

3.1.2 Ideal hydrodynamics and thermodynamics

The *ideal* superfluid energy-momentum tensor and conserved $U(1)$ current can be readily obtain by varying the action (3.2) w.r.t. $g_{\mu\nu}$ and A_μ respectively:

$$T^{\mu\nu}_{\text{ideal}} \equiv \frac{2}{\sqrt{-g}}\frac{\delta S}{\delta g_{\mu\nu}} = -2\frac{\partial F}{\partial X}\left(\nabla^\mu\rho\nabla^\nu\rho + \rho^2 D^\mu\psi D^\nu\psi\right) + (F-V)\Delta^{\mu\nu} + u^\mu u^\nu\left(T\frac{\partial}{\partial T} + \mu\frac{\partial}{\partial\mu} - 1\right)(F-V), \tag{3.4}$$

$$j^\mu_{\text{ideal}} \equiv \frac{1}{\sqrt{-g}}\frac{\delta S}{\delta A_\mu} = \frac{\partial(F-V)}{\partial\mu}u^\mu + \rho^2 D^\mu\psi, \tag{3.5}$$

respectively with $\Delta^{\mu\nu} = g^{\mu\nu} + u^\mu u^\nu$. Each of these can be rewritten as sum of a normal and a coherent superfluid component. Explicitly,

$$T^{\mu\nu}_{\text{ideal}} = T^{\mu\nu}_n - 2\frac{\partial F}{\partial X}\left(\nabla^\mu\rho\nabla^\nu\rho + \rho^2 D^\mu\psi D^\nu\psi\right), \quad T^{\mu\nu}_n := \mathcal{E}u^\mu u^\nu + P\Delta^{\mu\nu}, \quad j^\mu_{\text{ideal}} = j^\mu_n + j^\mu_\psi, \quad j^\mu_n := \mathcal{N}u^\mu \tag{3.6}$$

where $j^\mu_\psi := \rho^2 D^\mu\psi$ and

$$P := F - V, \quad \mathcal{E} := \left(T\frac{\partial}{\partial T} + \mu\frac{\partial}{\partial\mu} - 1\right)(F-V), \quad \mathcal{N} := \frac{\partial(F-V)}{\partial\mu} = \frac{\partial P}{\partial\mu}. \tag{3.7}$$

With the entropy density $\mathcal{S}$ defined as

$$\mathcal{S} := \frac{\partial P}{\partial T}\Big|_{\mu\text{ fixed}}, \tag{3.8}$$

the relations (3.7) imply the standard thermodynamic identity

$$P = -\mathcal{E} + T\mathcal{S} + \mu\mathcal{N}. \tag{3.9}$$

Note that P is distinct from p which appears in (3.3) as it is the generalized pressure which governs the normal fluid component. The coherent part in (3.4) which is proportional to $D^\mu\psi D^\nu\psi$

can be reinterpreted as a second fluid with a velocity field proportional to $D^\mu\psi$ and with an independent free energy. We refer the reader to [123, 141, 142] for more details. Note in our case we will also need a third fluid component with velocity field proportional to $\nabla^\mu\rho$ as evident from (3.4). However, such reinterpretations will not be necessary in what follows.

Varying the effective action (3.2) w.r.t. Σ, we obtain the equations of motion for ρ and ψ which are

$$2\nabla_\mu\left(\frac{\partial F}{\partial X}\nabla^\mu\rho\right)+\frac{\partial V}{\partial\rho}-2\rho\frac{\partial F}{\partial X}D_\mu\psi D^\mu\psi=0,\quad\text{and}\quad\nabla_\mu j^\mu_\psi=0. \tag{3.10}$$

The above equations of motion, in conjunction with $\nabla_\mu T^{\mu\nu}_{\text{ideal}}=0$ and $\nabla_\mu j^\mu_{\text{ideal}}=0$, imply the Euler equations

$$\nabla_\mu(\mathcal{S}u^\mu)=0,\quad\nabla_\mu(\mathcal{N}u^\mu)=0,\quad(T\mathcal{S}+\mu\mathcal{N})(u\cdot\nabla)u^\mu=-\left(\mathcal{S}\nabla^\mu_\perp T+\mathcal{N}\nabla_\perp{}^\mu\mu\right) \tag{3.11}$$

where $\nabla^\mu_\perp\equiv\Delta^{\mu\nu}\nabla_\nu$.

3.1.3 Adding dissipation

In order to further extend the effective theory, we need to add dissipation. This is achieved by adding additional terms to the energy-momentum tensor and the conserved current, which we denote as $\pi^{\mu\nu}$ and q^μ respectively, and which can be expanded in the form of derivatives of the Goldstone, velocity and temperature fields. The latter are called *constitutive relations* which should be determined/constrained by enforcing the existence of an entropy current with non-negative divergence. We therefore begin by writing

$$T^{\mu\nu}_n=\mathcal{E}u^\mu u^\nu+Pg^{\mu\nu}+\pi^{\mu\nu},\quad T^{\mu\nu}=T^{\mu\nu}_n-2\frac{\partial F}{\partial X}\left(\nabla^\mu\rho\nabla^\nu\rho+\rho^2D^\mu\psi D^\nu\psi\right),\quad j^\mu_n=\mathcal{N}u^\mu+q^\mu,\quad j^\mu=j^\mu_n+j^\mu_\psi \tag{3.12}$$

with $\mathcal{E}$, P and $\mathcal{N}$ as defined in (3.7). We choose a generalization of the Landau frame to define u^μ in the non-ideal case, so that $\pi^{\mu\nu}u_\nu=0$. Furthermore, we modify (3.10) by adding dissipative

sources θ_1 and θ_2 to the equations of motion of ρ and ψ respectively, so that

$$2\nabla_\mu\left(\frac{\partial F}{\partial X}\nabla^\mu\rho\right)+\frac{\partial V}{\partial\rho}-2\rho\frac{\partial F}{\partial X}D_\mu\psi D^\mu\psi=\theta_1,\quad \nabla_\mu j^\mu_\psi=\theta_2. \tag{3.13}$$

The above in conjunction with $\nabla_\mu T^{\mu\nu}=0$ and $\nabla_\mu j^\mu=0$ imply

$$\begin{aligned} T\nabla_\mu(\mathcal{S}u^\mu) &= -\theta_1(u\cdot\nabla)\rho-(\mu+(u\cdot D)\psi)\theta_2-\pi^{\mu\nu}(\nabla_\mu u_\nu)+\mu(\nabla\cdot q), &(3.14)\\ (\mathcal{S}T+\mathcal{N}\mu)(u\cdot\nabla)u^\mu &= -\mathcal{S}\nabla_\perp{}^\mu T-\mathcal{N}\nabla_\perp{}^\mu\mu-\nabla_{\perp\nu}\pi^{\mu\nu}+\theta_1\nabla_\perp{}^\mu\rho+\theta_2 D_\perp{}^\mu\psi &(3.15)\end{aligned}$$

where $D_\perp{}^\mu=\Delta^{\mu\nu}D_\nu$. As a consequence, we obtain a candidate entropy current $j^\mu_s=\mathcal{S}u^\mu-(\mu/T)(q^\mu+j^\mu_\psi)$ whose divergence turns out to be

$$\nabla_\mu j^\mu_s=-\frac{1}{T}(\nabla_\mu u_\nu)\pi^{\mu\nu}-((q+j_\psi)\cdot\nabla)\frac{\mu}{T}-\frac{1}{T}\theta_1(u\cdot\nabla)\rho-\frac{1}{T}\theta_2(u\cdot D)\psi. \tag{3.16}$$

The appropriate constitutive relations that lead to the positive definite divergence of the entropy current is then

$$\pi^{\mu\nu}=-2\eta\sigma^{\mu\nu}-\zeta\Delta^{\mu\nu}(\nabla\cdot u),\quad q^\mu+j^\mu_\psi=-\kappa\nabla^\mu\left(\frac{\mu}{T}\right),\quad \theta_1=-\kappa_1(u\cdot\nabla)\rho,\quad \theta_2=-\kappa_2(u\cdot D)\psi \tag{3.17}$$

with κ, η, ζ, κ_1 and κ_2 positive definite functions of T and μ (and in principle of ρ too). Also

$$\sigma^{\mu\nu}:=\frac{1}{2}\Delta^{\mu\alpha}\Delta^{\nu\beta}(\nabla_\alpha u_\beta+\nabla_\beta u_\alpha)-\frac{1}{3}\Delta^{\mu\nu}\nabla_\alpha u^\alpha$$

is the shear-stress tensor. We note that the constitutive relation for q^μ implies that the conserved $U(1)$ current is

$$j^\mu=nu^\mu-\kappa\nabla^\mu\left(\frac{\mu}{T}\right). \tag{3.18}$$

We readily validate our earlier claim from (3.16) and (3.17) that in equilibrium where entropy production is absent, we should satisfy the Josephson condition $(u\cdot D)\psi=0$, i. e. $(u\cdot\nabla)\psi=\mu$.

Furthermore, (3.13) implies that at equilibrium ρ should be in the (thermal) vacuum so that $\partial V/\partial\rho = 0$ in absence of spatial gradients of ψ. Note when $\nabla_{\perp\mu}\psi\nabla_{\perp}{}^{\mu}\psi \neq 0$, e. g. a constant, we can have ρ taking values away from the minima of V in equilibrium at any T and μ.

Finally in order to develop a MIS-type formulation, we simply replace the constitutive relations for $\pi^{\mu\nu}$ and j^{μ} in (3.17) by the dynamical equations

$$\begin{aligned}(u\cdot\nabla)(q^{\mu}+j^{\mu}_{\psi})+\frac{1}{\tau_q}(q^{\mu}+j^{\mu}_{\psi}) &= -\frac{1}{\tau_q}\kappa\nabla^{\mu}\left(\frac{\mu}{T}\right),\\ (u\cdot\nabla)\pi^{\mu\nu}+\frac{1}{\tau_\pi}\pi^{\mu\nu} &= -\frac{1}{\tau_\pi}\left(2\eta\sigma^{\mu\nu}+\zeta\Delta^{\mu\nu}\nabla\cdot u\right),\end{aligned} \tag{3.19}$$

with τ_π and τ_q being additional parameters that depend on T and μ (and in principle also on ρ). Clearly after the timescale of the respective relaxation times, $\pi^{\mu\nu}$ and $q^{\mu}+j^{\mu}_{\psi}$ will relax to their respective constitutive relations (3.17). This completes the construction of the MIS formalism for effective description of a relativistic superfluid. Finally we note that our construction is not quite reliable at very low temperatures where higher derivative terms can contribute also to the relaxation processes. In this context, one may use the formalism discussed in [144]. We can choose parameters such that for generic initial conditions with supercritical temperature (and also with a range of subcritical temperatures), the system never reaches sufficiently small temperatures while undergoing Bjorken flow.

3.2 Bjorken flow

In order to study Bjorken flow we need to consider the Milne background

$$\mathrm{d}s^2 = -\mathrm{d}\tau^2+\mathrm{d}x^2+\mathrm{d}y^2+\tau^2\mathrm{d}\xi^2 \tag{3.20}$$

and set $u^{\mu}=(1,\vec{0})$. Furthermore, we should consider all other variables $T,\mu,\rho,\psi,\pi^{\mu\nu}$ and q^{μ} to be dependent only on the proper time τ.

For a concrete example, let us consider F and V to be of the form given in (3.3). We further set $\mu = 0$ and $p = T^4$ as in a conformal equation of state. Conformality implies that

$$\eta = \frac{4}{3} C_\eta T^3, \quad \tau_\pi = \frac{C_{\tau\pi}}{T}, \quad \kappa_1 = C_{\kappa 1} T, \quad \kappa_2 = C_{\kappa 2} T^3 \tag{3.21}$$

where C_η, etc are constants and we set $\zeta = 0$. Note that $C_\eta = \eta/s$. Alternatively, we can parameterize[3] $\kappa_1 = C_{\kappa 1} T_c$ and $\kappa_2 = C_{\kappa 2} T_c^3$. None of the qualitative features that will feature in our discussion will depend on the details of such parametrizations. Denoting $\tau-$derivatives via a prime, the equations of motion (3.10) now take the form

$$\rho'' + \frac{\rho'}{\tau} + \lambda\rho^3 + \sigma(T - T_c)\rho - \rho\psi'^2 = -C_{\kappa 1} T \rho', \tag{3.22}$$

$$(\rho^2 \tau \psi')' = -C_{\kappa 2} T^3 \tau \psi'. \tag{3.23}$$

Furthermore, we consider a diagonal form of $\pi^{\mu\nu}$:

$$\pi^{\mu\nu} = \text{diag}\left(0, \frac{\Pi}{2}, \frac{\Pi}{2}, -\frac{\Pi}{\tau^2}\right). \tag{3.24}$$

It is convenient to use the dimensionless pressure anisotropy $\chi := 3\Pi/4T^4$. The conservation of the energy-momentum tensor $T^{\mu\nu}$ given in (3.12) provides the equation for the evolution of the temperature

$$\frac{\tau T'}{T} = \frac{1}{3}(\chi - 1) + \sigma \frac{\rho^2 + 2\tau\rho\rho'}{8T^3} + \frac{\tau}{4T^3}\left(C_{\kappa 1}\rho'^2 + C_{\kappa 2} T^2 \psi'^2\right). \tag{3.25}$$

Assuming p to be conformal, it is natural to modify the MIS equation (3.19) by replacing $u \cdot \nabla$ on the LHS with a Weyl-covariant derivative as in BRSSS formalism [1] so that the evolution

[3] In general η/s will be a complicated function of σ/T and T_c/T. The first parametrization (3.21) of η etc. is relevant at high temperatures when there is asymptotic freedom. At lower temperatures, the second parametrisation is relevant if $\sigma << T_c$.

of Π in terms of χ is given by

$$\tau\chi' + \frac{4}{3}\left(\chi - \frac{C_\eta}{C_{\tau\pi}}\right) + 4\chi\frac{\tau T'}{T} + \frac{\tau}{C_{\tau\pi}}\chi T = 0. \tag{3.26}$$

As such, we have a five-dimensional phase space given by T, χ, ψ', ρ and ρ' when we set $\mu = 0$ (for simplicity).

3.3 Results

Superfluid Bjorken flow has formidable complexity, but the results are best understood by considering possible attractor or saddle surfaces/curves/points first. It is easy to note from our equations that we can always consistently set $\Sigma = 0$. The evolution of T and χ are then exactly same as the case of ordinary Bjorken flow discussed in [25]. It is well known that the system flows to a unique hydrodynamic attractor curve given by $\chi_{\text{att}}(\tau T)$. However, we find this curve is actually a meta-stable curve near the $\Sigma = 0$ surface: typical solutions will approach this surface before departing at late times.

In addition, we find that the system has two fixed points! To see this we set for the moment $T = t_* T_c$, $\chi = 0$ (since any fixed point cannot have dissipation) and note that the equations of motion have solutions with $\psi' = 0$ and

$$\rho = \pm\rho_* = \pm\sqrt{\frac{\sigma T_c(1 - t_*)}{\lambda}} \tag{3.27}$$

since $\partial V/\partial\rho = 0$ at $\rho = \pm\rho_*$. Note setting ψ constant implies that we are moving on a line in the complex Σ plane, so ρ can assume any sign[4]. The equation for T given by (3.25) determines t_* via

$$\frac{1 - t_*}{t_*^3} = \frac{8\lambda T_c^2}{3\sigma^2} \tag{3.28}$$

[4]The situation is similar to motion to pure radial motion in a central potential with vanishing angular momentum. The constant radial coordinate $\phi = \phi_0$ jumps by π once the particle crosses the origin. If we want to keep ϕ continuous, then we can simply allow the radial coordinate to assume both signs.

in which we take $0 \leq t_* < 1$.

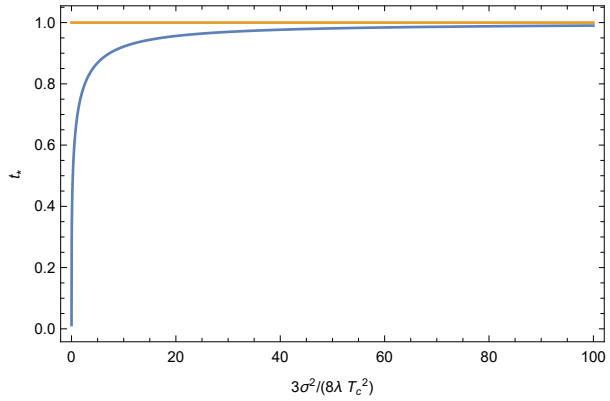

Figure 3.1: There is always a solution to (3.28) with $0 \leq t_* < 1$.

In Fig. 3.1, we see that irrespective of our choice of constants (σ, λ, T_c), we are always able to find a real solution within this range. Choosing $T_c = \sigma = \lambda = 1$, we find that $t_* \approx 0.551847$ and $\rho_* \approx 0.669442$.

The reader may readily note that (3.28) orginates from a specific choice of the equation of state i.e. $p(T)$. Also the fixed point is determined only by the quantum effective action (the ideal component) and is independent of the relaxation terms. The existence of such fixed points should therefore be generic in the Bjorken flow equations of the superfluid. The reason that such fixed points with constant temperature can exist in this expanding superfluid droplet is simply because the energy gained by non-reduction of temperature is compensated by the lower energy of the expanding vacuum with broken symmetry. Generally, of course the system will have even number of such fixed points since the symmetry breaking vacuua are doubly degenerate for fixed ψ and for any acceptable solution of t_*. At these symmetry breaking fixed points there is no entropy production because $\rho' = \psi' = \pi^{\mu\nu} = q^\mu = 0$. Since these are fixed points of an expanding system (with non-trivial velocity profile), these are not thermal.

We are now ready to report our results. The system of equations for the simple case (3.3) which give the evolution of (T, χ, ρ, ψ) under Bjorken flow with vanishing μ are (3.22), (3.23), (3.25) and (3.26). We recall that the phase space is five-dimensional when $\mu = 0$ with coordinates T, χ, ρ, ρ' and ψ'. The characteristics of the evolution of the system, however,

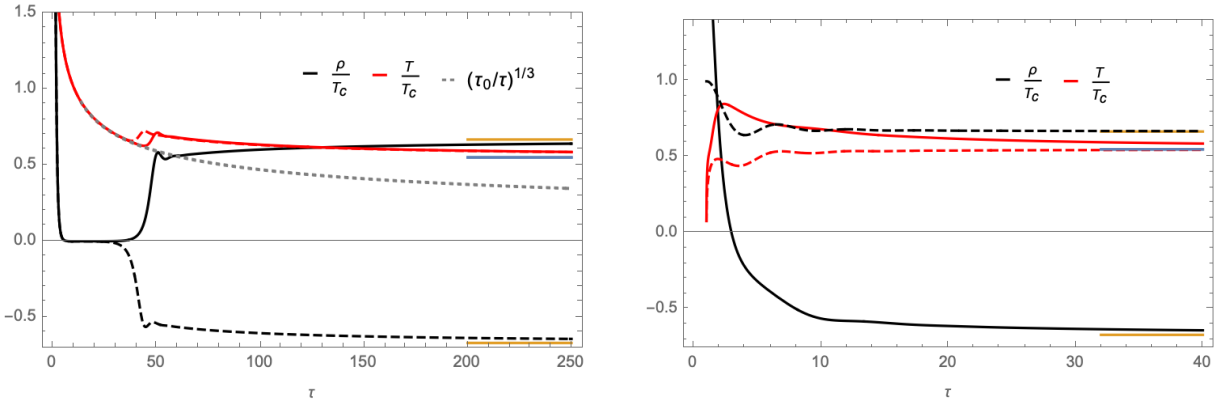

Figure 3.2: Evolution of the condensate and temperature for initial $T > T_c$ (left) and $T < T_c$ (right) for two different initial values of ρ, distinguished by solid and dashed lines. In the left panel with initial values of ρ as 1.947 and 1.954 (corresponding to the solid and dashed lines, respectively), at early times, the temperature (red lines) quickly goes to perfect-fluid type expansion $T \approx \tau^{-1/3}$ (shown as a gray dashed line) before switching to one of the symmetry breaking points at late time. This switching time corresponds to the rapid growth of the condensate, ρ, shown in black. At late times, both T and ρ asymptote to their respective final values, $t_\star$ and $\pm\rho_\star$, which we denote in both plots as blue and orange lines, respectively. In the right panel corresponding to initial values of ρ as 2 and 1 (solid and dashed lines, respectively), with initial $T < T_c$, the condensate rapidly approaches its asymptotic value. The evolution of the temperature is non-monotonic even at early times. In these plots $t_* \approx 0.551847$ and $\rho_* \approx 0.669442$ and we start with $\rho' = \psi' = 0$ and $\chi = 1$.

depend only on whether we initialize with $T > T_c$ or $T < T_c$.

For the purpose of generating plots, we choose $C_\eta = 1/(4\pi)$ and $C_{\tau\pi} = (2 - \ln 2)/(2\pi)$ as obtained by matching MIS with the holographic description of $\mathcal{N} = 4$ SYM theory at infinite 't Hooft coupling and for infinite number of colors [25]. Also we choose $C_{\kappa 1} = C_{\kappa 2} = 1$, and $\sigma = \lambda = 1$ in units $T_c = 1$. Likewise, we will count our proper time, τ, in units of $T_c = 1$.

Case 1 – initially $T > T_c$: In this case, the typical evolution of the system is as shown in the left panel of Fig. 3.2. Early on, both ρ and ψ' vanish very rapidly, particularly $\rho \approx \tau^{-1/2} e^{-\sqrt{\sigma T_c}\tau}$. The system approaches the $\Sigma = 0$ surface (with $\rho = \rho' = \psi' = 0$) where the evolution is purely hydrodynamic. As a result, the system gets trapped near the hydrodynamic attractor curve $\chi_{\rm att}(\tau T)$ where there is no symmetry breaking (ρ remains exponentially small). The entrapment occurs for a long time during which the system approaches a perfect fluid type expansion ($T \approx \tau^{-1/3}$) due to its evolution close to the attractor curve. However, at late time the system suddenly

reheats quickly and switches to one of the symmetry breaking fixed points with $T = t_* T_c$ and $\rho = \pm\rho_*$ (with $\psi' = 0$ and $\chi = 0$). Note that during the entire evolution of the system, the temperature remains above $t_* T_c$, including during the switching between the hydrodynamic attractor behavior and the final approach to its asymptotic value.

In Fig. 3.3, we further illustrate the above by fixing the initial temperature to $2T_c$ and initializing with $(\rho', \psi', \chi) = (0, 0, 1)$, but varying the initial value of ρ. As mentioned above, the qualitative features do not change if we choose initial values of T, ρ', ψ' and χ differently as long as $T > T_c$ initially. For any initial value of ρ, the system gets trapped close to the vertical $\rho = 0$ line, representing the hydrodynamic attractor curve where we have perfect-fluid like expansion $T \approx \tau^{-1/3}$ for a considerable time (see the inset) until it switches to one of the symmetry breaking fixed points marked with red and cyan colors. Varying initial values of ρ, we find alternating intervals in which the system chooses one of these fixed points at late times. The switching time depends on the initial condition and increases with the inital value of T very rapidly.

To study the basin of attraction of the fixed points, we fix the initial values $(\rho', \psi', \chi) = (0, 0, 1)$ and vary initial values of T and ρ. We readily observe from Fig. 3.4 that for initial values of T and $|\rho|$ greater than about $5T_c$ and $7T_c$, respectively, the basin of attraction of these two fixed points (marked with yellow and blue for ρ_* and $-\rho_*$, respectively) are interlaced in a complex manner, making long term prediction difficult. It is likely that the basin boundaries are fractal in these regimes.

We emphasize that even if the system is initialized with non-vanishing ρ' and ψ', it rapidly approaches the hydrodynamic attractor curve with vanishing Σ and lingers there for a long duration of time before rapidly switching to one of the fixed points. The basin of attraction of the fixed points has similar features.

If we start from the boundary of the basin of attraction of the two fixed points initially, then the system should get trapped by the hydrodynamic attractor curve on the vanishing Σ surface (with $\rho = \rho' = \psi' = 0$) and would asymptotically approach it without switching to any

of the fixed points.

Case 2 – starting with $T \leq T_c$: The evolution is qualitatively different to the previous case, although the system settles to one of the fixed points for a generic initial condition. As shown in Fig. 3.2, the temperature behaves non-monotonically at initial time even if we start with $T \approx t_* T_c$. The condensate ρ approaches $\pm\rho_*$ while ψ' and χ vanishes over the same timescale. Thus, the system approaches one of the fixed points without getting trapped near $\Sigma = 0$, unless the initial condition is close to the boundary of the basin of attraction as demonstrated in Fig. 3.3. In the latter case, the system evolves close to the hydrodynamic attractor for a certain period of time. This is expected because if we start from the boundary of the basins of attraction, then the system should approach the hydrodynamic attractor curve in the long run instead of evolving to one of the fixed points. We readily observe from Fig. 3.4 that the projections of the basin of attraction on $T - \rho$ plane separates into two simply connected regions.

In the following section, we analyze the MIS theory about thermal equilibrium and argue that the fixed points are actually unstable against inhomogeneous perturbations. The fate of this instability can be studied using our MIS framework.

3.4 Linearized fluctuations

Here, we compute the linearized fluctuations around thermal equilibrium at zero chemical potential. Note that in this section we are not considering an expanding fluid and we use the standard Minkowski coordinates. We show that the broken phases with $T \leq t_* T_c < T_c$ (with $t_* T_c$ corresponding to the value of the temperature at the fixed point of the Bjorken flow) are unstable in our MIS theory. While the non-hydrodynamic relaxation poles remain on the lower half-plane of complexified frequency, the speed of sound, the diffusion constant and the sound attenuation coefficient change sign at $T = t_* T_c$ and thus are negative for $T < t_* T_c$. This hydrodynamic instability should lead to spinodal decomposition [145, 146].

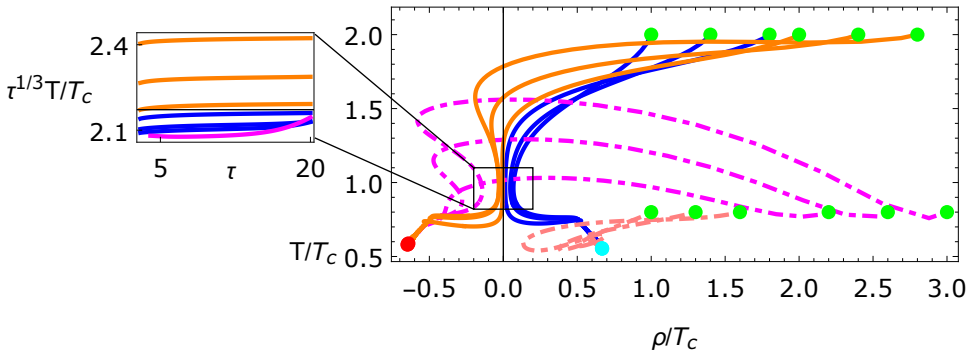

Figure 3.3: The evolution of the system is shown on the $T-\rho$ plane, a two-dimensional projection of the phase space. The initial values of T and ρ are marked by green dots and for all cases initial values of ρ', ψ' and χ are 0, 0 and 1, respectively. At late times, the system chooses one of the two fixed points marked in red and cyan. When $T = 2T_c$ initially, we find that the system quickly evolves to the vertical $\rho = 0$ line and gets trapped there for intermediate times. The inset plot shows that during this time $T \approx \tau^{-1/3}$ indicating that the system evolves close to the hydrodynamic attractor curve on $\Sigma = 0$ surface (with $\rho = \rho' = \psi' = 0$). If we start with $T = 0.8T_c$, then the system does not get trapped by the hydrodynamic attractor curve but merely passes through the vertical $\rho = 0$ line (except if we start close to the border separating the basin of attraction of the two fixed points, as shown by the magenta line in the inset).

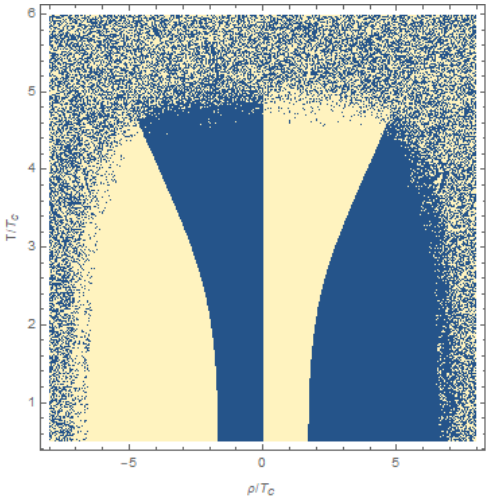

Figure 3.4: The projection of the basin of attractions of the two fixed points on the $T-\rho$ plane are shown here. The color coding is yellow for $+\rho_\star$ and blue for $-\rho_\star$. Note that below a certain value of temperature, there is a clear separation between a choice of initial conditions determining which $\rho_\star$ the system will evolve to. This is not the case for higher temperatures and higher $|\rho|$, where predictability from the initial conditions becomes difficult. The boundary of the basins of attraction is possibly a fractal at higher tempertures.

Without loss of generality, we take the momentum of the fluctuation in the z-direction. After recasting the equations of motion, (3.22) and (3.23), energy momentum tensor conservation (3.25) and MIS equation (3.26) in Minkowski coordinates and linearizing, we see that these equations are linear in $V \equiv (\delta T, \delta\rho, \delta\psi, \delta u, \delta\pi)$ in Fourier space. We can recast the equations in matrix form $Q(\omega, k) \cdot V = 0$, where Q is a 5×5 matrix. We find the dispersion relations by setting the determinant of Q to zero. The perturbations of the hydrodynamic variables are given by

$$\text{shear:} \quad \pi^{zx} \sim \delta\pi^{zx} e^{-i\omega t + ikz} \quad \text{and} \quad u^x \sim \delta u^x e^{-i\omega t + ikz}, \tag{3.29}$$

$$\text{sound:} \quad T \sim T_0 + \delta T e^{-i\omega t + ikz}, \quad \pi^{zz} \sim \delta\pi^{zz} e^{-i\omega t + ikz} \quad \text{and} \quad u^z \sim \delta u^z e^{-i\omega t + ikz}. \tag{3.30}$$

The fluctuations in the scalar sector are

$$\rho \sim \rho_0 + \delta\rho e^{-i\omega t + ikz} \quad \text{and} \quad \psi \sim \psi_0 + \delta\psi e^{-i\omega t + ikz}. \tag{3.31}$$

We distinguish between the broken and unbroken phase by the equilibrium value of the condensate.

3.4.1 Unbroken phase

When $\rho_0 = 0$, we are in the unbroken phase, $T > T_c$. In this case, the determinant of Q factors neatly into the phase, condensate and hydrodynamic dispersions. Since ρ_0 vanishes, the dispersion of the phase is trivial. We find the expected sound and shear modes of a conformal system (with $\eta = C_\eta T_0^3$)

$$\omega_{sound} = \pm\frac{k}{\sqrt{3}} - \frac{i\eta k^2}{2T_0^4} + O\left(k^3\right), \quad \text{and} \quad \omega_{shear} = -\frac{3i\eta k^2}{2T_0^4} + O(k^3), \tag{3.32}$$

as well as the non-hydrodynamic modes: one from the MIS equation and two from the scalar field

$$\omega_{relaxation} = -\frac{i}{\tau_\pi} + \mathcal{O}(k^2), \tag{3.33}$$

$$\omega_{scalar} = -\frac{1}{2}\left(i\kappa_1 \pm \sqrt{4\sigma(T_0 - T_c) - \kappa_1^2}\right) + \mathcal{O}\left(k^2\right), \tag{3.34}$$

respectively. Note that the superfluid mode is overdamped when $\kappa_1 > \sqrt{2\sigma(T_0 - T_c)}$.

3.4.2 Broken phase

Next, we turn our attention to the broken phase, $T < T_c$, and $\rho_0 = \pm\sqrt{\frac{\sigma(T_c - T_0)}{\lambda}}$. The dispersion relation of the phase is now no longer trivial, indicating the presence of a Goldstone mode

$$\rho_0^2(\omega^2 - k^2) + i\kappa_2\omega = 0. \tag{3.35}$$

Clearly we get two modes which at low k take the form

$$\omega_{diffusion} = -i\frac{\rho_0^2}{\kappa_2}k^2 + \mathcal{O}(k^4), \quad \omega_{relaxation} = -i\frac{\kappa_2}{\rho_0^2} + \mathcal{O}(k^2). \tag{3.36}$$

Thus one behaves as a diffusion mode (which has also been found in a hybrid system of a scalar field and holography in semihologaphic framework [16]) and the other as a relaxation mode in both sound and shear channels.

The shear sector in the broken phase with perturbations (3.29) has the following determinant

$$0 = \left(w^2 - k^2 - m_\sigma^2 + i\kappa_1\omega\right)\left(T_0\omega(\tau_\pi\omega + i)\left(8T_0^3 - 3\rho_0^2\sigma\right) - 6\eta k^2\right), \tag{3.37}$$

where we introduced the mass of the condensate, $m_\sigma^2 := 3\lambda\rho_0^2 + \sigma(T_c - T_0) = 4\sigma(T_c - T_0)$. The determinant factorizes into the condensate and hydrodynamic modes. For small k, we see that

the shear modes are

$$\omega_{QNM} = \frac{1}{2}\left(-i\kappa_1 \pm \sqrt{4m_\sigma^2 - \kappa_1^2}\right) + O(k^2), \tag{3.38}$$

$$\omega_{shear} = -\frac{6i\lambda\eta k^2}{8\lambda T_0^4 - 3\sigma^2(T_c - T_0)T_0} + O(k^3), \tag{3.39}$$

as well as the MIS mode (3.33). We call the first mode quasi-normal mode (QNM) simply because it has both real and imaginary parts at zero momentum (no analogy with black hole QNMs are implied here). We note that the diffusion constant has a pole in T_0 precisely when $T_0 = t_* T_c$ and its sign changes as we further lower T_0. A negative diffusion constant leads to what is known as uphill diffusion (against the concentration gradient) enhancing inhomogeneities and thus spinodal decomposition. As a side remark, the two scalar (condensate) modes become one diffusive mode in the limit $m_\sigma^2 \to 0$ (see the Goldstone sector discussed above), which in the context of the chiral phase transition can be thought of as the transition from pion propagating modes to the diffusive quark mode [147]. Of course, in the present context, we are working with a complex scalar field and not attempting to capture the $O(4)$ dynamics relevant for the chiral phase transition.

Finally, in the sound channel with perturbations (3.30), the dispersion takes the following form

$$\begin{aligned}
0 = {} & 48\eta k^2 \lambda T_0 \omega \left(4k^2\lambda T_0^2 - 8\lambda\sigma T_0^3 - 4\lambda T_0^2\left(-2\sigma T_c + w^2 + i\kappa_1 w\right) - \sigma^3 T_0 + \sigma^3 T_c\right) \\
& - (\tau_\pi w + i)\left(8\lambda T_0^3 + 3\sigma^2 T_0 - 3\sigma^2 T_c\right)\Big[- k\left(8k\lambda T_0^4 + 3k\sigma^2 T_0(T_0 - T_c)\right)\left(k^2 + 2\sigma(T_c - T_0) - w^2 - i\kappa_1 w\right) \\
& - 6T_0^2 w^2\left(-4k^2\lambda T_0^2 + 8\lambda\sigma T_0^3 + 4\lambda T_0^2\left(-2\sigma T_c + w^2 + i\kappa_1 w\right) + \sigma^3 T_0 - \sigma^3 T_c\right)\Big]
\end{aligned} \tag{3.40}$$

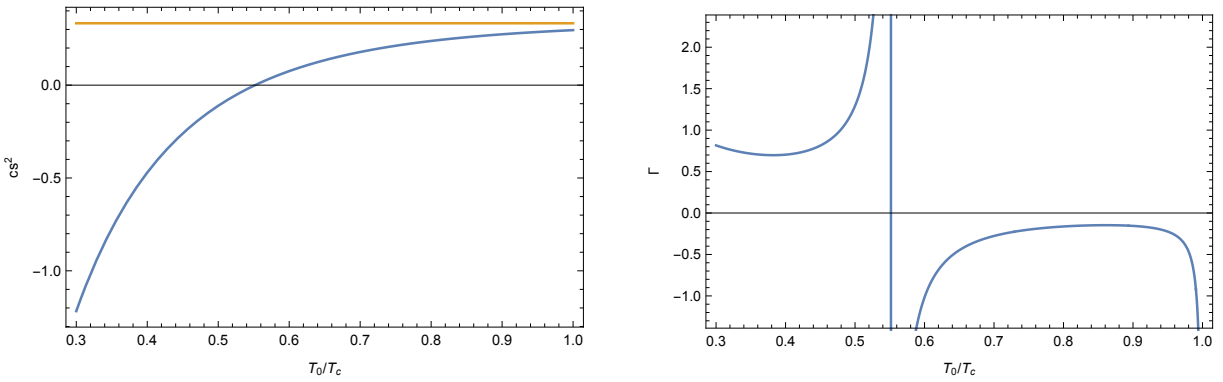

Figure 3.5: Left: the square of the speed of sound as a function of equilibrium temperature. As $T_0 \to t_* T_c$, the speed of sound vanishes, while as T_0 approaches the critical temperature T_c, it grows and monotonically reaches the conformal value, $1/3$. Right: the sound attenuation coefficient as a function of equilibrium temperature, which grows negative and large as T_0 approaches $t_* T_c$.

We see that in the small k limit, we have the following modes

$$\omega_{sound} = \pm c_s k - i\Gamma k^2 + O(k^3), \quad c_s^2 := \frac{8\lambda T_0^3 - 3\sigma^2(T_c - T_0)}{24\lambda T_0^3 + 3\sigma^2 T_0},$$
$$\Gamma := \frac{4\eta\lambda}{8\lambda T_0^4 - 3\sigma^2(T_c - T_0)T_0} + \frac{\kappa_1 \sigma \left(8\lambda T_0^3 - 3\sigma^2(T_c - T_0)\right)}{12 T_0 (T_c - T_0)\left(\sigma^2 + 8\lambda T_0^2\right)^2}, \tag{3.41}$$
$$\omega_{QNM} = \frac{1}{2}\left(-i\kappa_1 \pm \sqrt{-\kappa_1^2 + 8\sigma(T_c - T_0) + \frac{\sigma^3(T_c - T_0)}{\lambda T_0^2}}\right) + O(k^2). \tag{3.42}$$

Above, the first mode is clearly the sound mode but the square of the speed of sound c_s^2 becomes negative for $T_0 < t_* T_c$ triggering spinodal decomposition. In Fig. 3.5, we plot c_s^2 and the sound attenuation coefficient Γ which behaves similarly as the diffusion coefficient in the shear sector, diverging at $T_0 = t_* T_c$ and becoming negative as we further lower T_0.

We note that the instabilities occur only in the hydrodynamic sound and shear modes only for $T_0 \leq t_* T_c$. This indicates that the fixed points of the Bjorken flow could be unstable against inhomogeneous perturbations. However, when we start with supercritical temperatures (and a range of subcritical temperatures), the temperature remains above $t_* T_c$ for its entire evolution for a large class of initial conditions. We would like to investigate the fate of the instabilities of the fixed points using an appropriately modified MIS framework in the future.

Chapter 4

Schwinger Keldysh correlation function of Bjorken flow

One of the outstanding issues in the holographic duality, that maps strongly interacting quantum systems to semi-classical gravity in one higher dimension, is to understand the dictionary in real-time. The applications of the holographic approach to many-body physics are especially limited without explicit and implementable prescriptions for computing out-of-equilibrium correlation functions. Even in the weak-coupling limit, these correlation functions are fundamental tools for studying decoherence and thermalization, e.g. to understand how the commutator and the anti-commutator evolve to satisfy the fluctuation-dissipation relation leading to the emergence of the Kubo-Martin-Schwinger periodicity at an appropriate temperature, and how the occupation numbers of quasi-particles equilibrate or evolve to new fixed points [29, 116, 148, 149]. These correlation functions are actually indispensable for understanding dynamics far away from equilibrium in the strong coupling limit where the system cannot be described by quasi-particles. Although one can compute the one-point functions such as the energy-momentum tensor in real time using the correspondence between time-dependent geometries with regular horizons and states in the dual theory, with the remarkable fluid-gravity correspondence [1, 18, 38, 83] providing a primary example, and numerical relativity [112] pro-

viding a powerful tool, an explicit computation of a generating functional for hydrodynamic Schwinger-Keldysh correlation functions, as for instance, has not been achieved yet.[1]

As discussed in section 2.3, the object of interest is the generating functional

$$\exp(iW[J_1, J_2]) = \mathrm{Tr}\left(\hat{\rho}_0\, T_c \exp\left(-i \oint \mathrm{d}t \int \mathrm{d}^{d-1}x\; J(t,\mathbf{x})\hat{O}(t,\mathbf{x})\right)\right) \tag{4.1}$$

in the dual field theory, where $\hat{\rho}_0$ denotes the initial density matrix, $\oint$ the closed time Schwinger-Keldysh contour composed of the forward and backward arms — $\oint = \int_{-\infty}^{\infty} + \int_{\infty}^{-\infty}$, where the source $J(t,\mathbf{x})$ is specified such that it is $J_1(t,\mathbf{x})$ and $J_2(t,\mathbf{x})$ on the forward and backward arms of the contour, respectively, and T_c denotes contour ordering. Formally, we can rewrite the density-matrix as

$$\hat{\rho}_0 = \int [\mathcal{D}\phi_1][\mathcal{D}\phi_2]\; \rho_0(\phi_1,\phi_2)\, |\phi_1\rangle\langle\phi_2| \tag{4.2}$$

in terms of a basis $|\phi\rangle$ of field configurations, and construct the kernel

$$\mathcal{K}(\phi_1,\phi_2;J_1,J_2) = \langle\phi_2|T_c \exp\left(-i \oint \mathrm{d}t \int \mathrm{d}^{d-1}x\; J(t,\mathbf{x})\hat{O}(t,\mathbf{x})\right)|\phi_1\rangle. \tag{4.3}$$

Then the functional $W[J_1, J_1]$ can be obtained from

$$\exp(iW[J_1, J_2]) = \int [\mathcal{D}\phi_1][\mathcal{D}\phi_2]\; \rho_0(\phi_1,\phi_2)\mathcal{K}(\phi_1,\phi_2;J_1,J_2). \tag{4.4}$$

When $\hat{\rho}_0$ is the thermal density matrix, this computation simplifies drastically. One needs to just add an appendage of length T^{-1} at the end of the closed real time contour parallel to the negative imaginary axis, and impose periodic boundary conditions on the full contour implementing KMS periodicity [152].

[1] A limited number of observables can still be computed analytically or numerically. The equal time two-point functions can be computed via the geodesic approximation when the operator has a large scaling dimension, even out of equilibrium. The out-of-equilibrium retarded correlation function can also be computed by implementing linear causal response appropriately – see [150] for a general prescription. Furthermore, equal-time Green's function can be computed for operators with large anomalous scaling dimensions in the geodesic approximation and has been used to understand thermalization [151].

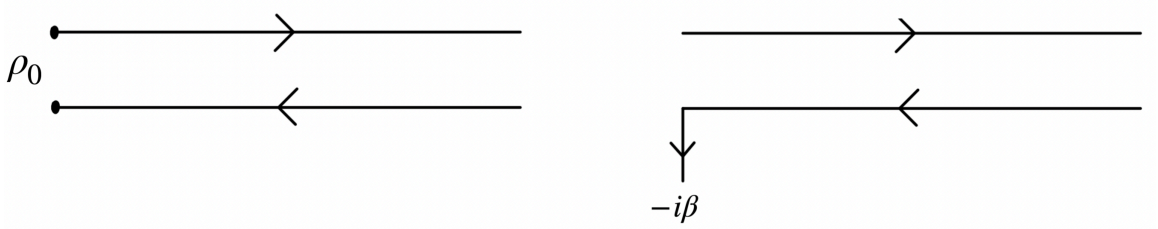

Figure 4.1: Left: The general Schwinger-Keldysh contour for an arbitrary initial density matrix $\hat{\rho}_0$. Field configurations need to be specified at the two ends of the closed time contour which are represented in bold. Right: In thermal equilibrium this simplifies. One needs an appendage to the contour extending along negative imaginary axis by $\beta = T^{-1}$ and then impose periodic boundary conditions for the full contour.

One can also expect a similar simplification for the Bjorken flow which provides the simplest example for evolution of an expanding system on the forward light cone (see Sec 2.1.4 for details). The state is assumed to have boost invariance, and also translational and rotational invariance along the transverse plane so that the energy-momentum tensor can be expressed only in terms of the energy density $T_{\tau\tau} = \epsilon(\tau)$ via Ward identities, where $\tau = \sqrt{t^2 - z^2}$ is the proper time of an observer co-moving with the flow and z being the longitudinal coordinate along which the expansion happens. At late time, $\epsilon(\tau)$ is described by hydrodynamics and thus it reaches a perfect fluid expansion, so that

$$\epsilon(\tau) \approx \epsilon_0 \left(\frac{\tau_0}{\tau}\right)^{\frac{d}{d-1}} . \tag{4.5}$$

In the hydrodynamic regime, it can be described by a single constant parameter, namely

$$\mu := \epsilon_0 \tau_0^{\frac{d}{d-1}} . \tag{4.6}$$

The full hydrodynamic series for $\epsilon(\tau)$ in powers of $\tau^{-\frac{d-2}{d-1}}$ (essentially a derivative expansion) is given in terms of μ (which is determined by initial conditions) and the transport coefficients which are determined by the fundamental microscopic theory. In this case, it is natural to ask whether there can be a simpler computation of the Schwinger-Keldysh partition function of $W[J_1, J_2]$ in the hydrodynamic limit, since just like the thermal case, the state can be essentially captured by a single parameter.

More generally, we would expect that general methods for computing $W[J_1, J_2]$ would exist in the hydrodynamic regime where the energy-momentum tensor and conserved currents are described only by the hydrodynamic variables, namely the four velocity $u^\mu(t, \mathbf{x})$, the energy density $\epsilon(t, \mathbf{x})$ (or equivalently the temperature $T(t, \mathbf{x})$), etc., and we would not require the knowledge of the detailed (off-diagonal) matrix elements $\rho(\phi_1, \phi_2)$ of the state or the kernel $\mathcal{K}(\phi_1, \phi_2; J_1, J_2)$ explicitly. In fact, $W[J_1, J_2]$ is related to the generalization of the thermodynamic free energy to hydrodynamics via Legendre transform, and the latter especially in the context of macroscopic spacetime configurations of conserved currents is also known as the large deviation functional [153] which can be computed in many models studied in classical non-equilibrium statistical mechanics.[2]

The primary aim of this chapter is to show how the explicit computation of $W[J_1, J_2]$ can be achieved by holographic methods in the hydrodynamic limit of the Bjorken flow. We will also present concrete steps for understanding how to go beyond the hydrodynamic limit and *recover* the initial state.

4.0.1 A brief historical review and summary of results

The first major advance in understanding thermal real-time correlation functions in holography was the Son-Starinets prescription for computing the retarded correlation function, according to which the ingoing boundary condition at the horizon implements the causal linear response in the classical gravity (large N and infinite strong coupling) approximation [155]. Using the Chesler and Yaffe method for causal time evolution in the bulk [112], this approach was suitably generalized to compute the out-of-equilibirum retarded correlation function in holography [150]. The first concrete implementation of the Schwinger-Keldysh contour in holography is due to Son and Herzog utilizing the eternal black hole geometry [59]. The two boundaries of

[2]The large deviation functional gives the probability for a macroscopic spacetime profile of a conserved charge or current density which does not necessarily satisfy the hydrodynamic equations. In a quantum system, the off-diagonal matrix elements in the basis of macroscopic field configurations for the conserved charges and currents eventually decohere, but the decoherence would be of interest. See [154] for a recent discussion on possibility of a quantum generalization of large deviation functional methods.

the eternal black hole were shown to provide the forward and backward arms of the Schwinger-Keldysh closed time contour with the backward arm displaced by $-i\beta/2$ (note $\beta = T^{-1}$) along the imaginary axis.

The most concrete prescription for real time gauge-gravity duality for general initial states is due to Skenderis and van Rees [31, 61]. This, however, requires detailed understanding of the state in terms of semiclassical field configurations of dual gravity, and is best defined for states which can be constructed using Euclidean path integrals. In this prescription, one explicitly constructs the bulk geometry corresponding to the boundary Schwinger-Keldysh contour with specified sources, and extends data on the field theory contour into the bulk in an appropriate manner. It is however, not easy to apply this approach to realistic computations for generic initial states. Furthermore, as mentioned above, we would expect a simpler approach in the hydrodynamic regime. We will compare this approach with ours in sec 4.5.

Our method is based on generalizing the recently proposed horizon cap prescription due to Crossley, Glorioso and Liu (CGL) [17] for the static black brane dual to the thermal state. Here the Schwinger-Keldysh contour is realized by a *horizon cap*, in which the ingoing Eddington-Finkelstein radial coordinate goes around the horizon in the complex plane in a little circle of radius ϵ (not to be confused with the energy density) before going back to the real axis and reaching the second boundary. Thus the two arms of the Schwinger-Keldysh contour at the two boundaries are connected continuously in the bulk through the bulk radial contour. The horizon cap implements the appropriate analytic continuation of bulk fields from one arm of the bulk geometry to the other with the sources J_1 and J_2 are specified independently at the two boundaries.

We provide a novel, elegant and simple proof that the CGL horizon cap prescription reproduces the KMS periodicity which relates the different Schwinger-Keldysh correlation functions, and furthermore also reproduces the Son-Starinets prescription for the retarded correlation function at arbitrary frequency and momenta. These were earlier verified only to the quadratic order in frequency [17]. Our proof relies on a simple and novel matrix factorization of ther-

mal correlation functions. This matrix factorization is crucial for the extension of the CGL method to the out-of-equilibrium hydrodynamic Bjorken flow and also for performing crucial consistency checks of the prescription as mentioned below.

The primary tool for extending the CGL prescription into the hydrodynamic regime is the existence of a Weyl rescaling of the Bjorken flow such that the temperature along with the energy and entropy densities becomes a constant at late time. Thus the late time perfect fluid expansion is mapped to a constant temperature. However, there is no time-reversal symmetry because the longitudinal direction expands and the transverse directions contract with proper time evolution in a way such that the total spatial volume density is a constant. This Weyl transformation can be lifted to a bulk diffeomorphism. At late proper time, the dual black hole's event horizon (and also the apparent horizon which coincides with it at late time) reaches a fixed location. The area and surface gravity of the event horizon (and therefore the entropy density and the the temperature of the dual state) remain constant at late time, but the event horizon shrinks in the directions transverse to the flow while expanding in the longitudinal direction. The latter necessitates the viscous and higher order corrections in hydrodynamics (in this Weyl rescaled version) so that the horizon is smooth (these corrections are rather obvious for the original Bjorken flow). The computation of viscous and higher order corrections is just a special case of the fluid/gravity correspondence [18] and has been worked out up to very high orders for the Bjorken flow [26]. The correlation functions for the Bjorken flow can be obtained simply by undoing the Weyl transformation. The Weyl anomaly could contribute to contact terms, which are diagonal in the Schwinger-Keldysh basis and state independent.

Crucially at late proper time, the Schwinger-Keldysh correlation functions can be mapped to the thermal correlation function after spacetime reparametrizations. This follows from the result that at leading order, the Klein-Gordon equation for the massive scalar field dual to the operator can be mapped to that in the static black brane, thus generalizing the result of Janik and Peschanski [156] for the homogeneous case after adequate spacetime reparametrizations manifested via the Weyl rescaling mentioned above. Furthermore the corrections due to

viscous and higher order derivative effects in the background can be incorporated systematically, however this requires a further non-trivial log correction to the time-reparametrization.

Let us present the crucial result for the limit of the perfect fluid expansion in some details. The d-dimensional background metric for the Bjorken flow is written in the Milne coordinates: τ, the rapidity $\zeta = \text{arctanh}(z/t)$ and the transverse coordinates $\vec{x}_\perp$, in which the Minkowski metric takes the form

$$\mathrm{d}s^2 = -\mathrm{d}\tau^2 + \tau^2 \mathrm{d}\zeta^2 + \mathrm{d}s_\perp^2 \tag{4.7}$$

It is convenient to define

$$\sigma = \tau^{\frac{d-2}{d-1}} \tau_0^{\frac{1}{d-1}}, \quad \hat{\zeta} = \zeta \tau_0. \tag{4.8}$$

Then the Milne metric above is Weyl equivalent to

$$\mathrm{d}s^2 = -\frac{(d-1)^2}{(d-2)^2}\mathrm{d}\sigma^2 + \frac{\sigma^2}{\tau_0^2}\mathrm{d}\hat{\zeta}^2 + \left(\frac{\sigma}{\tau_0}\right)^{-\frac{2}{d-2}} \mathrm{d}s_\perp^2. \tag{4.9}$$

Note that the spatial volume factor is unity although there is expansion and contraction along longitudinal and transverse directions respectively. The above metric should be set as the boundary metric of the dual AdS_{d+1} geometry ($d > 2$) which describes the Weyl rescaled Bjorken flow in the field theory, to implement our horizon cap prescription. Although there is no time-like Killing vector even at late time, the dual black hole's event horizon eventually attains a constant surface gravity and area, implying that the temperature, entropy and energy densities in the dual field theory become a constant.

In order to find the scalar Schwinger-Keldysh correlation function

$$G(\sigma_1, \sigma_2, \hat{\zeta}_1 - \hat{\zeta}_2, |\vec{x}_{\perp 1} - \vec{x}_{\perp 2}|) \tag{4.10}$$

(Note G is a 2×2 matrix in the Schwinger-Keldysh basis) at late time, it is useful to

define

$$\overline{\sigma} = \frac{1}{2}(\sigma_1 + \sigma_2), \quad \sigma_r = \sigma_1 - \sigma_2, \quad \widetilde{\zeta_r} = (\hat{\zeta}_1 - \hat{\zeta}_2)\frac{\overline{\sigma}}{\tau_0}, \quad \widetilde{x_{\perp r}} = |\vec{x}_{\perp 1} - \vec{x}_{\perp 2}|\left(\frac{\tau_0}{\overline{\sigma}}\right)^{\frac{1}{d-2}} \tag{4.11}$$

and take the limit $\overline{\sigma} \to \infty$ with other variables fixed. In this limit, the correlation function is essentially governed by the Weyl-transformed perfect fluid expansion in which the temperature and entropy density become constant although time-translation symmetry is not recovered as mentioned above. (Note due to boost invariance, and the transverse translational and rotational symmetries of the Bjorken flow, the correlation function should be functions of σ_1, σ_2, $\widetilde{\zeta_r}$ and $\widetilde{x_{\perp r}}$ only.) One of our main results is that the Schwinger-Keldysh correlation functions in this limit for holographic conformal field theories reduces to thermal correlation functions.[3] Undoing the Weyl transformation, we obtain the following correlation functions of the perfect fluid expansion in terms of those (denoted as G_β) of a static black brane dual to a thermal state:

$$\left(\frac{\tau_0}{\overline{\sigma}}\right)^{\frac{2\Delta_O}{d-2}} G_\beta\left(\frac{d-1}{d-2}\sigma_r, \sqrt{\widetilde{\zeta_r}^2 + \widetilde{x_{\perp r}}^2}\right). \tag{4.12}$$

(Here Δ_O is the scaling dimension of the scalar operator). Thus with the manifest spacetime reparametrizations, the correlation functions are thermal at a *fixed* temperature given by the constant surface gravity of the (Weyl-transformed) dual $d+1$-dimensional black hole horizon at late time when it reaches its final radial location $\varepsilon_0^{1/d}$. Explicitly, this temperature (which is equal to the static black brane temperature appearing in G_β) is given by

$$\beta = T_0^{-1} = \frac{4\pi\varepsilon_0^{1/d}}{d}, \quad \varepsilon_0 = \frac{16\pi G_N}{d-1}\epsilon_0, \tag{4.13}$$

with ϵ_0 defined in (4.5). The $d+1$-dimensional gravitational constant is related to the rank of the gauge group of the dual theory, as for instance in $\mathcal{N} = 4$ super Yang-Mills theory with $SU(N)$ gauge group in 4 dimensions, $G_N^{-1} = 2N^2/\pi$. Remarkably, we obtain a thermal fluctuation-

[3]The factors $(d-1)/(d-2)$, $\overline{\sigma}/\tau_0$ and $(\overline{\sigma}/\tau_0)^{-1/(d-2)}$ which appear with σ_r, $\hat{\zeta}_1 - \hat{\zeta}_2$ and $\vec{x}_{\perp 1} - \vec{x}_{\perp 2}$ below respecitively can be obtained readily from the Weyl rescaled metric (4.9) metric. These are $\sqrt{-g_{\sigma\sigma}}$, $\sqrt{g_{\hat{\zeta}\hat{\zeta}}}$ and $\sqrt{g_{ii}}$ respectively with g_{ii} denoting the components of the diagonal metric in the transverse spatial directions.

dissipation relation after the necessary spacetime reparametrizations when the state approaches perfect fluid expansion.

Since τ_0 has been chosen arbitrarily, let's consider a scaling $\tau_0 \to \xi\tau_0$ to see if there is any ambiguity in the above result. Note that G_β in (4.12) depends only on $T_0\sigma_r$ and $T_0\sqrt{\widetilde{\zeta_r}^2 + \widetilde{x_{\perp r}}^2}$ as it is a thermal correlation matrix of a CFT. Under this scaling, it is evident from (4.8) that $\sigma \to \xi^{\frac{1}{d-1}}\sigma$, and therefore $\sigma_r \to \xi^{\frac{1}{d-1}}\sigma_r$, $\overline{\sigma} \to \xi^{\frac{1}{d-1}}\overline{\sigma}$, $\widetilde{\zeta_r} \to \xi^{\frac{1}{d-1}}\widetilde{\zeta_r}$ and $\widetilde{x_{\perp r}} \to \xi^{\frac{1}{d-1}}\widetilde{x_{\perp r}}$. Also (4.5) and (4.13) give $\epsilon_0 \to \xi^{-\frac{d}{d-1}}\epsilon_0$ and $T_0 \to \xi^{-\frac{1}{d-1}}T_0$. Together these imply that G_β is invariant under $\tau_0 \to \xi\tau_0$ since $T_0\sigma_r$ and $T_0\widetilde{\zeta_r}$ and $T_0\widetilde{x_{\perp r}}$ are invariant this scaling. However, the Weyl factor in (4.12) scales as $\xi^{\frac{2\Delta_O}{d-1}}$ implying that the *dimensionless correlation function* $\overline{\sigma}^{-2\Delta_0}G$ is invariant under the scaling of τ_0. This holds to all orders.

It is worthwhile to emphasize that the correlation functions do not actually thermalize at late proper time, but assume a thermal form (4.12) only after spacetime reparametrizations. The latter is possible because the state itself loses memory of the initial conditions and reaches boost-invariant perfect fluid flow characterized only by a time-dependent temperature. Nevertheless, there is no time-like Killing vector, and therefore a thermal form is possible only after time-reparametrization and time-dependent rescaling of the spatial coordinates.

We can systematically include viscous and higher order corrections to the correlation functions. The correlation functions for the hydrodynamic Bjorken flow can be systematically obtained in an expansion of the form

$$G(\sigma_1, \sigma_2, \hat{\zeta}_1 - \hat{\zeta}_2, |\vec{x}_{\perp 1} - \vec{x}_{\perp 2}|) = \left(\frac{\tau_0}{\overline{\sigma}}\right)^{\frac{2\Delta_O}{d-2}} \sum_{n=0}^{\infty} \frac{1}{\overline{\sigma}^n \epsilon_0^{n/d}} G_n\left(T_0\sigma_r, T_0\widetilde{\zeta_r}, T_0\widetilde{x_{\perp r}}\right) \tag{4.14}$$

where G_0 coincides with the thermal correlation function G_β given by (4.12). Remarkably, the full series (for the hydrodynamic background) can be written as a bi-local generalization of the thermal form in the language of the matrix factorization mentioned above for the static black brane. The key points are

1. At each order in the late proper time expansion in $\overline{\sigma}^{-1}$, the behaviour of the bulk scalar

field at the horizon cap must be same as at the zeroth order with the latter in turn mapped to that in case of thermal equilibrium. This is required for consistency with field-theoretic identities.

2. The above is possible only when the horizon cap is pinned to the non-equilibrium event horizon.[4]

Our proposal passes many consistency tests. Firstly, using the general identity

$$G_R(x_1, x_2) = G_{11}(x_1, x_2) - G_{12}(x_1, x_2) \,,$$

we can show that even out of equilibrium the retarded response is obtained only from the ingoing mode which is analytic at the horizon cap in consistency with the general prescription of [150]. Secondly, the ansatz naturally reproduces the homogeneous transients (a non-trivial extension of the result of Janik and Peschanski [156] to higher orders). Also, our prescription ensures that the advanced response is always given by the outgoing mode which is regular (it has the same kind of branch cut at all orders as in thermal equilibrium, after Weyl rescaling of the Bjorken flow). We will show that this is needed for consistency in the gravitational setup also. The quadratic on-shell action and thus $W[J_1, J_2]$ originates only from the cross-terms between the in-going and out-going modes to all orders. This ensures a bi-local generalization of the thermal structure of the correlation functions in terms of the matrix factorization mentioned above, to all orders. Finally, our result that the horizon cap for the hydrodynamic Bjorken flow is pinned to the non-equilibrium event horizon captures the causal nature of the Schwinger-Dyson equations for the real-time (out-of-equilibrium) correlation functions in the dual field theory.[5]

[4]Note that the event horizon and the apparent horizon do not coincide when we consider second and higher orders in the proper time expansion for the Bjorken flow. In practice, we put the horizon cap at a fixed radial location and determine a proper residual gauge transformation at each order such that we satisfy the first condition mentioned above. We also find that this residual gauge fixing puts the event horizon at the same fixed location implying (in a gauge invariant way) that the horizon cap is pinned at the non-equilibrium event horizon.

The series (4.14) is not expected to be convergent, and therefore requires a trans-series completion with appropriate Stokes data which should be actually functions of σ_r, $\widetilde{\zeta_r}$ and $\widetilde{x_{\perp r}}$. We discuss their physical role in deciphering the information of the initial state which is lost in hydrodynamization, and also how they can be used to decode the interior of the event horizon.

The chapter is organized as follows. In section 4.1, we introduce the Crossley-Glorioiso-Liu (CGL) horizon cap prescription for the thermal Schwinger-Keldysh correlation functions in holography. We prove that the prescription indeed reproduces the KMS periodicity so that they are given just in terms of the retarded correlation function, and that the latter is exactly what we obtain from the Son-Starinets prescription. As mentioned, we use a new matrix factorization of thermal correlation functions. In section 4.2, based on the discussion of Bjorken flow and its Weyl rescaling in section 2.1.4 and holographic dual of Bjorken flow in section 2.2.4, we construct the holographic dual of Weyl rescaled Bjorken flow. As mentioned, this leads to a constant surface gravity and area at late time, although the event horizon stretches and expands in the directions longitudinal and transverse to the flow respectively. Additionally, we also discuss the proper residual gauge transformation corresponding to radial reparametrization.

In section 4.3, we study the probe bulk scalar field in the gravitational background dual to the hydrodynamic Bjorken flow and show how we can preserve the analytic structure of the horizon cap to all orders in the proper time expansion. Crucially, we find that it requires the horizon cap to be pinned to the non-equilibrium event horizon. In section 4.4, we use these results to extract the real-time correlation functions of the hydrodynamic Bjorken flow. After presenting the result for the perfect fluid limit in terms of a thermal propagator with spacetime reparametrizations, we show how we systematically obtain the corrections in a proper time expansion. We also discuss many non-trivial consistency checks of our results. In section 4.5, we present a discussion on how a trans-series completion of this expansion can lead to seeing the quantum fluctuations behind the non-equilibrium event horizon, and matching with initial

[5]The latter is manifest when written in terms of the coupled evolution of the statistical and spectral functions [29].

data lost during hydrodynamization.

4.1 The CGL horizon cap of the thermal black brane

The Crossley-Glorioso-Liu (CGL) horizon cap prescription is a simple proposal for the holographic realization of the Schwinger-Keldysh contour at thermal equilibrium [17]. The thermal nature of the correlation functions obtained from this prescription, including their consistency with the Kubo-Martin-Schwinger (KMS) periodicity, has been explicitly verified up to quadratic order in the small frequency expansion in [17]. In [17], it has also been verified that the retarded correlation function is implied by the ingoing boundary condition, as demanded by the Son-Starinets prescription [155] up to the quadratic order in frequency. These were sufficient to obtain a rudimentary effective theory of diffusion and dissipative hydrodynamics from holography [17, 157–167]. Here, we will present a novel and elegant proof that the CGL horizon cap indeed gives thermal correlation functions satisfying KMS periodicity, and that it also implies the Son-Starinets prescription for the retarded correlation function, at *any arbitrary frequency and momenta*.[6]

The generating functional for the thermal Schwinger-Keldysh correlation functions in a quantum field theory is[7]

$$e^{W[J_1,J_2]} = \mathrm{Tr}\left[\hat{\rho}_\beta T_c e^{i\int \mathrm{d}t \int \mathrm{d}^{d-1}x\,(\hat{O}_1(\mathbf{x},t)J_1(\mathbf{x},t)-\hat{O}_2(\mathbf{x},t)J_2(\mathbf{x},t))}\right] \tag{4.15}$$

with ρ_β denoting the thermal density matrix, 1 and 2 denoting the forward and backward arms of the contour, and T_c denoting (time) contour ordering. The contour ordering implies that (with

[6]The real-time prescription [61, 122] of van Rees and Skenderis leads to the ingoing boundary condition as shown in [31] in thermal equilibrium. Our methods discussed here discuss a natural generalization away from equilibrium for out-of-equilibrium, especially hydrodynamic states. For other approaches, see [166].

[7]Unless specified, we will always put the backward arm of the Schwinger-Keldysh time contour infinitesimally below the real axis. Also, we will often omit explicit mention of the appendage of the contour along the imaginary axis which creates the thermal state in the infinite past.

$\langle\cdot\rangle \equiv \mathrm{Tr}(\hat{\rho}_\beta \cdot))$

$$
\begin{aligned}
G_{11}(t-t', \mathbf{x}-\mathbf{x}') &= \frac{\delta^2 W}{\delta J_1(t,\mathbf{x})\delta J_1(t',\mathbf{x}')} = -i\langle T(\hat{O}(t,\mathbf{x})\hat{O}(t',\mathbf{x}'))\rangle, \\
-G_{12}(t-t', \mathbf{x}-\mathbf{x}') &= \frac{\delta^2 W}{\delta J_1(t,\mathbf{x})\delta J_2(t',\mathbf{x}')} = i\langle \hat{O}(t',\mathbf{x}')\hat{O}(t,\mathbf{x}))\rangle, \\
-G_{21}(t-t', \mathbf{x}-\mathbf{x}') &= \frac{\delta^2 W}{\delta J_2(t,\mathbf{x})\delta J_1(t',\mathbf{x}')} = i\langle \hat{O}(t,\mathbf{x})\hat{O}(t',\mathbf{x}'))\rangle, \\
G_{22}(t-t', \mathbf{x}-\mathbf{x}') &= \frac{\delta^2 W}{\delta J_2(t,\mathbf{x})\delta J_2(t',\mathbf{x}')} = -i\langle \overline{T}(\hat{O}(t,\mathbf{x})\hat{O}(t',\mathbf{x}'))\rangle.
\end{aligned}
\tag{4.16}
$$

Succinctly we can write the above as

$$
G_{ij}(x_1, x_2) = \frac{\delta^2 W}{\delta J_i(x_1)\delta J_j(x_2)}(-)^{i+j} \tag{4.17}
$$

with $(i, j) = (1, 2)$. The above holds even out of equilibrium with ρ_β in (4.15) replaced by an arbitrary initial state ρ_0.

It can readily be shown that the KMS periodicity (arising from the Tr in (4.15) after extending the contour along the negative imaginary axis by β as shown in Fig. 4.1) implies that the thermal correlation functions in Fourier space (with i and j standing for the 1 (forward) or 2 (backwards) arms of the contour) defined as

$$
G_{ij}(\omega, \mathbf{k}) = \int \mathrm{d}t\, \mathrm{d}^{\mathrm{d}-1}x\, e^{i\omega(t-t')} e^{-i\mathbf{k}\cdot(\mathbf{x}-\mathbf{x}')} G_{ij}(t-t', \mathbf{x}-\mathbf{x}') \tag{4.18}
$$

assume the form

$$
G_{ij} = \begin{pmatrix}
G_R(\omega,\mathbf{k})(1+n(\omega)) - G_A(\omega,\mathbf{k})n(\omega) & -(G_R(\omega,\mathbf{k}) - G_A(\omega,\mathbf{k})n(\omega) \\
-(G_R(\omega,\mathbf{k}) - G_A(\omega,\mathbf{k})(1+n(\omega)) & G_R(\omega,\mathbf{k})n(\omega) - G_A(\omega,\mathbf{k})(1+n(\omega))
\end{pmatrix}
\tag{4.19}
$$

where

$$
G_R(t-t', \mathbf{x}-\mathbf{x}') = -i\theta(t-t')\langle[\hat{O}(t,\mathbf{x}), \hat{O}(t',\mathbf{x}')]\rangle \tag{4.20}
$$

is the retarded propagator,

$$G_A(t-t', \mathbf{x}-\mathbf{x}') = -i\theta(t'-t)\langle[\hat{O}(t', \mathbf{x}'), \hat{O}(t, \mathbf{x})]\rangle \tag{4.21}$$

is the advanced propagator, and $n(\omega) = 1/(e^{\beta\omega} - 1)$ is the Bose-Einstein distribution function. It is easy to see from these definitions that

$$G_A^*(\omega, \mathbf{k}) = G_R(\omega, \mathbf{k}) \, . \tag{4.22}$$

The crucial element of the proof of why the CGL prescription works is a simple and general factorization property of thermal correlation functions in field theory (irrespective of whether the theory is holographic or not). The Schwinger-Keldysh thermal correlation functions (4.19) obtained by differentiating the real-time partition function at a temperature $T = \beta^{-1}$ can be factorized as shown below

$$G_{ij}(\omega, \mathbf{k}) = \sigma_3 \cdot \begin{pmatrix} A(\omega, \mathbf{k}) & B(\omega, \mathbf{k}) \\ A(\omega, \mathbf{k}) & B(\omega, \mathbf{k}) e^{\beta\omega} \end{pmatrix} \cdot \begin{pmatrix} a(\omega, \mathbf{k}) & b(\omega, \mathbf{k}) \\ a(\omega, \mathbf{k}) & b(\omega, \mathbf{k}) e^{\beta\omega} \end{pmatrix}^{-1} , \tag{4.23}$$

in which $\sigma_3 = \mathrm{diag}(1, -1)$ is the third Pauli matrix, and

$$G_R(\omega, \mathbf{k}) = \frac{A(\omega, \mathbf{k})}{a(\omega, \mathbf{k})} = \frac{B^*(\omega, \mathbf{k})}{b^*(\omega, \mathbf{k})} = G_A^*(\omega, \mathbf{k}). \tag{4.24}$$

Clearly $A \to \lambda A$, $B \to \tilde{\lambda} B$, $a \to \lambda a$ and $b \to \tilde{\lambda} b$ gives the same thermal matrix, so the factorization is unique up to the multiplicative complex functions $\lambda(\omega, \mathbf{k})$ and $\tilde{\lambda}(\omega, \mathbf{k})$.

The CGL horizon cap glues two copies of the black brane geometry, whose boundaries represent the forward and backward arms of the Schwinger-Keldysh time contour respectively, at the horizon as shown in Fig. 4.2. For reasons to become clear later, this prescription is easily implemented in the in-going Eddington-Finkelstein (EF) coordinates. The in-going EF radial coordinates of the two geometries, representing the forward (1) and backward (2) arms

of the time contour respectively, are displaced along the imaginary axis by $\mp\epsilon$ (i.e. $r_1 \to r_1 - i\epsilon$ and $r_2 \to r_2 + i\epsilon$). The smooth gluing is achieved by the encircling of the complexified radial coordinate around the horizon $r = r_h$ *clockwise* along a circle of radius $O(\epsilon)$ as it is analytically continued from the (first) copy dual to the forward contour to the (second) copy dual to the backward contour. The direction of time in the second copy has to be reversed so that full complexified bulk geometry has a single orientation. Therefore, the analytic continuation of the radial coordinate automatically necessitates the closed Schwinger-Keldysh time contour.

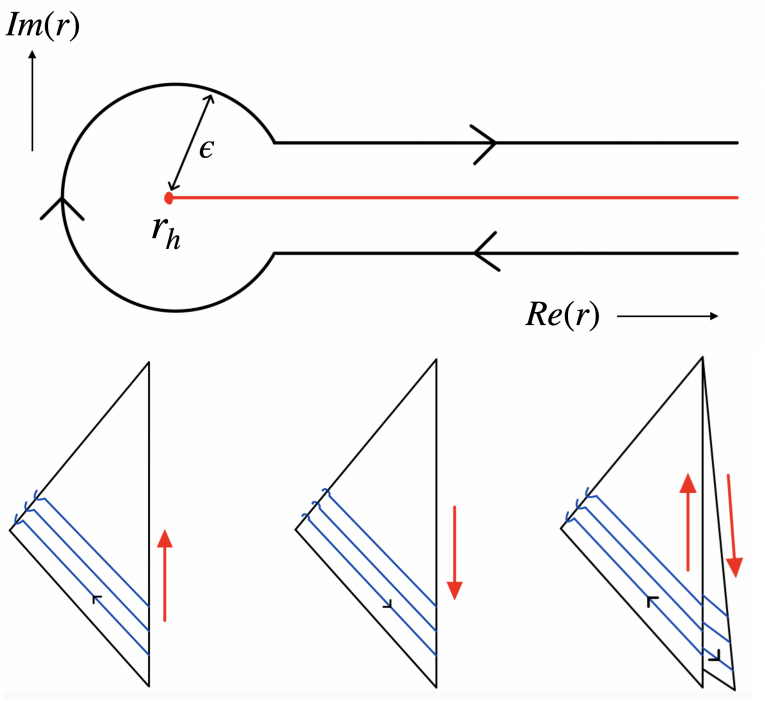

Figure 4.2: **Top:** The radial contour in the complexified two-sheeted black brane geometry on a constant time hypersurface. The radial coordinate goes around the horizon $r = r_h$ in the complex plane forming the *horizon cap*, and connects the two arms of the Schwinger-Keldysh contour at the two boundaries at a constant Lorentzian time. The analytic continuation along the horizon cap gives a well-defined Dirichlet value problem for the bulk fields in terms of their sources specified at the two boundaries. **Bottom:** Shows the time evolution of the radial contour (shown in blue lines) in the full complexified spacetime ending at the two Lorentzian arms at the two boundaries. The reversal of the direction of time in the second copy implies that the full complexified spacetime has a single orientation after the two copies are smoothly glued with the horizon cap.

Explicitly, the AdS_{d+1} static black brane geometry in the ingoing Eddington-

Finkelstein coordinates is

$$\mathrm{d}s^2 = -\frac{2}{r^2}\mathrm{d}r\mathrm{d}t - \frac{1}{r^2}\left(1 - r^d\varepsilon_0\right)\mathrm{d}t^2 + \frac{1}{r^2}(\mathrm{d}x_1^2 + \cdots + \mathrm{d}x_{d-1}^2) \tag{4.25}$$

where r is the bulk radial coordinate, t is the Eddington-Finkelstein time and the horizon is at $r = r_h = \varepsilon_0^{-1/d}$. The on-shell action for bulk fields in this geometry is identified with the generating functional of connected real-time correlation functions of the dual operators at the boundary. A bulk scalar field configuration can be written in the form

$$\Phi(r, t, \mathbf{x}) = \int \frac{\mathrm{d}\omega}{2\pi}\frac{\mathrm{d}^{d-1}k}{(2\pi)^{d-1}}\, e^{-i\omega t}e^{i\mathbf{k}\cdot\mathbf{x}}\Phi(r, \omega, \mathbf{k}). \tag{4.26}$$

On-shell, $\Phi(r, \omega, \mathbf{k})$ is a sum of two linearly independent solutions $\phi_{\mathrm{in}}(r, \omega, \mathbf{k})$ and $\phi_{\mathrm{out}}(r, \omega, \mathbf{k})$ which are in-going and out-going at the horizon respectively. Therefore,

$$\Phi(r, \omega, \mathbf{k}) = \phi_{\mathrm{in}}(r, \omega, \mathbf{k})p(\omega, \mathbf{k}) + \phi_{\mathrm{out}}(r, \omega, \mathbf{k})q(\omega, \mathbf{k}) \tag{4.27}$$

generally with $p(\omega, \mathbf{k})$ and $q(\omega, \mathbf{k})$ representing the arbitrary Fourier coefficients of the solutions which are in-going and out-going at the horizon respectively. The latter thus provide a basis of solutions for given ω and $\mathbf{k}$, and can be uniquely defined via the following conditions

$$\phi_{\mathrm{in}}(r_h, \omega, \mathbf{k}) = 1, \qquad \lim_{r\to r_h}\phi_{\mathrm{out}}(r, \omega, \mathbf{k})(r_h - r)^{-\frac{i\beta\omega}{2\pi}} = 1 \tag{4.28}$$

where

$$\beta = T^{-1} = \frac{4\pi r_h}{d} \tag{4.29}$$

is the inverse Hawking temperature of the black brane, and $r_h = \varepsilon_0^{-1/d}$ is the radial location of the horizon. Indeed, near the horizon ($r \approx r_h$),

$$\Phi(r, \omega, \mathbf{k}) \approx p(\omega, \mathbf{k}) + (r_h - r)^{\frac{i\beta\omega}{2\pi}}q(\omega, \mathbf{k}), \tag{4.30}$$

as should follow from the universal validity of the geometrical optics approximation at the horizon. The CGL horizon cap prescription for the analytic continuation of the radial coordinate from one copy of the bulk spacetime to another then implies that the Fourier coefficients of the on-shell solutions in the two copies are related by

$$p_2(\omega, \mathbf{k}) = p_1(\omega, \mathbf{k}), \qquad q_2(\omega, \mathbf{k}) = e^{\beta\omega} q_1(\omega, \mathbf{k}), \tag{4.31}$$

with 1 and 2 denoting the copies ending on the forward and backward arms of the time contour respectively at their boundaries. The on-shell solution in the full geometry can therefore be written in the following matrix form:

$$\begin{pmatrix} \Phi_1(r, t, \mathbf{x}) \\ \Phi_2(r, t, \mathbf{x}) \end{pmatrix} = \int \frac{\mathrm{d}\omega}{2\pi} \frac{\mathrm{d}^{d-1}k}{(2\pi)^{d-1}} \, e^{-i\omega t} e^{i\mathbf{k}\cdot\mathbf{x}} \mathcal{M}(r, \omega, \mathbf{k}) \cdot \begin{pmatrix} p(\omega, \mathbf{k}) \\ q(\omega, \mathbf{k}) \end{pmatrix} \tag{4.32}$$

with the matrix

$$\mathcal{M}(r, \omega, \mathbf{k}) = \begin{pmatrix} \phi_{\text{in}}(r, \omega, \mathbf{k}) & \phi_{\text{out}}(r, \omega, \mathbf{k}) \\ \phi_{\text{in}}(r, \omega, \mathbf{k}) & e^{\beta\omega} \phi_{\text{out}}(r, \omega, \mathbf{k}) \end{pmatrix} \tag{4.33}$$

providing a basis of solutions for the entire complexified spacetime comprising of the two copies smoothly glued at the horizon. The sources $J_1(\omega, \mathbf{k})$ and $J_2(\omega, \mathbf{k})$ specified at the two boundaries (see below) implement the Dirichlet boundary conditions that determine $p(\omega, \mathbf{k})$ and $q(\omega, \mathbf{k})$ uniquely for real frequencies and momenta, and thus yielding a unique bulk field configuration in the full complexified spacetime.

According to the holographic dictionary, the generating functional for the connected correlation functions is identified with the on-shell action for the scalar field dual to the operator $\hat{O}$, on the full complexified spacetime, i.e.

$$W[J_1, J_2] = iS_{\text{on-shell}}. \tag{4.34}$$

Assuming minimal coupling to gravity, the on-shell quadratic action for the bulk scalar field Φ

dual to a scalar operator takes the form

$$S_{on-shell} = S_{in-in} + S_{in-out} + S_{out-out}. \tag{4.35}$$

The first piece S_{in-in} is quadratic in the ingoing mode. Since the ingoing mode is analytic at the horizon, the contributions from the two arms cancel each other out (as the solutions are the same on the two arms) while the circle around the horizon does not contribute as well. Therefore, $S_{in-in} = 0$. Note if we keep the in-going mode alone, then $J_1 = J_2$. In the field theory, $W[J_1 = J_2] = 0$ because the partition function e^W with the same unitary evolution forward and backward in time, equals unity. Therefore, $S_{in-in} = 0$ is consistent with field theory.

The second piece S_{in-out}, which is the sum of cross-terms between the in and out-going modes, has a branch point at the horizon. Integrating over the two arms amounts to integrating around a branch cut, and results in the two boundary terms on-shell, i.e.

$$S_{in-out} = S_{bdy1} + S_{bdy2}. \tag{4.36}$$

The third piece $S_{out-out}$ has a possibility of a pole at the horizon, i.e. $(r_h - r)^{-1}$ terms in the Lagrangian density arising from the radial derivative acting on the non-analytic piece $(r_h - r)^{\frac{i\beta\omega}{2\pi}}$, which we denote collectively as S_ϵ. Essentially S_ϵ gets contributions from the following two terms:

$$S_\epsilon \propto \int \mathrm{d}\omega \int \mathrm{d}^d k \oint_\epsilon \mathrm{d}r \sqrt{-G}\Big(G^{rr}\partial_r\phi^*_{out}\partial_r\phi_{out} + G^{rt}\left(\partial_r\phi^*_{out}\partial_t\phi_{out} + \partial_r\phi_{out}\partial_t\phi^*_{out}\right)\Big). \tag{4.37}$$

Remarkably, the poles originating from these two terms cancel each other out (note β is given by (4.29)) resulting in $S_\epsilon = 0$. The remaining terms quadratic in the outgoing mode are analytic, so that $S_{out-out}$ is also the sum of two boundary terms. These two boundary terms cancel each other out as in the in-going case. On the gravitational side, the easy way to see this is by first writing the contributions from the forward and backward arms of the contour separately. The

boundary contributions from one arm in the integrand would be proportional to

$$\phi_b(-\omega,k)(\partial_r\phi)_b(\omega,k)+\cdots$$

with ϕ_b and $(\partial_r\phi)_b$ denoting the boundary values of ϕ and its radial derivative respectively, and $\cdots$ include counter-terms too. The contributions from the forward and backward parts of the contour come with opposite signs. If we consider the terms quadratic in the out-going mode, then $\phi_b(\omega,k)$ picks up a factor of $e^{\beta\omega}$ while $\phi_b(-\omega,k)$ picks up a factor of $e^{-\beta\omega}$ via analytic continuation through the horizon cap, and the product of these factors is unity. Therefore, the contributions from the forward and backward contours cancel out leading to $S_{out-out}=0$.

It is useful to see this also from the field theory perspective. If we keep the outgoing modes only, then $J_2(\omega,\mathbf{k})=J_1(\omega,\mathbf{k})e^{\beta\omega}$. In any field theory [162]

$$\begin{aligned} W[J_1(t,\mathbf{x}),J_2(t,\mathbf{x})] &= W_T[J_2(t-i\beta,\mathbf{x}),J_1(t,\mathbf{x})], \\ \text{i.e. } W[J_1(t,\mathbf{x}),J_2(t+i\beta,\mathbf{x})] &= W_T[J_2(t,\mathbf{x}),J_1(t,\mathbf{x})] \end{aligned} \tag{4.38}$$

where W_T stands for the time-reversed process in which we specify with the same density matrix in the future instead of the initial time.[8] For $J_1(t,\mathbf{x})=J_2(t,\mathbf{x})=J(\omega,\mathbf{k})$, this amounts to

$$W_T[J(\omega,\mathbf{k}),J(\omega,\mathbf{k}))]=W[J(\omega,\mathbf{k}),J(\omega,\mathbf{k})e^{\beta\omega}].$$

The LHS of the above equation vanishes because once again the forward and backward evolution with the same source are inverses of each other (there is no operator insertion in the past now although the state is specified in the future). Therefore, the RHS of the above equation should vanish too, implying that

$$W[J_2(\omega,\mathbf{k})=J_1(\omega,\mathbf{k})e^{\beta\omega}]=0. \tag{4.39}$$

[8] Succinctly, $W[J_1,J_2]=\mathrm{Tr}(\rho_0\tilde{U}[J_2]U[J_1])$ where $U[J_1]$ is forward evolution with source J_1 and $\tilde{U}[J_2]$ is backward evolution with source J_2. Similarly, $W_T[J_1,J_2]=\mathrm{Tr}(\tilde{U}[J_2]\rho_0U[J_1])=\mathrm{Tr}(\rho_0U[J_1]\tilde{U}[J_2])$.

Thus, $S_{out-out} = 0$ is consistent with field theory. See also footnote 12 for a more straightforward verification that the thermal correlators in the dual theory originate from S_{in-out} alone.

The upshot is that we obtain only two boundary contributions from the cross-term between the in-going and out-going modes, so that

$$S_{on-shell} \equiv S_{in-out} = S_{bdy1} + S_{bdy2} \tag{4.40}$$

where S_{bdy1} and S_{bdy2} are the contributions from the two boundaries after taking into account counter-terms necessary for holographic renormalization [60]. This implies that

$$S_{\text{on-shell}}[J_1, J_2] = \int \mathrm{d}t \int \mathrm{d}^{d-1}x \left(\langle O_1(t,\mathbf{x})\rangle J_1(t,\mathbf{x}) - \langle O_2(t,\mathbf{x})\rangle J_2(t,\mathbf{x})\right) \tag{4.41}$$

with

$$\begin{aligned}
\begin{pmatrix} J_1(\omega,\mathbf{k}) \\ J_2(\omega,\mathbf{k}) \end{pmatrix} &= \mathcal{S}(\omega,\mathbf{k}) \cdot \begin{pmatrix} p(\omega,\mathbf{k}) \\ q(\omega,\mathbf{k}) \end{pmatrix}, \\
\begin{pmatrix} \langle O_1(\omega,\mathbf{k})\rangle \\ \langle O_2(\omega,\mathbf{k})\rangle \end{pmatrix} &= \mathcal{R}(\omega,\mathbf{k}) \cdot \begin{pmatrix} p(\omega,\mathbf{k}) \\ q(\omega,\mathbf{k}) \end{pmatrix} \\
&= (\mathcal{R}\cdot\mathcal{S}^{-1})(\omega,\mathbf{k}) \cdot \begin{pmatrix} J_1(\omega,\mathbf{k}) \\ J_2(\omega,\mathbf{k}) \end{pmatrix}.
\end{aligned} \tag{4.42}$$

The matrices $\mathcal{R}$ and $\mathcal{S}$ are defined as follows. Let the asymptotic ($r \approx 0$) expansions of the in-going and out-going modes be[9]

$$\begin{aligned}
\phi_{\text{in}}(r,\omega,\mathbf{k}) &= r^{d-\Delta}(a_0(\omega,\mathbf{k}) + \cdots) + r^{\Delta}(A_0(\omega,\mathbf{k}) + \cdots), \\
\phi_{\text{out}}(r,\omega,\mathbf{k}) &= r^{d-\Delta}(b_0(\omega,\mathbf{k}) + \cdots) + r^{\Delta}(B_0(\omega,\mathbf{k}) + \cdots).
\end{aligned} \tag{4.43}$$

[9]The scaling dimension Δ is related to the mass via $\Delta = \frac{d}{2} + \sqrt{\frac{d^2}{4} + m^2L^2}$ with L being the AdS radius.

Then

$$\mathcal{S}(\omega,\mathbf{k}) = \begin{pmatrix} a_0(\omega,\mathbf{k}) & b_0(\omega,\mathbf{k}) \\ a_0(\omega,\mathbf{k}) & e^{\beta\omega} b_0(\omega,\mathbf{k}) \end{pmatrix} = \lim_{r\to 0} r^{\Delta-d}\mathcal{M}(r,\omega,\mathbf{k}) \tag{4.44}$$

and[10]

$$\mathcal{R}(\omega,\mathbf{k}) = (2\Delta-d)\begin{pmatrix} A_0(\omega,\mathbf{k}) & B_0(\omega,\mathbf{k}) \\ A_0(\omega,\mathbf{k}) & e^{\beta\omega} B_0(\omega,\mathbf{k}) \end{pmatrix} + \cdots . \tag{4.45}$$

The $\cdots$ above stands for (state-independent) contact terms which we ignore. Denoting

$$\widehat{G}(\omega,\mathbf{k}) = (\sigma_3\cdot\mathcal{R}\cdot\mathcal{S}^{-1})(\omega,\mathbf{k}), \tag{4.46}$$

(with $\sigma_3 = \mathrm{diag}(1,-1)$) we find from (4.41), (4.42), (4.44), (4.45) and (4.46) that[11]

$$\begin{aligned} S_{\text{on-shell}}[J_1,J_2] &= \int \frac{\mathrm{d}\omega}{2\pi}\frac{\mathrm{d}^{d-1}k}{(2\pi)^{d-1}}(J_1(-\omega,-\mathbf{k})\langle O_1(\omega,\mathbf{k})\rangle - J_2(-\omega,-\mathbf{k})\langle O_2(\omega,\mathbf{k})\rangle) \\ &= \int \frac{\mathrm{d}\omega}{2\pi}\frac{\mathrm{d}^{d-1}k}{(2\pi)^{d-1}}(J_1(-\omega,-\mathbf{k})\ J_2(-\omega,-\mathbf{k}))\cdot\widehat{G}(\omega,\mathbf{k})\cdot\begin{pmatrix} J_1(\omega,\mathbf{k}) \\ J_2(\omega,\mathbf{k})\end{pmatrix}. \end{aligned} \tag{4.47}$$

Therefore, the identification (4.34) together with (4.16) implies that,[12]

$$G_{ij}(\omega,\mathbf{k}) = \frac{\partial^2 S_{\text{on-shell}}}{\partial J_i(-\omega,-\mathbf{k})\partial J_j(\omega,\mathbf{k})}(2\pi)^d = \widehat{G}(\omega,\mathbf{k}), \tag{4.48}$$

From the matrix factorization of thermal correlation functions given by (4.23), we readily find from (4.44), (4.45) and (4.46) that the correlation functions obtained by differentiating the on-shell gravitational action are thermal, i.e. assume the form (4.19) provided[13]

$$G_R(\omega,\mathbf{k}) = (2\Delta-d)\frac{A_0(\omega,\mathbf{k})}{a_0(\omega,\mathbf{k})}, \qquad G_A(\omega,\mathbf{k}) = (2\Delta-d)\frac{B_0(\omega,\mathbf{k})}{b_0(\omega,\mathbf{k})}. \tag{4.49}$$

[10] Note that, asymptotically, $\mathcal{M}(r,\omega,\mathbf{k}) = r^{d-\Delta}(\mathcal{S}(\omega,\mathbf{k})+\cdots) + r^{\Delta}(\mathcal{R}(\omega,\mathbf{k})+\cdots)$.

[11] $J_i(\omega,\mathbf{k}) = \int \mathrm{d}t\,\mathrm{d}^{d-1}x\, e^{i\omega t}e^{-i\mathbf{k}\cdot\mathbf{x}}J_i(t,\mathbf{x})$.

[12] The reader can check that substituting $p(\omega,\mathbf{k})+q(\omega,\mathbf{k}) = J_1(\omega,\mathbf{k})$ and $p(\omega,\mathbf{k})+q(\omega,\mathbf{k})e^{\beta\omega} = J_2(\omega,\mathbf{k})$ in the on-shell action (4.47), and using the thermal form of the propagators below, that indeed only cross-terms between p and q, i.e. the in and out-going modes appear. There are no contributions from terms quadratic in p or in q, implying that $S_{in-in} = S_{out-out} = 0$ as claimed above, and also $S_{on-shell} = S_{in-out}$.

[13] It is obvious that to map to the factorization in (4.23), we have to set $A = (2\Delta-d)A_0$, $B = (2\Delta-d)B_0$, $a = a_0$ and $b = b_0$.

Remarkably, the above are exactly the Son-Starinets prescriptions [155] for the retarded and advanced propagators according to which they are obtained from the in-going and out-going boundary conditions at the horizon respectively. Furthermore, since the out-going mode is time reverse of the in-going mode (which is not manifest in the Eddington-Finkelstein gauge but can be evident from transforming to Schwarzchild-like coordinates),[14] we should have

$$\frac{B_0^*(\omega,\mathbf{k})}{b_0^*(\omega,\mathbf{k})} = \frac{A_0(\omega,\mathbf{k})}{a_0(\omega,\mathbf{k})}, \quad \text{i.e.} \quad G_A^*(\omega,\mathbf{k}) = G_R(\omega,\mathbf{k}) \quad \text{holds.} \tag{4.50}$$

We therefore conclude that the CGL horizon cap prescription reproduces the Son-Starinets prescription for the retarded propagator together with KMS periodicity and the thermal structure of the correlation functions at any frequency and momentum. A similar approach was adopted earlier by Son and Herzog by identifying the two sides of the eternal black hole with the forward and backward arms of the Schwinger-Keldysh contour [168]. However, in this case, the backward part of the time contour needs to be shifted by $\beta/2$ along the negative imaginary axis. The main advantage of the CGL prescription is that we do not need an eternal black hole geometry for its implementation suggesting that its non-equilibrium generalization would be generically more feasible. Furthermore, it is also not clear if out-of-equilibrium correlation functions can be analytically continued in their time arguments as required by the Son and Herzog implementation of the Schwinger-Keldysh contour. Also it should be possible to define integration over bulk vertices and bulk quantum loops in the CGL prescription as well via the analytic structure of the complexified spacetime with the horizon cap. However, this is outside the scope of the present work, and therefore we do not further discuss about this issue. Finally, we note that the arguments presented here are simpler compared to [17] since we do not employ an expansion about $\omega = 0$ which obscures the analytic continuation at the horizon cap by producing $(\log \omega)^n$ terms.

[14] Note that the notion of in/outgoing modes are gauge-invariant up to overall multiplicative factors, but these cancel out in the ratio of the normalizable to the non-normalizable modes. This is why the Son-Starinets prescription is also gauge-invariant.

4.2 Gravitational setup of Weyl rescaled Bjorken flow

The implementation of the CGL prescription to dynamical asymptotically AdS_{d+1} (anti-de Sitter) bulk geometry dual to the Bjorken flow in the field theory, is achieved by Weyl rescaling the Bjorken flow at the boundary. The Weyl rescaled Bjorken flow as shown in 2.1.4, at late time maps the perfect fluid to a flow with a constant temperature. Though there is no time translational symmetry, at late time due to contraction and expansion in the longitudinal and transverse direction, the temperature along with the energy density and entropy density maps to a constant.

In the bulk it is implemented by an appropriate diffeomorphism. As a result of this transformation, the state reaches a constant temperature and entropy density at late proper time instead of attaining perfect fluid expansion. The dual black hole also attains a horizon with constant surface gravity and area. However, even at late proper time there is no time-like Killing vector – the directions longitudinal and transverse to the flow expand and contract respectively such that the horizon area remains constant at late proper time. Along with the Weyl transformation of the metric and the energy-momentum tensor described in 2.1.4, the holographic dual also produces the Weyl anomaly. The Weyl transformation will be an important tool in implementing the horizon cap prescription out of equilibrium.

Additionally, we will focus on the residual gauge freedom which allows us to fix the non-equilibrium event or apparent horizon at a fixed radial location. We will see that it is crucial to pin the horizon cap at the non-equilibrium event horizon for regularity, and therefore this gauge freedom will play an important role. This gauge freedom as shown in chapter 2, does not affect the dual metric or the dual energy-momentum tensor (and is thus a proper gauge transformation) of the dual Bjorken flow. Similarly, the boundary metric or the dual energy-momentum tensor remains invariant in the case of Weyl scaled Bjorken flow.

The holographic dual of the Weyl scaled Bjorken flow in a d-dimensional conformal theory is a $(d+1)$-dimensional geometry which satisfies the Einstein's equations with a negative

cosmological constant:

$$R_{MN} - \frac{1}{2}RG_{MN} - \frac{d(d-1)}{2L^2}G_{MN} = 0. \tag{4.51}$$

In what follows, we will set $L = 1$ for convenience. In addition to the field theory coordinates, we need an extra radial coordinate to describe the dual geometry. The state of the conformal theory dual to a specific solution of (4.51), lives at the boundary ($\rho = 0$) in the boundary metric, which is defined as

$$g^{\rm b}_{\mu\nu} = \lim_{\rho\to 0}\rho^2 G_{\mu\nu} \tag{4.52}$$

where a and b stand for the field theory indices. Since we are considering the Weyl rescaled version of the Bjorken flow, the boundary metric should coincide with (2.63).

Before considering the Weyl rescaled Bjorken flow, it is useful to first understand the vacuum solution, which is pure (maximally symmetric) AdS_{d+1} spacetime with the desired boundary metric. In the ingoing Eddington-Finkelstein gauge, the vacuum state in the Weyl scaled metric (2.63) is dual to

$$\begin{aligned} {\rm d}s^2 &= -\frac{2}{v^2}\frac{d-1}{d-2}{\rm d}v{\rm d}\sigma - \frac{1}{v^2}\left(\frac{(d-1)^2}{(d-2)^2} + \frac{2(d-1)v}{(d-2)^2\sigma}\right){\rm d}\sigma^2 + \frac{1}{\tau_0^2}\left(1+\frac{\sigma}{v}\right)^2 {\rm d}\hat{\zeta}^2 \\ &\quad + \frac{1}{v^2}\left(\frac{\sigma}{\tau_0}\right)^{-\frac{2}{d-2}} {\rm d}s_\perp^2, \end{aligned} \tag{4.53}$$

where v is the radial coordinate. These bulk metrics (2.99) and (4.53) are related by the diffeomorphism

$$\tau = \tau_0^{-\frac{1}{d-2}}\sigma^{\frac{d-1}{d-2}}, \quad r = v\left(\frac{\sigma}{\tau_0}\right)^{\frac{1}{d-2}}. \tag{4.54}$$

For both cases, (2.99) and (4.53), we obtain the boundary metrics (2.52) and (2.63) from (4.52), after replacing ρ with r and v, respectively. Any Weyl transformation at the boundary is dual to a bulk diffeomorphism. Since the boundary metrics (2.52) and (2.63) are related by a Weyl transformation, (4.54) is simply a specific instance of this general feature of holographic duality.

Note that τ and σ are related exactly by the time reparametrization (2.61) at the boundary.[15] Holographic renormalization discussed in 2.2.2 provides the framework for extracting the $\langle T_{\mu\nu}\rangle$ corresponding to the state in the field theory dual to a specific asymptotically AdS_{d+1} bulk geometry. For the bulk geometry (2.99), $\langle T_{\mu\nu}\rangle = 0$ in the dual vacuum state living in the flat Milne metric (2.52) at the boundary. On the other hand, for the vacuum state living on the Weyl transformed Milne metric (2.63) which is dual to the bulk geometry (4.53), $\langle T_{\mu\nu}\rangle = 0$ only if d is odd. For even d, holographic renormalization reproduces the Weyl anomaly of the dual field theory. In the case of $d = 4$, we obtain (using minimal subtraction scheme)

$$\langle \widetilde{T}_{\mu\nu}\rangle = \frac{1}{8\pi G_N}\mathcal{A}_{\mu\nu} \tag{4.55}$$

with

$$\begin{aligned}\mathcal{A}_{\mu\nu} &= \frac{1}{16}\left(\frac{4}{3}\widetilde{R}_{\mu\nu}\widetilde{R} - 2\widetilde{R}_{\mu\rho}\widetilde{R}^{\rho}{}_{\nu} - \tilde{g}_{\mu\nu}\left(\frac{1}{2}\widetilde{R}^2 - \widetilde{R}_{\rho\sigma}\widetilde{R}^{\rho\sigma}\right)\right),\\ &= \mathrm{diag}\left(-\frac{1}{32\sigma^4}, -\frac{11}{648\sigma^2\tau_0^2}, \frac{25\tau_0}{648\sigma^5}, \frac{25\tau_0}{648\sigma^5}\right)\end{aligned} \tag{4.56}$$

where $\tilde{g}$ denotes the Weyl rescaled background metric (2.63), $\widetilde{R}_{\mu\nu}$ is the Ricci tensor built out of it, etc. It is easy to verify that

$$\widetilde{\nabla}_\mu \widetilde{T}^{\mu}{}_{\nu} = 0, \tag{4.57}$$

i.e. energy and momentum is conserved in the Weyl rescaled background metric (2.63) (with $\widetilde{\nabla}$ being the covariant derivative built out of it), and

$$\widetilde{T}^{\mu}{}_{\mu} = -\frac{1}{8\pi G_N}\left(\frac{1}{24}\widetilde{R}^2 - \frac{1}{8}\widetilde{R}_{\rho\sigma}\widetilde{R}^{\rho\sigma}\right) = \frac{1}{8\pi G_N}\frac{2}{27\sigma^4}. \tag{4.58}$$

[15] Diffeomorphisms such as (4.54) which implement global transformations on the dual state are called improper diffeomorphisms which are always part of residual gauge freedom after gauge fixing in the bulk. The latter can also have additional proper diffeomorphisms which do not affect the dual physical quantities.

Using

$$\frac{1}{G_N} = \frac{2N^2}{\pi}, \tag{4.59}$$

we can readily find that (4.58) reproduces the Weyl anomaly of $SU(N)$ $\mathcal{N} = 4$ super-symmetric Yang-Mills theory [104, 105].

In order to construct a regular horizon cap, it is useful to change coordinates from r and τ to v and σ following (4.54) as in the case of the spacetime dual to the vacuum state. Note, it follows from (2.100) that v and s are the same. In these new coordinates, the metric (2.97) takes the form:

$$\begin{aligned} \mathrm{d}s^2 &= -\frac{2}{v^2}\frac{d-1}{d-2}\mathrm{d}v\mathrm{d}\sigma - \frac{1}{v^2}\left(\frac{(d-1)^2}{(d-2)^2}A(v,\sigma) + \frac{2(d-1)v}{(d-2)^2\sigma}\right)\mathrm{d}\sigma^2 \\ &\quad + \frac{1}{\tau_0^2}\left(1+\frac{\sigma}{v}\right)^2 e^{L(v,\sigma)}\mathrm{d}\hat{\zeta}^2 + \frac{1}{v^2}\left(\frac{\sigma}{\tau_0}\right)^{-\frac{2}{d-2}} e^{K(v,\sigma)}\mathrm{d}s_\perp^2, \end{aligned} \tag{4.60}$$

and is dual to Bjorken flow on the Weyl rescaled background metric (2.63) at the boundary. Holographic renormalization and the constraints of the Einstein's equations (4.51) imply that the energy-momentum tensor of the dual Bjorken flow takes the form

$$\langle \widetilde{T}_{\mu\nu} \rangle = T^W_{\mu\nu} + \frac{1}{8\pi G_N}\mathcal{A}_{\mu\nu} \tag{4.61}$$

where $T^W_{\mu\nu}$ takes the general Bjorken form with non-vanishing components given by (2.64) in which

$$\tilde{\epsilon}(\sigma) = -\frac{d-1}{16\pi G_N}\frac{(d-1)^2}{(d-2)^2}a_d(\sigma), \tag{4.62}$$

and $\mathcal{A}_{\mu\nu}$ is the Weyl anomaly appearing for even d. Comparing with (2.116), we indeed verify that the bulk diffeomorphism (4.54) implements the Weyl transformation and time reparametrization in the dual theory (with the Weyl factor given by (2.62)) and also reproduces its Weyl anomaly. Particularly, for $d = 4$, we recall that $\mathcal{A}_{\mu\nu}$ is simply given by (4.56). The anomalous term is state-independent (and is always the same as in the Weyl transformed vacuum state). We again note that $\langle \widetilde{T}_{\mu\nu} \rangle$ is invariant under the residual gauge symmetry since it

is independent of $a_1(\tau)$ after we implement the gravitational constraints following the previous discussion.

Obviously, the late proper time expansion (2.102) takes the form

$$\begin{aligned} A(v,\sigma) &= 1-\varepsilon_0 v^d+\sum_{i=1}^{\infty}\left(\varepsilon_0^{1/d}\sigma\right)^{-i} a_{(i)}(\varepsilon_0^{1/d}v), \\ L(v,\sigma) &= \sum_{i=1}^{\infty}\left(\varepsilon_0^{1/d}\sigma\right)^{-i} l_{(i)}(\varepsilon_0^{1/d}v), \\ K(v,\sigma) &= \sum_{i=1}^{\infty}\left(\varepsilon_0^{1/d}\sigma\right)^{-i} k_{(i)}(\varepsilon_0^{1/d}v). \end{aligned} \tag{4.63}$$

Explicitly, for $d = 4$ as mentioned in section 2.2.4 the first order equations takes the similar form ,

$$\begin{aligned} a_{(1)}(x) &= \alpha_1\frac{x(1+x^4)}{3}+\frac{2x^4(1+x)}{3}, \\ k_{(1)}(x) &= \alpha_1\frac{x}{3}+\frac{1}{2}g(x), \\ l_{(1)}(x) &= \alpha_1\frac{x}{3}-g(x), \end{aligned} \tag{4.64}$$

with

$$g(x)=\frac{4}{3}x-\frac{1}{3}\ln(x^2+1)-\frac{2}{3}\ln(x+1)-\frac{2}{3}\arctan x. \tag{4.65}$$

Above α_1 is the dimensionless parameter associated with the residual gauge freedom as mentioned earlier. At any order in the late proper time expansion, the terms multiplying α_1 in (4.64) remain the same, however we should replace α_1 by α_n at the n-th order. It is also easy to see that $g(x)$ is finite at $x = 1$ implying that the metric is regular (with no naked singularity) at the perturbative horizon

$$v_h=\varepsilon_0^{-1/d}+O(\sigma^{-1}). \tag{4.66}$$

At late proper time the dual black brane has a constant surface gravity and area although the directions longitudinal to the flow keep expanding and those transvere to the flow keep contracting.

The above metric reproduces the late proper time expansion of $\widetilde{\epsilon}(\sigma)$ which takes the form (2.65) with ϵ_0 given by (2.116) and λ_n taking specific values for a given d. Particularly, for any d, we obtain

$$\lambda_1 = -\frac{1}{(d-1)^{\frac{d-1}{d}}(16\pi G_N)^{1/d}}. \tag{4.67}$$

It is easy to verify from (2.58) and the equation of state (see (2.117))

$$T = \beta^{-1} = \frac{d}{4\pi}\varepsilon_0^{1/d}, \quad \epsilon = \frac{d-1}{16\pi G_N}\varepsilon_0 = \frac{d-1}{16\pi G_N}\left(\frac{4\pi T}{d}\right)^d \tag{4.68}$$

that (4.67) implies via (2.58) that

$$\frac{\eta}{s} = \frac{1}{4\pi}\,, \tag{4.69}$$

for any $d > 2$. For details of d=2 see Appendix B

4.3 The bulk scalar field and the horizon cap of the Bjorken flow

The key to obtaining the real time correlation functions is solving the dynamics of the scalar field in the gravitational background dual to the Bjorken flow. The starting point, however, is to construct the analogue of the bulk Schwinger-Keldysh contour with the horizon cap for the gravitational background itself. This is straightforward. The metric dual to the Weyl scaled Bjorken flow (given by Eqs. (4.60) and (4.63)) reaches a constant horizon temperature at late time although the boundary metric has time-dependent spatial components. Since we would be working perturbatively in the late proper time expansion, we will fix the horizon cap at the constant late-time value $v = \varepsilon_0^{-1/d}$ to all orders in the perturbative late proper time expansion while keeping the residual gauge freedom of radial reparametrization unfixed as mentioned above. The metric is analytic to all orders at the horizon cap. Therefore, there is no modification to the metric on the other arm of the bulk spacetime as it is reached via the complexified v contour encircling the horizon as shown in Fig. 4.2 (as emphasized earlier, there is no analytic

continuation in σ and other coordinates). Exactly the same gravitational background is valid on both arms of the complex v contour. It is also easy to see that the on-shell Einstein-Hilbert action on the two arms cancel each other out implying that the dual (non-)equilibrium partition function in absence of additional sources (and with the same boundary metric on the two arms) is exactly zero, as should be the case.[16]

There is a crucial subtlety to this rather simple construction. We should worry about the residual gauge symmetries at first and higher orders in the late proper time expansion. In what follows, we will show that the analytic behavior of the sourced scalar field retains its equilibrium nature to all orders in the late proper time expansion at the horizon cap, provided the residual gauge symmetry is fixed in a unique way at each order. This addresses an issue which would have arisen if we had fixed the residual gauge symmetries to keep the apparent or the event horizon at $v = \varepsilon_0^{-1/d}$ to all orders in the late proper time expansion. However the location of these two horizons differ at second and higher orders in the proper time expansion. We find that the gauge fixing which implements the regularity of the horizon cap is exactly the same which fixes the event (but not the apparent) horizon at $v_h = \varepsilon_0^{1/d}$ up to third order in the proper time expansion in the case of AdS_4 and AdS_5. Although we do not have an analytic proof that this feature will continue to hold at higher orders, we expect it to be the case as we explicitly find that the gauge fixing is independent of the mass of the bulk scalar field, and it should also hold for fermion, vector and higher rank tensor fields.

To see the main advantage of working in the v and σ coordinates, note that the explicit form of the leading order metric (as evident from Eqs. (4.60) and (4.63)) is:

$$\begin{aligned} \mathrm{d}s^2 &= -\frac{2}{v^2}\frac{d-1}{d-2}\mathrm{d}v\mathrm{d}\sigma - \frac{1}{v^2}\left(\frac{(d-1)^2}{(d-2)^2}(1-v^d\varepsilon_0+\mathcal{O}(\sigma^{-1}))+\frac{2(d-1)v}{(d-2)^2\sigma}\right)\mathrm{d}\sigma^2 \\ &\quad +\frac{1}{\tau_0^2}\left(1+\frac{\sigma}{v}\right)^2(1+\mathcal{O}(\sigma^{-1}))\mathrm{d}\hat{\zeta}^2+\frac{1}{v^2}\left(\frac{\sigma}{\tau_0}\right)^{-\frac{2}{d-2}}(1+\mathcal{O}(\sigma^{-1}))\mathrm{d}s_\perp^2. \end{aligned} \tag{4.70}$$

[16] In the field theory, this is equivalent to the statement that $W[J_1 = J_2 = 0] = 0$.

It is useful to define the *comoving momenta* which depend on σ

$$\kappa_L = k_L \frac{\tau_0}{\sigma}, \quad \vec{\kappa}_T = \vec{k}_T \left(\frac{\tau_0}{\sigma}\right)^{-\frac{1}{d-2}}. \tag{4.71}$$

such that it takes care of the longitudinal expansion and transverse contraction of the boundary metric. A natural ansatz for the scalar field consistent with boost invariance of the background geometry is:

$$\Phi(v, \sigma, \hat{\zeta}, \vec{x}_\perp) \approx e^{i\left(-\frac{d-1}{d-2}\omega\sigma + k_L\hat{\zeta} + \vec{k}_T\cdot\vec{x}_\perp\right)} f(v, \omega, \kappa_L, \vec{\kappa}_T). \tag{4.72}$$

where remarkably there is no explicit σ dependence in f (only implicitly through κ_L and $\vec{\kappa}_T$) while in the phase we have the usual fixed conjugate momenta k_L and $\vec{k}_T$. This is exact at leading order and can be further corrected to obtain a systematic expansion of the equations of motion in powers of σ^{-1} as shown below. Particularly, the Klein Gordon equation $(\Box - m^2)\Phi = 0$ for the bulk scalar field at the leading order σ^0 is then[17]

$$\mathcal{D}f = O(\sigma^{-1}) \tag{4.73}$$

where

$$\mathcal{D} = v^2(1 - v^d\varepsilon_0)\partial_v^2 - v(d - 1 - 2iv\omega + v^d\varepsilon_0)\partial_v - (m^2 + v(v(\kappa_L^2 + \kappa_T^2) + i(d-1)\omega)). \tag{4.74}$$

Remarkably, the left hand side of (4.73) is just the Klein Gordon equation for the massive bulk scalar in the AdS_{d+1} static black brane geometry (4.25) at temprature β^{-1} given by (4.68), with v substituting for r, and ω, κ_L and $\vec{\kappa}_T$ identified with the canonical frequency and momenta. The implication is that f will have exactly the same solutions at the leading order as in the static black brane geometry and therefore the same analytic structure at the horizon cap at the leading order. For the homogeneous ($k_L = \vec{k}_T = 0$) and massless case, this result reduces to the observation made by Janik and Peschanski [156] in the context of the transients of the Bjorken

[17] To obtain this we should substitute k_L and $\vec{k}_T$ in (4.72) by the redefined momenta (4.71) and remember to differentiate f w.r.t. σ as the redefined momenta (4.71) depend on σ.

flow.

Note that the dependence of f in (4.72) on the co-moving momenta imply that we do not have separation of variables, but this should not be expected as the background at late time corresponds to an expanding boost-invariant perfect fluid, which has no time-like Killing vector. Nevertheless, the map to the Laplacian of a static black hole geometry is possible at leading order because the boost invariant perfect fluid is given only by a time-dependent temperature.

The ansatz (4.72) can be corrected to incorporate the viscous and all higher order corrections to the gravitational Bjorken flow background systematically while ensuring the regularity of the horizon cap after fixing the residual gauge freedom perturbatively in late proper time expansion. This modified ansatz involves an expansion in σ^{-1} with coefficients which are functions of v, ω and the co-moving momenta, such that the equations of motion can be solved systematically in σ^{-1} expansion as well. Obviously, this implies that we also take into account the implicit dependence of the co-moving momenta on σ while obtaining the equations of motion order by order in σ^{-1}.

Explicitly, the ansatz for the bulk scalar field in the full complexified spacetime with 1 and 2 labelling the sheets of the bulk spacetime ending at the forward and backward arms of the Schwinger-Keldysh contour respectively at their boundaries is

$$\begin{aligned}\begin{pmatrix}\Phi_1(v,\sigma,\hat{\zeta},\vec{x}_\perp)\\ \Phi_2(v,\sigma,\hat{\zeta},\vec{x}_\perp)\end{pmatrix} &= \int \mathrm{d}\omega \mathrm{d}k_L \mathrm{d}^{d-2}k_T\ e^{i\left(k_L\hat{\zeta}+\vec{k}_T\cdot\vec{x}_\perp\right)} e^{-i\frac{d-1}{d-2}\omega\sigma}\left(\frac{\sigma}{\tau_0}\right)^{i\gamma_0(\omega/\varepsilon_0^{1/d})} \\ &\quad \sum_{n=0}^{\infty}\left(\varepsilon_0^{1/d}\sigma\right)^{-n}\mathcal{M}_n(v,\omega,\kappa_L,\vec{\kappa}_T)\cdot\begin{pmatrix}p(\omega,k_L,k_T)\\ q(\omega,k_L,k_T)\end{pmatrix}\end{aligned} \tag{4.75}$$

where

$$\mathcal{M}_n(v,\omega,\kappa_L,\vec{\kappa}_T)=\begin{pmatrix}\phi_{n,in}(v,\omega,\kappa_L,\vec{\kappa}_T) & \phi_{n,out}(v,\omega,\kappa_L,\vec{\kappa}_T)\\ \phi_{n,in}(v,\omega,\kappa_L,\vec{\kappa}_T) & e^{\beta\omega}\phi_{n,out}(v,\omega,\kappa_L,\vec{\kappa}_T)\end{pmatrix}. \tag{4.76}$$

Above, in (4.75), a non-analytic term proportional to $\sigma^{i\gamma_0}$ has been introduced with γ_0 being a new dimensionless function of only $\omega/\varepsilon_0^{1/d}$. This non-analytic factor is crucial to have a regular

horizon cap as shown below. However, it does not affect the zeroth order equation of motion which takes the form of the Laplacian on a static black brane as discussed above. For any ω, (4.75) has the appearance of a trans-series in σ^{-1} with ω characterizing the continuous instanton exponent. Note p and q are functions of ω, k_L and k_T (and not the redefined momenta κ_L and $\vec{\kappa}_T$), since we are integrating over ω, k_L and k_T, and utilizing the superposition principle to obtain the general solution with right behaviour at the horizon cap. However $\mathcal{M}_n$ depend on κ_L and $\vec{\kappa}_T$, and therefore they have non-trivial derivatives w.r.t. σ. The coefficients p and q, which are functions of the ordinary momenta (k_L and $\vec{k}_T$), and coefficients of the in-going and out-going modes respectively (see more below), are determined by imposing Dirichlet boundary conditions at the two boundaries.

The structure of $\mathcal{M}_n$ in (4.76) is determined as follows. Note that at the zeroth order, i.e. at $n = 0$, we obtain exactly the solutions of the static black brane as noted above. We can choose the basis of solutions which are in-going and out-going at the horizon, and satisfying the normalization conditions given by (4.28). Explicitly, near the perturbative horizon $v = \varepsilon_0^{1/d}$ where the horizon cap is located, they take the forms[18]

$$\begin{aligned}\phi_{0,in} &= 1 + \sum_{k=1}^{\infty} p_{0,k} \left(\varepsilon_0^{-1/d} - v\right)^k , \\ \phi_{0,out} &= \left(\varepsilon_0^{-1/d} - v\right)^{i \frac{2\omega}{d\varepsilon_0^{1/d}}} \left(1 + \sum_{k=1}^{\infty} q_{0,k} \left(\varepsilon_0^{-1/d} - v\right)^k\right),\end{aligned} \tag{4.77}$$

respectively. Note we have used (4.68) to set $\beta\omega/(2\pi) = 2\omega/(d\varepsilon_0^{1/d})$. For $n \geq 1$, $\phi_{n,in}$ and $\phi_{n,out}$ represent corrections to these zeroth order solutions as discussed below. In (4.76), we have assumed that $\phi_{n,in}$ and $\phi_{n,out}$ have the same behavior at the horizon cap $v = v_h = \varepsilon_0^{-1/d}$ for $n \geq 1$as in the case of the equilibrium (or equivalently at the zeroth order). This indeed turns out to be the case with appropriate residual gauge fixing as mentioned before and explicitly shown below.[19]

[18] $\phi_{0,in} \to 1$ and $\left(\varepsilon_0^{-1/d} - v\right)^{-i \frac{2\omega}{d\varepsilon_0^{1/d}}} \phi_{0,out} \to 1$ as $v \to \varepsilon_0^{-1/d}$ are just normalizations.

[19] In the following section, we show that preserving the near-horizon behavior to all orders is required for satisfying many consistency conditions, such as ensuring that the retarded correlation function is given by causal response.

At higher orders, the equations determining $\phi_{n,in}$ and $\phi_{n,out}$ can be obtained from expanding $(\Box - m^2)\Phi = 0$ in the late proper time expansion after substituting k_L and $\vec{k}_T$ in (4.75) by the redefined momenta (4.71), and isolating the σ^{-n} term. We obtain that $\phi_{n,in}$ and $\phi_{n,out}$ satisfies the linear inhomogeneous ordinary differential equations

$$\mathcal{D}\phi_{n,in} = \mathcal{S}_{n,in}, \quad \mathcal{D}\phi_{n,out} = \mathcal{S}_{n,out}, \tag{4.78}$$

with $\mathcal{D}$ being the same operator (4.74), which is simply that corresponding to the Klein-Gordon equation for the static black brane at temperature β^{-1} given by (4.68), at all orders. The sources $\mathcal{S}_{n,in}$ and $\mathcal{S}_{n,out}$ are functions of v, ω, κ_L and $\vec{\kappa}_T$, and depend on $\phi_{m,in}$ and $\phi_{m,out}$ respectively for $m < n$. Both of these sources also depend on the functions $a_{(i)}$, $k_{(i)}$ and $l_{(i)}$, which appear in the late proper time expansion (4.63) of the background metric, with $i \leq n$. Note that the source is linear in the bulk field Φ, and therefore splits into $\mathcal{S}_{n,in}$ and $\mathcal{S}_{n,out}$ at each order in the σ^{-1} expansion for $n \geq 1$. Since $\phi_{n,in}$ for $n \geq 1$ corrects $\phi_{0,in}$, we include the particular solution with only $\phi_{m,in}$ (and $m < n$) appearing in the source term $\mathcal{S}_{n,in}$ in it. The particular solutions sourced by $\phi_{m,out}$ with $0 \leq m < n$ which appear in $\mathcal{S}_{n,out}$ are added by definition to $\phi_{n,out}$ similarly.

The regularity of the horizon cap implies that at first and higher orders in the proper time expansion, we should have

$$\begin{aligned} \lim_{v \to \varepsilon_0^{-1/d}} \left(\varepsilon_0^{-1/d} - v\right)^{-i\frac{2\omega}{d\varepsilon_0^{1/d}}} \phi_{n,out}(v, \omega, \kappa_L, \vec{\kappa}_T) &= -i\gamma_{n,out}(\omega, \kappa_L, \vec{\kappa}_T), \\ \lim_{v \to \varepsilon_0^{-1/d}} \phi_{n,in}(v, \omega, \kappa_L, \vec{\kappa}_T) &= -i\gamma_{n,in}(\omega, \kappa_L, \vec{\kappa}_T), \end{aligned} \tag{4.79}$$

with $\gamma_{n,out}$s and $\gamma_{n,in}$s as new functions of ω, κ_L and $\vec{\kappa}_T$ for $n \geq 1$. This will ensure that the analytical dependence of the field on v at the horizon cap $v = v_h = \varepsilon_0^{-1/d}$ is the same to all orders in the proper time expansion. Note that at the zeroth order, the analogous conditions for $\phi_{0,in}$ and $\phi_{0,out}$ are simply given by 1 on the RHS in both cases by choice (see (4.77)). We will show that the $\gamma_{n,out}$s and $\gamma_{n,in}$s can be determined uniquely for $n \geq 1$ via horizon cap regularity and field theory identities.

Firstly, note that (4.79) implies that $\phi_{n,in}$ and $\phi_{n,out}$ can be written in the form

$$\phi_{n,in} = \phi_{n(p),in} - i\gamma_{n,in}\ \phi_{0,in}, \quad \phi_{n,out} = \phi_{n(p),out} - i\gamma_{n,out}\ \phi_{0,out} \tag{4.80}$$

for $n \geq 1$ such that $\phi_{n(p),in}$ and $\phi_{n(p),out}$ are the particular solutions of the inhomogeneous ordinary differential equations (4.78). Both $\phi_{n(p),in}$ and $\phi_{n(p),out}$ are determined by the sources $\mathcal{S}_{n,in}$ and $\mathcal{S}_{n,out}$, and are proportional to the coefficients p and q, respectively (i.e. they vanish when $p = q = 0$). Near the horizon cap $v \approx \varepsilon_0^{1/d}$, we explicitly find that $\phi_{n(p),in}$ and $\phi_{n(p),out}$ behave as

$$\begin{aligned} \lim_{v\to\varepsilon_0^{-1/d}} \left(\varepsilon_0^{-1/d} - v\right)^{-i\frac{2\omega}{d\varepsilon_0^{1/d}}} \phi_{n(p),out} &= O\left(\varepsilon_0^{-1/d} - v\right), \\ \lim_{v\to\varepsilon_0^{-1/d}} \phi_{n(p),in} &= O\left(\varepsilon_0^{-1/d} - v\right), \end{aligned} \tag{4.81}$$

respectively. Equivalently,

$$\begin{aligned} \phi_{n(p),out} &= \left(\varepsilon_0^{-1/d} - v\right)^{i\frac{2\omega}{d\varepsilon_0^{1/d}}} \sum_{k=1}^{\infty} q_{n,k} \left(\varepsilon_0^{-1/d} - v\right)^k, \\ \phi_{n(p),in} &= \sum_{k=1}^{\infty} p_{n,k} \left(\varepsilon_0^{-1/d} - v\right)^k \end{aligned} \tag{4.82}$$

where the coefficients should be determined by the equations of motion. For the outgoing solution, we find that this behavior is possible only when the residual gauge parameter α_n appearing in the background metric and $\gamma_{n,out}$ are chosen appropriately to cancel double and single poles appearing in the equation of motion (4.78) at the horizon cap for each $n \geq 1$. Furthermore, α_ns are simply numerical constants (as they are defined to be), and $\gamma_{n,out}$s are linear functions of $\omega/\varepsilon_0^{1/d}$ only. Thus the outgoing solutions appearing in $\mathcal{M}_n$ in our ansatz (4.75) are determined uniquely. As discussed before, and will be explicitly shown again in the next section this completely determines the advanced propagator of the Bjorken flow. The non-equilibrium retarded propagator then is also determined uniquely, since even out of equilibrium, the advanced and retarded propagators are related by the exchange of the spatial and temporal arguments. Utilizing this, we can determine $\gamma_{n,in}$s uniquely as well for $n \geq 1$ as will be shown in the next section.

In this section, we will focus mainly on the outgoing mode.

It is easy to see that (4.81) (equivalently (4.82)) implies that $\gamma_{n,in}$ and $\gamma_{n,out}$ are simply the coefficients of the homogeneous solutions of the equations of motion (4.78) for $n \geq 1$. Therefore $\gamma_{n,in}$ and $\gamma_{n,out}$ appear in $\mathcal{S}_{m,in}$ and $\mathcal{S}_{m,out}$ respectively for $m > n$. We will illustrate by example how requiring the regularity condition (4.81) (equivalently (4.82)) at the n-th order determines $\gamma_{n-1,out}$ along with the gauge parameter α_n (which is a constant) recursively.

Unlike the case of the outgoing mode, the ingoing mode is always analytic at the horizon cap. Therefore, we need to use consistency conditions for the Schwinger-Keldysh correlation functions to determine $\gamma_{n,in}$s for $n \geq 1$. However, γ_0 in the ansatz (4.75) appears in both the in-going and out-going modes. Our construction passes a significant consistency test that the same function $\gamma_0(\omega/\varepsilon_0^{1/d})$ determines the homogeneous transients (sourceless solutions which are ingoing at the horizon) with the argument $\omega/\varepsilon_0^{1/d}$ taking values corresponding to the appropriately rescaled quasi-normal mode frequencies of the static black hole, as will be discussed in section 4.4.5. This is remarkable as we determine the function γ_0 analytically by imposing the regularity condition (4.82) on the outgoing mode at the horizon cap.

In what follows, we illustrate how we determine the outgoing mode and the residual gauge fixing uniquely in the case of AdS_5. Let us first see how we determine γ_0 and α_1 at the first order in the proper time expansion. This requires the first order correction to the background metric given by (4.64) and (4.65). We find that the equation of motion (4.78) for $\phi_{1,out}$ explicitly takes the following form near the horizon cap $v \approx \varepsilon_0^{1/4}$ up to overall proportionality factors:

$$\begin{aligned}
&\frac{1}{(\varepsilon_0^{1/4}v-1)^2}\frac{\omega}{4\varepsilon_0^{1/4}}(\alpha_1+3)(\omega\varepsilon_0^{-1/4}+2i)\\
&+\frac{1}{(\varepsilon_0^{1/4}v-1)}\frac{i\omega}{\varepsilon_0^{1/4}}\left(\frac{2\kappa_L^2+2\kappa_T^2-m^2-3\omega^2+240\omega\varepsilon_0^{1/4}}{24\varepsilon_0^{1/2}}(\alpha_1+3)\right.\\
&\qquad\left.+\frac{(16+5\alpha_1)\omega^2-4\gamma_0\omega\varepsilon_0^{1/4}}{\varepsilon_0^{1/2}}\right)+\cdots,
\end{aligned} \tag{4.83}$$

with $\cdots$ denoting terms which are regular at $v=\varepsilon_0^{1/4}$ if $\phi_{1,out}$ is of the form (4.82). See Appendix

D for more details. We readily see that in order to have a solution of the desired form (4.81) we must impose

$$\alpha_1 = -3, \quad \gamma_0 = \frac{\omega}{4\varepsilon_0^{1/4}} \tag{4.84}$$

so that the double and single pole terms of the equation of motion appearing at the horizon cap vanish. The double pole term determines α_1 and the single pole term determines γ_0. As claimed before, we find that γ_0 is indeed a simple linear function of $\omega/\varepsilon_0^{1/4}$ (rather just proportional to it) while the gauge parameter α_1 is a numerical constant as it should be.

At the second order in the proper time expansion, similarly α_2 and γ_1 are determined by the vanishing of the double and single pole terms in the equation of motion for $\phi_{2,out}$ respectively. Here we have to utilize the explicit second order correction to the background metric given in Appendix B. Explicitly,

$$\alpha_2 = \frac{1}{72}\left(20 + 9\pi - 12\ln 2\right), \quad \gamma_1 = \frac{1}{16}\left(4i - \frac{9\pi + 4 - 24\ln 2}{9}\frac{\omega}{\varepsilon_0^{1/4}}\right). \tag{4.85}$$

We find once again α_2 is just a numerical constant as it should be and γ_1 is a linear function of $\omega/\varepsilon_0^{1/4}$.

It is indeed crucial that the $\gamma_{n,out}$s for $n \geq 0$ are functions of ω only and are independent of κ_L and $\vec{\kappa}_T$ which depend on σ. Otherwise, the central assumption (4.79) (and thus (4.82)) are not valid for the outgoing mode at the horizon cap, and should be corrected by log terms. The latter would have implied that the behavior near the horizon cap at first and higher orders is different from the zeroth order which is the same as in thermal equilibrium. Note that the ansatz for the ingoing mode in (4.82) remains valid to all orders even if $\gamma_{n,in}$s depend on κ_L and $\vec{\kappa}_T$. The coefficients $p_{n,k}$ in (4.82) also involve derivatives of $\gamma_{m,in}$s w.r.t. κ_L and $\vec{\kappa}_T$ with $m < n$. See Appendix D for more details.

Finally, we have explicitly verified that the values of the residual gauge parameters α_1 and α_2 are such that the event horizon is pinned to the horizon cap $v = v_h = \varepsilon_0^{-1/d}$ at the first and second orders respectively for both AdS_4 and AdS_5. Note that the apparent horizon

differs from the event horizon from second order onwards, so the evolving apparent horizon is behind the horizon cap. See Appendix C for details. We expect that this feature persists to all orders so that although the interior of the event horizon is excised, the full double sheeted geometry with the horizon cap still covers the entire bulk regions which can send signals to the boundary.[20] This feature mirrors the causal nature [29] of the Schwinger-Dyson equations for the correlation functions in the field theory. We will discuss more about the consistency of this result in Sec 4.4.5.

The quadratic on-shell action for the bulk scalar field is the sum of three pieces, namely S_{in-in} and $S_{out-out}$ which are quadratic in the in-going and out-going modes respectively, and the cross-term S_{in-out}. As in the thermal case discussed in section 4.1, $S_{in-in} = 0$. The in-going mode is analytic at the horizon and the contributions from the forward and backward arms of the radial contour cancel out. Once again this is required for consistency, as if we keep only the in-going mode by setting $q = 0$ in (4.75), then $J_1 = J_2$ and $W[J_1 = J_2] = 0$ for an arbitrary initial (non-thermal) state. (Recall W is identified with $iS_{on-shell}$.) The cross term S_{in-out} has a branch point at the horizon cap and the integration over the radial contour results in the two boundary terms like in the thermal case discussed in section 4.1. $S_{out-out}$ potentially has a single pole $(v_h - v)^{-1}$ divergence which we denote as S_ϵ. Explicitly,

$$\begin{aligned} S_\epsilon \;\propto\; & \int \mathrm{d}\omega \int \mathrm{d}k_L \int \mathrm{d}^{d-2}k_T \oint_\epsilon \mathrm{d}v \sqrt{-G}\Big(G^{vv}\partial_v\phi^*_{n,out}\partial_v\phi_{n,out} \\ & + G^{v\sigma}\left(\partial_v\phi^*_{n,out}\partial_\sigma\phi_{n,out} + \partial_v\phi_{n,out}\partial_\sigma\phi^*_{n,out}\right) + \cdots \Big) \end{aligned} \tag{4.86}$$

at the n-th order in the late proper time expansion. We have verified that $S_\epsilon = 0$ for the solution with the regular behaviour at the horizon cap given by (4.79), obtained for the appropriate choices of α_n and $\gamma_{n-1,out}$ as discussed above. One can also check that terms like $\phi^*_{k,out}\,\phi_{l,out}$ with $k + l \leq 2n$ also do not contribute to S_ϵ. However, our arguments for $S_{out-out} = 0$ for the thermal case in section 4.1 do not go through here since they rely on the KMS boundary condition.

[20] Although we do not have a rigorous proof to all orders, we believe that this follows from the general result that the event horizon is generated by null geodesics which also determine the singularities arising in the equation of motion at the horizon cap.

Nevertheless, since the pole at the horizon vanishes, $S_{out-out}$ is the sum of two boundary terms as well.

Since we preserve the horizon cap regularity at each order, the analytic continuation of the out-going mode across the horizon cap at each order works exactly in the same way as in the case of thermal equilibrium, i.e. $\phi_{n,out}(\omega, v, \kappa_L, \kappa_T)$ picks up a factor of $e^{\beta\omega}$ as evident from (4.80) and (4.82). Repeating the argument in section 4.1, each boundary term in $S_{out-out}$ involves one $\phi_b(\omega, \kappa_L, \kappa_T)$ and another $\phi_b(-\omega, \kappa_L, \kappa_T)$ (with b standing for the boundary value) or the corresponding boundary values of the radial derivatives. Also the contribution from the forward and backward arms come with opposite signs. While $\phi_b(\omega, \kappa_L, \kappa_T)$ picks up a $e^{\beta\omega}$ factor via analytic continuation across the horizon cap, $\phi_b(-\omega, \kappa_L, \kappa_T)$ picks up a $e^{-\beta\omega}$ factor, and these multiply to unity. Therefore, the boundary term contributions from the two arms cancel out resulting in $S_{out-out} = 0$.

Finally, as in the thermal case the on-shell action is simply the sum of two boundary terms (including the counter-terms for holographic renormalization) obtained from S_{in-out}. We can then readily differentiate this on-shell action to obtain the Schwinger-Keldysh correlation functions of the Bjorken flow.

As shown in the following section, the boundary correlation functions obtained solely from S_{in-out} ensure that the (non-equilibrium) retarded correlation function is given always by linear causal response. Furthermore, a major consistency check is that we reproduce the homogeneous transients as poles of the retarded Green's function in complexified ω not only at the leading order as computed in [156], but also at the subleading orders as shown in Appendix F and discussed further below. We will discuss more consistency tests in section 4.4.5.

4.4 The real time out-of-equilibrium correlation functions

4.4.1 Some useful relations and their consequences

Some crucial identities are valid for the Schwinger-Keldysh correlation functions even in out-of-equilibrium states. The first such identity of interest is

$$\begin{aligned} G_R(x_1,x_2) &= -i\theta(x_1^0-x_2^0)\mathrm{Tr}(\rho[\hat{O}(x_1),\hat{O}(x_2)]) \\ &= -i\Big(\mathrm{Tr}(\rho\,\mathrm{T}(\hat{O}(x_1)\hat{O}(x_2))) - \mathrm{Tr}(\rho\hat{O}(x_2)\hat{O}(x_1))\Big) \\ &= G_{11}(x_1,x_2) - G_{12}(x_1,x_2). \end{aligned} \tag{4.87}$$

Similarly, we can arrive at the identity

$$\begin{aligned} G_A(x_1,x_2) &= i\theta(x_2^0-x_1^0)\mathrm{Tr}(\rho[\hat{O}(x_1),\hat{O}(x_2)]) \\ &= -i\Big(\mathrm{Tr}(\rho\,\mathrm{T}(\hat{O}(x_1)\hat{O}(x_2))) - \mathrm{Tr}(\rho\hat{O}(x_1)\hat{O}(x_2))\Big) \\ &= G_{11}(x_1,x_2) - G_{21}(x_1,x_2). \end{aligned} \tag{4.88}$$

These identities give the retarded and advanced correlation functions in the usual Schwinger-Keldysh basis. The definitions of the correlation functions also imply that in any arbitrary state

$$G_{11}(x_1,x_2) = G_{11}(x_2,x_1), \quad G_{12}(x_1,x_2) = G_{21}(x_2,x_1), \quad G_{22}(x_1,x_2) = G_{22}(x_2,x_1). \tag{4.89}$$

Finally, it is obvious also that in any arbitrary (non-equilibrium) state

$$G_R(x_1,x_2) = G_A(x_2,x_1). \tag{4.90}$$

We will show that these identities imply the following for the horizon cap of the Bjorken flow. Firstly, will use (4.87) to show that the retarded correlation function is always obtained from the ingoing mode, and (4.88) to show that the advanced correlation function is always obtained

from the outgoing mode. Secondly, due to (4.90), we can uniquely determine $\gamma_{n,in}$ for $n \geq 1$. These coefficients cannot be determined by the regularity condition (4.79) of the horizon cap unlike $\gamma_{n,out}$ as discussed previously, but together with $\gamma_{n,out}$ they provide unique solution of the bulk scalar field for specified sources at the two boundaries via our ansatz (4.75). We will also see that by satisfying (4.90) we can also ensure the validity of (4.89).

Another important issue is the Weyl transformation. Consider a background metric $g_{\mu\nu}$ and its Weyl rescaled version $\Omega^2(x)g_{\mu\nu}$ such that $\Omega(x)$ is a non-vanishing function. Disregarding Weyl anomaly, the correlations functions of a scalar primary operator $\hat{O}$ of conformal dimension Δ_O in a conformal field theory living in these two background metrics would be related by

$$\mathrm{Tr}(\tilde{\rho}\hat{O}(x_1)\cdots\hat{O}(x_n))_{\Omega^2 g_{\mu\nu}} = \Omega^{-\Delta_O}(x_1)\cdots\Omega^{-\Delta_O}(x_n)\mathrm{Tr}(\rho\hat{O}(x_1)\cdots\hat{O}(x_n))_{g_{\mu\nu}} \tag{4.91}$$

where $\tilde{\rho} = U^\dagger \rho U$ with U denoting the unitary operator implementing the Weyl transformation. In the context of the holographic Bjorken flow, the states ρ and $\tilde{\rho}$ would be described by the holographic geometries whose boundary metrics are the Milne metric and its Weyl rescaled version respectively, and the respective energy-momentum tensors are also appropriately Weyl transformed including the correct holographic Weyl anomaly. This has been described in detail already in section 4.2.

We have seen that it is easier to implement the out-of-equilibrium horizon cap prescription in the Weyl transformed geometry (state) in which the temperature and entropy density become a constant at late proper time, and the Klein-Gordon equation in the bulk assumes the form of that in a static black brane at the leading order. It is convenient to compute the correlation functions in this background first, and then go back to the usual Bjorken flow background by Weyl transformation. In this case, we should use

$$\Omega^{\Delta_O}(\tau_1)\Omega^{\Delta_O}(\tau_2)\widetilde{G}(x_1, x_2)$$

with $\widetilde{G}(x_1, x_2)$ being the correlation functions computed after Weyl rescaling to obtain the cor-

relation functions in the usual Bjorken flow background with Ω given by (2.61) and (2.62). We disregard Weyl anomalies since they are not state-dependent (same as in vacuum).

Note that the full correlation functions to all orders in the late proper time expansion should depend on $\hat{\zeta}_1$ and $\hat{\zeta}_2$ only through the relative separation $\hat{\zeta}_1 - \hat{\zeta}_2$ in rapidity due to the boost invariance of the background, and similarly only on $|\vec{x}_{\perp 1} - \vec{x}_{\perp 2}|$ due to translation and rotation symmetries of the background in the transverse spatial plane.

We note that we can practically use the Weyl transformation to compute the correlation functions is because we are in the boost invariant hydrodynamic regime where the state is characterized only by a proper time dependent temperature. A Weyl rescaling makes the temperature constant at late time leading us to set-up a perturbative derivative expansion controlled by a fixed dimensionful parameter. However, there will contributions to the correlation functions in the form of a generalized trans-series which depends on the initial conditions, and are not constructed from hydrodynamic data. Such contributions which represent transients leading to hydrodynamization of correlation functions are discussed in section 4.5. In this section, we discuss the Schwinger-Keldysh correlation functions in the hydrodynamic regime using a well-defined late proper time expansion.

4.4.2 General structure of the hydrodynamic correlation functions

It is useful to define a new variable

$$s(\sigma) = \frac{d-1}{d-2}\sigma - \tilde{\gamma}_0 \varepsilon_0^{-1/d} \ln(\sigma/\tau_0) \tag{4.92}$$

with $\tilde{\gamma}_0 = \gamma_0 \varepsilon_0^{1/d}/\omega$ being a numerical constant (independent of ω). We have already seen that the smoothness of the horizon cap requires that in the case of AdS_5, $\tilde{\gamma}_0 = 1/4$ (see (4.84)).[21] In terms of this variable, we can readily see from (4.75) that the non-normalizable mode of the

[21] In the case of AdS_4, $\tilde{\gamma}_0 = 2/3$.

scalar field in the gravitational background dual to the Bjorken flow takes the form:

$$\begin{pmatrix} J_1(\sigma,\hat{\zeta},\vec{x}_\perp) \\ J_2(\sigma,\hat{\zeta},\vec{x}_\perp) \end{pmatrix} = \int \mathrm{d}\omega \mathrm{d}k_L \mathrm{d}^{d-2}k_T \; e^{-i\omega s(\sigma)} e^{i\left(k_L\hat{\zeta}+\vec{k}_T\cdot\vec{x}_\perp\right)} \sum_{n=0}^{\infty}\left(\varepsilon_0^{1/d}\sigma\right)^{-n}\mathcal{S}_n(\omega,\kappa_L,\vec{\kappa}_T)\cdot\begin{pmatrix} p(\omega,k_L,k_T) \\ q(\omega,k_L,k_T)\end{pmatrix} \tag{4.93}$$

and similarly, the expectation value of the dual operator (up to state-independent contact terms) is

$$\begin{pmatrix} \langle O_1(\sigma,\hat{\zeta},\vec{x}_\perp)\rangle \\ \langle O_2\rangle(\sigma,\hat{\zeta},\vec{x}_\perp) \end{pmatrix} = (2\Delta_O - d)\int \mathrm{d}\omega \mathrm{d}k_L \mathrm{d}^{d-2}k_T \; e^{-i\omega s(\sigma)} e^{i\left(k_L\hat{\zeta}+\vec{k}_T\cdot\vec{x}_\perp\right)} \sum_{n=0}^{\infty}\left(\varepsilon_0^{1/d}\sigma\right)^{-n}\mathcal{R}_n(\omega,\kappa_L,\vec{\kappa}_T)\cdot\begin{pmatrix} p(\omega,k_L,k_T) \\ q(\omega,k_L,k_T)\end{pmatrix} \tag{4.94}$$

where $\mathcal{S}_n$ and $\mathcal{R}_n$ can be defined from the asymptotic expansion of $\mathcal{M}_n$:

$$\mathcal{M}_n(v,\omega,\kappa_L,\vec{\kappa}_T) = v^{d-\Delta_O}\left(\mathcal{S}_n(\omega,\kappa_L,\vec{\kappa}_T)+\cdots\right) + v^{\Delta_O}\left(\mathcal{R}_n(\omega,\kappa_L,\vec{\kappa}_T)+\cdots\right), \tag{4.95}$$

and the labels 1 and 2 stand for the sheets of the bulk spacetime ending on the forward and backward arms of the Schwinger-Keldysh contour respectively.

It is also useful to define

$$\begin{aligned} \mathcal{R}(\sigma,\omega,\kappa_L,\vec{\kappa}_T) &= \sum_{n=0}^{\infty}\left(\varepsilon_0^{1/d}\sigma\right)^{-n}\mathcal{R}_n(\omega,\kappa_L,\vec{\kappa}_T), \\ \mathcal{S}(\sigma,\omega,\kappa_L,\vec{\kappa}_T) &= \sum_{n=0}^{\infty}\left(\varepsilon_0^{1/d}\sigma\right)^{-n}\mathcal{S}_n(\omega,\kappa_L,\vec{\kappa}_T). \end{aligned} \tag{4.96}$$

Clearly (4.76) leads to

$$\begin{aligned}
\mathcal{S}(\sigma,\omega,\kappa_L,\vec{\kappa}_T) &= \begin{pmatrix} a(\sigma,\omega,\kappa_L,\vec{\kappa}_T) & b(\sigma,\omega,\kappa_L,\vec{\kappa}_T) \\ a(\sigma,\omega,\kappa_L,\vec{\kappa}_T) & e^{\beta\omega} b(\sigma,\omega,\kappa_L,\vec{\kappa}_T) \end{pmatrix}, \\
\mathcal{R}(\sigma,\omega,\kappa_L,\vec{\kappa}_T) &= \begin{pmatrix} A(\sigma,\omega,\kappa_L,\vec{\kappa}_T) & B(\sigma,\omega,\kappa_L,\vec{\kappa}_T) \\ A(\sigma,\omega,\kappa_L,\vec{\kappa}_T) & e^{\beta\omega} B(\sigma,\omega,\kappa_L,\vec{\kappa}_T) \end{pmatrix}
\end{aligned} \tag{4.97}$$

where

$$\begin{aligned}
\phi_{in}(v,\sigma,\omega,\kappa_L,\vec{\kappa}_T) &= \sum_{n=0}^{\infty} \left(\varepsilon_0^{1/d}\sigma\right)^{-n} \phi_{n,in}(v,\omega,\kappa_L,\vec{\kappa}_T), \\
\phi_{out}(v,\sigma,\omega,\kappa_L,\vec{\kappa}_T) &= \sum_{n=0}^{\infty} \left(\varepsilon_0^{1/d}\sigma\right)^{-n} \phi_{n,out}(v,\omega,\kappa_L,\vec{\kappa}_T),
\end{aligned} \tag{4.98}$$

gives us $a(\sigma,\omega,\kappa_L,\vec{\kappa}_T)$, $A(\sigma,\omega,\kappa_L,\vec{\kappa}_T)$, $b(\sigma,\omega,\kappa_L,\vec{\kappa}_T)$ and $B(\sigma,\omega,\kappa_L,\vec{\kappa}_T)$ from their following near boundary expansions

$$\begin{aligned}
\phi_{in}(v,\sigma,\omega,\kappa_L,\vec{\kappa}_T) &= v^{d-\Delta_O}\left(a(\sigma,\omega,\kappa_L,\vec{\kappa}_T)+\cdots\right) + v^{\Delta_O}\left(A(\sigma,\omega,\kappa_L,\vec{\kappa}_T)+\cdots\right), \\
\phi_{out}(v,\sigma,\omega,\kappa_L,\vec{\kappa}_T) &= v^{d-\Delta_O}\left(b(\sigma,\omega,\kappa_L,\vec{\kappa}_T)+\cdots\right) + v^{\Delta_O}\left(B(\sigma,\omega,\kappa_L,\vec{\kappa}_T)+\cdots\right).
\end{aligned} \tag{4.99}$$

It should also be obvious that if we define a_n, A_n, b_n and B_n via

$$\begin{aligned}
\phi_{n,in}(v,\omega,\kappa_L,\vec{\kappa}_T) &= v^{d-\Delta_O}\left(a_n(\omega,\kappa_L,\vec{\kappa}_T)+\cdots\right) + v^{\Delta_O}\left(A_n(\omega,\kappa_L,\vec{\kappa}_T)+\cdots\right), \\
\phi_{n,out}(v,\sigma,\omega,\kappa_L,\vec{\kappa}_T) &= v^{d-\Delta_O}\left(b_n(\omega,\kappa_L,\vec{\kappa}_T)+\cdots\right) + v^{\Delta_O}\left(B_n(\omega,\kappa_L,\vec{\kappa}_T)+\cdots\right).
\end{aligned} \tag{4.100}$$

then

$$\begin{aligned}
a(\sigma,\omega,\kappa_L,\vec{\kappa}_T) &= \sum_{n=0}^{\infty}\left(\varepsilon_0^{1/d}\sigma\right)^{-n} a_n(\omega,\kappa_L,\vec{\kappa}_T),\\
A(\sigma,\omega,\kappa_L,\vec{\kappa}_T) &= \sum_{n=0}^{\infty}\left(\varepsilon_0^{1/d}\sigma\right)^{-n} A_n(\omega,\kappa_L,\vec{\kappa}_T),\\
b(\sigma,\omega,\kappa_L,\vec{\kappa}_T) &= \sum_{n=0}^{\infty}\left(\varepsilon_0^{1/d}\sigma\right)^{-n} b_n(\omega,\kappa_L,\vec{\kappa}_T),\\
B(\sigma,\omega,\kappa_L,\vec{\kappa}_T) &= \sum_{n=0}^{\infty}\left(\varepsilon_0^{1/d}\sigma\right)^{-n} B_n(\omega,\kappa_L,\vec{\kappa}_T).
\end{aligned} \tag{4.101}$$

The correlation function can be extracted simply from the on-shell action, which as shown in the previous section, is the sum of the two boundary terms obtained from S_{in-out}. The computations are similar to the case of the thermal equilibrium discussed before. The general structure of the correlation function with $\{a,b\}=\{1,2\}$ standing for the forward and backward arms of the Schwinger-Keldysh contour (using (2.66)) is (see Appendix E for more details)

$$\begin{aligned}
\widetilde{G}_{ab}(\sigma_1,\sigma_2,\hat{\zeta}_1-\hat{\zeta}_2,|\vec{x}_{\perp 1}-\vec{x}_{\perp 2}|) &= \frac{1}{\sqrt{-\widetilde{g}_1}\sqrt{-\widetilde{g}_2}}\frac{\delta^2 S_{\,on-shell}[J_1,J_2]}{\delta J_a(\sigma_1,\hat{\zeta}_1,\vec{x}_{\perp 1})\delta J_b(\sigma_2,\hat{\zeta}_2,\vec{x}_{\perp 2})}(-)^{a+b}\\
&= \frac{(d-2)^2}{(d-1)^2}\int \mathrm{d}\omega \mathrm{d}k_L \mathrm{d}^{d-2}k_T\, e^{-i\omega(s(\sigma_1)-s(\sigma_2))}\\
&\quad e^{ik_L(\hat{\zeta}_1-\hat{\zeta}_2)+i\vec{k}_T\cdot(\vec{x}_{\perp 1}-\vec{x}_{\perp 2})}\widehat{G}_{ab}(\sigma_1,\sigma_2,\omega,k_L,\vec{k}_T),
\end{aligned} \tag{4.102}$$

where (compare with the thermal case (4.46) – recall σ_3 is the Pauli matrix)

$$\begin{aligned}
\widehat{G}(\sigma_1,\sigma_2,\omega,k_L,\vec{k}_T) &= \frac{2\Delta_O-d}{2}\Big(s'(\sigma_2)\,\sigma_3\ \cdot\mathcal{R}(\sigma_1,\omega,\kappa_{L1},\vec{\kappa}_{T1})\cdot\ \mathcal{S}^{-1}(\sigma_2,\omega,\kappa_{L2},\vec{\kappa}_{T2})\\
&\quad +(\text{transpose},\ \sigma_1\leftrightarrow\sigma_2,\omega\to-\omega,\kappa_{L1}\leftrightarrow-\kappa_{L2},\vec{\kappa}_{T1}\leftrightarrow-\vec{\kappa}_{T2})\Big)
\end{aligned} \tag{4.103}$$

with

$$\kappa_{L1}=k_L\frac{\tau_0}{\sigma_1},\quad \kappa_{L2}=k_L\frac{\tau_0}{\sigma_2},\quad \vec{\kappa}_{T1}=\vec{k}_T\left(\frac{\tau_0}{\sigma_1}\right)^{-1/(d-2)},\quad \vec{\kappa}_{T2}=\vec{k}_T\left(\frac{\tau_0}{\sigma_2}\right)^{-1/(d-2)}. \tag{4.104}$$

The transpose above denotes matrix transposition, $\leftrightarrow$ denotes exchange operation and $\rightarrow$ replacement. The second term in (4.103) is produced by the symmetrization due to the differentiation in (4.102).

Explicitly, (compare with the thermal case given by Eq (4.47))

$$\begin{aligned}
\widehat{G}_{11}(\sigma_1,\sigma_2,\omega,k_L,\vec{k}_T) &\equiv \widehat{G}_R(\sigma_1,\sigma_2,\omega,k_L,\vec{k}_T)(1+n(\omega)) - \widehat{G}_A(\sigma_1,\sigma_2,\omega,k_L,\vec{k}_T)n(\omega),\\
\widehat{G}_{12}(\sigma_1,\sigma_2,\omega,k_L,\vec{k}_T) &\equiv \left(\widehat{G}_R(\sigma_1,\sigma_2,\omega,k_L,\vec{k}_T) - \widehat{G}_A(\sigma_1,\sigma_2,\omega,k_L,\vec{k}_T)\right)n(\omega),\\
\widehat{G}_{21}(\sigma_1,\sigma_2,\omega,k_L,\vec{k}_T) &\equiv \left(\widehat{G}_R(\sigma_1,\sigma_2,\omega,k_L,\vec{k}_T) - \widehat{G}_A(\sigma_1,\sigma_2,\omega,k_L,\vec{k}_T)\right)(1+n(\omega)),\\
\widehat{G}_{22}(\sigma_1,\sigma_2,\omega,k_L,\vec{k}_T) &\equiv \widehat{G}_R(\sigma_1,\sigma_2,\omega,k_L,\vec{k}_T)n(\omega) - \widehat{G}_A(\sigma_1,\sigma_2,\omega,k_L,\vec{k}_T)(1+n(\omega)),
\end{aligned} \tag{4.105}$$

with $n(\omega) = 1/(e^{\beta\omega}-1)$ is the Bose-Einstein distribution and

$$\begin{aligned}
\widehat{G}_R(\sigma_1,\sigma_2,\omega,k_L,\vec{k}_T) &\equiv \frac{(d-2)^2}{(d-1)^2}(2\Delta_O - d)\frac{s'(\sigma_1)+s'(\sigma_2)}{2}\\
&\quad \frac{A\left(\sigma_1,\omega,\kappa_{L1},\vec{\kappa}_{T1}\right)}{a\left(\sigma_2,\omega,\kappa_{L2},\vec{\kappa}_{T2}\right)},\\
\widehat{G}_A(\sigma_1,\sigma_2,\omega,k_L,\vec{k}_T) &\equiv \frac{(d-2)^2}{(d-1)^2}(2\Delta_O - d)\frac{s'(\sigma_1)+s'(\sigma_2)}{2}\\
&\quad \frac{B\left(\sigma_1,\omega,\kappa_{L1},\vec{\kappa}_{T1}\right)}{b\left(\sigma_2,\omega,\kappa_{L2},\vec{\kappa}_{T2}\right)}.
\end{aligned} \tag{4.106}$$

Above $\equiv$ denotes equality up to terms which vanish after the frequency and momentum integration in (4.102) and β is given by (4.68).

In order that (4.105) and (4.106) follow from (4.103), and also for the general identities (4.90) and (4.89) to be satisfied, we should have

$$\frac{A\left(\sigma_1,\omega,\kappa_{L1},\vec{\kappa}_{T1}\right)}{a\left(\sigma_2,\omega,\kappa_{L2},\vec{\kappa}_{T2}\right)} \equiv \frac{B\left(\sigma_2,-\omega,-\kappa_{L1},-\vec{\kappa}_{T1}\right)}{b\left(\sigma_1,-\omega,-\kappa_{L2},-\vec{\kappa}_{T2}\right)}, \tag{4.107}$$

i.e.

$$\widehat{G}_R\left(\sigma_1,\sigma_2,\omega,\kappa_{L1},\vec{\kappa}_{T1}\right) \equiv \widehat{G}_A\left(\sigma_2,\sigma_1,-\omega,-\kappa_{L2},-\vec{\kappa}_{T2}\right). \tag{4.108}$$

As mentioned, we will show in section 4.4.4 that the above can be satisfied by appropriate

choices of $\gamma_{n,in}s$ at each order in the late proper time expansion where we go to large values of the average reparametrized proper time $\overline{\sigma} = (\sigma_1 + \sigma_2)/2$ with fixed difference $\sigma_r = \sigma_1 - \sigma_2$. Thus we see that the correlation functions of the hydrodynamic Bjorken flow has a hidden and simple bi-local thermal structure to all orders in the late proper time expansion. We will show this satisfies crucial consistency tests.

Using (4.105) and (4.106), and the identities (4.87) and (4.88) which are valid out-of-equilibrium, we readily see that the actual retarded and advanced propagators of the Weyl transformed Bjorken flow is

$$\begin{aligned}
\widetilde{G}_R(\sigma_1,\sigma_2,\hat{\zeta}_1-\hat{\zeta}_2,|\vec{x}_{\perp 1}-\vec{x}_{\perp 2}|) &= \frac{(d-2)^2}{(d-1)^2}(2\Delta_O-d)\frac{s'(\sigma_1)+s'(\sigma_2)}{2} \\
&\int \mathrm{d}\omega \mathrm{d}k_L \mathrm{d}^{d-2}k_T\, e^{-i\omega(s(\sigma_1)-s(\sigma_2))} \\
&e^{ik_L(\hat{\zeta}_1-\hat{\zeta}_2)+i\vec{k}_T\cdot(\vec{x}_{\perp 1}-\vec{x}_{\perp 2})}\frac{A\left(\sigma_1,\omega,\kappa_{L1},\vec{k}_{T1}\right)}{a\left(\sigma_2,\omega,\kappa_{L2},\vec{k}_{T2}\right)}, \\
\widetilde{G}_A(\sigma_1,\sigma_2,\hat{\zeta}_1-\hat{\zeta}_2,|\vec{x}_{\perp 1}-\vec{x}_{\perp 2}|) &= \frac{(d-2)^2}{(d-1)^2}(2\Delta_O-d)\frac{s'(\sigma_1)+s'(\sigma_2)}{2} \\
&\int \mathrm{d}\omega \mathrm{d}k_L \mathrm{d}^{d-2}k_T\, e^{-i\omega(s(\sigma_1)-s(\sigma_2))} \\
&e^{ik_L(\hat{\zeta}_1-\hat{\zeta}_2)+i\vec{k}_T\cdot(\vec{x}_{\perp 1}-\vec{x}_{\perp 2})}\frac{B\left(\sigma_1,\omega,\kappa_{L1},\vec{k}_{T1}\right)}{b\left(\sigma_2,\omega,\kappa_{L2},\vec{k}_{T2}\right)}.
\end{aligned} \tag{4.109}$$

Therefore, it follows from (4.106) that indeed the retarded propagator is obtained purely from the out-of-equilibrium ingoing mode and the advanced propagator is also obtained from the out-of-equilibrium outgoing mode as claimed before. Note that at the zeroth order these results are automatic as it reduces to the thermal case described earlier.[22]

Finally, to obtain the Schwinger-Keldysh correlation function of the Bjorken flow, we should implement the Weyl transformation. Using (2.62), the Weyl transformation finally yields

[22]The bi-local thermal structure of hydrodynamic correlation functions in holography was argued earlier in [169] via Wigner transform. However the arguments here were less rigorous and relied on the possibility of obtaining correlation functions utilizing only one copy of the non-equilibrium background where the interior of the perturbative horizon could be removed.

the correlation function of the Bjorken flow:

$$G(\sigma_1,\sigma_2,\hat{\zeta}_1-\hat{\zeta}_2,|\vec{x}_{\perp 1}-\vec{x}_{\perp 2}|)=\left(\frac{\tau_0}{\sigma_1}\right)^{\frac{\Delta_O}{d-2}}\left(\frac{\tau_0}{\sigma_2}\right)^{\frac{\Delta_O}{d-2}}\widetilde{G}(\sigma_1,\sigma_2,\hat{\zeta}_1-\hat{\zeta}_2,|\vec{x}_{\perp 1}-\vec{x}_{\perp 2}|). \tag{4.110}$$

4.4.3 In the limit of the perfect fluid expansion

At very late proper time, the Bjorken flow is simply a perfect fluid expansion. For the Weyl transformed Bjorken flow which reaches a specific final temperature, the scalar field in the dual gravitational geometry can be mapped to that in the static thermal black brane spacetime at the leading order in the late proper time expansion. This naturally implies that the Schwinger-Keldysh correlation functions at late proper time should be related to the corresponding thermal correlation functions via appropriate spacetime-reparametrizations. After undoing the Weyl transformation, we should obtain the Schwinger-Keldysh correlation functions of the perfect fluid expansion.

To obtain the correlation function in the perfect fluid expansion, we first take the limit in $\widetilde{G}$ given by Eqs. (4.102)-(4.106), where we take the average reparametrized proper time coordinate $\overline{\sigma}=(1/2)(\sigma_1+\sigma_2)$ to infinity keeping the relative reparametrized proper time coordinate $\sigma_r=\sigma_1-\sigma_2$ fixed, and also $\hat{\zeta}_1-\hat{\zeta}_2$ and $\vec{x}_{\perp 1}-\vec{x}_{\perp 2}$ fixed. In this limit,

$$\kappa_{L1},\,\kappa_{L2}\to\overline{\kappa}_L,\quad \vec{\kappa}_{T1},\,\vec{\kappa}_{T2}\to\overline{\vec{\kappa}}_T \tag{4.111}$$

where

$$\overline{\kappa}_L=k_L\frac{\tau_0}{\overline{\sigma}},\quad \overline{\vec{\kappa}}_T=\vec{k}_T\left(\frac{\tau_0}{\overline{\sigma}}\right)^{-1/(d-2)}. \tag{4.112}$$

As shown in the previous section, both ϕ_{in} and ϕ_{out} assume the form in the static black brane geometry, and therefore

$$\widehat{G}_R\to\frac{A_0(\omega,\overline{\kappa}_L,\overline{\vec{\kappa}}_T)}{a_0(\omega,\overline{\kappa}_L,\overline{\vec{\kappa}}_T)},\quad \widehat{G}_A\to\frac{B_0(\omega,\overline{\kappa}_L,\overline{\vec{\kappa}}_T)}{b_0(\omega,\overline{\kappa}_L,\overline{\vec{\kappa}}_T)}, \tag{4.113}$$

given by the corresponding static black brane results and therefore all Schwinger-Keldysh correlation functions after the momentum integrals shown in (4.102) should assume the thermal form, i.e.

$$\widetilde{G} \to G_\beta\left(\sigma_1-\sigma_2, (\hat{\zeta}_1-\hat{\zeta}_2)\frac{\overline{\sigma}}{\tau_0}, |\vec{x}_{\perp 1}-\vec{x}_{\perp 2}|\left(\frac{\tau_0}{\overline{\sigma}}\right)^{\frac{1}{d-2}}\right) \tag{4.114}$$

with G_β denoting the thermal correlation functions. In order to obtain the above form, we change variables in the momentum integrals from k_L and $\vec{k}_T$ to $\overline{\kappa}_L$ and $\overline{\vec{\kappa}}_T$. Note the Jacobian of this transformation is identity. We also need to change the integration variable ω to $\omega = \omega(d-1)/(d-2)$ which yields a Jacobian $(d-2)/(d-1)$. Furthermore, we have used

$$s'(\sigma_1),\ s'(\sigma_2) \to \frac{d-1}{d-2}. \tag{4.115}$$

The factor $(d-2)^2/(d-1)^2$ in (4.102) is cancelled by one factor of $(d-1)/(d-2)$ each from the Jacobian and s'.

Finally, the Weyl transformation in the late proper time limit gives

$$G \to \left(\frac{\tau_0}{\overline{\sigma}}\right)^{\frac{2\Delta_Q}{d-2}} G_\beta\left(\frac{d-1}{d-2}(\sigma_1-\sigma_2), (\hat{\zeta}_1-\hat{\zeta}_2)\frac{\overline{\sigma}}{\tau_0}, |\vec{x}_{\perp 1}-\vec{x}_{\perp 2}|\left(\frac{\tau_0}{\overline{\sigma}}\right)^{\frac{1}{d-2}}\right) \tag{4.116}$$

the Schwinger-Keldysh correlation functions of the perfect fluid expansion. Since the static black brane has full rotational invariance in terms of the reparametrized spacetime coordinates, we may also write

$$G \to \left(\frac{\tau_0}{\overline{\sigma}}\right)^{\frac{2\Delta_Q}{d-2}} G_\beta\left(\frac{d-1}{d-2}(\sigma_1-\sigma_2), \sqrt{(\hat{\zeta}_1-\hat{\zeta}_2)^2\frac{\overline{\sigma}^2}{\tau_0^2}+|\vec{x}_{\perp 1}-\vec{x}_{\perp 2}|^2\left(\frac{\tau_0}{\overline{\sigma}}\right)^{\frac{2}{d-2}}}\right) \tag{4.117}$$

for the correlation functions in the limit of the late time perfect fluid expansion. The explicit analytic forms of the thermal holographic propagators is known, see [166, 170] as for instance.

It is obvious that we are actually resumming over the associated $\overline{\sigma}$ factors in the spatial factors $\hat{\zeta}_1-\hat{\zeta}_2$ and $\vec{x}_{\perp 1}-\vec{x}_{\perp 2}$. For brevity we will denote the variables as $\sigma_r = \sigma_1-\sigma_2$ (as defined

before) and

$$\widetilde{\zeta_r} = (\hat{\zeta}_1 - \hat{\zeta}_2)\frac{\overline{\sigma}}{\tau_0}, \quad \widetilde{x_{\perp r}} = |\vec{x}_{\perp 1} - \vec{x}_{\perp 2}|\left(\frac{\tau_0}{\overline{\sigma}}\right)^{\frac{1}{d-2}} . \tag{4.118}$$

The late proper time expansion of the Schwinger-Keldysh correlation function then amounts to the following series

$$G(x_1, x_2) = \left(\frac{\tau_0}{\overline{\sigma}}\right)^{\frac{2\Delta_O}{d-2}} \sum_{n=0}^{\infty} \frac{1}{\overline{\sigma}^n \varepsilon_0^{n/d}} G_n\left(\sigma_r, \widetilde{\zeta_r}, \widetilde{x_{\perp r}}\right) + \cdots \tag{4.119}$$

with $\cdots$ denoting trans-series type completion about which we will discuss more below.

Since the choice of τ_0 determines the effective final temperature $T = \beta^{-1}$ via (4.68), let's consider a scaling $\tau_0 \to \xi\tau_0$ to see if there is any ambiguity in the above result. Note that G_β in (4.117) depends only on $T\sigma_r$ and $T\sqrt{\widetilde{\zeta_r}^2 + \widetilde{x_{\perp r}}^2}$ as it is a thermal correlation matrix of a CFT. Under this scaling, it is evident from (4.8) that $\sigma \to \xi^{\frac{1}{d-1}}\sigma$, and therefore $\sigma_r \to \xi^{\frac{1}{d-1}}\sigma_r$, $\overline{\sigma} \to \xi^{\frac{1}{d-1}}\overline{\sigma}$, $\widetilde{\zeta_r} \to \xi^{\frac{1}{d-1}}\widetilde{\zeta_r}$ and $\widetilde{x_{\perp r}} \to \xi^{\frac{1}{d-1}}\widetilde{x_{\perp r}}$. Also $\epsilon_0 \to \xi^{-\frac{d}{d-1}}\epsilon_0$ and $T \to \xi^{-\frac{1}{d-1}}T$ as discussed earlier in section 2.1.4. Together these imply that G_β and also G_n in (4.119) are invariant under $\tau_0 \to \xi\tau_0$ since $T\sigma_r$ and $T\widetilde{\zeta_r}$ and $T\widetilde{x_{\perp r}}$ are invariant this scaling. However, the Weyl factor in (4.12) scales as $\xi^{\frac{2\Delta_O}{d-1}}$ implying that the *dimensionless correlation function* $\overline{\sigma}^{-2\Delta_0}G$ is invariant under the scaling of τ_0.

4.4.4 First and higher orders in the late proper time expansion

From the form of the Schwinger-Keldysh correlation functions given by Eqs. (4.102)-(4.106) which are valid to all orders, we can readily go beyond the perfect fluid limit systematically and construct the late proper time expansion (4.119). The contribution to the first order correction comes from the following terms:

1. The phase factor,

$$e^{-i\omega(s(\sigma_1)-s(\sigma_2))} \to e^{-i\omega\sigma_r\frac{d-1}{d-2}}\left(1 + i\omega\tilde{\gamma}_0\varepsilon_0^{-1/d}\frac{\sigma_r}{\overline{\sigma}} + \mathcal{O}\left(\overline{\sigma}^{-2}\right)\right) . \tag{4.120}$$

2. The Jacobian

$$s'(\sigma_1) \text{ and } s'(\sigma_2) \to \frac{d-1}{d-2} - \frac{\tilde{\gamma}_0}{\overline{\sigma}\varepsilon_0^{1/d}} + O\left(\overline{\sigma}^{-2}\right) . \tag{4.121}$$

3. Late-time expansion of the matrices $\mathcal{R}$ and $\mathcal{S}$ given by (4.97) in $\overline{\sigma}^{-1}$. This also includes the κ_L and $\vec{\kappa}_T$ dependence. For instance, consider any generic function $f(\kappa_{L1})$ and $f(\vec{\kappa}_{T1})$,

$$\begin{aligned} f(\kappa_{L1}) &= f(\overline{\kappa}_L) - \partial_{\overline{\kappa}_L} f(\overline{\kappa}_L) \frac{\sigma_r \overline{\kappa}_L}{2\overline{\sigma}} , \\ f(\vec{\kappa}_{T1}) &= f\left(\vec{\overline{\kappa}}_T\right) + \partial_{\vec{\overline{\kappa}}_T} f\left(\vec{\overline{\kappa}}_T\right) \frac{\sigma_r \vec{\overline{\kappa}}_T}{2(d-2)\overline{\sigma}} , \end{aligned} \tag{4.122}$$

and similarly for $f(\kappa_{L2})$ and $f(\vec{\kappa}_{T2})$.

From (4.103), we obtain

$$\begin{aligned} \widehat{G}_1 &= \frac{(2\Delta_0 - d)}{2} \frac{d-2}{d-1} \sigma_3 . \Big[\mathcal{R}_0 . \mathcal{S}^{-1}{}_1 + \mathcal{R}_1 . \mathcal{S}^{-1}{}_0 + \left(\mathcal{R}_0 . \partial_{\overline{\kappa}_L} \mathcal{S}^{-1}{}_0 - \partial_{\overline{\kappa}_L} \mathcal{R}_0 . \mathcal{S}^{-1}{}_0 \right) \frac{\sigma_r \overline{\kappa}_L}{2} \\ &- \left(\mathcal{R}_0 . \partial_{\vec{\overline{\kappa}}_T} \mathcal{S}^{-1}{}_0 - \partial_{\vec{\overline{\kappa}}_T} \mathcal{R}_0 . \mathcal{S}^{-1}{}_0 \right) \frac{\sigma_r \vec{\overline{\kappa}}_T}{2(d-2)} - \tilde{\gamma}_0 \varepsilon_0^{-1/d} \frac{d-2}{d-1} \mathcal{R}_0 . \mathcal{S}^{-1}{}_0 \Big] \left(\omega, \overline{\kappa}_L, \vec{\overline{\kappa}}_T \right) \\ &+ \left(\text{transpose}, \ \omega \to -\omega, \ \overline{\kappa}_L \to -\overline{\kappa}_L, \ \vec{\overline{\kappa}}_T \to -\vec{\overline{\kappa}}_T \right) . \end{aligned} \tag{4.123}$$

An easier way to read off the first order correction is to use (4.105) and (4.106), and consider similar $\overline{\sigma}^{-1}$ expansion of $\widehat{G}_R$ and $\widehat{G}_A$. Collecting first order terms from (4.106), as for instance, we obtain

$$\begin{aligned} \widehat{G}_{R,1} &= \frac{(2\Delta_0 - d)}{2} \frac{d-2}{d-1} \Bigg[\frac{2A_1}{a_0} - \frac{2A_0 a_1}{a_0^2} + \frac{A_0 \sigma_r}{a_0^2} \left(\frac{\vec{\overline{\kappa}}_T}{d-2} \partial_{\vec{\overline{\kappa}}_T} - \overline{\kappa}_L \partial_{\overline{\kappa}_L} \right) a_0 \\ &+ \frac{\sigma_r}{a_0} \left(\frac{\vec{\overline{\kappa}}_T}{(d-2)} \partial_{\vec{\overline{\kappa}}_T} - \overline{\kappa}_L \partial_{\overline{\kappa}_L} \right) A_0 - \frac{\tilde{\gamma}_0 \varepsilon_0^{-1/d} A_0}{a_0} \frac{d-2}{d-1} \Bigg] \left(\omega, \overline{\kappa}_L, \vec{\overline{\kappa}}_T \right) \end{aligned} \tag{4.124}$$

and

$$\begin{aligned} \widehat{G}_{A,1} &= \frac{(2\Delta_0 - d)}{2} \frac{d-2}{d-1} \Bigg[\frac{2B_1}{b_0} - \frac{2B_0 b_1}{b_0^2} + \frac{B_0 \sigma_r}{b_0^2} \left(\frac{\vec{\overline{\kappa}}_T}{d-2} \partial_{\vec{\overline{\kappa}}_T} - \overline{\kappa}_L \partial_{\overline{\kappa}_L} \right) b_0 \\ &+ \frac{\sigma_r}{b_0} \left(\frac{\vec{\overline{\kappa}}_T}{(d-2)} \partial_{\vec{\overline{\kappa}}_T} - \overline{\kappa}_L \partial_{\overline{\kappa}_L} \right) B_0 - \frac{\tilde{\gamma}_0 \varepsilon_0^{-1/d} B_0}{b_0} \frac{d-2}{d-1} \Bigg] \left(\omega, \overline{\kappa}_L, \vec{\overline{\kappa}}_T \right) . \end{aligned} \tag{4.125}$$

This allows us to finally determine $\gamma_{1,in}$ and similarly $\gamma_{n,in}$ for $n > 1$ as follows. After integrating over the frequency and momentum integrals (i.e. doing integrals over ω, k_L and $\vec{k}_T$) as in (4.109), we obtain the first order correction in the series expansion of the type (4.119):

$$G_R(x_1, x_2) = \sum_{n=0}^{\infty} \frac{1}{\overline{\sigma}^n \varepsilon_0^{n/d}} G_{R,n}\left(\sigma_r, \widetilde{\zeta}_r, \widetilde{x_{\perp r}}\right), \tag{4.126}$$

and similarly for $G_A(x_1, x_2)$. For the identities (4.87) and (4.88) to be satisfied, we therefore need (note that $\widetilde{x_{\perp r}}$ is invariant under $x_1 \leftrightarrow x_2$)

$$G_{R,n}\left(-\sigma_r, -\widetilde{\zeta}_r, \widetilde{x_{\perp r}}\right) = G_{A,n}\left(\sigma_r, \widetilde{\zeta}_r, \widetilde{x_{\perp r}}\right) \tag{4.127}$$

at each n, which can be ensured by appropriate choices of $\gamma_{n,in}(\omega, \kappa_L, \vec{\kappa}_T)$ at each order for $n \geq 1$, since they determine both A_n and a_n. In turn, this justifies the bi-local thermal structure (4.105) and (4.106) which implies via (4.87) and (4.88) that the retarded correlation originates purely from the ingoing mode and the advanced correlation function purely from the outgoing mode at all orders. We emphasize that although $\gamma_{n,out}$s are only functions of the frequency ω, $\gamma_{n,in}$s are functions of both frequency and momenta.

With $\gamma_{n,in}$ determined we know the RHS of (4.124) completely. Doing the frequency and momenta integrals shown in (4.102), we can obtain the first and similarly higher order corrections to all Schwinger-Keldysh propagators.

4.4.5 Consistency checks

The general result for the hidden bi-local thermal structure of the hydrodynamic correlation functions given by Eqs. (4.102)-(4.106) to all orders satisfies a simple consistency check. When $J_1 = J_2$, i.e. when the sources are the same at the two boundaries, we have only the in-going

solution which is analytic. The on-shell solution also vanishes. When $J_1 = J_2$, we have

$$\langle O_1(x_1)\rangle = \int_{x_2} (G_{11}(x_1, x_2)J_1(x_2) - G_{12}(x_1, x_2)J_2(x_2)) = \int_{x_2} G_R(x_1, x_2)J_1(x_2),$$

on the forward arm, and thus we see that the response in the forward arm is indeed given by the retarded correlation function, and this also follows from the bi-local thermal structure of the hydrodynamic correlation functions resulting in (4.109) as shown above. We can also see that the analytic in-going mode is indeed always related to causal response from the full non-linear evolution (we just consider the forward arm here). There is a unique regular solution to Einstein's gravity minimally coupled to a scalar field corresponding to an initial condition for the bulk scalar field $\Phi(v, \zeta, \vec{x}_\perp)$ at a constant Eddington-Finkelstein time hypersurface when the boundary source $J(\sigma, \zeta, \vec{x}_\perp)$ is specified for all time in the future. This solution can be obtained via a Chebyshev grid in the radial direction [112] which implies analyticity at the horizon, and thus the causal evolution is built out of analytic ingoing modes. Our result then should follow in the linearized limit. The way to implement this explicitly was shown earlier in [150] which is thus reproduced by the horizon cap prescription.[23]

A more non-trivial consistency check involves the outgoing mode. Consider an outgoing mode with frequency ω and momenta k_L and $\vec{k}_T$ in the Bjorken flow background. Evidently, from the discussion before, to all orders in the late proper time expansion, we have

$$J_2(\omega, k_L, \vec{k}_T) = e^{\beta\omega} J_1(\omega, k_L, \vec{k}_T)$$

with β defined by ε_0 as in (4.68). Therefore, on the forward arm (where we choose to do the k_L

[23] See [171] for the non-equilibrium retarded correlation function in a hydrodynamic expansion, and [172, 173] for AdS-Vaidya and states corresponding to quenches, etc. The latter uses the prescription of [150].

and $\vec{k}_T$ integrations first)

$$\begin{aligned}
\langle O_1(x_1)\rangle &= \int \mathrm{d}\omega \int \mathrm{d}^d x_2 e^{-i\omega(s(\sigma_1)-s(\sigma_2))}(\widehat{G}_{11}(\omega,x_1,x_2)J_1(\omega,\vec{x}_2) - \widehat{G}_{12}(\omega,x_1,x_2)J_2(\omega,\vec{x}_2)) \\
&= \int \mathrm{d}\omega \int \mathrm{d}^d x_2 e^{-i\omega(s(\sigma_1)-s(\sigma_2))}(\widehat{G}_{11}(\omega,x_1,x_2) - \widehat{G}_{12}(\omega,x_1,x_2)e^{\beta\omega})J_1(\omega,\vec{x}_2) \\
&= \int \mathrm{d}\omega \int \mathrm{d}^d x_2 e^{-i\omega(s(\sigma_1)-s(\sigma_2))}(\widehat{G}_{11}(\omega,x_1,x_2) - \widehat{G}_{21}(\omega,x_1,x_2))J_1(\omega,\vec{x}_2) \\
&= \int \mathrm{d}\omega \int \mathrm{d}^{\mathrm{d}} x_2 e^{-i\omega(s(\sigma_1)-s(\sigma_2))}\widehat{G}_A(\omega,x_1,x_2)J_1(\omega,\vec{x}_2) \\
&= \int \mathrm{d}^d x_2 G_A(x_1,x_2)J_1(x_2).
\end{aligned}$$

Above, we have used the result from (4.105) that $\widehat{G}_{12}e^{\beta\omega} = \widehat{G}_{21}$ and also the identity (4.88). Thus indeed we see that the outgoing mode gives advanced response. Note for both $J_2 = e^{\beta\omega}J_1$ and $\widehat{G}_{12}e^{\beta\omega} = \widehat{G}_{21}$ (used above) to hold, we need absence of log terms at the horizon, which follows if $\gamma_{n,out}$s are functions of ω only. The out-going solution which satisfies the regularity condition (4.82) at the horizon cap indeed has this property with $\gamma_{n,out}$ determined from the cancellation of the double and single poles of the equation of motion being a linear function of ω and independent of κ_L and $\vec{k}_T$.

Furthermore, let us consider transients which are ingoing solutions with vanishing sources at the boundary. To be simplistic, let us consider the homogeneous transients first. Since we can map the leading order solution to the static black brane background, we should have

$$\omega = \omega_Q \ ,$$

where ω_Q corresponds to the homogeneous quasinormal mode frequencies of the static black brane, as noted by Janik and Peschanski. A non-trivial consistency test of our ansatz for the bulk scalar field is that the condition for the sources to vanish at the first subleading order is

$$\gamma_0 = \gamma_0(\omega_Q),$$

i.e. for AdS_5 we should have

$$\gamma_0(\omega) = \frac{\omega_Q}{4\varepsilon_0^{1/4}}.$$

The details of the numerical verification are shown in Appendix F. These transients can be added to the solution with specific sources since the equation of the scalar field is linear and are needed for matching with arbitrary initial conditions for the bulk scalar field, as discussed below. The case of the inhomogeneous transients is complicated since the effective momenta κ_L and $\vec{\kappa}_T$ also depend on the proper time, and will be examined in a later work.

Our key result that the horizon cap is pinned to the non-equilibrium event horizon is consistent with the feature in non-equilibrium quantum field theory that the evolution of the Schwinger-Keldysh correlation functions, which can be written in the form of the Schwinger-Dyson equations for the commutator and anti-commutator via functional derivatives of the two-particle irreducible effective action, is causal and uniquely determined once we give the initial conditions for these in the initial state [29]. The bulk analogue is that the evolution of the field configuration on the full complexified geometry with the horizon cap should be uniquely and causally determined for given initial conditions. For this to hold, the horizon cap should cover the spacetime outside the event horizon, which is indeed the case.

4.5 On initial conditions and seeing behind the event horizon

The discussion on initial conditions is subtle.[24] We only discuss this briefly here and hope to address it fully in the future. For the full complexified geometry, in order to obtain a unique solution for the bulk scalar field on both arms, we need to specify $\Phi_1(v, \zeta, \vec{x}_\perp)$ and $\Phi_2(v, \zeta, \vec{x}_\perp)$ at an initial time σ_0 on both arms, and also the sources $J_1(\sigma, \zeta, \vec{x}_\perp)$ and $J_2(\sigma, \zeta, \vec{x}_\perp)$ at the two boundaries for all times in the future. Our horizon cap prescription leads to unique solutions for the in-going and out-going modes corresponding to $J_1(\sigma, \zeta, \vec{x}_\perp)$ and $J_2(\sigma, \zeta, \vec{x}_\perp)$ in a large proper time expansion, however it is not guaranteed we can match with arbitrary initial conditions

[24] We thank Kostas Skenderis for discussions on these issues.

$\Phi_1(v,\zeta,\vec{x}_\perp)$ and $\Phi_2(v,\zeta,\vec{x}_\perp)$ at $\sigma = \sigma_0$. This is a conceptual problem although the matching with data for the initial density matrix is a separate issue from obtaining the correlation functions in the limit where the state hydrodynamizes and forgets most details of the initial conditions; we have concerned ourselves with the latter here. The two arms of the Schwinger-Keldysh contour specify the two in-states which have overlap, in principle, with arbitrary bulk field configurations at initial time, corresponding to $\Phi_1(v,\zeta,\vec{x}_\perp)$ and $\Phi_2(v,\zeta,\vec{x}_\perp)$ respectively. The full on-shell gravitational action beyond the hydrodynamic limit should yield the matrix element

$$\langle\Phi_1|T_c\left(\exp\left(-i\oint J(x)\hat{O}(x)\right)\right)|\Phi_2\rangle \tag{4.128}$$

with T_c denotes time-ordering in the closed time contour, and $\langle\Phi_1|$ and $\langle\Phi_2|$ denoting states in the dual field theory corresponding to the semi-classical bulk field configurations.[25]

This issue can be partly addressed by allowing for the ingoing transients discussed above. These do not change the sources at the two boundaries but they modify the initial conditions at the two slices. However, this is not enough because we have a pair of initial conditions, one each for each arm. The transients are analytic at the horizon cap and do not affect the initial conditions on the two arms independently. Although this needs to be investigated further, presently we may conclude that one may not be able to obtain semi-classical solutions corresponding to arbitrary in-in states meaning that decoherence, which suppresses some off-diagonal matrix elements, is built in the semi-classical gravity approximation. This issue is also relevant for the general approach of Skenderis and Balt van Rees [61]. We also note that there is possibility of adding other semi-classical complex saddles of the gravitational action which do not have a natural hydrodynamic limit.

There is another independent route for matching with initial conditions. The late proper time expansion of the correlation functions (4.119) is divergent, and would require a trans-series

[25] In the approach of Skenderis and van Rees [61], the in-in states are defined using Euclidean path integrals. Even in this approach it is unclear if one can glue arbitrary in-in states by bulk geometries. See [174, 175] for some discussions on this issue.

completion which would naively be of the form (like multi-instanton series)

$$
\begin{aligned}
G(x_1,x_2) &= \prod_{\alpha=1}^{\infty}\left(\sum_{n_\alpha=0}^{\infty}\left(C_\alpha(\sigma_r,\widetilde{\zeta_r},\widetilde{x_{\perp r}})\overline{\sigma}^{\gamma_\alpha(\sigma_r,\widetilde{\zeta_r},\widetilde{x_{\perp r}})}e^{-\xi_\alpha(\sigma_r,\widetilde{\zeta_r},\widetilde{x_{\perp r}})\overline{\sigma}}\right)^{n_\alpha}\right)\\
&\quad \Gamma_{n_1,n_2,\dots}(\overline{\sigma},\sigma_r,\widetilde{\zeta_r},\widetilde{x_{\perp r}}) \quad \text{with}\\
\Gamma_{n_1,n_2,\dots}(\overline{\sigma},\sigma_r,\widetilde{\zeta_r},\widetilde{x_{\perp r}}) &= \sum_{k=0}^{\infty}\Gamma_{k;n_1,n_2,\dots}(\sigma_r,\widetilde{\zeta_r},\widetilde{x_{\perp r}})\overline{\sigma}^{-k}.
\end{aligned}
\tag{4.129}
$$

This is a generalization of the trans-series for $\epsilon(\sigma)$ for the Bjorken flow which completes the divergent asymptotic hydrodynamic series at large proper time [25, 26, 91]. Above $\Gamma_{n_\alpha=0}$ coincides with the matrix hydrodynamic power series (4.119) which we have explicitly computed here; while generally $\Gamma_{n_1,n_2,\dots}$ is a similar matrix power series in $\overline{\sigma}^{-1}$ whose coefficients are related to those of (4.119) for each fixed σ_r, $\widetilde{\zeta_r}$ and $\widetilde{x_{\perp r}}$. Physically, the functions $\xi_\alpha(\sigma_r,\widetilde{\zeta_r},\widetilde{x_{\perp r}})$ and $\gamma_\alpha(\sigma_r,\widetilde{\zeta_r},\widetilde{x_{\perp r}})$ govern the hydrodynamic relaxation of the Green's function for fixed separations of the reparametrized spacetime arguments x_1 and x_2. It is possible that these functions are approximately constants. Crucially the Stokes data $C_\alpha(\sigma_r,\widetilde{\zeta_r},\widetilde{x_{\perp r}})$ are determined by initial conditions. Instead of being constants as in the case of $\epsilon(\tau)$, the Stokes data are now functions.

The mathematical formulation of the trans-series is required to formulate a precise way to capture information about the initial state via Stokes data, and therefore the quantum fluctuations behind the event horizon. In order to match with the initial conditions, we should add the transients and therefore the Stokes data to hydrodynamic gravitational background as well. Furthermore, additional Stokes data for the evolving event horizon which can be captured by the time-dependent residual gauge transformation is needed too (recall that the residual gauge transformation itself is expressed in the large proper time expansion for which a trans-series completion is necessary like for $\epsilon(\sigma)$). One could interpret the latter feature as the horizon hair (more precisely a proper residual gauge transformation) playing a crucial role in decoding the interior of the event horizon.[26]

[26] See [176, 177] for recent reviews on current progress in resolving black hole information paradoxes with substantial discussion on the role played by *hair* degrees of freedom at the horizon.

Chapter 5

Thermalisation in Semi-holography

One of the salient features of the theory of strong interactions is its asymptotic freedom, which is the feature that the interactions of the quarks and gluons are asymptotically weaker with the increase in their energies. The discovery of this feature by Gross, Politzer and Wilczek [178, 179] holds both physical as well as computational significance in understanding QCD matter formed in heavy ion collisions. Physically, it means that in a range of temperatures where we find a crossover between the confined state of quarks and gluons at low energies and a deconfined state at high energies, one needs to combine both non-perturbative and perturbative computational approaches for interpreting various phenomena. Such a combined approach should also be relevant for understanding the evolution of matter formed in heavy ion collisions. The behaviour of high transverse momentum quarks and gluons-like partons called jets, particularly the mechanism via which they lose their energy as they plough through QGP can be qualitatively and quantitatively explained by perturbative QCD [180, 181]. However, various evidences such as elliptic flow and rapid thermalisation in QGP suggest strong interaction with perfect fluid like behaviour.

The mechanism of thermalization of the quark-gluon plasma has been intensely investigated [36, 182, 183], but the most significant questions like what are the main processes contributing to rapid thermalisation and how can they be inferred from experimental data still

require better understanding. To capture the essence of thermalisation and other phenomena in such a complex many-body system with (emergent) quantum gauge fields, it is necessary to combine perturbative and non-perturbative approaches, especially when the system is effectively in the range of temperatures $T_c - 3T_c$, where T_c is the deconfinement temperature. One such approach is the semi-holographic formalism which provides such a unified and consistent framework. In this framework, one considers two subsectors described by perturbative and holographic approaches respectively. These two sectors are coupled by a democratic coupling scheme (reviewed below), which is consistent with the Wilsonian renormalization group and furthermore allows the dynamics of both subsystems to be solved in a self-consistent manner.

In this chapter, we begin with review of semi-holographic formalism with the example of effective metric coupling and then study how the perturbative and non-perturbative sectors thermalize together. At the outset, there is a puzzle. In the large N limit, the full semi-holographic system has two entropy currents, and can be stuck in *pseudo-equilibrium* states where the entropy production is zero while the perturbative and non-perturbative sectors can reach two different physical temperatures. We first prove that only the global equilibrium state, where the two subsectors have the same physical temperatures, has maximum entropy in a micro-canonical ensemble with a fixed total energy. We further show that if we consider a generic state in which simple observables like the full energy-momentum tensor is like in a pseudo-equilibrium state, the total entropy of this non-equilibrium state is that of global equilibrium. The latter implies that for a generic (typical) state, thermalization occurs isentropically in the large N limit with no von-Neumann entropy production. The relaxation to global equilibrium is irreversible.

We explicitly study thermalization in semi-holography in the approximation where the dynamics of each subsystem can be described by BRSSS theory (2.50). We construct non-equilibrium states that have total entropy commensurate with that of the global equilibrium state. We show that the full (isolated) system relaxes to the global equilibrium state (within numerical approximation) so that the final and initial entropies are the same. In BRSSS theory,

the entropy current takes the form of su^μ, where u^μ is defined by the energy current and s is a (non-)equilibrium entropy density (2.49). The entropy current has positive definite divergence implying entropy production is always positive. However, this does not necessarily imply that the entropy density s itself is monotonic. We find that the relaxation process does produce entropy but it is small. Generically transfer of entropy between the subsectors occurs although the total initial and final entropies are the same.

Finally, we interpret this result in terms of the full quantum dynamics where we argue that the von-Neumann and Renyi entropies of the subsystems and the full system should remain invariant during thermalization in the large N limit. Nevertheless, the information of the basis in which the subsystem density matrices are diagonal is lost although the eigenvalues do not change along time evolution. This irreversibility can be captured by different notions of entropies as borne out in effective semi-holographic dynamics.

5.1 Semi-holography

Semi-holography has been proposed as an effective framework which incorporates both the perturbative and non-perturbative degrees of freedom consistently in a wide range of energy scales. The term "Semi-holography" was coined by Faulker and Polchinski [10] in the context of holographic non-Fermi liquid models, in which they coupled a dynamical boundary field to IR-CFT. Later, this formulation was implemented in heavy ion collisions by Mukhopadhyay and Iancu [12] where a classical Yang-Mill field defining the weakly coupled gluon modes is coupled to the strongly coupled conformal field theories having a gravity dual.

The semi-holographic framework proposes democratic formulation [62] in which at any energy scale, the full theory is defined by both the weakly coupled perturbative sectors as well the strongly coupled non-perturbative sector having a classical gravity dual in the large N limit. The two sectors otherwise isolated from each other, are allowed to interact by deforming the marginal and relevant couplings of each sector and promoting them as local algebraic func-

tions of the operators of the other sector. This sort of deformation ensures renormalisability of the effective action of the full system. The democratic coupling determined from this action principle allows to construct low energy dynamics of the full system from the effective low energy description of the individual sector. The two sectors living in their respective effective metric background are assumed to share same topological space such that we can describe the full system including these sectors using same coordinate. Moreover, the energy-momentum tensor of the full system is conserved in the physical background while the subsectors are closed in their respective background metric and are allowed to exchange energy and momentum defined with respect to the physical background metric.

The dynamics of the full system is solved by solving the dynamics of the individual sectors iteratively in a self-consistent manner [12]. The iterative method specifies the initial conditions for the dynamical variables of each sector including the boundary condition of the bulk field. At each iteration, the initial conditions are kept fixed and the individual sectors are solved independently with their effective metrics and couplings determined self-consistently. When the iteration converges, the energy-momentum tensor of the full system becomes conserved in the physical background metric. Convergence of the dynamics of the full system has been confirmed in various numerical investigations where it has been shown that the convergence is highly non-trivial [184, 185]. This iterative method with proper initial conditions for heavy-ion collisions has been described in [12].

As previously stated, the democratic formulation allows for the coarse-grained description of the entire system from the effective coarse-grained dynamics of individual sectors. This allows phenomenological construction, in which the stress tensor of the entire system is a polynomial of the stress tensors of the subsectors, and thus a hydrodynamic description of the individual sector is sufficient to develop the physical system. However, this property is unique to democratic coupling in a semi-holographic framework; otherwise, in systems such as water-oil mixtures, we must know the nature of intermolecular interactions in addition to the hydrodynamic descriptions of water and oil to define the mixture using hydrodynamic the-

ory. To better understand the preceding discussion, we consider the example of metric coupling (rank-2 tensor) [20] which is relevant for the following chapter.

Effective Metric coupling

Consider a dynamical system $\mathcal{F}$ in a fixed metric background $g^{(B)}_{\mu\nu}$. The physical system is composed of two sub-sectors $\mathcal{U}$ and $\tilde{\mathcal{U}}$ which corresponds to the perturbative and non-perturbative degrees of freedom. The two sub-sectors live on their respective metric background $g_{\mu\nu}$ and $\tilde{g}_{\mu\nu}$. The effective action of the system that captures the deformation of the marginal/relevant coupling of the individual sectors and their interaction is defined as,

$$\begin{aligned} S_{tot}[\phi,\tilde{\phi},g_{\mu\nu},\tilde{g}_{\mu\nu},g^{(B)}_{\mu\nu}] &= S[\phi,g_{\mu\nu}]+\tilde{S}[\tilde{\phi},\tilde{g}_{\mu\nu}]+\int d^Dx\Big[\frac{1}{2\gamma}\sqrt{-g^{(B)}}\,tr[(g-g^{(B)}).(\tilde{g}-g^{(B)})] \\ &- \frac{\gamma'}{2\gamma}\sqrt{-g^{(B)}}\,\frac{(tr[g.g^{(B)}]-D)(tr[\tilde{g}.g^{(B)}]-D)}{\gamma+\gamma' D}\Big]. \end{aligned} \tag{5.1}$$

$D = d+1$ is the dimension of the spacetime and . denotes trace operation. S and $\tilde{S}$ is the effective action of the respective sectors, $\mathcal{U}$ and $\tilde{\mathcal{U}}$. ϕ and $\tilde{\phi}$ denotes all the matter fields in the two sub-sectors. γ and γ' are the dimensionful semi-holographic coupling of mass dimension $-D$ whose ratio gives the dimensionless coupling r, $r := -\frac{\gamma'}{\gamma}$. g, $\tilde{g}$ and $g^{(B)}$ are the determinant of the effective metrics of the sub-sectors and the background physical metric. The effective metrics $g_{\mu\nu}$ and $\tilde{g}_{\mu\nu}$ act as an auxiliary field and captures the marginal deformation of the respective sectors. As mentioned earlier, the deformation is taken care of by promoting the effective metrics as a local algebraic function of the operator of the complementary system. The algebraic equations of the effective metric are obtained by varying the action (5.1) with respect to the individual effective metrics. The lowest-order metric coupling equations that dictate the coupling between the sub-sectors are,

$$g_{\mu\nu} = g^{(B)}_{\mu\nu}+\frac{\sqrt{-\tilde{g}}}{\sqrt{-g^{(B)}}}\Big[\gamma\,\tilde{t}^{\,\alpha\beta}g^{(B)}_{\alpha\mu}g^{(B)}_{\beta\nu}+\gamma'\,tr(\tilde{t}.g^{(B)})g^{(B)}_{\mu\nu}\Big], \tag{5.2}$$

$$\tilde{g}_{\mu\nu} = g^{(B)}_{\mu\nu}+\frac{\sqrt{-g}}{\sqrt{-g^{(B)}}}\Big[\gamma\,t^{\alpha\beta}g^{(B)}_{\alpha\mu}g^{(B)}_{\beta\nu}+\gamma'\,tr(t.g^{(B)})g^{(B)}_{\mu\nu}\Big], \tag{5.3}$$

$\tilde{t}^{\alpha\beta}$, and $t^{\alpha\beta}$ are the energy-momentum tensor of the respective subsectors,

$$t^{\alpha\beta} = -\frac{2}{\sqrt{-g}}\frac{\partial S}{\partial g_{\alpha\beta}}, \qquad \tilde{t}^{\alpha\beta} = -\frac{2}{\sqrt{-\tilde{g}}}\frac{\partial \tilde{S}}{\partial \tilde{g}_{\alpha\beta}}. \tag{5.4}$$

These energy-momentum tensors of the sub-sectors are conserved with respect to their effective metric background i.e., they satisfy the ward identities,

$$\nabla_\alpha t^{\alpha\beta} = 0, \qquad \tilde{\nabla}_\alpha \tilde{t}^{\alpha\beta} = 0 \tag{5.5}$$

where ∇ and $\tilde{\nabla}$ are the covariant derivatives with respect to the effective metrics. Further, the energy-momentum tensor of the full system $\mathcal{F}$ can be obtained as a polynomial of the energy-momentum of the individual sectors by varying the action (5.1) with respect to the background metric $g^{(B)}_{\mu\nu}$,

$$T^{\mu\nu} := -\frac{2}{\sqrt{-g^{(B)}}}\frac{\partial S_{tot}}{\partial g^{(B)}_{\mu\nu}}, \tag{5.6}$$

$$T^{\mu}_{\nu} = \frac{1}{2}\left((t^{\mu}_{\nu} + t^{\gamma}_{\mu})\frac{\sqrt{-g}}{\sqrt{-g^{(B)}}} + (\tilde{t}^{\mu}_{\nu} + \tilde{t}^{\gamma}_{\mu})\frac{\sqrt{-\tilde{g}}}{\sqrt{-g^{(B)}}}\right) + \Delta K \delta^{\nu}_{\mu} \tag{5.7}$$

where

$$\begin{aligned}\Delta K = &- \frac{\gamma}{2}\left(t^{\rho\alpha}\frac{\sqrt{-g}}{\sqrt{-g^{(B)}}}\right) g^{(B)}_{\alpha\beta}\left(\tilde{t}^{\,\beta\sigma}\frac{\sqrt{-\tilde{g}}}{\sqrt{-g^{(B)}}}\right) g^{(B)}_{\sigma\rho} \\ &- \frac{\gamma'}{2}\left(t^{\alpha\beta}\frac{\sqrt{-g}}{\sqrt{-g^{(B)}}}\right) g^{(B)}_{\alpha\beta}\left(\tilde{t}^{\,\sigma\rho}\frac{\sqrt{-\tilde{g}}}{\sqrt{-g^{(B)}}}\right) g^{(B)}_{\sigma\rho}.\end{aligned} \tag{5.8}$$

The full energy-momentum tensor T^{μ}_{ν} is conserved in the physical background $g^{(B)}_{\mu\nu}$ provided that the coupling equations and the sub-sector Ward identities are satisfied,

$$\nabla^{(B)}_{\mu} T^{\mu}_{\nu} = 0. \tag{5.9}$$

5.2 Thermodynamic and statistical consistencies

A crucial test of this democratic coupling scheme of the semi-holographic framework is its thermodynamic consistency. We note that once we specify the equations of states of the subsystem at the same physical temperature, we not only define the global temperature but also the energy-momentum tensor of the full system, and thus the total energy and total pressure. On the other hand, from the total energy and total pressure, we can also derive the global temperature via thermodynamic identities. Do these two global temperatures agree? Precisely, thermodynamic consistency implies that for any democratic effective metric coupling rule with a total conserved energy-momentum tensor (5.9), the global temperature $\mathcal{T}$ given by the (same) physical temperature of the subsystems will satisfy the thermodynamic identities

$$\mathcal{E} + \mathcal{P} = \mathcal{S}\mathcal{T}, \qquad d\mathcal{E} = \mathcal{T} d\mathcal{S} \tag{5.10}$$

where $\mathcal{E}$ is the total energy density, $\mathcal{P}$ is the total pressure of the full system, and $\mathcal{S}$ is the appropriate total entropy.

Here we review the proof of thermodynamic consistency, following the generic discussion in [20]. Suppose we consider a full system $\mathcal{F}$ living in a $d-$dimensional spacetime whose metric characterised by static gravitational potential $\phi(x)$ (not a function of time) reads as,

$$g^{(B)}_{\mu\nu} = \text{diag}(-e^{-2\phi(\mathbf{x})}, \underbrace{1, \cdots, 1}_{d-1}). \tag{5.11}$$

The two sub-sectors $\mathcal{U}$ and $\tilde{\mathcal{U}}$ interacting via their effective metric are assumed to equilibrate to individual temperature T_1 and T_2. This parameterizes the effective metrics of the sub-sectors in a static, homogeneous and isotropic form,

$$g_{\mu\nu} = diag\Big(- a(\mathbf{x})^2, \underbrace{b(\mathbf{x})^2, \cdots, b(\mathbf{x})^2}_{d-1} \Big), \qquad \tilde{g}_{\mu\nu} = diag\Big(- \tilde{a}(\mathbf{x})^2, \underbrace{\tilde{b}(\mathbf{x})^2, \cdots, \tilde{b}(\mathbf{x})^2}_{d-1} \Big), \tag{5.12}$$

which leads to the following form of the energy-momentum tensor of the subsystems,

$$t^{\mu\nu} = diag\Bigg(\frac{\varepsilon(T_1(\mathbf{x}))}{a(\mathbf{x})^2}, \underbrace{\frac{P(T_1(\mathbf{x}))}{b(\mathbf{x})^2}, \cdots, \frac{P(T_1(\mathbf{x}))}{b(\mathbf{x})^2}}_{d-1}\Bigg), \tag{5.13}$$

$$\tilde{t}^{\mu\nu} = diag\Bigg(\frac{\tilde{\varepsilon}(T_2(\mathbf{x}))}{\tilde{a}(\mathbf{x})^2}, \underbrace{\frac{\tilde{P}(T_2(\mathbf{x}))}{\tilde{b}(\mathbf{x})^2}, \cdots, \frac{\tilde{P}(T_2(\mathbf{x}))}{\tilde{b}(\mathbf{x})^2}}_{d-1}\Bigg) \tag{5.14}$$

where $\varepsilon(\tilde{\varepsilon})$ and $P(\tilde{P})$ are the energy density and pressure of the respective subsystem. With this form of the energy-momentum tensor of the individual sectors, the effective metric coupling equations will still be a polynomial which in the lowest order (5.2) read as,

$$\begin{aligned}
e^{-2\phi(\mathbf{x})} - a(\mathbf{x})^2 &= \left(\frac{e^{-\phi(\mathbf{x})}(d-1)\tilde{P}(T_2(\mathbf{x}))\, r\, \gamma}{\tilde{b}(\mathbf{x})^2} + \frac{(1-r)\, e^{-3\phi(\mathbf{x})}\gamma\, \tilde{\varepsilon}(T_2(\mathbf{x}))}{\tilde{a}(\mathbf{x})^2}\right)\tilde{a}(\mathbf{x})\tilde{b}(\mathbf{x})^{d-1}, \\
b(\mathbf{x})^2 - 1 &= \left(\frac{(1-(d-1)r)\, e^{\phi(\mathbf{x})}\, \tilde{P}(T_2(\mathbf{x}))}{\tilde{b}(\mathbf{x})^2} + \frac{e^{-\phi(\mathbf{x})}\, r\, \gamma\, \varepsilon(T_2(\mathbf{x}))}{\tilde{a}(\mathbf{x})^2}\right)\tilde{a}(\mathbf{x})\tilde{b}(\mathbf{x})^{d-1}, \\
e^{-2\phi(\mathbf{x})} - \tilde{a}(\mathbf{x})^2 &= \left(\frac{e^{-\phi(\mathbf{x})}(d-1)P(T_1(\mathbf{x}))\, r\, \gamma}{b(\mathbf{x})^2} + \frac{(1-r)e^{-3\phi(\mathbf{x})}\, \gamma\, \varepsilon(T_1(\mathbf{x}))}{a(\mathbf{x})^2}\right)a(\mathbf{x})b(\mathbf{x})^{d-1}, \\
\tilde{b}(\mathbf{x})^2 - 1 &= \left(\frac{(1-(d-1)r)\, e^{\phi(\mathbf{x})}\, P(T_1(\mathbf{x}))}{b(\mathbf{x})^2} + \frac{e^{-\phi(\mathbf{x})}r\, \gamma\, \varepsilon(T_1(\mathbf{x}))}{a(\mathbf{x})^2}\right)a(\mathbf{x})b(\mathbf{x})^{d-1}
\end{aligned} \tag{5.15}$$

where for $\phi(\mathbf{x}) \to 0$ we smoothly recovers the flat-space solution.

To define global equilibrium in a system one needs to ensure that the full-system temperature $\mathcal{T}$ as well as the subsystem temperatures T_1 and T_2 are related to each other. The temperatures of the system can be specified by the inverse of the Euclidean time circle which is a constant at global equilibrium,

$$\mathcal{T}^{-1} = \int_0^\beta \sqrt{-g_{00}^{(B)}}d\tau, \tag{5.16}$$

$$T_1^{-1} = \int_0^\beta \sqrt{-g_{00}}d\tau = a\beta = a\mathcal{T}^{-1}, \tag{5.17}$$

$$T_2^{-1} = \int_0^\beta \sqrt{-\tilde{g}_{00}}d\tau = \tilde{a}\beta = \tilde{a}\mathcal{T}^{-1}. \tag{5.18}$$

This gives

$$e^{-\phi(\mathbf{x})}\mathcal{T}(\mathbf{x}) = a(\mathbf{x})T_1(\mathbf{x}) = \tilde{a}(\mathbf{x})T_2(\mathbf{x}) = \mathcal{T}_0. \tag{5.19}$$

Therefore the space of equilibrium solutions is parameterized by the single parameter $\mathcal{T}_0$ and this defines the global equilibrium condition. Following this one needs to verify the compatibility of the condition with the energy-momentum tensor of the subsystem and the full system. Using the Ward identity (5.5), one can show that the conservation of the thermal energy-momentum tensor of the individual sectors with respect to their effective metric implies,

$$\frac{\partial_i P}{\varepsilon + P} + \frac{\partial_i a}{a} = 0, \qquad \frac{\partial_i \tilde{P}}{\tilde{\varepsilon} + \tilde{P}} + \frac{\partial_i \tilde{a}}{\tilde{a}} = 0 \tag{5.20}$$

where ∂_i is space derivative. Then using the thermodynamic identities,

$$\varepsilon + P = T_1 s_1, \qquad \tilde{\varepsilon} + \tilde{P} = T_2 s_2, \tag{5.21}$$

we can write the conservation equation as,

$$\partial_i\Big(\ln(T_1 a)\Big) = 0, \qquad \partial_i\Big(\ln(T_2 \tilde{a})\Big) = 0 \tag{5.22}$$

which is consistent with the global equilibrium condition (5.19). Here s_1 and s_2 are the entropy densities of the respective systems.

The energy-momentum tensor of the full system following the construction of the effective metric coupling can be parameterised as,

$$T^{\mu\nu} = \Big(e^{-2\phi(\mathbf{x})}\mathcal{E}(\mathcal{T}(\mathbf{x})), \underbrace{\mathcal{P}(T(\mathbf{x})), \cdots, \mathcal{P}(T(\mathbf{x}))}_{d-1}\Big) \tag{5.23}$$

which is conserved in the background metric (5.11). The conservation equation (5.9) gives,

$$\frac{\partial_i \mathcal{P}}{\mathcal{E}+\mathcal{P}} - \partial_i \phi = 0. \tag{5.24}$$

Also from (5.19) and (5.22) we get,

$$\frac{\partial_i \mathcal{T}}{\mathcal{T}} - \partial_i \phi = 0, \tag{5.25}$$

and therefore,

$$\frac{\partial_i \mathcal{T}}{\mathcal{T}} - \frac{\partial_i \mathcal{P}}{\mathcal{E}+\mathcal{P}} = 0 \tag{5.26}$$

which along with the thermodynamic identity $\mathcal{E}+\mathcal{P} = \mathcal{T}\mathcal{S}$ gives,

$$\partial_i \mathcal{P} = \mathcal{S}\partial_i \mathcal{T}. \tag{5.27}$$

This relation holds for arbitrary smooth $\phi(\mathbf{x})$ i.e.,

$$d\mathcal{P} = \mathcal{S}d\mathcal{T} \tag{5.28}$$

which together with $\mathcal{E}+\mathcal{P} = \mathcal{T}\mathcal{S}$ becomes,

$$d\mathcal{E} = \mathcal{T}d\mathcal{S} \tag{5.29}$$

where the variation is taken by changing the parameter $\mathcal{T}_0$. Note that we can give the desired proof in the flat space by considering $\phi(\mathbf{x}) \to 0$.

Furthermore, consistency with statistical mechanics implies a specific form of the total entropy $\mathcal{S}$. Since the two subsystems are effectively isolated in their self-consistent effective metrics (although exchanging energy and momentum when viewed from the actual physical metric background), the total entropy should be just a sum of the entropy densities after ac-

counting for the respective self-consistent effective spatial volume densities.

It is easy to show that $\mathcal{S}$ obtained from the thermodynamic identities satisfies statistical consistency for any democratic effective metric coupling. The form of energy-momentum tensor of the full system (5.9) with one contravariant and one covariant index indicates that the explicit interaction terms in ΔK is always diagonal and appears with opposite signs for $\mathcal{E}$ and $\mathcal{P}$. This leads to,

$$(\varepsilon + P)ab^{d-1} + (\tilde{\varepsilon} + \tilde{P})\tilde{a}\tilde{b}^{d-1} = (\mathcal{E} + \mathcal{P})e^{-\phi(\mathbf{x})}. \tag{5.30}$$

Then from the thermodynamic identities we get,

$$T_1 s_1 ab^{d-1} + T_2 \tilde{a} s_2 \tilde{b}^{d-1} = \mathcal{T}\mathcal{S}e^{-\phi(\mathbf{x})}. \tag{5.31}$$

The global equilibrium condition (5.19) implies the total entropy $\mathcal{S}$ is a sum of the individual entropy of the sub-sectors with some spatial volume factor correction,

$$\mathcal{S} = s_1 b^{d-1} + s_2 \tilde{b}^{d-1}. \tag{5.32}$$

More generally, total entropy current $\mathcal{S}^\mu$ can be defined as

$$\mathcal{S}^\mu := \frac{\sqrt{-g}}{\sqrt{-g^{(B)}}} s_1^\mu + \frac{\sqrt{-\tilde{g}}}{\sqrt{-g^{(B)}}} s_2^\mu \tag{5.33}$$

where s_1^μ and s_2^μ are respective subsystem entropy currents (which in equilibrium take the forms $s_1^\mu = s_1 u^\mu$ and $s_2^\mu = s_2 \tilde{u}^\mu$). It is easy to see that $\nabla_\mu s_1^\mu \geq 0$ & $\tilde{\nabla}_\mu s_2^\mu \geq 0$ implying

$$\nabla_\mu^{(B)} \mathcal{S}^\mu \geq 0. \tag{5.34}$$

In equilibrium, $\mathcal{S}^\mu = \mathcal{S}U^\mu$ with U^μ being the thermal frame of the full system. Note the definition of entropy current (5.33) holds generally even out of equilibrium.

5.3 Global equilibrium has maximum total entropy

In the preceding section, it has been shown that global equilibrium satisfies both thermodynamic as well as statistical consistencies. However, the interaction of the individual sectors via their effective metric allows the subsystems to equilibrate to a state with different temperatures T_1 and T_2. This makes it less obvious that at global equilibrium the total entropy of the full system is maximum. For our coupling scheme to be valid, one needs to ensure that the global equilibrium must have maximum entropy in a micro-canonical ensemble with constant total energy. In what follows, we prove that this is indeed the case.

In a micro-canonical ensemble, the isolation of the full system implies that the total energy $\mathcal{E} = \mathcal{E}_0$ is a constant while the individual sectors interact via their effective metric and equilibrate with temperatures T_1 and T_2, leading the full system to a pseudo-equilibrium state. The condition that the total energy $\mathcal{E}$ is a constant relates the temperatures T_1 and T_2 of the two subsectors, and hence in a microcanonical ensemble, the space of pseudo-equilibrium solutions is characterised by one parameter, say, λ. We observe that the extremization of total entropy on a manifold of pseudo-equilibrium solutions with constant energy $\mathcal{E}_0$, parameterised by λ, implies global equilibrium.

We demonstrate this for an isolated system $\mathcal{F}$ with two subsectors $\mathcal{U}$ and $\tilde{\mathcal{U}}$ defined by arbitrary equations of states (EoS), $P(\varepsilon)$ and $\tilde{P}(\tilde{\varepsilon})$. The full system lives in Minkowski spacetime defined by the metric

$$g^{(B)}_{\mu\nu} = \eta_{\mu\nu} = \text{diag}(-1, \underbrace{1, \cdots, 1}_{d-1}). \tag{5.35}$$

The two sectors live in their individual effective metrics $g_{\mu\nu}$ and $\tilde{g}_{\mu\nu}$ given by

$$g_{\mu\nu} = \text{diag}\left(-a(\lambda)^2, \underbrace{b(\lambda)^2, \cdots, b(\lambda)^2}_{d-1}\right), \qquad \tilde{g}_{\mu\nu} = \text{diag}\left(-\tilde{a}(\lambda)^2, \underbrace{\tilde{b}(\lambda)^2, \cdots, \tilde{b}(\lambda)^2}_{d-1}\right). \tag{5.36}$$

These two sectors interact via the metric coupling (5.15) and equilibrate to a pseudo-equilibrium

state with temperatures T_1 and T_2. The full system is characterised by six equations. The four equations are derivative of metric coupling equations (5.15) and the other two equations are $\partial\mathcal{E}/\partial\lambda = 0$ and $\partial\mathcal{S}/\partial\lambda = 0$. $\mathcal{S}$ is given by the thermodynamic identity, $\mathcal{T}\mathcal{S} = \mathcal{P} + \mathcal{E}$ where $\mathcal{E}$ and $\mathcal{P}$ (from (5.6) using (5.13)) is defined as,

$$\begin{aligned}
\mathcal{E} &= \epsilon(T_1)ab^{d-1} + \tilde{\epsilon}(T_2)\tilde{a}\tilde{b}^{d-1} \\
&+ \frac{\gamma}{2}\left(\frac{\epsilon(T_1)\tilde{\epsilon}(T_2)}{a^2\tilde{a}^2} + \frac{(d-1)P(T_1)\tilde{P}(T_1)}{b^2\tilde{b}^2}\right)ab^{d-1}\tilde{a}\tilde{b}^{d-1} \\
&+ \frac{\gamma'}{2}\left(-\frac{\epsilon(T_1)}{a^2} + \frac{(d-1)P(T_1)}{b^2}\right)\left(-\frac{\tilde{\epsilon}(T_2)}{\tilde{a}^2} + \frac{(d-1)\tilde{P}(T_2)}{\tilde{b}^2}\right)ab^{d-1}\tilde{a}\tilde{b}^{d-1}, \qquad (5.37) \\
\mathcal{P} &= P(T_1)ab^{d-1} + \tilde{P}(T_2)\tilde{a}\tilde{b}^{d-1} \\
&+ \frac{\gamma}{2}\left(\frac{\epsilon(T_1)\tilde{\epsilon}(T_2)}{a^2\tilde{a}^2} + \frac{(d-1)P(T_1)\tilde{P}(T_1)}{b^2\tilde{b}^2}\right)ab^{d-1}\tilde{a}\tilde{b}^{d-1} \\
&+ \frac{\gamma'}{2}\left(-\frac{\epsilon(T_1)}{a^2} + \frac{(d-1)P(T_1)}{b^2}\right)\left(-\frac{\tilde{\epsilon}(T_2)}{\tilde{a}^2} + \frac{(d-1)\tilde{P}(T_2)}{\tilde{b}^2}\right)ab^{d-1}\tilde{a}\tilde{b}^{d-1}. \qquad (5.38)
\end{aligned}$$

Here all the variables are functions of a single parameter λ. Now using the the thermodynamic identities (5.21) and the thermodynamic relation $dP = s_1 dT_1$ ($d\tilde{P} = s_2 dT_2$), we get

$$\frac{d\varepsilon}{d\lambda} = \frac{1}{c_s(\lambda)^2}\frac{dP}{d\lambda}, \qquad \frac{d\tilde{\varepsilon}}{d\lambda} = \frac{1}{\tilde{c}_s(\lambda)^2}\frac{d\tilde{P}}{d\lambda}, \qquad (5.39)$$

and

$$\frac{dP}{d\lambda} = \frac{P(\lambda) + \varepsilon(\lambda)}{T_1(\lambda)}\frac{dT_1}{d\lambda}, \qquad \frac{d\tilde{P}}{d\lambda} = \frac{\tilde{P}(\lambda) + \tilde{\varepsilon}(\lambda)}{T_2(\lambda)}\frac{dT_2}{d\lambda}, \qquad (5.40)$$

where

$$s_1(\lambda) = \frac{P(\lambda) + \varepsilon(\lambda)}{T_1(\lambda)}, \qquad s_2(\lambda) = \frac{\tilde{P}(\lambda) + \tilde{\varepsilon}(\lambda)}{T_2(\lambda)}, \qquad (5.41)$$

and $c_s^2 = \frac{dP}{d\varepsilon}$ $\left(\tilde{c}_s^2 = \frac{d\tilde{P}}{d\tilde{\varepsilon}}\right)$ is the speed of sound of the two sectors. This expresses the equations (5.39) and (5.40) in terms of $\frac{dT_1}{d\lambda}$ $\left(\frac{dT_2}{d\lambda}\right)$ which in turn gives the six equations in terms of $\frac{dT_1}{d\lambda}$ $\left(\frac{dT_2}{d\lambda}\right)$. Then these six equations can be written in matrix form with coefficient vector A =

$(T_1'(\lambda), T_2'(\lambda), a'(\lambda), b'(\lambda), \tilde{a}'(\lambda), \tilde{b}'(\lambda))$ as

$$Q.A = 0, \tag{5.42}$$

with Q being a 6×6 matrix and prime denotes derivative wrt λ. This set of equations admits a non-trivial solution when $\det(Q) = 0$. We find that this $\det(Q) = 0$ condition (explicit equation is given in (5.43)) implies the global equilibrium relation (5.19) i.e, $T_1(\lambda)a(\lambda) = T_2(\lambda)\tilde{a}(\lambda)$.

$$\det(Q) = \Big(a(\lambda)T_1(\lambda) - \tilde{a}(\lambda)T_2(\lambda)\Big)\Big(\cdots\Big). \tag{5.43}$$

The complete expression of the second term is large and can be found in appendix G. Note that one of the multiplicative factors in the equation (5.43) is $(T_1 a - T_2\tilde{a})$, which means that equation (5.43) ensures that the global equilibrium condition is always satisfied (unless the second multiplicative in (5.43) vanishes identically).

Therefore the condition $\mathcal{E} = \mathcal{E}_0$ gives a one-parameter family of curves (parameterized by the parameter $\mathcal{E}_0$ or equivalently by λ) in the 2-dimensional space of $T_1(\lambda)$ and $T_2(\lambda)$. The second condition $\det(Q) = 0$ (5.43) gives another curve in the 2-dimensional space of $T_1(\lambda)$ and $T_2(\lambda)$. The intersection of these two curves is the global equilibrium of the full system at constant total energy $\mathcal{E}_0$.

5.4 Numerical study of thermalization

We numerically illustrate the above proof of thermalization by considering two conformal equations of state with constant total energy $\mathcal{E}_0$ of the full system. The corresponding plot is shown in Fig. 5.1 where we have considered a $d = 3$ dimensional system whose sub-sectors are defined by the conformal equations of states, $\varepsilon = 2P = 2n_1 T_1^3$ and $\tilde{\varepsilon} = 2\tilde{P} = 2n_2 T_2^3$. The Fig. 5.1 corresponds to unequal n_1 and n_2.

We observe in Fig. 5.1 that the global thermalization measure $(T_1 a - T_2\tilde{a})$ indeed van-

ishes with the maximum entropy of the full system. Thus ensuring that the global equilibrium is accompanied by the maximum total entropy. We also find that the entropy of one subsystem always increases while that of the other subsystem decreases at any point on the equilibrium phase diagram. However, the second law of thermodynamics states that the entropy current has positive divergence, which implies that there exists non-decreasing entropy current for each of the subsectors along with the full system. Then the question arises, how will the dynamics of the full system evolve towards global equilibrium from an arbitrary pseudo-equilibrium state?

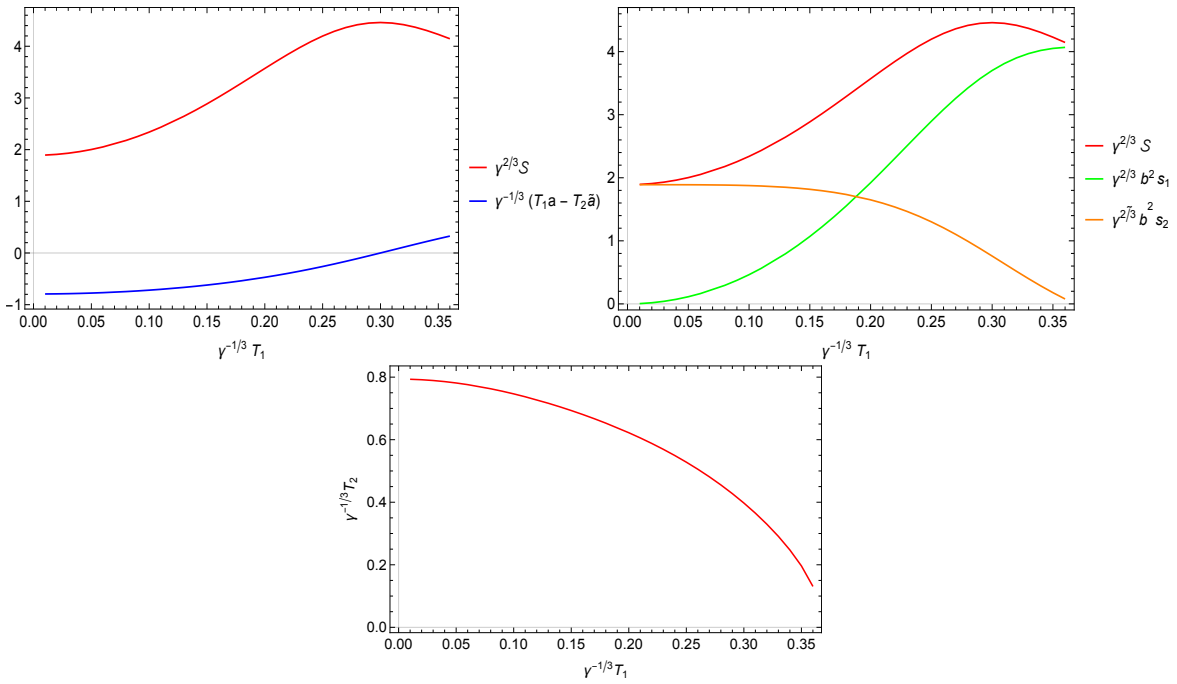

Figure 5.1: The left plot shows full system entropy in red and global equilibrium measure $(aT_1 - \tilde{a}T_2)$ in blue as function of T_1. The entropy becomes maximum when the measure of global equilibrium vanishes. On the right, the plot shows the subsystem entropies and the full system entropy as function of T_1. The lower plot shows (pseudo-)equilibrium phase space, $T_2(T_1)$. Here $n_1 = 10, n_2 = 1, \mathcal{E}_0 = 1, r = 2, \gamma = 1$.

5.4.1 Resolution

The above question is addressed in terms of perturbations added to some pseudo-equilibrium state. On adding perturbation to any arbitrary pseudo-equilibrium state, the entropy of one of the subsystems can decrease while that of the other can increase owing to the interaction between the two sectors. The dynamics will eventually increase the entropies of both subsystems,

resulting in another pseudo-equilibrium state. However, if the initial decrease in one of the subsystem entropy is more than the subsequent increase in its entropy, then there will be an overall decrease in the entropy, which is consistent with the second law of thermodynamics.

Moreover, it has been observed that the fluctuations in total entropy become negative once the system reaches global thermal equilibrium, Fig. 5.2. This means that these fluctuations are exponentially suppressed because the probability of macroscopic fluctuation in a microcanonical ensemble is proportional to Exp(ΔS).

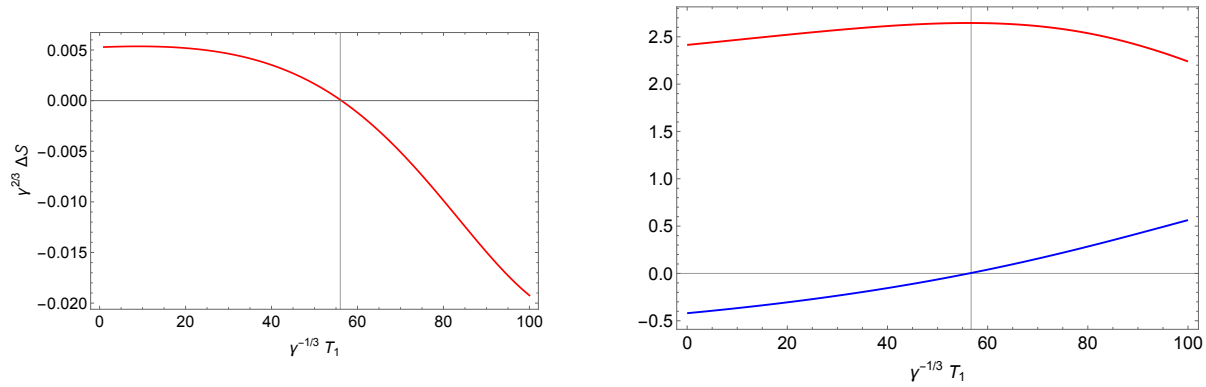

Figure 5.2: The plot show the nature of $\Delta\mathcal{S}$, and global equilibrium measure as function of T_1.

5.5 Isentropic thermalization

Following the generic proof of thermalization in a hybrid system constructed via the metric coupling technique in semi-holographic framework, we study thermalization, preferably isentropic thermalization in a dynamical system. The proposal of isentropic thermalization as discussed below,

Consider an arbitrary pseudo-equilibrium state given by subsystem temperatures T_1 and T_2 in which the energy-momentum tensor of the full system is diagonal with total energy $\mathcal{E}$ and total pressure $\mathcal{P}$. We perturb this pseudo-equilibrium state by demanding the following four conditions: the total energy $\mathcal{E}$ of the full system should remain constant, the total isotropic pressure $\mathcal{P}$ should remain unchanged, the total anisotropic diagonal pressure and the total (spa-

tial) off-diagonal component of non-equilibrium stress-tensor should vanish. Together these four conditions imply that the full energy-momentum tensor of the perturbed state remains the same as that of the pseudo-equilibrium state. In addition, we also put a fifth maximal entropy condition which means the total entropy of the full system $\mathcal{S}$ is equal to that in global thermal equilibrium. Therefore with these five conditions, we assume to obtain a one-parameter family of generically non-equilibrium states, which are macroscopically in pseudo-equilibrium (since the total energy-momentum tensor is the same) but are more extreme non-equilibrium and have maximal entropy as that of global equilibrium. Then any of these one-parameter families of fluctuations will relax to global equilibrium such that the total entropy remains constant in time. This leads to isentropic thermalization.

Further, the question of thermalization, not only isentropically but also without entropy transfer between subsystems, i.e. isentropically within each subsystem also introduces one more condition. This condition can simply ensure that the subsystem entropy is also the same as in global equilibrium (the other one automatically sets to the global equilibrium value) i.e., isentropic within each subsystem. Although isentropic thermalisation is generic, the isentropic within each subsystem is not – typically there is isentropic thermalization with entropy transfer.

5.5.1 Dynamical system: BRSSS theory

We investigate isentropic thermalization in semi-holography in the approximation where the dynamics of each subsystem can be described by the first-order BRSSS formalism[1], similar to the modified MIS (2.50). We study the system in a $d = 3-$ dimensional spacetime where the full system lives on the flat spacetime given by the Minkowski metric,

$$g^{(B)}_{\mu\nu} \equiv \eta_{\mu\nu} = \text{diag}(-1, 1, 1) \tag{5.44}$$

[1]Here we consider the system to be in flat space and have linear velocity. Hence, the BRSSS expansion is truncated at first order following the discussion in section 2.1.3.

and the two subsystems defined by the conformal equation of state, live on the effective metrics of the form,

$$g_{\mu\nu} = \begin{pmatrix} -a_{11}(t)^2 & 0 & 0 \\ 0 & a_{22}(t)^2 & a_{23}(t) \\ 0 & a_{23}(t) & a_{33}(t)^2 \end{pmatrix} \quad \text{and} \quad \tilde{g}_{\mu\nu} = \begin{pmatrix} -\tilde{a}_{11}(t)^2 & 0 & 0 \\ 0 & \tilde{a}_{22}(t)^2 & \tilde{a}_{23}(t) \\ 0 & \tilde{a}_{23}(t) & \tilde{a}_{33}(t)^2 \end{pmatrix}. \tag{5.45}$$

The full system along with the subsystems are conserved in their respective background metric i.e. the full system energy-momentum tensor, T^{μ}_{ν}, satisfies the ward identity (5.9) and the individual system energy momentum tensor $t^{\mu\nu}$ and $\tilde{t}^{\mu\nu}$ satisfies the ward identity (5.5). The energy-momentum tensors of the subsystems are defined as,

$$t^{\mu\nu} = (\varepsilon + P)u^{\mu}u^{\nu} + Pg^{\mu\nu} + \pi^{\mu\nu} \quad \text{and} \quad \tilde{t}^{\mu\nu} = (\tilde{\varepsilon} + \tilde{P})\tilde{u}^{\mu}\tilde{u}^{\nu} + \tilde{P}\tilde{g}^{\mu\nu} + \tilde{\pi}^{\mu\nu}, \tag{5.46}$$

where the time-like fluid velocity $u^{\mu}(\tilde{u}^{\mu})$ of each subsystem is given by,

$$u^{\mu} = \text{diag}(1/a_{11}(t), 0, 0) \quad \text{and} \quad \tilde{u}^{\mu} = \text{diag}(1/\tilde{a}_{11}(t), 0, 0), \tag{5.47}$$

and the shear stress tensor which is the first order dissipative term of (5.46) is considered to be,

$$\pi^{\mu\alpha}.g_{\alpha\nu} \equiv \pi^{\mu}_{\nu} = \begin{pmatrix} 0 & 0 & 0 \\ 0 & -\frac{\pi_d(t)}{2} & \pi_{od}(t) \\ 0 & \frac{\pi_d(t)}{a_{33}(t)} + \frac{a_{22}(t)^2\pi_{od}(t)}{a_{33}(t)^2} & \frac{\pi_d(t)}{2} \end{pmatrix}, \tag{5.48}$$

$$\tilde{\pi}^{\mu\alpha}.\tilde{g}_{\alpha\nu} \equiv \tilde{\pi}^{\mu}_{\nu} = \begin{pmatrix} 0 & 0 & 0 \\ 0 & -\frac{\tilde{\pi}_d(t)}{2} & \tilde{\pi}_{od}(t) \\ 0 & \frac{\tilde{\pi}_d(t)}{\tilde{a}_{33}(t)} + \frac{\tilde{a}_{22}(t)^2\tilde{\pi}_{od}(t)}{\tilde{a}_{33}(t)^2} & \frac{\tilde{\pi}_d(t)}{2} \end{pmatrix}. \tag{5.49}$$

Here we have used the Landau frame convention (refer to chapter 2 for details) and traceless

condition due to conformality to get the above form of $\pi^{\mu\nu}$ and $\tilde{\pi}^{\mu\nu}$, i.e.,

$$\text{Orthogonality:} \qquad u_\nu \pi^{\mu\nu} = 0 \qquad \text{and} \qquad \tilde{u}_\nu \tilde{\pi}^{\mu\nu} = 0. \tag{5.50}$$

$$\text{Traceless:} \qquad \pi^\mu_\mu = 0 \qquad \text{and} \qquad \tilde{\pi}^\mu_\mu = 0. \tag{5.51}$$

Above $\pi_d(\tilde{\pi}_d)$ is the diagonal anisotropy and $\pi_{od}(\tilde{\pi}_{od})$ is the off diagonal anisotropy of the subsystem. Further, following the relaxation type equation (2.50), the shear stress tensor can be promoted to a dynamical variable as,

$$\left[\pi^{\mu\nu} + \tau_\pi D\pi^{\mu\nu}\right] + \frac{3}{2}\tau_\pi \pi^{\mu\nu}\nabla_\alpha u^\alpha = -\eta\sigma^{\mu\nu} \tag{5.52}$$

$$\left[\tilde{\pi}^{\mu\nu} + \tilde{\tau}_\pi \tilde{D}\tilde{\pi}^{\mu\nu}\right] + \frac{3}{2}\tilde{\tau}_\pi \tilde{\pi}^{\mu\nu}\tilde{\nabla}_\alpha \tilde{u}^\alpha = -\tilde{\eta}\tilde{\sigma}^{\mu\nu} \tag{5.53}$$

where $\tau_\pi(\tilde{\tau}_\pi)$ and $\eta(\tilde{\eta})$ are the transport coefficients known as relaxation time and shear viscosity and $\sigma^{\mu\nu}$ and $\tilde{\sigma}^{\mu\nu}$ are defined as,

$$\sigma^{\mu\nu} := \frac{1}{2}(\nabla_\alpha u_\beta + \nabla_\beta u_\alpha)\Delta^{\alpha\beta}\Delta^{\mu\nu} - \frac{1}{2}\nabla_\lambda u^\lambda \Delta^{\mu\nu},$$
$$\tilde{\sigma}^{\mu\nu} := \frac{1}{2}(\tilde{\nabla}_\alpha \tilde{u}_\beta + \tilde{\nabla}_\beta \tilde{u}_\alpha)\tilde{\Delta}^{\alpha\beta}\tilde{\Delta}^{\mu\nu} - \frac{1}{2}\tilde{\nabla}_\lambda \tilde{u}^\lambda \tilde{\Delta}^{\mu\nu}$$

where $\Delta^{\mu\nu}$ and $\tilde{\Delta}^{\mu\nu}$ are the spatial projections defined before. The full system is governed by fourteen equations, seven for each subsystem: one ward identity, two equations from MIS and four coupling equations and hence seven variables: ε, π_d, π_{od}, a_{11}, a_{22}, a_{33} and a_{23} of each subsystem. The equations are given in the appendix H. Note in this system the entropy densities s_1, s_2 and $\mathcal{S}$ are defined as in (2.49),

$$s_1 = \frac{\varepsilon + P}{T_1} - \frac{\tau_\pi}{4\eta T_1}\pi^{\mu\nu}\pi_{\mu\nu}, \tag{5.54}$$

$$s_2 = \frac{\tilde{\varepsilon} + \tilde{P}}{T_2} - \frac{\tilde{\tau}_\pi}{4\tilde{\eta} T_2}\tilde{\pi}^{\mu\nu}\tilde{\pi}_{\mu\nu}, \tag{5.55}$$

$$\mathcal{S} = \frac{\sqrt{-g}}{\sqrt{-g^{(B)}}}s_1 + \frac{\sqrt{-\tilde{g}}}{\sqrt{-g^{(B)}}}s_2. \tag{5.56}$$

This ensures positive divergence of entropy current in the system.

We numerically investigate the system to study isentropic thermalisation. We set the following specification (5.57) to the sub-systems such that one of the sub-systems behaves as weakly coupled and the other as strongly coupled. We also set the coupling strength γ to unity and $r = 2$.

$$\eta = \frac{1}{4\pi}\frac{\varepsilon + P}{T_1}, \qquad \tilde{\eta} = \frac{100}{4\pi}\frac{\tilde{\varepsilon} + \tilde{P}}{T_2}, \qquad \tau_\pi = \frac{2 - \ln 2}{2\pi T_1}, \qquad \tilde{\tau}_\pi = \frac{5 * 100}{4\pi T_2}, \qquad n_1 = n_2 = 1. \tag{5.57}$$

As mentioned earlier, we consider the system to be isolated and in micro-canonical ensemble which fixes the total energy $\mathcal{E}$ to a constant $\mathcal{E}_0$. Initially the system is assumed to be in a global equilibrium state with maximum entropy of the full system. The system is then driven to a non-equilibrium state whose entropy is as large as that of global equilibrium by perturbing the energy-momentum tensor of the sub-systems. Eventually, the dynamics take the full system towards global equilibrium state as shown in Fig. 5.3. The entropy of one sub-system which behaves as a hard sector remains constant while the other varies with time. This shows that there exist non-equilibrium states whose entropy is as large as that of the global equilibrium entropy and entropy production occurs only in the soft sector. Further, we hold the perturbation constant and vary the full system temperature up to a large value. We observe (Fig. 5.4) that the entropy production on the scale of perturbation vanishes in the limit of large temperature and also the departure of the final state of the system from the global equilibrium in the scale of perturbation decreases as we go to the higher temperature. This shows that equilibration happens isentropically compare to the scale of perturbation in the infinite temperature limit.

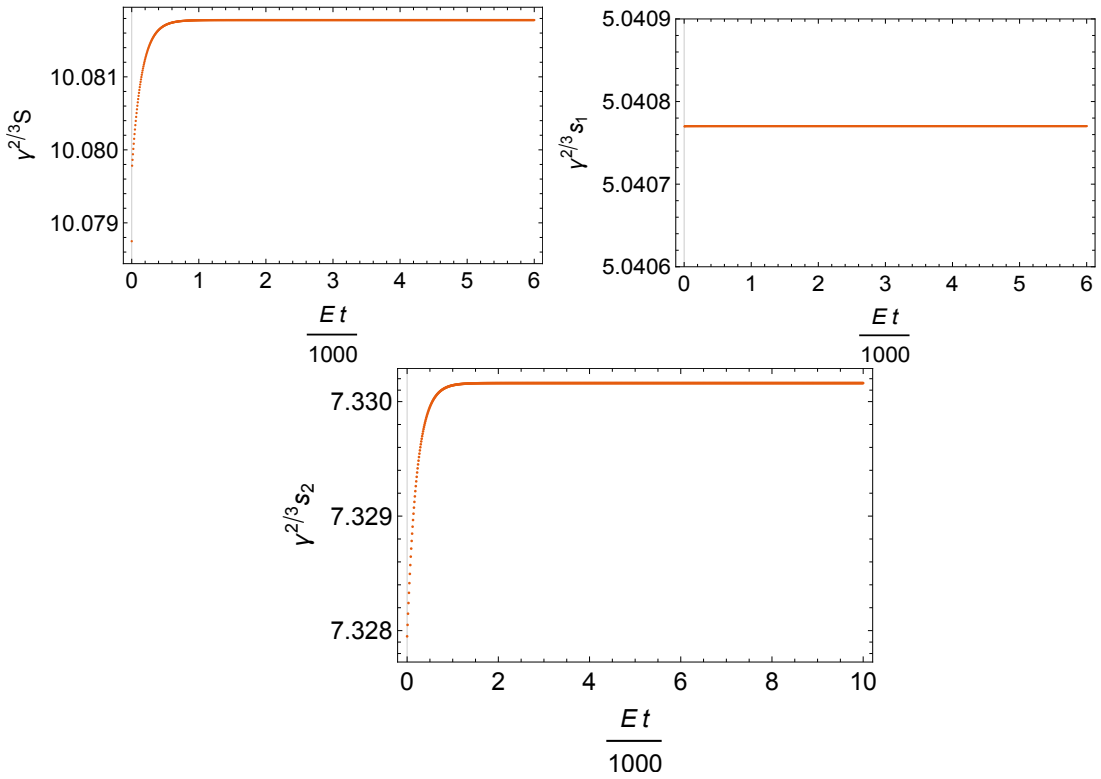

Figure 5.3: The plot shows the evolution of the entropy of the full system and the individual system over time for constant full system energy $\mathcal{E}_0 = 6\gamma$. Here the x-axis is the dimensionless time $\mathcal{E}t$ scaled by a factor of $1/1000$ to fit in the plot.

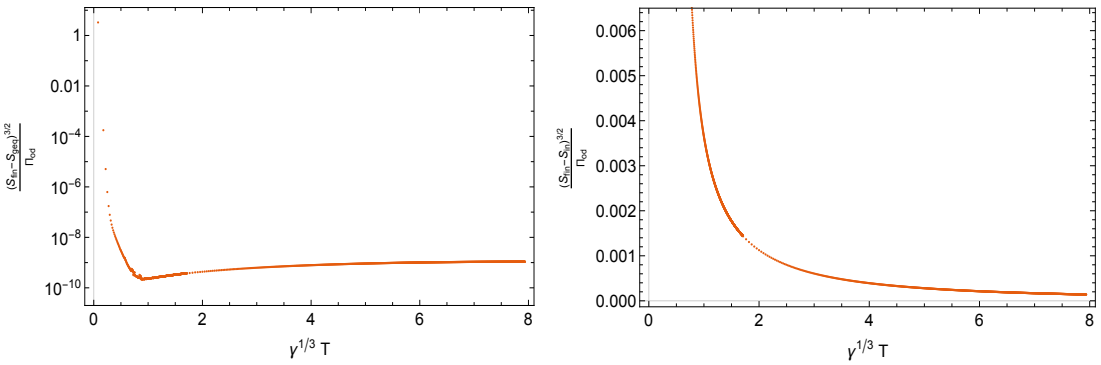

Figure 5.4: The first plot shows that the ratio of entropy production to the scale of perturbation vanishes at high temperatures. The second plot shows that in the large T limit, the departure of the final state from the global equilibrium in the scale of perturbation vanishes.

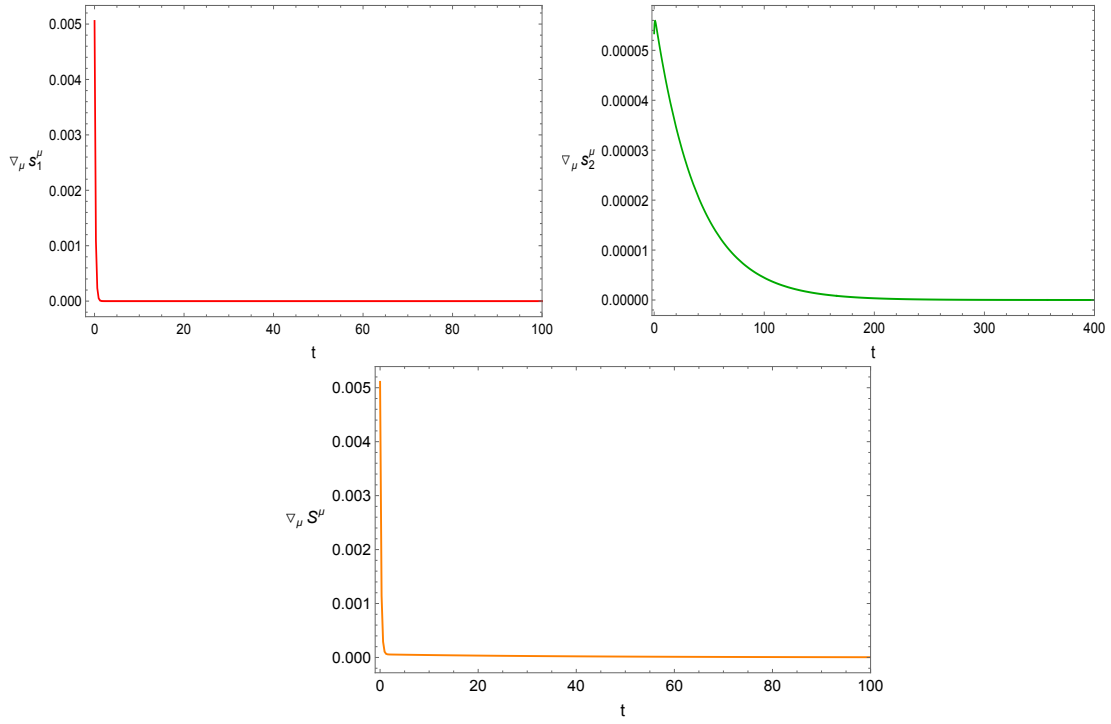

Figure 5.5: The plot shows the positive divergence of the entropy current of the full system and individual systems.

5.6 Quantum formulation of large N dynamics and isentropic thermalization

In order to see how thermalization can occur without producing entropy, it is useful to study the quantum formulation of the semi-holographic dynamics in the large N limit.

To simplify the discussion, we consider scalar coupling between the two sectors. However, our formulation readily generalizes to the case of the effective metric coupling we have discussed above. The scalar coupling can be obtained from the action:

$$S = S_1[J_1] + S_2[J_2] + \frac{1}{\alpha}\int (J_1 - J_0)(J_2 - J_0). \tag{5.58}$$

Varying with respect to the effective J_1 and J_2 in presence of an external source J_0, we obtain

the algebraic coupling equations:

$$J_1 = J_0 + \alpha O_2, \qquad J_2 = J_0 + \alpha O_1 \tag{5.59}$$

where

$$O_1 = \frac{\delta S_1}{\delta J_1}, \quad O_2 = \frac{\delta S_2}{\delta J_2}. \tag{5.60}$$

In absence of the effective metric coupling, the subsystems also live in flat spacetime effectively.

Now consider a generic state ρ_{12} of the full system which will be entangled typically and the reduced density matrices of the subsectors are

$$\rho_1 = Tr_2(\rho_{12}), \qquad \rho_2 = Tr_1(\rho_{12}). \tag{5.61}$$

The expectation values of the operators in the subsystems are

$$\langle O_1 \rangle = Tr(\rho_1 O_1), \qquad \langle O_2 \rangle = Tr(\rho_2 O_2). \tag{5.62}$$

In the large N limit, the full dynamics can be formulated in terms of the Hamiltonians H_1 and H_2 of the two sectors:

$$\hat{H}_1 = \hat{H}_{10} + \int J_1 \hat{O}_1, \quad \hat{H}_2 = \hat{H}_{20} + \int J_2 \hat{O}_2 \tag{5.63}$$

where $\hat{H}_{10}$ and $\hat{H}_{20}$ are the undeformed Hamiltonians of the subsystems (with hats distinguishing operators from c-numbers explicitly), and the effective sources J_1 and J_2 are given by (5.59) but with O_1 and O_2 replaced by the expectation values:

$$J_1 = J_0 + \alpha \langle O_2 \rangle, \qquad J_2 = J_0 + \alpha \langle O_1 \rangle. \tag{5.64}$$

In this limit, the time evolution is simply

$$\rho_{12} \to U_1 \otimes U_2 \, \rho_{12} \, U_1^\dagger \otimes U_2^\dagger \tag{5.65}$$

where U_1 and U_2 are the unitary time evolution operators obtained from H_1 and H_2, respectively. It follows that the subsystem density matrices have the evolution,

$$\rho_1 \to U_1 \rho_1 U_1^\dagger, \quad \rho_2 \to U_2 \rho_2 U_2^\dagger. \tag{5.66}$$

The iterative procedure to solve the dynamics of the full system is as follows. Let the initial state ρ_{12} be typical (and thus entangled). In the first step of the iteration, set $J_1 = J_2 = J_0$. Obtain $\langle O_1 \rangle$ and $\langle O_2 \rangle$. Evolve the full system in time via (5.65). In the second step, compute $\langle O_1 \rangle$ and $\langle O_2 \rangle$, and evolve the full system again via (5.65) but now with the deformed subsystem Hamiltonians. Subsequently, repeat this by evolving the full system with the subsystem Hamiltonians in which $\langle O_1 \rangle$ and $\langle O_2 \rangle$ are obtained from the second iteration, and keep on repeating until we find convergence. When convergence is achieved, the energy-momentum tensor of the full system is conserved. It is to be noted that at each step of the iteration, the subsystems undergo relevant/marginal deformations if the operators O_1 and O_2 have the required mass dimensions. Therefore, the full quantum evolution is well-defined at each step of the iteration.

In [16, 184], the semi-holographic dynamics with a scalar coupling was solved in the above iterative procedure, and convergence was achieved to an excellent approximation in just four iterations. However, in these works, the boundary system was a scalar/gauge field and the holographic system had a dual description in terms of a gravitational system coupled to a bulk scalar. The full dynamics was solved in classical approximation both in the bulk and boundary. Further, in [186], the full semi-holographic dynamics has been solved in this iterative procedure in a lower dimensional example with the boundary system quantized. Specifically, a quantum harmonic oscillator or a qubit is coupled to a SYK-type system dual to $NAdS_2$ holographic

geometry with a bulk scalar field.

In the large N formulation of quantum dynamics, we readily note that since the subsystems are evolved unitarily, the subsystem entropies and also the full system von Neumann entropies should remain invariant under time evolution. Nevertheless, the dynamics in this approximation is similar to a non-linear unitary mean field channel, where the non-linearity arises from replacing the operators O_1 and O_2 by their expectation values. In [186], it has been found that the boundary qubit reaches its lowest energy state while preserving the purity due to unitary evolution – the eigenvalues of its density matrix do not change but the information of the initial basis in which the density matrix becomes diagonal is lost since the final basis is that in which the subsystem Hamiltonian is diagonal. As the qubit reaches its lowest energy state, the holographic system approaches a thermal state dual to a black hole. In this case, since one degree of freedom is interacting with a large N holographic system, we expect the former to reach the lowest energy state due to equipartition of energy, as indeed observed. Therefore, the self-consistent non-linear unitary evolution leads to thermalization. Although the von Neumann entropy (and also Renyi entropies) of the boundary qubit does not change, it thermalizes by going to the lowest energy state which commutes with the Hamiltonian. The thermalization here is aided by the inherent second law in gravitational dynamics with the dynamics of the time reparametrization mode solved semi-classically and self-consistently.

The extrapolation to higher dimensions, and with a large quantum system with a commensurate dimensional Hilbert space coupled to a holographic system is as follows. Generally, if we consider a typical state ρ_{12} of the full isolated system, which could be out of equilibrium, and in which we specify simple observables such as the full system energy-momentum tensor (to be, as for instance, same as in pseudo-equilibrium), then this state generically should have maximum possible entropy, same as in global equilibrium. Furthermore, the full system will relax to global equilibrium without any change in subsystem and full system entropies.

We have shown that when we approximate the dynamics of both systems by BRSSS theories, we have non-equilibrium states with full system entropy close to global equilibrium,

which is the maximal possible entropy. Even though the perturbations are large compared to the difference in entropy, the full system is thermalized with very little entropy production.

We expect that if we couple kinetic theory to a holographic system, and solve the kinetic equations together with the gravitational dynamics, we can show that generically we should have isentropic thermalization. Unlike BRSSS, one can turn on higher moments of the distribution function and initial radial profiles of the bulk metric in a way in which a large number of parameters specifying the initial state contribute to the entropies but not to the initial energy-momentum tensors. (These parameters do not affect the coupling equations which give the effective metrics.) Thus we hope to achieve isentropic thermalization typically in the large N approximation consistently with the full quantum formulation described here. Particularly, we want to check if random initial conditions with fixed total energy indeed thermalize with small entropy perturbation compared with the scale of non-equilibrium perturbations

Finally, we note that the non-equilibrium entropy we obtain in effective descriptions like BRSSS, kinetic theory or dual gravity need not be the von Neumann entropy. A possible non-equilibrium entropy can be obtained by first measuring the energies of the subsystems so that the off-diagonal components of the respective density matrices in the energy basis are removed, and then computing the von Neumann entropy. Note that the thermal entropy remains the same with such a definition since the thermal density matrix is diagonal in the energy basis. We propose to examine if such a non-equilibrium entropy can be more appropriate to measure the irreversibility of thermalization and also understand the transfer of entropies between subsystems.

Chapter 6

Discussion

6.1 Summary

The discovery of hydrodynamic attractors in the context of heavy ion collisions, as well as the salient features of QCD such as chiral symmetry breaking and asymptotic freedom, motivates the thesis' investigation of far-away from equilibrium dynamics in the context of the Bjorken model of QGP. In this thesis, we explore the interplay between continuous symmetry breaking and hydrodynamization in a far-away from equilibrium system and also compute real-time hydrodynamic correlation functions of a system that hydrodynamizes at a late time. In addition, we also explore thermalisation in semi-holography.

After reviewing the necessary theoretical background of relativistic hydrodynamic theory, AdS/CFT correspondence and Schwinger-Keldysh correlation function in chapter 2, in chapter 3 we develop the MIS formalism for superfluids, extending the quantum effective action approach and study the Bjorken flow. We find that the dynamics of the system is governed by the existence of the conventional hydrodynamic attractor with unbroken symmetries and new fixed points determined by the potential for the condensate and the equation of state of the system. Particularly, if the initial temperature is above T_c, we find that the Josephson condition is satisfied by the phase very rapidly while the condensate becomes exponentially small over a

similar timescale and undergoes slow-roll during which the system gets trapped in the vicinity of the conventional hydrodynamic attractor. This persists for a long time until the system reheats and switches over to one of the symmetry-breaking fixed points. If the initial temperature is below T_c, the system does not generically get trapped by the conventional hydrodynamic attractor but rather evolves to one of the fixed points. In both cases, the hydrodynamic attractor traps the system forever if we start with initial conditions at the border of the basin of attraction of the fixed points.

As mentioned earlier, we expect that our key result that the superfluid Bjorken flow is governed by a combination of hydrodynamic attractors and an even number of non-dissipative fixed points should be a generic phenomenological feature. The fixed points are determined by the ideal component of the dynamics obtained from the quantum effective action with the relaxation mechanism playing no role while the hydrodynamic attractor appears in any strong coupling or weak coupling description of thermalization. Further, the analysis of fluctuations in thermal equilibrium indicates that the system has superfluid modes as seen in other effective theories and also unstable hydrodynamic modes when the temperature corresponds to values lower than that at the fixed points. This indicates that the fixed points are unstable against spinodal decomposition which needs further investigation in future by introducing inhomogeneities in the initial conditions and using our MIS theory with necessary improvements.

Chapter 4 studies the computation of real-time correlation functions of the hydrodynamic Bjorken flow by implementing CGL prescription of horizon cap to a dynamical, asymptotically AdS_{d+1} geometry whose boundary dual is Bjorken flow. We believe that our method for computing this correlation function can be generalized to generic situations where the state hydrodynamizes, meaning that the dynamics of one-point functions can be captured by an asymptotic series expansion which is generated by the hydrodynamic evolution of the temperature and velocity fields. The key would be to see if there exist Weyl transformations with non-trivial spacetime dependence which can map the flow at late time to a configuration with constant temperature and entropy density although time translation symmetry may not be present. In

this case, as demonstrated here for the Bjorken flow, the dual black hole would attain a horizon with constant surface gravity and area at late time, although a time-like Killing vector may be eternally absent. The event horizon's shape would fluctuate in space and time keeping the total area fixed when entropy production ceases in this limit. Nevertheless, with appropriate space-time reparametrizations, the horizon cap prescription can be made to work as in the case of the Bjorken flow provided at the leading order in the large (suitably reparametrized) time expansion the equation of motion of bulk fields can be mapped to that on a static black brane.

Chapter 5 discusses a part of the ongoing work on thermalisation in semi-holography. In this chapter, we review semi-holographic formalism with the example of metric coupling and then provide a generic proof of thermalisation in a hybrid system coupled democratically in this formalism. Indeed, it has been observed that the entropy of a full system in a micro-canonical ensemble maximises when the physical temperatures of the respective sectors coincide at any fixed total energy. This claim has been further supported by studying a two-fluid model of BRSSS formalism. Here we have shown that there exist generic non-equilibrium states whose entropy is as large as that of the global equilibrium entropy. Moreover, we observe that equilibration happens isentropically compared to the scale of perturbations in the infinite temperature limit. Finally, we have developed a quantum understanding of the thermalization of an isolated hybrid system in the context of quantum theory in the large N limit.

6.2 Outlook

The effective description of the superfluid in MIS formalism has been studied with $U(1)$ symmetry breaking where we have coupled the expectation value of the order parameter to the fluid. However, it will be more generic to couple the fluctuation of the order parameter to the fluid rather than the expectation value of the order parameter. The expectation value will appear dynamically. This can be achieved by using the mean-field approximation technique [187]. Further, in the context of chiral symmetry, one can study this boost-invariant expanding super-

fluid formalism using $O(4)$ pion physics and incorporate explicit symmetry breaking along with the spontaneous one by adding a term like $\mathcal{M}\Sigma^\dagger + \mathcal{M}^\dagger\Sigma$ [52], where Σ is the field invariant under $O(4)$ symmetry and $\mathcal{M}$ is a matrix that can be taken to unity and is responsible for explicit symmetry breaking. The incorporation of pion physics with hydrodynamics can increase the prediction power of hydrodynamics to understand the evolution of nuclear matter formed in a heavy-ion collision.

It would be important to study the Bjorken expansion of the superfluid in a UV-complete setup at strong coupling, particularly in a holographic model. Of particular interest would be to understand if the approach to the hydrodynamic attractor and subsequent switching to the symmetry-breaking fixed points occurs rapidly as in the MIS setup. Furthermore, to be of relevance to the quark-gluon plasma we will need to consider interacting multi-component systems as in [123]. Our model is essentially that of the quark sector. The gluonic degrees of freedom should be introduced as a separate fluid. Furthermore, it may be necessary to include both weakly coupled and strongly coupled degrees of freedom. Such hybrid fluid models with a higher dimensional hydrodynamic attractor have been discussed in [20, 63]. In the case of a multicomponent system, the reheating transition of the superfluid to the fixed point may not be possible or may not occur irreversibly because of the transfer of energy to the other components of the full system.

Bjorken flow captures the dynamics occurring along the direction of expansion. To capture the dynamics of transverse direction for a better understanding of the evolution of far-from-equilibrium systems such as QGP, it will be interesting to investigate the Gubser flow [188]. Gubser flow attractor has been studied widely [189–193] due to its relevance to heavy ion colliders. However, its holographic dual has been left unexplored. We pursue this direction to formulate a holographic dual of Gubser flow such that it can be used to study holographic attractors and also compute Schwingker Keldysh correlation functions as discussed in chapter 4.

Another important problem would be to understand the Borel resummation of the hy-

drodynamic series (4.119) and compute the Schwinger-Keldysh correlation functions of the holographic hydrodynamic attractor [26]. Furthermore, the late-time thermal nature of the correlation functions in terms of the reparametrized spacetime arguments could be of phenomenological relevance in heavy ion collisions, especially regarding the dynamics of heavy quarks and bound states, and jets in the expanding quark-gluon plasma [194].

Our prescription can be used to construct the quantum generalization of classical stochastic hydrodynamics (see [9, 28] for reviews) in holographic theories by considering the backreaction of the fluctuations on the background geometry systematically. In this direction, one can incorporate the quantum effect in correlation functions by computing the boundary propagator using 2PI effective action. This is especially important in the context of superfluid fluctuations since quantum dynamics is important at coherence time and length scales which are shorter than the scattering time and the mean free path respectively (see [154] for an excellent related discussion)– non-linearities can potentially cause novel non-trivial effects such as quantum corrections to the long time tails.[1]

Thermalisation studied in the BRSSS theory could capture isentropic thermalisation with a diagonal and isotropic form of the energy-momentum tensor of the full system. To get a better understanding of isentropic thermalisation, one can study the hybrid system of two RTA kinetic theories coupled via a democratic coupling or black hole dynamics coupled to a RTA kinetic theory or BRSSS theory.

The methods developed in the thesis have been discussed from the perspective of QCD matter formed in heavy ion collision. However, this can be generalised to other non-equilibrium processes. In the context of the effective description of dissipative superfluid, it would be interesting to explore more general forms of expanding flows, particularly those with spherical symmetry (see [195] for a relevant model). As the superfluid condensate is naturally driven to slow roll on a hydrodynamic attractor with a natural mechanism of exit from the slow roll, while reheating of the system upon switching to one of the fixed points, this raises the possibility that

[1]For recent work on the role of classical fluctuations of the superfluid order parameter in modifying transport properties see [8].

one can use such a superfluid as an inflaton in cosmology with a natural preheating mechanism in place.

Further, a more general goal in the horizon prescription to compute the Schwinger Keldysh correlation function is to develop a quantum generalization of the large deviation function in classical non-equilibrium statistical mechanics, which is essentially a generalization of the equilibrium free energy to the hydrodynamic regime, assigning, for instance, the probability to a microscopic hydrodynamic configuration which may not satisfy the hydrodynamic equations. The approach (of [166]) which constructs an effective action at finite temperature from the complexified bulk spacetime will be very relevant for such developments. More generally, the horizon cap method can be used to study holographic (evaporating) black holes interacting with heat baths or dynamical reservoirs, and understand the reconstruction of the islands [177, 196] (which include the black hole interior) from Hawking quanta. In such cases, semi-holographic formulations for open quantum systems (see [16, 197] and also [166] for instance) can provide useful models.

Appendix A

Weyl covariant derivative

The Weyl covariant derivative is a derivative operator which maps a Weyl covariant tensor to another Weyl covariant tensor of one higher rank. The action of a Weyl covariant derivative $\mathcal{D}_\alpha$ on a tensor $Q^{\mu\cdots}_{\nu\cdots}$ of weight w as defined in [83, 86] is given by

$$\mathcal{D}_\alpha Q^{\mu\cdots}_{\nu\cdots} \equiv \nabla_\alpha Q^{\mu}_{\nu} + wA_\alpha Q^{\mu\cdots}_{\nu\cdots} + (g_{\alpha\lambda}A^\mu - \delta^\mu_\alpha A_\alpha - \delta^\mu_\alpha A_\alpha)Q^{\lambda\cdots}_{\nu\cdots} + \cdots - (g_{\alpha\nu}A^\lambda - \delta^\alpha A_\nu - \delta^\lambda_\nu A_\alpha)Q^{\mu\cdots}_{\lambda\cdots} - \cdots \tag{A.1}$$

where A_μ is the connection one-form whose form in the context of fluid dynamicscan be determined from the condition that the Weyl covariant derivative of the fluid velocity u^μ is required to be transverse and traceless, i.e.

$$u^\alpha \mathcal{D}_\alpha u^\mu = 0, \qquad \mathcal{D}_\mu u^\mu = 0. \tag{A.2}$$

This defines A_μ to be,

$$A_\mu = u^\lambda \nabla_\lambda u_\mu - \frac{1}{d-1} u_\mu \nabla^\lambda u_\lambda \tag{A.3}$$

where d is the dimension of the system. For a conformally invariant tensor $Q^{\mu\cdots}_{\nu\cdots}$, $Q^{\mu\cdots}_{\nu\cdots} = e^{-w\phi}\tilde{Q}^{\mu\cdots}_{\nu\cdots}$ the action of Weyl covariant derivative will be

$$\mathcal{D}_\alpha Q^{\mu\cdots}_{\nu\cdots} = e^{-w\phi}\tilde{D}_\alpha \tilde{Q}^{\mu\cdots}_{\nu\cdots} \tag{A.4}$$

which means that the Weyl covariant derivative of a conformally invariant tensor transforms homogeneously with the same weight w as the tensor itself. Further, the derivative $\mathcal{D}_\alpha$ defined in terms of the Weyl connection ∇^{Weyl}_α as $\mathcal{D}_\alpha = \nabla^{Weyl}_\alpha + wA_\alpha$ implies metric compatibility i.e., $\mathcal{D}_\alpha g_{\mu\nu} = 0$ with $w = -2$ for $g_{\mu\nu}$.

Appendix B

Detailed form of the particular equation of the second order Einstein equation of the five-dimensional metric dual to the Bjorken flow

Here we write the particular solutions of the second-order expansion of Einstein's equations based on the ansatz (2.97) along with (2.102),

$$
\begin{aligned}
PI_{1,2} &= \frac{1}{12}\Big(8x^2 + 6\log\left(x^2+1\right) - \alpha_1^2(x+2)x - 4\alpha_1(x+2)x \\
&+ 16x + 4\log(x+1) + 2(2-6x)\arctan(x) + 4\Big), \\
PI_{3,2} &= \frac{x}{108}\Big(\alpha_1^2\left(-9x^5 - 6x^4 + 3x + 6\right) - 4\alpha_1\left(9x^5 + 12x^4 - 9x - 8\right) \\
&+ 4\Big(-9x^5 - 9\left(x^4+1\right)\arctan(x) + x^3 + 9x^3\log\left(x^2+1\right) + 9x + 16\Big)\Big),
\end{aligned}
$$

$$
\begin{aligned}
PI_{2,2} &= Re\Bigg[\frac{1}{24}\Big(-24x^2-\frac{16x}{x^3+x^2+x+1}+16x+(4+4i)\arctan(x)^2-(1-i)\log^2(i-x)\\
&+ 4\log^2(x+1)-2\log^2(-i+x)-(3+i)\log^2(i+x)-4\log^2\left(x^2+1\right)+(2+8i)\arctan\left(\frac{x+1}{1-x}\right)\\
&+ 2i\pi\arctan(x)-8\arctan(x)+(2-8i)\arctan\left(\frac{x-1}{x+1}\right)-\pi\log(2)+4\pi\log\left(1+e^{-2i\arctan(x)}\right)\\
&- 16\arctan(x)\log\left(1+e^{2i\arctan(x)}\right)+8\arctan(x)\log\left(1-ie^{2i\arctan(x)}\right)+2\pi\log\left(1-ie^{2i\arctan(x)}\right)\\
&+ 6\log(1-x)-(4+4i)\log\left(\left(\frac{1}{2}+\frac{i}{2}\right)(ix+1)\right)\log(x+1)\\
&+ 2\log(x+1)+4\log(x-1)\log\left(\left(\frac{1}{2}+\frac{i}{2}\right)(-i+x)\right)-(6+2i)\log\left(\frac{1}{2}(ix+1)\right)\log(i+x)\\
&+ 4\log(x-1)\log\left(\left(\frac{1}{2}-\frac{i}{2}\right)(i+x)\right)+(4+4i)\log(x+1)\log\left(\left(-\frac{1}{2}-\frac{i}{2}\right)(i+x)\right)\\
&- (2-2i)\log(i-x)\log\left(-\frac{1}{2}i(i+x)\right)-4\log(-i+x)\log\left(-\frac{1}{2}i(i+x)\right)\\
&+ (2-2i)\log(i-x)\log\left(x^2+1\right)-4\log(x-1)\log\left(x^2+1\right)\\
&+ 4\log(-i+x)\log\left(x^2+1\right)+(6+2i)\log(i+x)\log\left(x^2+1\right)\\
&+ 2\pi\log\left(x^2+1\right)-4\log\left(x^2+1\right)+8\log(x+1)\log\left(1-\left(\frac{1}{2}-\frac{i}{2}\right)(x+1)\right)\\
&- 4\pi\log\left(\sin\left(\arctan(x)+\frac{\pi}{4}\right)\right)+2\pi\log\left(\frac{x+1}{\sqrt{x^2+1}}\right)-(6-2i)\mathrm{Li}_2\left(\frac{ix}{2}+\frac{1}{2}\right)\\
&+ 8i\mathrm{Li}_2\left(-e^{2i\arctan(x)}\right)-4i\mathrm{Li}_2\left(ie^{2i\arctan(x)}\right)\\
&+ 4\mathrm{Li}_2\left(\left(-\frac{1}{2}+\frac{i}{2}\right)(x-1)\right)+4\mathrm{Li}_2\left(\left(-\frac{1}{2}-\frac{i}{2}\right)(x-1)\right)+(4+4i)\mathrm{Li}_2\left(\left(\frac{1}{2}+\frac{i}{2}\right)(x+1)\right)\\
&+ (4-4i)\mathrm{Li}_2\left(\left(\frac{1}{2}-\frac{i}{2}\right)(x+1)\right)-(6+2i)\mathrm{Li}_2\left(-\frac{1}{2}i(i+x)\right)+\Big(-\frac{8x}{x^3+x^2+x+1}+8x\\
&+ (2+4i)\arctan\left(\frac{x+1}{1-x}\right)-4\arctan(x)+(2-4i)\arctan\left(\frac{x-1}{x+1}\right)\Big)\alpha_1-\frac{8}{x^3+x^2+x+1}\Big)\Bigg],
\end{aligned}
$$

where $\mathrm{Li}_2(x)$ is the polylogarithmic function of order 2. The expressions for the particular solution get increasingly complicated at higher orders. However, the simple structure of the homogeneous solutions remain the same at every order. The integration constants associated with the homogeneous solutions can be fixed at every order as mentioned in the 2.2.4.

Appendix C

The event horizon and the apparent horizon of the Bjorken flow

This appendix is devoted to a comparative discussion between the event horizon and the apparent horizon in the dynamical geometry dual to the Bjorken flow.

C.1 Event horizon:

Classically, the event horizon marks the null hypersurface from which no signal can come out, i.e, the outgoing null rays become tangential to the hypersurface. To determine its location in the geometry given by (4.60), consider radial null geodesics in this spacetime whose equation is given by,

$$\frac{\partial v}{\partial \sigma} + \frac{v^2}{2}\frac{d-2}{d-1} g_{\sigma\sigma} = 0 \,, \qquad \text{with} \qquad g_{\sigma\sigma} = \frac{1}{v^2}\left(\frac{(d-1)^2}{(d-2)^2} A(v,\sigma) + \frac{2(d-1)v}{(d-2)^2\sigma}\right) . \tag{C.1}$$

For a static geometry, $v_E = cons.$ and the event horizon is simply given by the zero of $g_{\sigma\sigma}$. However, in a dynamical geometry, the event horizon will depend on σ. Consider the late-time

expansion of the horizon of the form,

$$v(\sigma) \equiv v_E(\sigma) = \sum_{i=0} v_{Ei}\, \sigma^{-i} \tag{C.2}$$

Now to determine v_{Ei}, we use the equation (C.1) along with the known late-time expansion of $A(v, \sigma)$,

$$A(v, \sigma) = 1 - \varepsilon_0\, v^d + \frac{1}{\varepsilon_0^{1/d}\sigma} a_1(v) + \frac{1}{\varepsilon_0^{2/d}\sigma^2} a_2(v) + \cdots \tag{C.3}$$

At leading order, we have

$$v_{E0} = 1/\varepsilon_0^{1/d}$$

in any spacetime dimensions $d + 1$. The sub-leading corrections to the event horizon depend on the residual gauge parameters. For instance, the first and second sub-leading corrections in $d = 4$[1] are,

$$\begin{aligned} v_{E1} &= \frac{(3 + \alpha_1)}{6\varepsilon_0^{1/2}}\,, \\ v_{E2} &= \frac{72\alpha_2 - 9\pi - 20 + 12\log(2)}{216\varepsilon_0^{3/4}}\,, \end{aligned} \tag{C.4}$$

where α_1 and α_2 are the residual gauge parameters associated with the late-time expansion of $A(v, \sigma)$. Now the gauge parameters can be uniquely fixed by demanding regularity of the horizon cap. In $d = 4$, this gives (recall (4.84) and (4.85))

$$\begin{aligned} \alpha_1 &= -3, \\ \alpha_2 &= \frac{9\pi + 20 - 12\log(2)}{72}. \end{aligned} \tag{C.5}$$

These values, in turn fix the event horizon to $1/\varepsilon_0^{1/d}$ upto the second subleading order. Thus, regularization of the horizon cap leads to vanishing of the sub-leading corrections v_{Ei} (for $i > 0$) to the static event horizon. We expect this feature to remain true to all orders in the late-time

[1]For $d = 3$, the first sub-leading correction is $v_{E1} = \frac{5(5+3\alpha_1)}{3\varepsilon_0^{2/3}}$, which again depends on the residual parameter. However, these corrections do not have a universal form like the leading order.

expansion.

C.2 Apparent horizon:

The apparent horizon is a null hypersurface that acts as a boundary between the trapped and un-trapped regions, whose location is given by the product of the expansion parameters $\theta_{\pm}$, i.e. $\Theta = e^f \theta_+ \theta_-$, where the factor e^f is defined below. The trapped region is characterized by $\Theta > 0$, where the light rays directed outward propagates inward, whereas in the un-trapped region the light rays directed outward propagates outward and is characterized by $\Theta < 0$. Therefore $\Theta = 0$ gives the location of the apparent horizon.

Here we will adopt the dual-null formalism [198–201] to study location of the apparent horizon, where one defines a pair of null hypersurfaces $\Sigma^{\pm}$ parameterised by scalars $\zeta^{\pm}$, with associated one-forms $n^{\pm} = -\mathrm{d}\zeta^{\pm}$. The null normal vector associated with these hypersurfaces are given by,

$$l^{\mu}_{\pm} = e^{-f} g^{\mu\nu} n^{\mp}_{\nu} \, ,$$

where e^f is the normalization factor given by,

$$e^f = -g^{\mu\nu} n^{-}_{\mu} n^{+}_{\nu} \, .$$

Next we define the expansion parameters $\theta_{\pm}$,

$$\theta_{\pm} = \mathcal{L}_{\pm} Log(\mu) \, ,$$

where μ is the spatial volume element of the geometry in which the hypersurfaces are defined and $\mathcal{L}_{\pm}$ is the lie derivative along the null normal vectors, $l_{\pm}$. Finally we introduce the invariant[2]

[2]This parameter Θ is invariant under reparameterisation of the scalar $\zeta^{\pm} \to \xi^{\pm}(\zeta^{\pm})$ or interchange of $\zeta^{\pm} \to \zeta^{\mp}$ as discussed in [199].

quantity $\Theta = e^f \theta_+ \theta_-$, whose zero gives the location of the apparent horizon.

In case of our geometry (4.60), we consider a pair of null hypersurface defined by constant values of the retarded and advanced radial null coordinates, whose normal one-forms are given by,

$$n^- = -\mathcal{N}^- \mathrm{d}\sigma, \qquad n^+ = -\mathcal{N}^+ \Big(\Big(\frac{2v}{\sigma} + (d-1) A(v,\sigma) \Big) \mathrm{d}\sigma + 2(d-2) \mathrm{d}v \Big), \tag{C.6}$$

and the null normal vectors $l^\mu_\pm$ along with the normalisation factor e^f and the volume element μ reads,

$$\begin{aligned} e^f &= \frac{2(d-2)^2}{d-1} \mathcal{N}^+ \mathcal{N}^- v^2 \,, \\ l^\mu_+ &= \left(\frac{1}{2(d-2)\mathcal{N}^+}, 0, 0, \vec{0} \right) \,, \\ l^\mu_- &= \left(-\frac{\sigma(d-1)A(v,\sigma) + 2v}{2(d-2)\mathcal{N}^- \sigma}, 1/\mathcal{N}^-, 0, \vec{0} \right) \,, \\ \mu &= \frac{\sigma + v}{v^3 \sigma} \sqrt{e^{2K(v,\sigma) + L(v,\sigma)}} \,. \end{aligned} \tag{C.7}$$

where $\mathcal{N}^+$ and $\mathcal{N}^-$ are the overall normalizability factor that can be determined by the integrability condition $\mathrm{d}(\mathrm{d}n^\pm) = 0$. This ensures that the one-forms (C.6) and (C.7) are exact. However there is no need of computing them explicitly, as when we compute Θ the contribution of $\mathcal{N}^+$ and $\mathcal{N}^-$ from e^f will cancel with the ones coming from θ_- and θ_+.

Now since the apparent horizon depends on σ, one can consider a late-time expansion of the apparent horizon similar to the event horizon as,

$$v_A(\sigma) = \sum_{i=0} v_{Ai}\, \sigma^{-i}.$$

To determine the coefficients v_{Ai} we solve $\Theta = 0$ at every order. In case of any spacetime dimensions $d+1$, the leading order result is universal and turns out to be

$$v_{A0} = 1/\varepsilon_0^{1/d} ,$$

which coincides with the event horizon. However, the sub-leading corrections are dimension dependent. For $d = 4$, the first and second sub-leading corrections to the leading terms are

$$\begin{aligned} v_{A1} &= \frac{3+\alpha_1}{6\varepsilon_0^{1/2}} , \\ v_{A2} &= \frac{72\alpha_2 - 9\pi - 8 + 12\log(2)}{216\,\varepsilon_0^{3/4}} . \end{aligned} \tag{C.8}$$

Note that, for $\alpha_1 = -3$ the first order correction to the apparent horizon vanishes similar to the case of the event horizon. However, at second order, the value of α_2 (given by (4.85)) for which the the correction to the event horizon vanishes, now renders $v_{A2} > 0$. So the apparent horizon will lie inside the event horizon (see Figure C.1). Again, we expect this feature to remain true at higher orders as well.

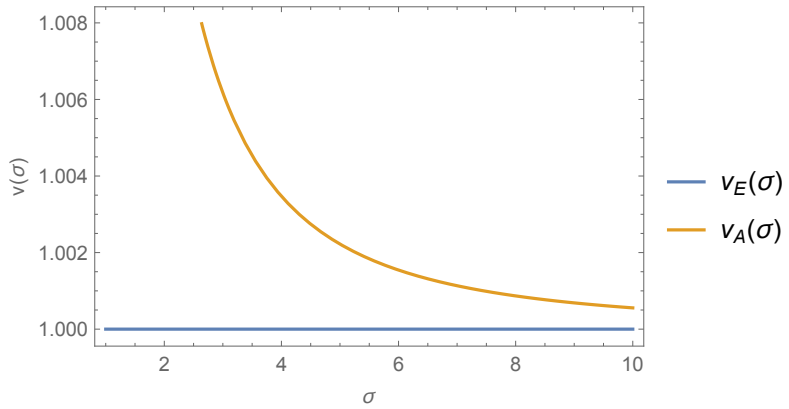

Figure C.1: The figure shows the evolution of the event horizon(blue curve) and the apparent horizon(yellow curve) in the dynamical geometry dual to the Bjorken flow, upto second order in late-time expansion. Here ε_0 is set to 1 and the gauge parameters α_1 and α_2 are so chosen that the event horizon is fixed to 1. The apparent horizon always lies inside the event horizon (at greater v).

Appendix D

More details of the bulk scalar field in the AdS_5 Bjorken flow background

In this appendix, we will provide brief details of the solution of Klein-Gordon equation at the leading (4.73) and first subleading order (4.78) (for $n = 1$) and validate the near-horizon behaviours (4.77) and (4.81) for the same. To be specific, we will consider the example of $d = 4$.

At leading order, the homogenous Klein-Gordon equation (4.73) simply takes the form of that in a static black brane geometry. So we can expand the solution in the standard basis provided by the ingoing and outgoing modes. Near the horizon, these modes admit the following expansions

$$\phi_{0,in}(v,\omega,\kappa_L,\vec{\kappa}_T) = p_0\left[1+(\varepsilon_0^{-1/4}-v)\frac{\left(\kappa_L^2+\vec{\kappa}_T^2-m^2\varepsilon_0^{1/2}+3i\varepsilon_0^{-1/4}\omega\right)}{2\left(2\varepsilon_0^{1/4}-i\omega\right)}+\mathcal{O}((\varepsilon_0^{-1/4}-v)^2)+\cdots\right] \tag{D.1}$$

$$(\varepsilon_0^{-1/4}-v)^{-\frac{i\omega}{2\varepsilon_0^{-1/4}}}\phi_{0,out}(v,\omega,\kappa_L,\vec{\kappa}_T)=q_0\Bigg[1+(\varepsilon_0^{-1/4}-v)\frac{\left(2\kappa_L^2+2\vec{\kappa}_T^2-2m^2\varepsilon_0^{1/2}-3i\omega\right)}{4\left(2\varepsilon_0^{1/4}+i\omega\right)}$$
$$+O((\varepsilon_0^{-1/4}-v)^2)+\cdots\Bigg]. \quad \text{(D.2)}$$

Now, without loss of generality, we can set $p_0 = 1$ and $q_0 = 1$. Then, in the limit $v \to \varepsilon_0^{-1/4}$ we reproduce the behaviours given in (4.77).

At the first subleading order ($n = 1$), the Klein-Gordon equation is given by (4.78) with

$$S_{1,in} = \tilde{\mathcal{S}}\phi_{0,in}(v,\omega,\kappa_L,\vec{\kappa}_T)$$

$$S_{1,out} = \tilde{\mathcal{S}}\phi_{0,out}(v,\omega,\kappa_L,\vec{\kappa}_T) \quad \text{(D.3)}$$

where,

$$\begin{aligned}
\tilde{\mathcal{S}} &= -\frac{v}{6\varepsilon_0^{1/4}}\Bigg(\alpha_1\varepsilon_0^{1/4}v\left(2\kappa_L^2v+2\vec{\kappa}_T^2v+3i\omega\right)+2v\left(2\kappa_L^2-\vec{\kappa}_T^2\right)\tan^{-1}\left(\varepsilon_0^{1/4}v\right)+4(\kappa_L^2+\vec{\kappa}_T^2)\varepsilon_0^{1/4}v^2 \\
&+ (2\kappa_L^2-\vec{\kappa}_T^2)v\Big(\log\left(\varepsilon_0^{1/2}v^2+1\right)+2\log\left(\varepsilon_0^{1/4}v+1\right)\Big)+12i\gamma_0\varepsilon_0^{1/4}+6i\varepsilon_0^{1/4}v\omega\Bigg) \\
&- \frac{1}{6}v\Bigg((4\varepsilon_0^{3/4}v^5+2\alpha_1\varepsilon_0v^6+4\varepsilon_0v^6+2\alpha_1v^2+4v^2)\partial_v^2+(2\varepsilon_0v^5-\alpha_1v-8i\gamma_0v+4\varepsilon_0^{3/4}v^4+\alpha_1\varepsilon_0v^5-2v)\partial_v \\
&- 12\kappa_L\partial_{\kappa_L}+6\vec{\kappa}_T\partial_{\vec{\kappa}_T}-4\vec{\kappa}_Tv\partial_{\vec{\kappa}_T}\partial_v+8\kappa_Lv\partial_{\kappa_L}\partial_v\Bigg). \quad \text{(D.4)}
\end{aligned}$$

The action of $\tilde{\mathcal{S}}$ on $\phi_{0,out}$ gives rise to singular terms having poles of order one and two at the horizon, as mentioned in (4.83). Upon removing these poles by suitably fixing α_1 and γ_0 as in (4.84), the particular solution at the first subleading order for the outgoing mode admits the

near-horizon expansion,

$$
\begin{aligned}
(\varepsilon_0^{-1/4}-v)^{-\frac{i\omega}{2\varepsilon_0^{-1/4}}}\phi_{1(p),out}(\omega,v,\kappa_L,\vec{\kappa}_T) &= \frac{(\varepsilon_0^{-1/4}-v)}{48\varepsilon_0^{1/4}+24i\omega}\Big(-2\kappa_L^2(\pi-7+\log(64))+\vec{\kappa}_T^2(\pi+2+\log(64)) \\
&- 2m^2\varepsilon_0^{1/2}-4i\varepsilon_0^{1/4}\omega-\omega^2\Big)+O((\varepsilon_0^{-1/4}-v)^2)+\cdots
\end{aligned}
\tag{D.5}
$$

However, for the ingoing mode no such divergent terms appear and we simply have the following near horizon exapnsion

$$
\begin{aligned}
\phi_{1(p),in}(\omega,v,\kappa_L,\vec{\kappa}_T) &= \Big(\kappa_L^2\left(-4\varepsilon_0^{1/4}(\pi-7+\log(64))+2i\omega(\pi-3+\log(64))\right) \\
&+ \vec{\kappa}_T^2\left(2\varepsilon_0^{1/4}(\pi+2+\log(64))-i\omega(\pi+6+\log(64))\right) \\
&- 4m^2\varepsilon_0^{3/4}+2im^2\varepsilon_0^{1/2}\omega+6\varepsilon_0^{1/4}\omega^2+12i\varepsilon_0^{1/2}\omega\Big)\frac{(\varepsilon_0^{-1/4}-v)}{24\left(2\varepsilon_0^{1/4}-i\omega\right)^2} \\
&+ O((\varepsilon_0^{-1/4}-v)^2)+\cdots
\end{aligned}
\tag{D.6}
$$

Clearly, in the limit $v \to \varepsilon_0^{-1/4}$, we reproduce (4.81) for $d = 4$ and $n = 1$. Similar behaviour persists at higher orders as well.

Appendix E

Derivation of Eqs. (4.102)

The source and vev of the dual operator at the boundary are given by

$$J(\sigma_2,\hat{\zeta}_2,\vec{x}_{\perp 2}) = \int \mathrm{d}\omega \mathrm{d}k_L \mathrm{d}^{d-2}k_T \; e^{-i\omega s(\sigma_2)} e^{i\left(k_L\hat{\zeta}_2+\vec{k}_T\cdot\vec{x}_{\perp 2}\right)} \; \mathcal{S}(\sigma_2,\omega,\kappa_L,\vec{\kappa}_T)\cdot Q(\omega,k_L,k_T), \tag{E.1}$$

$$\langle O(\sigma_1,\hat{\zeta}_1,\vec{x}_{\perp 1})\rangle = (2\Delta_O - d)\int \mathrm{d}\omega \mathrm{d}k_L \mathrm{d}^{d-2}k_T \; e^{-i\omega s(\sigma_1)} e^{i\left(k_L\hat{\zeta}_1+\vec{k}_T\cdot\vec{x}_{\perp 1}\right)} \; \mathcal{R}(\sigma_1,\omega,\kappa_L,\vec{\kappa}_T)\cdot Q(\omega,k_L,k_T)\,, \tag{E.2}$$

where

$$J(\sigma,\hat{\zeta},\vec{x}_\perp) = \begin{pmatrix} J_1(\sigma,\hat{\zeta},\vec{x}_\perp) \\ J_2(\sigma,\hat{\zeta},\vec{x}_\perp)\end{pmatrix}, \quad \langle O(\sigma,\hat{\zeta},\vec{x}_\perp)\rangle = \begin{pmatrix} \langle O_1(\sigma,\hat{\zeta},\vec{x}_\perp)\rangle \\ \langle O(\sigma,\hat{\zeta},\vec{x}_\perp)\rangle\end{pmatrix}, \quad Q(\omega,k_L,k_T) = \begin{pmatrix} p(\omega,k_L,k_T) \\ q(\omega,k_L,k_T)\end{pmatrix}.$$

To extract the SK Green's function, we first invert (E.1) to get,

$$Q(\omega,k_L,k_T) = \int \mathrm{d}\sigma_2 \mathrm{d}\hat{\zeta}_2 \mathrm{d}^{d-2}x_{\perp 2} \; s'(\sigma_2) \; e^{i\omega s(\sigma_2)} e^{-i\left(k_L\hat{\zeta}_2+\vec{k}_T\cdot\vec{x}_{\perp 2}\right)} \; \mathcal{S}^{-1}(\sigma_2,\omega,\kappa_L,\vec{\kappa}_T)\cdot J(\sigma_2,\hat{\zeta}_2,\vec{x}_{2\perp}). \tag{E.3}$$

Finally, plugging it back to (E.2) and using linear response theory,

$$\langle O(\sigma_1,\hat{\zeta}_1,\vec{x}_{\perp 1})\rangle = \int \mathrm{d}\sigma_2 \mathrm{d}\hat{\zeta}_2 \mathrm{d}^{d-2}\vec{x}_{\perp 2} \; \widetilde{G}(\sigma_1,\sigma_2,\hat{\zeta}_1,\hat{\zeta}_2,\vec{x}_{\perp 1},\vec{x}_{\perp 2})\, J(\sigma_2,\hat{\zeta}_2,\vec{x}_{\perp 2})$$

we read off the SK Green's function

$$\widetilde{G}(\sigma_1,\sigma_2,\hat{\zeta}_1-\hat{\zeta}_2,\vec{x}_{\perp 1}-\vec{x}_{\perp 2}) = \int \mathrm{d}\omega \mathrm{d}k_L \mathrm{d}^{d-2}k_T\, e^{-i\omega(s(\sigma_1)-s(\sigma_2))} e^{ik_L(\hat{\zeta}_1-\hat{\zeta}_2)+i\vec{k}_T\cdot(\vec{x}_{\perp 1}-\vec{x}_{\perp 2})}\widehat{G}(\sigma_1,\sigma_2,\omega,k_L,\vec{k}_T) \tag{E.4}$$

where,

$$\widehat{G}(\sigma_1,\sigma_2,\omega,k_L,\vec{k}_T) = \frac{1}{2}\Big(s'(\sigma_2)\,\sigma_3\ \cdot\mathcal{R}\,(\sigma_1,\omega,\kappa_{L1},\vec{\kappa}_{T1})\cdot\ \mathcal{S}^{-1}\,(\sigma_2,\omega,\kappa_{L2},\vec{\kappa}_{T2}) + (\text{transpose},\ \sigma_1\leftrightarrow\sigma_2,\omega\to-\omega,\kappa_{L1}\leftrightarrow-\kappa_{L2},\vec{\kappa}_{T1}\leftrightarrow-\vec{\kappa}_{T2})\Big) \tag{E.5}$$

with,

$$\kappa_{L1}=k_L\frac{\tau_0}{\sigma_1},\quad \kappa_{L2}=k_L\frac{\tau_0}{\sigma_2},\quad \vec{\kappa}_{T1}=\vec{k}_T\left(\frac{\tau_0}{\sigma_1}\right)^{-1/(d-2)},\quad \vec{\kappa}_{T2}=\vec{k}_T\left(\frac{\tau_0}{\sigma_2}\right)^{-1/(d-2)}.$$

Firstly, note that the variable conjugate to the momentum ω is the reparametrized time $s(\sigma)$ whereas the boundary quantites depend on σ. This gives rise to the factor $s'(\sigma_2)$ in (E.3) as the Jacobian of the transformation $s(\sigma_2)\to\sigma_2$. Also note that, due to translational invariance along the spatial directions, the matrices $\mathcal{S}$ and $\mathcal{R}$ are independent of $\hat{\zeta}$ and $\vec{x}_\perp$. Hence, on carrying out the momentum integrals in (E.4), we would get $\widetilde{G}(\sigma_1,\sigma_2,\hat{\zeta}_1,\hat{\zeta}_2,\vec{x}_{\perp 1},\vec{x}_{\perp 2})\equiv\widetilde{G}(\sigma_1,\sigma_2,\hat{\zeta}_1-\hat{\zeta}_2,\vec{x}_{\perp 1}-\vec{x}_{\perp 2})$.

Appendix F

Transients and γ_0

The quasinormal frequencies and transients capture the causal response of a black hole to small perturbations. Typically, for a black hole these are determined using the spectral representation method. However, here we adapt a simpler approach for the computation of the same.

For the homogeneous transients, consider the field ansatz (4.75) with only the ingoing modes of a massless scalar, i.e.

$$\Phi(v,\sigma) \;=\; \int \mathrm{d}\omega\; e^{-i\frac{d-1}{d-2}\omega\sigma}\left(\frac{\sigma}{\tau_0}\right)^{i\gamma_0(\omega/\varepsilon_0^{1/d})} \sum_{n=0}^{\infty}\left(\varepsilon_0^{1/d}\sigma\right)^{-n}\phi_{n,in}(v,\omega)p(\omega)\,, \tag{F.1}$$

where $\phi_{n,in}(v,\omega)$ obeys the same equations (4.73) and (4.78) (and hence admit the solutions (4.77) and (4.80)) with $\kappa_L, \vec{\kappa_T} = 0$. The residual gauge parameters α_i appearing in the subleading solutions are fixed such that at every order, the event horizon is pinned at $v_h = \varepsilon_0^{-1/4}$ with associated Hawking temperature $T = \varepsilon_0^{1/4}/\pi$. For concreteness, we will again consider $d = 4$.

Recall that, at leading order, the ingoing mode(with zero spatial momentum) admits the the near-horizon expansion

$$\phi_{0,in}(v,\omega) = 1 + \frac{3i\varepsilon_0^{1/4}\omega}{2\left(2\varepsilon_0^{1/4} - i\omega\right)}(\varepsilon_0^{-1/4} - v) + O((\varepsilon_0^{-1/4} - v)^2) + \cdots \tag{F.2}$$

To compute the transients, we introduce the dimensionless decay rate $\lambda = \omega/\pi T$ and also scale the horizon to set $v_h = 1$. In terms of the dimensionless parameter, the solution (F.2) when expanded near the boundary $v = 0$ reads,

$$\phi_{0,in}(v = 0, \lambda) \equiv a_0(\lambda) = 1 - \frac{3\lambda}{2\,(2i + \lambda)} + \cdots \tag{F.3}$$

The QNM corresponds to $a_0(\lambda_{qnm}) = 0$, implying that there is no contribution to the source from the leading order field. The lowest QNM frequency obtained in this method turns out to be

$$\lambda_{qnm} = -2.7668i \pm 3.11945\ ,$$

which agrees with the one obtained from spectral representation method upto order 10^{-10}.

Similarly at subleading orders $n > 0$, the sources can be made to vanish, i.e. $a_{n>0}(\lambda_{qnm}) = 0$ by suitably fixing γ_0 (for $n = 1$) and $\gamma_{n,in}$ (for $n > 1$) as functions of λ_{qnm}. For example, corresponding to this lowest λ_{qnm}, $\gamma_0(\lambda_{qnm})$ obtained by setting $a_1(\lambda_{qnm}) = 0$ at the first subleading order is,

$$\gamma_0(\lambda_{qnm}) = -0.68669i \pm 0.779863\ , \tag{F.4}$$

which turns out to be same as the one computed from the outgoing mode analysis (4.84),

$$\gamma_0 = \frac{\omega_Q}{4\varepsilon_0^{1/4}} = \frac{\lambda_{qnm}}{4} = -0.68669i \pm 0.779863\ . \tag{F.5}$$

These two results agree up to order 10^{-9}.

See [202] for recent relevant work in the large D limit.

Appendix G

Determinant Q

The form of the full determinant Q reads as,

$$
\begin{aligned}
\det(Q) =& \gamma^{5/3}\left(a(\lambda)T_1(\lambda) - \tilde{a}(\lambda)T_2(\lambda)\right)\frac{4b(\lambda)\tilde{b}(\lambda)\left(P(\lambda)+\varepsilon(\lambda)\right)\left(\tilde{P}(\lambda)+\tilde{\varepsilon}(\lambda)\right)}{\tilde{a}(\lambda)c_s(\lambda)^2\tilde{c}_s(\lambda)^2T_1(\lambda)^2T_2(\lambda)^2} \\
& \Bigg(-4a(\lambda)^3\tilde{a}(\lambda)^3b(\lambda)^2\tilde{b}(\lambda)^2 \\
& + \gamma^2\Big(4a(\lambda)^2\tilde{a}(\lambda)^2b(\lambda)^2\tilde{b}(\lambda)^2P(\lambda)\tilde{P}(\lambda) \\
& + 4a(\lambda)^4\tilde{a}(\lambda)^4c_s(\lambda)^2\tilde{c}_s(\lambda)^2(P(\lambda)+\varepsilon(\lambda))(\tilde{P}(\lambda)+\tilde{\varepsilon}(\lambda)) + b(\lambda)^4\tilde{b}(\lambda)^4\varepsilon(\lambda)\tilde{\varepsilon}(\lambda) \\
& + r\Big(4a(\lambda)^2b(\lambda)^2P(\lambda)\left(-3\tilde{a}(\lambda)^2\tilde{b}(\lambda)^2\tilde{P}(\lambda) + 2\tilde{a}(\lambda)^4\tilde{c}_s(\lambda)^2(\tilde{P}(\lambda)+\tilde{\varepsilon}(\lambda)) - \tilde{b}(\lambda)^4\tilde{\varepsilon}(\lambda)\right) \\
& +8a(\lambda)^4\tilde{a}(\lambda)^2c_s(\lambda)^2(P(\lambda)+\varepsilon(\lambda))\left(\tilde{b}(\lambda)^2\tilde{P}(\lambda) - 2\tilde{a}(\lambda)^2\tilde{c}_s(\lambda)^2(\tilde{P}(\lambda)+\tilde{\varepsilon}(\lambda))\right) \\
& -2b(\lambda)^4\tilde{b}(\lambda)^2\varepsilon(\lambda)\left(2\tilde{a}(\lambda)^2\tilde{P}(\lambda) + \tilde{b}(\lambda)^2\tilde{\varepsilon}(\lambda)\right)\Big) \\
& + r^2\left(-4a(\lambda)^2b(\lambda)^2P(\lambda) + 4a(\lambda)^4c_s(\lambda)^2(P(\lambda)+\varepsilon(\lambda)) - b(\lambda)^4\varepsilon(\lambda)\right) \\
& \left(-4\tilde{a}(\lambda)^2\tilde{b}(\lambda)^2\tilde{P}(\lambda) + 4\tilde{a}(\lambda)^4\tilde{c}_s(\lambda)^2(\tilde{P}(\lambda)+\tilde{\varepsilon}(\lambda)) - \tilde{b}(\lambda)^4\tilde{\varepsilon}(\lambda)\right)\Big) \\
& + \gamma^4\Big(-a(\lambda)\tilde{a}(\lambda)b(\lambda)^2\tilde{b}(\lambda)^2\left(c_s(\lambda)^2P(\lambda)\varepsilon(\lambda) + c_s(\lambda)^2\varepsilon(\lambda)^2 + P(\lambda)^2\right) \\
& \left(\tilde{c}_s(\lambda)^2\tilde{P}(\lambda)\tilde{\varepsilon}(\lambda) + \tilde{c}_s(\lambda)^2\tilde{\varepsilon}(\lambda)^2 + \tilde{P}(\lambda)^2\right) \\
& + 6ra(\lambda)\tilde{a}(\lambda)b(\lambda)^2\tilde{b}(\lambda)^2\left(c_s(\lambda)^2P(\lambda)\varepsilon(\lambda) + c_s(\lambda)^2\varepsilon(\lambda)^2 + P(\lambda)^2\right) \\
& \left(\tilde{c}_s(\lambda)^2\tilde{P}(\lambda)\tilde{\varepsilon}(\lambda) + \tilde{c}_s(\lambda)^2\tilde{\varepsilon}(\lambda)^2 + \tilde{P}(\lambda)^2\right) \\
& - 9r^2a(\lambda)\tilde{a}(\lambda)b(\lambda)^2\tilde{b}(\lambda)^2\left(c_s(\lambda)^2P(\lambda)\varepsilon(\lambda) + c_s(\lambda)^2\varepsilon(\lambda)^2 + P(\lambda)^2\right) \\
& \left(\tilde{c}_s(\lambda)^2\tilde{P}(\lambda)\tilde{\varepsilon}(\lambda) + \tilde{c}_s(\lambda)^2\tilde{\varepsilon}(\lambda)^2 + \tilde{P}(\lambda)^2\right)\Big)\Bigg)
\end{aligned}
\tag{G.1}
$$

Appendix H

Equations for isentropic thermalisation in modified MIS

Here we give the explicit form of the ward identity and MIS equations of the subsystems and the coupling equations.

- The Ward identity (5.5) reads as,

$$
\begin{aligned}
0 =& 6\varepsilon'(t)a_{11}(t)a_{33}(t)\Big(a_{22}(t)^2a_{33}(t)^2 - a_{23}(t)^2\Big) \\
&+ \varepsilon(t)a_{33}(t)\Big(a_{22}(t)a_{33}(t)\left(a_{22}(t)\left(3a_{11}(t)a'_{33}(t) - 8a_{33}(t)a'_{11}(t)\right) + 3a_{11}(t)a_{33}(t)a'_{22}(t)\right) \\
&+ 8a_{23}(t)^2a'_{11}(t) - 3a_{11}(t)a_{23}(t)a'_{23}(t)\Big) \\
&+ \pi_d(t)a_{11}(t)\Big(- a_{22}(t)a_{33}(t)^3a'_{22}(t) + a_{22}(t)^2a_{33}(t)^2a'_{33}(t) + a_{23}(t)\left(a_{33}(t)a'_{23}(t) - 2a_{23}(t)a'_{33}(t)\right)\Big) \\
&- 2\pi_{od}(t)a_{11}(t)a_{22}(t)\Big(a_{23}(t)\left(a_{33}(t)a'_{22}(t) + a_{22}(t)a'_{33}(t)\right) - a_{22}(t)a_{33}(t)a'_{23}(t)\Big) \qquad \text{(H.1)}
\end{aligned}
$$

- The two MIS equations (2.50) are

$$
\begin{aligned}
0 =& \pi_d'(t)\Big(\tau_\pi a_{23}(t)^2 a_{33}(t)^2 - \tau_\pi a_{22}(t)^2 a_{33}(t)^4\Big) + \pi_{od}'(t)\Big(2\tau_\pi a_{23}(t)^3 - 2\tau_\pi a_{22}(t)^2 a_{23}(t) a_{33}(t)^2\Big) \\
&+ \pi_d(t)\Big(a_{11}(t) a_{33}(t)^2 \left(a_{23}(t)^2 - a_{22}(t)^2 a_{33}(t)^2\right)\Big) + 2\pi_{od}(t)\Big(a_{11}(t) a_{23}(t) \left(a_{23}(t)^2 - a_{22}(t)^2 a_{33}(t)^2\right)\Big) \\
&+ \eta\Big(2a_{22}(t) a_{33}(t)^4 a_{22}'(t) - 2a_{22}(t)^2 a_{33}(t)^3 a_{33}'(t) - 2a_{23}(t) a_{33}(t)^2 a_{23}'(t) + 4a_{23}(t)^2 a_{33}(t) a_{33}'(t)\Big)
\end{aligned}
\tag{H.2}
$$

$$
\begin{aligned}
0 =& \pi_d'(t)\Big(\tau_\pi a_{22}(t)^2 a_{23}(t) a_{33}(t)^3 - \tau_\pi a_{23}(t)^3 a_{33}(t)\Big) + \pi_{od}'(t)\Big(2\tau_\pi a_{22}(t)^4 a_{33}(t)^3 - 2\tau_\pi a_{22}(t)^2 a_{23}(t)^2 a_{33}(t)\Big) \\
&+ \pi_{od}(t)\Big(2a_{11}(t) a_{22}(t)^2 a_{33}(t) \left(a_{22}(t)^2 a_{33}(t)^2 - a_{23}(t)^2\right) - 2\tau_\pi a_{22}(t) a_{23}(t)^2 a_{33}(t) a_{22}'(t) \\
&+ 2\tau_\pi a_{22}(t)^3 a_{33}(t)^3 a_{22}'(t) + 2\tau_\pi a_{22}(t)^2 a_{23}(t)^2 a_{33}'(t) - 2\tau_\pi a_{22}(t)^4 a_{33}(t)^2 a_{33}'(t)\Big) \\
&+ \pi_d(t)\Big(a_{11}(t) a_{23}(t) a_{33}(t) \left(a_{22}(t)^2 a_{33}(t)^2 - a_{23}(t)^2\right) + \tau_\pi a_{22}(t)^2 a_{33}(t)^3 a_{23}'(t) \\
&- 2\tau_\pi a_{22}(t)^2 a_{23}(t) a_{33}(t)^2 a_{33}'(t) - \tau_\pi a_{23}(t)^2 a_{33}(t) a_{23}'(t) + 2\tau_\pi a_{23}(t)^3 a_{33}'(t)\Big) \\
&+ \eta\Big(-2a_{22}(t) a_{23}(t) a_{33}(t)^3 a_{22}'(t) + 2a_{22}(t)^2 a_{33}(t)^3 a_{23}'(t) - 2a_{22}(t)^2 a_{23}(t) a_{33}(t)^2 a_{33}'(t)\Big)
\end{aligned}
\tag{H.3}
$$

- The coupling equations are:

$$
\begin{aligned}
1 - a_{11}(t)^2 &= \tilde{a}_{11}(t)\sqrt{\tilde{a}_{22}(t)^2\tilde{a}_{33}(t)^2 - \tilde{a}_{23}(t)^2}\Big(\gamma\frac{\tilde{\varepsilon}(t)}{\tilde{a}_{11}(t)^2} + \gamma r\Big(-\frac{\tilde{\varepsilon}(t)}{\tilde{a}_{11}(t)^2} \\
&+ \frac{\tilde{a}_{33}(t)^2((t) - \tilde{\pi}_d(t)) - 2\tilde{a}_{23}(t)\tilde{\pi}_{od}(t)}{2\tilde{a}_{22}(t)^2\tilde{a}_{33}(t)^2 - 2\tilde{a}_{23}(t)^2} \\
&+ \frac{\tilde{a}_{22}(t)^2\left(\tilde{a}_{33}(t)^2(\tilde{\pi}_d(t) + \tilde{\varepsilon}(t)) - 2\tilde{a}_{23}(t)\tilde{\pi}_{od}(t)\right) - 2\tilde{a}_{23}(t)^2\tilde{\pi}_d(t)}{2\tilde{a}_{22}(t)^2\tilde{a}_{33}(t)^4 - 2\tilde{a}_{23}(t)^2\tilde{a}_{33}(t)^2}\Big)\Big) \qquad \text{(H.4)}
\end{aligned}
$$

$$
\begin{aligned}
a_{22}(t)^2 - 1 &= \tilde{a}_{11}(t)\sqrt{\tilde{a}_{22}(t)^2\tilde{a}_{33}(t)^2 - \tilde{a}_{23}(t)^2}\Big(\gamma\frac{\left(\tilde{a}_{33}(t)^2(\tilde{\varepsilon}(t) - \tilde{\pi}_d(t)) - 2\tilde{a}_{23}(t)\tilde{\pi}_{od}(t)\right)}{2\tilde{a}_{22}(t)^2\tilde{a}_{33}(t)^2 - 2\tilde{a}_{23}(t)^2} \\
&- \gamma r\Big(-\frac{\tilde{\varepsilon}(t)}{\tilde{a}_{11}(t)^2} + \frac{\tilde{a}_{33}(t)^2(\tilde{\varepsilon}(t) - \tilde{\pi}_d(t)) - 2\tilde{a}_{23}(t)\tilde{\pi}_{od}(t)}{2\tilde{a}_{22}(t)^2\tilde{a}_{33}(t)^2 - 2\tilde{a}_{23}(t)^2} \\
&+ \frac{\tilde{a}_{22}(t)^2\left(\tilde{a}_{33}(t)^2(\tilde{\pi}_d(t) + \tilde{\varepsilon}(t)) - 2\tilde{a}_{23}(t)\tilde{\pi}_{od}(t)\right) - 2\tilde{a}_{23}(t)^2\tilde{\pi}_d(t)}{2\tilde{a}_{22}(t)^2\tilde{a}_{33}(t)^4 - 2\tilde{a}_{23}(t)^2\tilde{a}_{33}(t)^2}\Big)\Big) \qquad \text{(H.5)}
\end{aligned}
$$

$$
\begin{aligned}
a_{33}(t)^2 - 1 &= \tilde{a}_{11}(t)\sqrt{\tilde{a}_{22}(t)^2\tilde{a}_{33}(t)^2 - \tilde{a}_{23}(t)^2}\Big(\gamma\frac{(\tilde{a}_{22}(t)^2(\tilde{a}_{33}(t)^2(\tilde{\pi}_d(t) + \tilde{\varepsilon}(t))}{2\tilde{a}_{22}(t)^2\tilde{a}_{33}(t)^4 - 2\tilde{a}_{23}(t)^2\tilde{a}_{33}(t)^2} \\
&+ \gamma\frac{-2\tilde{a}_{23}(t)\tilde{\pi}_{od}(t)) - 2\tilde{a}_{23}(t)^2\tilde{\pi}_d(t))}{2\tilde{a}_{22}(t)^2\tilde{a}_{33}(t)^4 - 2\tilde{a}_{23}(t)^2\tilde{a}_{33}(t)^2} \\
&- \gamma r\Big(-\frac{\tilde{\varepsilon}(t)}{\tilde{a}_{11}(t)^2} + \frac{\tilde{a}_{33}(t)^2(\tilde{\varepsilon}(t) - \tilde{\pi}_d(t)) - 2\tilde{a}_{23}(t)\tilde{\pi}_{od}(t)}{2\tilde{a}_{22}(t)^2\tilde{a}_{33}(t)^2 - 2\tilde{a}_{23}(t)^2} \\
&+ \frac{\tilde{a}_{22}(t)^2\left(\tilde{a}_{33}(t)^2(\tilde{\pi}_d(t) + \tilde{\varepsilon}(t)) - 2\tilde{a}_{23}(t)\tilde{\pi}_{od}(t)\right) - 2\tilde{a}_{23}(t)^2\tilde{\pi}_d(t)}{2\tilde{a}_{22}(t)^2\tilde{a}_{33}(t)^4 - 2\tilde{a}_{23}(t)^2\tilde{a}_{33}(t)^2}\Big)\Big) \qquad \text{(H.6)}
\end{aligned}
$$

$$
a_{23}(t) = \gamma\frac{\tilde{a}_{11}(t)\sqrt{\tilde{a}_{22}(t)^2\tilde{a}_{33}(t)^2 - \tilde{a}_{23}(t)^2}\left(2\tilde{a}_{22}(t)^2\tilde{\pi}_{od}(t) + \tilde{a}_{23}(t)(\tilde{\pi}_d(t) - \tilde{\varepsilon}(t))\right)}{2\tilde{a}_{22}(t)^2\tilde{a}_{33}(t)^2 - 2\tilde{a}_{23}(t)^2} \qquad \text{(H.7)}
$$

- Similarly the seven equations for the other subsystem can be written by replacing $a_{11}(t) \to \tilde{a}_{11}(t)$, $a_{22}(t) \to \tilde{a}_{22}(t)$, $a_{33}(t) \to \tilde{a}_{33}(t)$, $a_{23}(t) \to \tilde{a}_{23}(t)$, $\varepsilon(t) \to \tilde{\varepsilon}(t)$, $\pi_d(t) \to \tilde{\pi}_d(t)$, $\pi_{od}(t) \to \tilde{\pi}_{od}(t)$ and vice versa.

Bibliography

[1] Rudolf Baier, Paul Romatschke, Dam Thanh Son, Andrei O. Starinets, and Mikhail A. Stephanov. Relativistic viscous hydrodynamics, conformal invariance, and holography. *JHEP*, 04:100, 2008.

[2] W. Israel and J.M. Stewart. Transient relativistic thermodynamics and kinetic theory. *Annals Phys.*, 118:341–372, 1979.

[3] Maximilian Attems, Jorge Casalderrey-Solana, David Mateos, Daniel Santos-Oliván, Carlos F. Sopuerta, Miquel Triana, and Miguel Zilhão. Paths to equilibrium in non-conformal collisions. *JHEP*, 06:154, 2017.

[4] Michal P. Heller, Romuald A. Janik, and Przemyslaw Witaszczyk. The characteristics of thermalization of boost-invariant plasma from holography. *Phys. Rev. Lett.*, 108:201602, 2012.

[5] Alexander Soloviev. Hydrodynamic attractors in heavy ion collisions: a review. *Eur. Phys. J. C*, 82(4):319, 2022.

[6] H.-T. Ding, P. Hegde, O. Kaczmarek, F. Karsch, Anirban Lahiri, S.-T. Li, Swagato Mukherjee, H. Ohno, P. Petreczky, C. Schmidt, and P. Steinbrecher and. "chiral phase transition temperature in (2+1)-flavor qcd. *Physical Review Letters*, 123(6), aug 2019.

[7] Olaf Kaczmarek, Frithjof Karsch, Anirban Lahiri, Lukas Mazur, and Christian Schmidt. Qcd phase transition in the chiral limit. 2020.

[8] Eduardo Grossi, Alexander Soloviev, Derek Teaney, and Fanglida Yan. Soft pions and transport near the chiral critical point. *Phys. Rev. D*, 104(3):034025, 2021.

[9] Pavel Kovtun. Lectures on hydrodynamic fluctuations in relativistic theories. *Journal of Physics A: Mathematical and Theoretical*, 45(47):473001, nov 2012.

[10] Thomas Faulkner and Joseph Polchinski. Semi-holographic fermi liquids. *Journal of High Energy Physics*, 2011(6), jun 2011.

[11] Ayan Mukhopadhyay and Giuseppe Policastro. Phenomenological characterization of semiholographic non-fermi liquids. *Physical Review Letters*, 111(22), nov 2013.

[12] Edmond Iancu and Ayan Mukhopadhyay. A semi-holographic model for heavy-ion collisions. *Journal of High Energy Physics*, 2015(6), jun 2015.

[13] J. D. Bjorken. Highly Relativistic Nucleus-Nucleus Collisions: The Central Rapidity Region. *Phys. Rev. D*, 27:140–151, 1983.

[14] Alberto Nicolis. Low-energy effective field theory for finite-temperature relativistic superfluids. 8 2011.

[15] D.T. Son. Low-energy quantum effective action for relativistic superfluids. 4 2002.

[16] Sukrut Mondkar, Ayan Mukhopadhyay, Anton Rebhan, and Alexander Soloviev. Quasinormal modes of a semi-holographic black brane and thermalization. *JHEP*, 11:080, 2021.

[17] Paolo Glorioso, Michael Crossley, and Hong Liu. A prescription for holographic Schwinger-Keldysh contour in non-equilibrium systems. 12 2018.

[18] Sayantani Bhattacharyya, Veronika E Hubeny, Shiraz Minwalla, and Mukund Rangamani. Nonlinear Fluid Dynamics from Gravity. *JHEP*, 02:045, 2008.

[19] Romuald A. Janik. Viscous plasma evolution from gravity using AdS/CFT. *Phys. Rev. Lett.*, 98:022302, 2007.

[20] Aleksi Kurkela, Ayan Mukhopadhyay, Florian Preis, Anton Rebhan, and Alexander Soloviev. Hybrid Fluid Models from Mutual Effective Metric Couplings. *JHEP*, 08:054, 2018.

[21] Wikipedia contributors. Qcd matter, 2023.

[22] H. Niemi and G. S. Denicol. How large is the knudsen number reached in fluid dynamical simulations of ultrarelativistic heavy ion collisions?, 2014.

[23] Wojciech Florkowski, Michal P. Heller, and Michal Spalinski. New theories of relativistic hydrodynamics in the LHC era. *Rept. Prog. Phys.*, 81(4):046001, 2018.

[24] Michal Spalinski. On the hydrodynamic attractor of Yang-Mills plasma. *Phys. Lett. B*, 776:468–472, 2018.

[25] Michal P. Heller and Michal Spalinski. Hydrodynamics Beyond the Gradient Expansion: Resurgence and Resummation. *Phys. Rev. Lett.*, 115:072501, 2015.

[26] Michal P. Heller, Romuald A. Janik, and Przemyslaw Witaszczyk. Hydrodynamic Gradient Expansion in Gauge Theory Plasmas. *Phys. Rev. Lett.*, 110(21):211602, 2013.

[27] François Gelis. *Quantum Field Theory*. Cambridge University Press, 7 2019.

[28] Hong Liu and Julian Sonner. Holographic systems far from equilibrium: a review. 10 2018.

[29] Juergen Berges. Introduction to nonequilibrium quantum field theory. *AIP Conf. Proc.*, 739(1):3–62, 2004.

[30] Szabolcs Borsanyi. Nonequilibrium field theory from the 2PI effective action. *PoS*, JHW2005:004, 2006.

[31] Balt C. van Rees. Real-time gauge/gravity duality and ingoing boundary conditions. *Nucl. Phys. B Proc. Suppl.*, 192-193:193–196, 2009.

[32] Jana N. Guenther. Overview of the qcd phase diagram – recent progress from the lattice, 2020.

[33] Ulrich Heinz and Raimond Snellings. Collective flow and viscosity in relativistic heavy-ion collisions. *Annual Review of Nuclear and Particle Science*, 63(1):123–151, oct 2013.

[34] DEREK A. TEANEY. VISCOUS HYDRODYNAMICS AND THE QUARK GLUON PLASMA. In *Quark-Gluon Plasma 4*, pages 207–266. WORLD SCIENTIFIC, feb 2010.

[35] Raimond Snellings. Elliptic flow: a brief review. *New Journal of Physics*, 13(5):055008, may 2011.

[36] Jürgen Berges, Michal P. Heller, Aleksas Mazeliauskas, and Raju Venugopalan. Qcd thermalization: Ab initio approaches and interdisciplinary connections. *Reviews of Modern Physics*, 93(3), aug 2021.

[37] Paul Romatschke and Ulrike Romatschke. Viscosity information from relativistic nuclear collisions: How perfect is the fluid observed at RHIC? *Physical Review Letters*, 99(17), oct 2007.

[38] G. Policastro, Dan T. Son, and Andrei O. Starinets. The Shear viscosity of strongly coupled N=4 supersymmetric Yang-Mills plasma. *Phys. Rev. Lett.*, 87:081601, 2001.

[39] P. K. Kovtun, D. T. Son, and A. O. Starinets. Viscosity in strongly interacting quantum field theories from black hole physics. *Physical Review Letters*, 94(11), mar 2005.

[40] Paul Romatschke and Ulrike Romatschke. *Relativistic Fluid Dynamics In and Out of Equilibrium: And Applications to Relativistic Nuclear Collisions*. Cambridge Monographs on Mathematical Physics. Cambridge University Press, 2019.

[41] Chun Shen and Li Yan. Recent development of hydrodynamic modeling in heavy-ion collisions, 2020.

[42] Ingo Müller. Zum Paradoxon der Wärmeleitungstheorie. *Z. Phys.*, 198:329–344, 1967.

[43] Ines Aniceto and Michal Spalinski. Resurgence in extended hydrodynamics. *Physical Review D*, 93(8), apr 2016.

[44] M. Strickland. The non-equilibrium attractor for kinetic theory in relaxation time approximation. *Journal of High Energy Physics*, 2018(12), dec 2018.

[45] Michal P. Heller, Aleksi Kurkela, Michal Spalinski, and Viktor Svensson. Hydrodynamization in kinetic theory: Transient modes and the gradient expansion. *Physical Review D*, 97(9), may 2018.

[46] Krishna Rajagopal and Frank Wilczek. Static and dynamic critical phenomena at a second order QCD phase transition. *Nuclear Physics B*, 399(2-3):395–425, jul 1993.

[47] Mark G. Alford, Krishna Rajagopal, and Frank Wilczek. Color flavor locking and chiral symmetry breaking in high density QCD. *Nucl. Phys. B*, 537:443–458, 1999.

[48] Mark Alford. Color superconductivity in ultra-dense quark matter. *PoS*, LAT2006:001, 2006.

[49] Robert D. Pisarski and Frank Wilczek. Remarks on the chiral phase transition in chromodynamics. *Phys. Rev. D*, 29:338–341, Jan 1984.

[50] Adrien Florio, Eduardo Grossi, Alexander Soloviev, and Derek Teaney. Dynamics of the o(4) critical point in qcd. *Physical Review D*, 105(5), mar 2022.

[51] D. T. Son. Hydrodynamics of nuclear matter in the chiral limit. *Physical Review Letters*, 84(17):3771–3774, apr 2000.

[52] Eduardo Grossi, Alexander Soloviev, Derek Teaney, and Fanglida Yan. Transport and hydrodynamics in the chiral limit. *Phys. Rev. D*, 102(1):014042, 2020.

[53] Kapitza P. Viscosity of liquid helium below the λ-point. *Nature*, 141(74), jan 1938.

[54] MISENER A. ALLEN J.F. Flow phenomena in liquid helium ii. *Nature*, 142(74), oct 1938.

[55] L. Landau. Theory of the superfluidity of helium ii. *Phys. Rev.*, 60:356–358, Aug 1941.

[56] B. Carter and I. M. Khalatnikov. Equivalence of convective and potential variational derivations of covariant superfluid dynamics. *Phys. Rev. D*, 45:4536–4544, Jun 1992.

[57] Seth J. Putterman. Superfluid hydrodynamics. 3, 1974.

[58] Julian Schwinger. Brownian motion of a quantum oscillator. *Journal of Mathematical Physics*, 2(3):407–432, 1961.

[59] C. P. Herzog and D. T. Son. Schwinger-Keldysh propagators from AdS/CFT correspondence. *JHEP*, 03:046, 2003.

[60] Kostas Skenderis. Lecture notes on holographic renormalization. *Class. Quant. Grav.*, 19:5849–5876, 2002.

[61] Kostas Skenderis and Balt C. van Rees. Real-time gauge/gravity duality: Prescription, Renormalization and Examples. *JHEP*, 05:085, 2009.

[62] Souvik Banerjee, Nava Gaddam, and Ayan Mukhopadhyay. Illustrated study of the semi-holographic nonperturbative framework. *Physical Review D*, 95(6), mar 2017.

[63] Toshali Mitra, Sukrut Mondkar, Ayan Mukhopadhyay, Anton Rebhan, and Alexander Soloviev. Hydrodynamic attractor of a hybrid viscous fluid in Bjorken flow. *Phys. Rev. Res.*, 2(4):043320, 2020.

[64] Anton Rebhan Sukrut Mondkar, Ayan Mukhopadhyay and Alexander Soloviev. Linear response in mis semi-holography. *Manuscript under preparation*.

[65] John Adams et al. Experimental and theoretical challenges in the search for the quark gluon plasma: The STAR Collaboration's critical assessment of the evidence from RHIC collisions. *Nucl. Phys. A*, 757:102–183, 2005.

[66] B. B. Back et al. The PHOBOS perspective on discoveries at RHIC. *Nucl. Phys. A*, 757:28–101, 2005.

[67] I. Arsene et al. Quark gluon plasma and color glass condensate at RHIC? The Perspective from the BRAHMS experiment. *Nucl. Phys. A*, 757:1–27, 2005.

[68] K. Adcox et al. Formation of dense partonic matter in relativistic nucleus-nucleus collisions at RHIC: Experimental evaluation by the PHENIX collaboration. *Nucl. Phys. A*, 757:184–283, 2005.

[69] Paul Romatschke. Relativistic fluid dynamics far from local equilibrium. *Physical Review Letters*, 120(1), jan 2018.

[70] Jakub Jankowski and Michal Spalinski. Hydrodynamic Attractors in Ultrarelativistic Nuclear Collisions. 3 2023.

[71] N. D. Birrell and P. C. W. Davies. *Quantum Fields in Curved Space*. Cambridge Monographs on Mathematical Physics. Cambridge Univ. Press, Cambridge, UK, 2 1984.

[72] M. J. Duff. Twenty years of the Weyl anomaly. *Class. Quant. Grav.*, 11:1387–1404, 1994.

[73] Ofer Aharony, Steven S. Gubser, Juan Martin Maldacena, Hirosi Ooguri, and Yaron Oz. Large N field theories, string theory and gravity. *Phys. Rept.*, 323:183–386, 2000.

[74] J D Brown. Action functionals for relativistic perfect fluids. *Classical and Quantum Gravity*, 10(8):1579–1606, aug 1993.

[75] Jyotirmoy Bhattacharya, Sayantani Bhattacharyya, and Mukund Rangamani. Non-dissipative hydrodynamics: Effective actions versus entropy current. *JHEP*, 02:153, 2013.

[76] Sergei Dubovsky, Lam Hui, Alberto Nicolis, and Dam Thanh Son. Effective field theory for hydrodynamics: Thermodynamics, and the derivative expansion. *Physical Review D*, 85(8), apr 2012.

[77] Wikipedia contributors. Lagrangian and eulerian specification of the flow field — Wikipedia, the free encyclopedia, 2022. [Online; accessed 15-March-2023].

[78] Sergei Dubovsky, Lam Hui, Alberto Nicolis, and Dam Thanh Son. Effective field theory for hydrodynamics: thermodynamics, and the derivative expansion. *Phys. Rev. D*, 85:085029, 2012.

[79] Paul Romatschke. New Developments in Relativistic Viscous Hydrodynamics. *Int. J. Mod. Phys. E*, 19:1–53, 2010.

[80] Peter Kostädt and Mario Liu. Causality and stability of the relativistic diffusion equation. *Phys. Rev. D*, 62:023003, Jun 2000.

[81] Paul Romatschke. Relativistic Viscous Fluid Dynamics and Non-Equilibrium Entropy. *Class. Quant. Grav.*, 27:025006, 2010.

[82] Sayantani Bhattacharyya, R. Loganayagam, Ipsita Mandal, Shiraz Minwalla, and Ankit Sharma. Conformal Nonlinear Fluid Dynamics from Gravity in Arbitrary Dimensions. *JHEP*, 12:116, 2008.

[83] Mukund Rangamani. Gravity and Hydrodynamics: Lectures on the fluid-gravity correspondence. *Class. Quant. Grav.*, 26:224003, 2009.

[84] Amaresh Jaiswal. Relativistic third-order dissipative fluid dynamics from kinetic theory. *Phys. Rev. C*, 88:021903, 2013.

[85] Michael Haack and Amos Yarom. Nonlinear viscous hydrodynamics in various dimensions using AdS/CFT. *JHEP*, 10:063, 2008.

[86] R. Loganayagam. Entropy Current in Conformal Hydrodynamics. *JHEP*, 05:087, 2008.

[87] Sangyong Jeon and Ulrich Heinz. Introduction to Hydrodynamics. *Int. J. Mod. Phys. E*, 24(10):1530010, 2015.

[88] Inês Aniceto, Ricardo Schiappa, and Marcel Vonk. The resurgence of instantons in string theory, 2011.

[89] Hiroaki S. Yamada and Kensuke S. Ikeda. A numerical test of pade approximation for some functions with singularity, 2013.

[90] T. Schäfer and E. V. Shuryak. Instantons in QCD. *Reviews of Modern Physics*, 70(2):323–425, apr 1998.

[91] Gokce Basar and Gerald V. Dunne. Hydrodynamics, resurgence, and transasymptotics. *Phys. Rev. D*, 92(12):125011, 2015.

[92] Inês Aniceto, Gokce Basar, and Ricardo Schiappa. A Primer on Resurgent Transseries and Their Asymptotics. *Phys. Rept.*, 809:1–135, 2019.

[93] Ines Aniceto, Ben Meiring, Jakub Jankowski, and Michal Spalinski. The large proper-time expansion of Yang-Mills plasma as a resurgent transseries. *JHEP*, 02:073, 2019.

[94] Daniele Dorigoni. An Introduction to Resurgence, Trans-Series and Alien Calculus. *Annals Phys.*, 409:167914, 2019.

[95] Michal P. Heller. Holography, Hydrodynamization and Heavy-Ion Collisions. *Acta Phys. Polon. B*, 47:2581, 2016.

[96] Toshali Mitra, Sukrut Mondkar, Ayan Mukhopadhyay, Anton Rebhan, and Alexander Soloviev. Hydrodynamization in hybrid Bjorken flow attractors. 11 2022.

[97] Gerard 't Hooft. Dimensional reduction in quantum gravity. *Conf. Proc. C*, 930308:284–296, 1993.

[98] Leonard Susskind. The World as a hologram. *J. Math. Phys.*, 36:6377–6396, 1995.

[99] Juan Martin Maldacena. The Large N limit of superconformal field theories and supergravity. *Adv. Theor. Math. Phys.*, 2:231–252, 1998.

[100] Martin Ammon and Johanna Erdmenger. *Gauge/gravity duality: Foundations and applications*. Cambridge University Press, Cambridge, 4 2015.

[101] David Tong. String Theory. 1 2009.

[102] Peter Breitenlohner and Daniel Z. Freedman. Positive Energy in anti-De Sitter Backgrounds and Gauged Extended Supergravity. *Phys. Lett. B*, 115:197–201, 1982.

[103] Peter Breitenlohner and Daniel Z. Freedman. Stability in Gauged Extended Supergravity. *Annals Phys.*, 144:249, 1982.

[104] M. Henningson and K. Skenderis. The Holographic Weyl anomaly. *JHEP*, 07:023, 1998.

[105] Vijay Balasubramanian and Per Kraus. A Stress tensor for Anti-de Sitter gravity. *Commun. Math. Phys.*, 208:413–428, 1999.

[106] Sebastian de Haro, Sergey N. Solodukhin, and Kostas Skenderis. Holographic reconstruction of space-time and renormalization in the AdS / CFT correspondence. *Commun. Math. Phys.*, 217:595–622, 2001.

[107] Robert M. Wald. *General Relativity*. Chicago Univ. Pr., Chicago, USA, 1984.

[108] Seungjoon Hyun, Won Tae Kim, and Julian Lee. Statistical entropy and AdS / CFT correspondence in BTZ black holes. *Phys. Rev. D*, 59:084020, 1999.

[109] Romuald A. Janik and Robert B. Peschanski. Asymptotic perfect fluid dynamics as a consequence of Ads/CFT. *Phys. Rev. D*, 73:045013, 2006.

[110] Shunichiro Kinoshita, Shinji Mukohyama, Shin Nakamura, and Kin-ya Oda. A Holographic Dual of Bjorken Flow. *Prog. Theor. Phys.*, 121:121–164, 2009.

[111] Guillaume Beuf, Michal P. Heller, Romuald A. Janik, and Robi Peschanski. Boost-invariant early time dynamics from AdS/CFT. *JHEP*, 10:043, 2009.

[112] Paul M. Chesler and Laurence G. Yaffe. Numerical solution of gravitational dynamics in asymptotically anti-de Sitter spacetimes. *JHEP*, 07:086, 2014.

[113] Michael E. Peskin and Daniel V. Schroeder. *An Introduction to quantum field theory*. Addison-Wesley, Reading, USA, 1995.

[114] L. V. Keldysh. Diagram technique for nonequilibrium processes. *Zh. Eksp. Teor. Fiz.*, 47:1515–1527, 1964.

[115] Esteban A. Calzetta and Bei-Lok B. Hu. *Nonequilibrium Quantum Field Theory*. Oxford University Press, 2009.

[116] L M Sieberer, M Buchhold, and S Diehl. Keldysh field theory for driven open quantum systems. *Reports on Progress in Physics*, 79(9):096001, aug 2016.

[117] Alex Kamenev. *Field Theory of Non-Equilibrium Systems*. Cambridge University Press, 2011.

[118] Ulrich Heinz. Thermalization at rhic. *AIP Conference Proceedings*, 739(1):163–180, 2004.

[119] Juergen Berges and Jurgen Cox. Thermalization of quantum fields from time reversal invariant evolution equations. *Phys. Lett. B*, 517:369–374, 2001.

[120] J. Berges, S. Borsanyi, and C. Wetterich. Prethermalization. *Phys. Rev. Lett.*, 93:142002, 2004.

[121] Hong Liu and Julian Sonner. Holographic systems far from equilibrium: a review, 2018.

[122] Kostas Skenderis and Balt C. van Rees. Real-time gauge/gravity duality. *Phys. Rev. Lett.*, 101:081601, 2008.

[123] Andreas Schmitt. *Introduction to Superfluidity: Field-theoretical approach and applications*, volume 888. 2015.

[124] J Goldstone. Field theories with superconductor solutions. *Il Nuovo Cimento (1955-1965)*, 19(1):154–164, January 1961.

[125] Yoichiro Nambu. Quasi-particles and gauge invariance in the theory of superconductivity. *Phys. Rev.*, 117:648–663, Feb 1960.

[126] Y. Nambu and G. Jona-Lasinio. Dynamical model of elementary particles based on an analogy with superconductivity. i. *Phys. Rev.*, 122:345–358, Apr 1961.

[127] Jeffrey Goldstone, Abdus Salam, and Steven Weinberg. Broken symmetries. *Phys. Rev.*, 127:965–970, Aug 1962.

[128] Derek A. Teaney. *Viscous Hydrodynamics and the Quark Gluon Plasma*, pages 207–266. 2010.

[129] Jürgen Berges, Michal P. Heller, Aleksas Mazeliauskas, and Raju Venugopalan. Thermalization in QCD: theoretical approaches, phenomenological applications, and interdisciplinary connections. 5 2020.

[130] Allan Adams, Lincoln D. Carr, Thomas Schaefer, Peter Steinberg, and John E. Thomas. Strongly Correlated Quantum Fluids: Ultracold Quantum Gases, Quantum Chromodynamic Plasmas, and Holographic Duality. *New J. Phys.*, 14:115009, 2012.

[131] Anupam Mazumdar and Graham White. Review of cosmic phase transitions: their significance and experimental signatures. *Rept. Prog. Phys.*, 82(7):076901, 2019.

[132] Paul Romatschke. Relativistic Fluid Dynamics Far From Local Equilibrium. *Phys. Rev. Lett.*, 120(1):012301, 2018.

[133] Paul Romatschke and Ulrike Romatschke. *Relativistic Fluid Dynamics In and Out of Equilibrium*. Cambridge Monographs on Mathematical Physics. Cambridge University Press, 5 2019.

[134] Hong Liu and Paolo Glorioso. Lectures on non-equilibrium effective field theories and fluctuating hydrodynamics. *PoS*, TASI2017:008, 2018.

[135] Haruki Watanabe and Hitoshi Murayama. Redundancies in Nambu-Goldstone Bosons. *Phys. Rev. Lett.*, 110(18):181601, 2013.

[136] Alberto Nicolis, Riccardo Penco, and Rachel A. Rosen. Relativistic Fluids, Superfluids, Solids and Supersolids from a Coset Construction. *Phys. Rev. D*, 89(4):045002, 2014.

[137] Lasma Alberte, Matteo Baggioli, Andrei Khmelnitsky, and Oriol Pujolas. Solid Holography and Massive Gravity. *JHEP*, 02:114, 2016.

[138] Alberto Nicolis, Riccardo Penco, Federico Piazza, and Riccardo Rattazzi. Zoology of condensed matter: Framids, ordinary stuff, extra-ordinary stuff. *JHEP*, 06:155, 2015.

[139] Prahar Mitra, Matteo Ippoliti, R.N. Bhatt, S.L. Sondhi, and Kartiek Agarwal. Cooling arbitrary near-critical systems using hyperbolic quenches. *Phys. Rev. B*, 99(10):104308, 2019.

[140] Jake A.P. Glidden, Christoph Eigen, Lena H. Dogra, Timon A. Hilker, Robert P. Smith, and Zoran Hadzibabic. Bidirectional dynamic scaling in an isolated Bose gas far from equilibrium. 6 2020.

[141] Mark G. Alford, S.Kumar Mallavarapu, Andreas Schmitt, and Stephan Stetina. From a complex scalar field to the two-fluid picture of superfluidity. *Phys. Rev. D*, 87(6):065001, 2013.

[142] Mark G. Alford, S. Kumar Mallavarapu, Andreas Schmitt, and Stephan Stetina. From field theory to superfluid hydrodynamics of dense quark matter. In *Compact Stars in the QCD Phase Diagram III*, 4 2013.

[143] Alexander Haber, Andreas Schmitt, and Stephan Stetina. Instabilities in relativistic two-component (super)fluids. *Phys. Rev. D*, 93(2):025011, 2016.

[144] Richard A. Davison, Luca V. Delacrétaz, Blaise Goutéraux, and Sean A. Hartnoll. Hydrodynamic theory of quantum fluctuating superconductivity. *Phys. Rev. B*, 94(5):054502, 2016. [Erratum: Phys.Rev.B 96, 059902 (2017)].

[145] D. Boyanovsky, H.J. de Vega, and D.J. Schwarz. Phase transitions in the early and the present universe. *Ann. Rev. Nucl. Part. Sci.*, 56:441–500, 2006.

[146] Oliver R. Stockdale, Matthew T. Reeves, Xiaoquan Yu, Guillaume Gauthier, Kwan Goddard-Lee, Warwick P. Bowen, Tyler W. Neely, and Matthew J. Davis. Universal

dynamics in the expansion of vortex clusters in a dissipative two-dimensional superfluid. *Phys. Rev. Research*, 2:033138, Jul 2020.

[147] Eduardo Grossi, Alexander Soloviev, Derek Teaney, and Fanglida Yan. Manuscript in preparation.

[148] Markus Heyl. Dynamical quantum phase transitions: a review. *Rept. Prog. Phys.*, 81(5):054001, 2018.

[149] Takashi Mori, TatsuhikoN. Ikeda, Eriko Kaminishi, and Masahito Ueda. Thermalization and prethermalization in isolated quantum systems: a theoretical overview. *J. Phys. B*, 51(11):112001, 2018.

[150] Souvik Banerjee, Takaaki Ishii, Lata Kh Joshi, Ayan Mukhopadhyay, and P. Ramadevi. Time-dependence of the holographic spectral function: Diverse routes to thermalisation. *JHEP*, 08:048, 2016.

[151] V. Balasubramanian, A. Bernamonti, J. de Boer, N. Copland, B. Craps, E. Keski-Vakkuri, B. Muller, A. Schafer, M. Shigemori, and W. Staessens. Holographic Thermalization. *Phys. Rev. D*, 84:026010, 2011.

[152] Michel Le Bellac. *Thermal Field Theory*. Cambridge Monographs on Mathematical Physics. Cambridge University Press, 1996.

[153] Hugo Touchette. The large deviation approach to statistical mechanics. *Physics Reports*, 478(1):1–69, 2009.

[154] Denis Bernard. Can the macroscopic fluctuation theory be quantized? *Journal of Physics A: Mathematical and Theoretical*, 54(43):433001, oct 2021.

[155] Dam T. Son and Andrei O. Starinets. Minkowski space correlators in AdS / CFT correspondence: Recipe and applications. *JHEP*, 09:042, 2002.

[156] Romuald A. Janik and Robert B. Peschanski. Gauge/gravity duality and thermalization of a boost-invariant perfect fluid. *Phys. Rev. D*, 74:046007, 2006.

[157] Jewel K. Ghosh, R. Loganayagam, Siddharth G. Prabhu, Mukund Rangamani, Akhil Sivakumar, and V. Vishal. Effective field theory of stochastic diffusion from gravity. *JHEP*, 05:130, 2021.

[158] Michael Crossley, Paolo Glorioso, and Hong Liu. Effective field theory of dissipative fluids. *JHEP*, 09:095, 2017.

[159] Paolo Glorioso, Michael Crossley, and Hong Liu. Effective field theory of dissipative fluids (II): classical limit, dynamical KMS symmetry and entropy current. *JHEP*, 09:096, 2017.

[160] Paolo Glorioso, Hong Liu, and Srivatsan Rajagopal. Global Anomalies, Discrete Symmetries, and Hydrodynamic Effective Actions. *JHEP*, 01:043, 2019.

[161] Kristan Jensen, Raja Marjieh, Natalia Pinzani-Fokeeva, and Amos Yarom. A panoply of Schwinger-Keldysh transport. *SciPost Phys.*, 5(5):053, 2018.

[162] Hong Liu and Paolo Glorioso. Lectures on non-equilibrium effective field theories and fluctuating hydrodynamics. *PoS*, TASI2017:008, 2018.

[163] Jan de Boer, Michal P. Heller, and Natalia Pinzani-Fokeeva. Holographic Schwinger-Keldysh effective field theories. *JHEP*, 05:188, 2019.

[164] Bidisha Chakrabarty, Joydeep Chakravarty, Soumyadeep Chaudhuri, Chandan Jana, R. Loganayagam, and Akhil Sivakumar. Nonlinear Langevin dynamics via holography. *JHEP*, 01:165, 2020.

[165] Temple He, R. Loganayagam, Mukund Rangamani, and Julio Virrueta. An effective description of momentum diffusion in a charged plasma from holography. *JHEP*, 01:145, 2022.

[166] Chandan Jana, R. Loganayagam, and Mukund Rangamani. Open quantum systems and Schwinger-Keldysh holograms. *JHEP*, 07:242, 2020.

[167] Temple He, R. Loganayagam, Mukund Rangamani, Akhil Sivakumar, and Julio Virrueta. The timbre of Hawking gravitons: an effective description of energy transport from holography. *JHEP*, 09:092, 2022.

[168] Dam T. Son and Derek Teaney. Thermal Noise and Stochastic Strings in AdS/CFT. *JHEP*, 07:021, 2009.

[169] Ayan Mukhopadhyay. Nonequilibrium fluctuation-dissipation relation from holography. *Phys. Rev. D*, 87(6):066004, 2013.

[170] Matthew Dodelson, Alba Grassi, Cristoforo Iossa, Daniel Panea Lichtig, and Alexander Zhiboedov. Holographic thermal correlators from supersymmetric instantons. 6 2022.

[171] Souvik Banerjee, Ramakrishnan Iyer, and Ayan Mukhopadhyay. The holographic spectral function in non-equilibrium states. *Phys. Rev. D*, 85:106009, 2012.

[172] Lata Kh Joshi, Ayan Mukhopadhyay, Florian Preis, and Pichai Ramadevi. Exact time dependence of causal correlations and nonequilibrium density matrices in holographic systems. *Phys. Rev. D*, 96(10):106006, 2017.

[173] Casey Cartwright and Matthias Kaminski. Correlations far from equilibrium in charged strongly coupled fluids subjected to a strong magnetic field. *JHEP*, 09:072, 2019.

[174] Juan F. Pedraza, Andrea Russo, Andrew Svesko, and Zachary Weller-Davies. Sewing spacetime with Lorentzian threads: complexity and the emergence of time in quantum gravity. *JHEP*, 02:093, 2022.

[175] Pedro Jorge Martinez and Guillermo A. Silva. Thermalization of holographic excited states. *JHEP*, 03:003, 2022.

[176] Suvrat Raju. Lessons from the information paradox. *Phys. Rept.*, 943:1–80, 2022.

[177] Tanay Kibe, Prabha Mandayam, and Ayan Mukhopadhyay. Holographic spacetime, black holes and quantum error correcting codes: A review. *Eur. Phys. J. C*, 82:463, 2022.

[178] David J. Gross and Frank Wilczek. Ultraviolet behavior of non-abelian gauge theories. *Phys. Rev. Lett.*, 30:1343–1346, Jun 1973.

[179] H. David Politzer. Reliable perturbative results for strong interactions? *Phys. Rev. Lett.*, 30:1346–1349, Jun 1973.

[180] Jean-Paul Blaizot and Yacine Mehtar-Tani. Jet Structure in Heavy Ion Collisions. *Int. J. Mod. Phys. E*, 24(11):1530012, 2015.

[181] Charles Gale, Sangyong Jeon, and Bjoern Schenke. Hydrodynamic Modeling of Heavy-Ion Collisions. *Int. J. Mod. Phys. A*, 28:1340011, 2013.

[182] Ulrich W. Heinz. Thermalization at RHIC. *AIP Conf. Proc.*, 739(1):163–180, 2004.

[183] Michael Strickland. Thermalization and isotropization in heavy-ion collisions. *Pramana*, 84(5):671–684, 2015.

[184] Christian Ecker, Ayan Mukhopadhyay, Florian Preis, Anton Rebhan, and Alexander Soloviev. Time evolution of a toy semiholographic glasma. *JHEP*, 08:074, 2018.

[185] Ayan Mukhopadhyay, Florian Preis, Anton Rebhan, and Stefan A. Stricker. Semi-Holography for Heavy Ion Collisions: Self-Consistency and First Numerical Tests. *JHEP*, 05:141, 2016.

[186] Tanay Kibe, Sukrut Mondkar, Ayan Mukhopadhyay, and Hareram Swain. Black hole complementarity from microscopic models. 2023.

[187] Lev Pitaevskii and Sandro Stringari. 65Superfluidity. In *Bose-Einstein Condensation and Superfluidity*. Oxford University Press, 01 2016.

[188] Steven S. Gubser. Symmetry constraints on generalizations of Bjorken flow. *Phys. Rev. D*, 82:085027, 2010.

[189] Ashutosh Dash and Victor Roy. Hydrodynamic attractors for Gubser flow. *Phys. Lett. B*, 806:135481, 2020.

[190] Gabriel S. Denicol and Jorge Noronha. Hydrodynamic attractor and the fate of perturbative expansions in Gubser flow. *Phys. Rev. D*, 99(11):116004, 2019.

[191] Chandrodoy Chattopadhyay, Ulrich Heinz, Subrata Pal, and Gojko Vujanovic. Higher order and anisotropic hydrodynamics for Bjorken and Gubser flows. *Phys. Rev. C*, 97(6):064909, 2018.

[192] Alireza Behtash, C. N. Cruz-Camacho, and M. Martinez. Far-from-equilibrium attractors and nonlinear dynamical systems approach to the Gubser flow. *Phys. Rev. D*, 97(4):044041, 2018.

[193] Alireza Behtash, Syo Kamata, Mauricio Martinez, and Haosheng Shi. Global flow structure and exact formal transseries of the Gubser flow in kinetic theory. *JHEP*, 07:226, 2020.

[194] Wit Busza, Krishna Rajagopal, and Wilke van der Schee. Heavy Ion Collisions: The Big Picture, and the Big Questions. *Ann. Rev. Nucl. Part. Sci.*, 68:339–376, 2018.

[195] Solomon Endlich, Alberto Nicolis, and Junpu Wang. Solid Inflation. *JCAP*, 10:011, 2013.

[196] Ahmed Almheiri, Raghu Mahajan, Juan Maldacena, and Ying Zhao. The Page curve of Hawking radiation from semiclassical geometry. *JHEP*, 03:149, 2020.

[197] Lata Kh Joshi, Ayan Mukhopadhyay, and Alexander Soloviev. Time-dependent $NAdS_2$ holography with applications. *Phys. Rev. D*, 101(6):066001, 2020.

[198] Shunichiro Kinoshita, Shinji Mukohyama, Shin Nakamura, and Kin ya Oda. A holographic dual of bjorken flow. *Progress of Theoretical Physics*, 121(1), jan 2009.

[199] S. A. Hayward. General laws of black hole dynamics. *Phys. Rev. D*, 49:6467–6474, 1994.

[200] Sean A. Hayward. Energy and entropy conservation for dynamical black holes. *Phys. Rev. D*, 70:104027, 2004.

[201] Pau Figueras, Veronika E. Hubeny, Mukund Rangamani, and Simon F. Ross. Dynamical black holes and expanding plasmas. *JHEP*, 04:137, 2009.

[202] Jorge Casalderrey-Solana, Christopher P. Herzog, and Ben Meiring. Holographic Bjorken Flow at Large-D. *JHEP*, 01:181, 2019.